Vol. 67 • No. 5

May 2024

Microwave Journal

IMS 16-21 June

SPECIAL FOCUS: 5G/6G

horizon house®
Founded in 1958
mwjournal.com

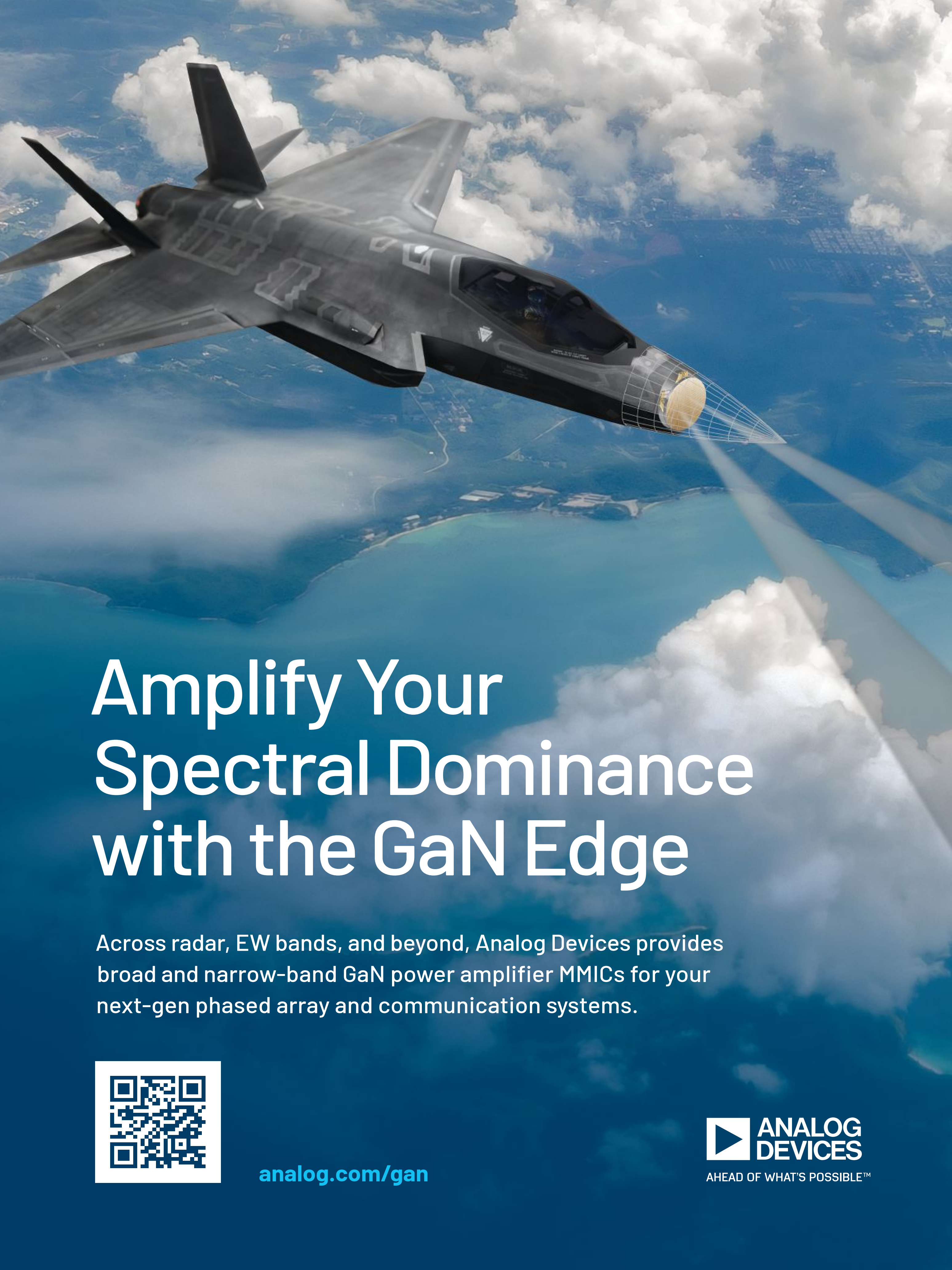

Amplify Your Spectral Dominance with the GaN Edge
Across radar, EW bands, and beyond, Analog Devices provides broad and narrow-band GaN power amplifier MMICs for your next-gen phased array and communication systems.
analog.com/gan
ANALOG DEVICES
AHEAD OF WHAT'S POSSIBLE™

ADVANCED TECHNOLOGY FOR MISSION CRITICAL APPLICATIONS

DORADO JQL FERROCOM

MEET US @IMS2024
BOOTH #543

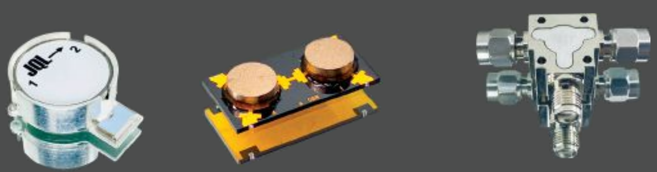

ISOLATORS & CIRCULATORS

SURFACE MOUNT, MICROSTRIP, DROP-IN, COAXIAL WAVEGUIDES

EMS

DESIGN & ASSEMBLY OF ELECTRONIC BOARDS

FILTERS & MULTIPLEXERS

CERAMIC
CERAMIC WAVEGUIDE
CAVITY & DISCRETE

MICROWAVE ANTENNA

SINGLE POLARIZATION
DUAL POLARIZATION
6 GHZ TO 80 GHZ

+1-(888) 236-9828 (US)
+1-(630) 246-7833 (INTL)

MADE IN USA

FOR MORE PRODUCT INFORMATION
GET IN TOUCH WITH US

1255 ARMOUR BLVD
MUNDELEIN, IL 60060
USA

+1-(888) 236-9828 (US)
+1-(630) 246-7833 (INTL)

JQLTECHNOLOGIES.COM

SALES@JQLTECHNOLOGIES.COM

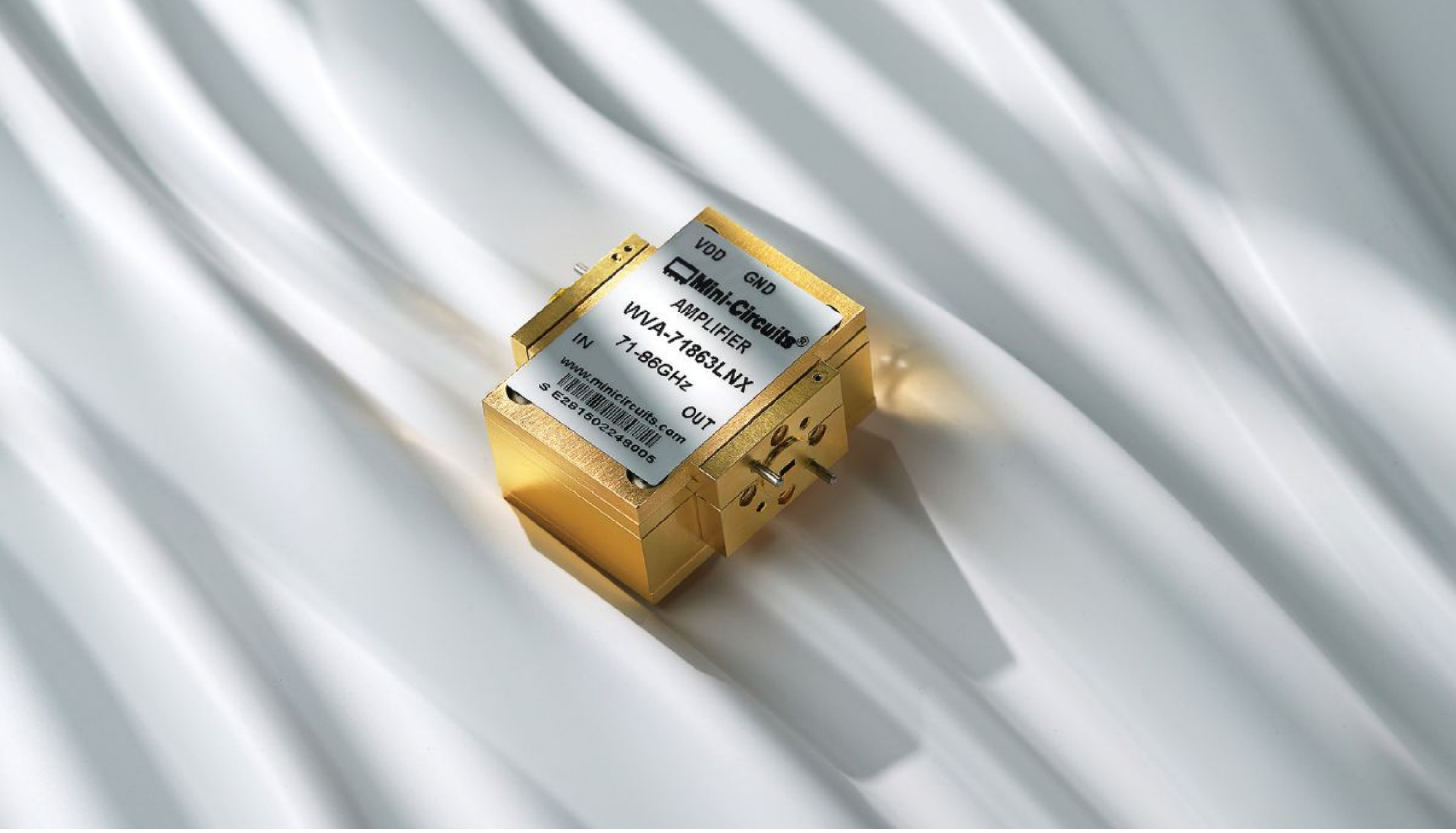

DC TO 95 GHz

High-Frequency Products

For mmWave Test Applications

Waveguide Amplifiers

WVA-71863HP(X)+

Medium power
Key features:

- 71 to 86 GHz
- WR12 Waveguide Interface
- +24.5 dBm P_{SAT}
- 39 dB Gain

WVA-71863LNX+

Medium power
Key features:

- 71 to 86 GHz
- WR12 Waveguide Interface
- 4.5 dB Noise Figure
- 39 dB Gain

E-Band Amplifiers

ZVA-50953G+

E-Band Medium Power Amplifier

- 50 to 95 GHz
- +21 dBm P_{OUT} at Saturation
- 28 dB gain
- ±2.0 dB gain flatness
- Single supply voltage, +10 to +15V

ZVA-71863HP+

E-Band Medium Power Amplifier

- 71 to 86 GHz
- +24 dBm P_{OUT} at Saturation
- 38 dB gain
- ±1.5 dB gain flatness
- Single supply voltage, +10 to +15V

ZVA-71863LNX+

E-Band Low Noise Amplifier

- 71 to 86 GHz
- 4.5 dB noise figure
- 37 dB gain
- +13.8 dBm P1dB, +18 dBm P_{SAT}
- Single-supply voltage, +10 to +15V

K — V-Band Amplifiers

ZVA-35703+

Medium Power Amplifier

- 35 to 71 GHz
- +21 dBm P_{SAT}
- 17.5 dB gain
- ±1.5 dB gain flatness
- Single supply voltage, +10 to +15V

ZVA-543HP+

Medium Power Amplifier

- 18 to 54 GHz
- +29 dBm P_{SAT}
- High gain, 31 dB
- ±2.0 dB gain flatness
- Single supply voltage, +10 to +15V

ZVA-0.5W303G+

Medium Power Amplifier

- 10 MHz to 30 GHz
- 0.5W P_{OUT} at Saturation
- ±1.5 dB gain flatness
- 4.2 dB noise figure
- Single +12V bias voltage

Additional High Frequency Products

BIAS TEES

DIGITAL STEP ATTENUATORS

I/Q MIXERS

MIXERS

MULTIPLIERS

POWER DETECTORS

SWITCHES

& MORE

Mini-Circuits®


RF-LAMBDA
THE LEADER OF RF BROADBAND SOLUTIONS
BROADBAND SSPA / EMC BENCHTOP
SOLID STATE POWER AMPLIFIER
0.1-22GHZ
ULTRA BROADBAND SSPA
RFLUPA01M22GA
4W 0.1-22GHZ
RFLUPA0218GB
20W 1-19GHZ
300W 6-18GHZ SOLID STATE BROADBAND
400W 8-11GHZ
SOLID STATE BROADBAND
0.1-6GHZ VHZ,
UHF, L, S, C BAND
RFLUPA02G06GC
100W 2-6GHZ
RFLUPA0706GD
30W 0.7-6GHZ
MADE IN USA
6-18GHZ C, X, KU BAND
RFLUPA08G11GA
50W 8-11GHZ
RFLUPA0618GD
60W 6-18GHZ
RFLUPA06G12GB
25W 6-12GHZ
18-50GHZ K, KA, V BAND
RFLUPA18G47GC
2W 18-47GHZ
RFLUPA27G34GB
15W 27-34GHZ
RFLUPA47G53GA2
10W 47-53GHZ
RFLUPA27G34GB
30W 18-40GHZ
BENCHTOP RF MICROWAVE SYSTEM POWER AMPLIFIER
RAMP00G06GA- 30W 0.01-6GHZ
RAMP39G48GA- 4W 39-48GHZ
RAMP01G22GA- 8W 1-22GHZ
RAMP27G34GA- 8W 27-34GHZ
www.rflambda.com
sales@rflambda.com
1-888-976-8880
1-972-767-5998
San Diego, CA, US
Carrollton, TX, US
Ottawa, ONT, Canada
Frankfurt, Germany

Drop-ins, Modules & IMAs to 100 GHz

Get on the Grid

X-Microwave offers a modular design system technology that is revolutionizing the RF and Microwave industry. RF and Microwave engineers use X-MWblock® modular building blocks to rapidly evaluate, prototype, and produce high-end RF and Microwave systems faster, easier, and at lower cost.

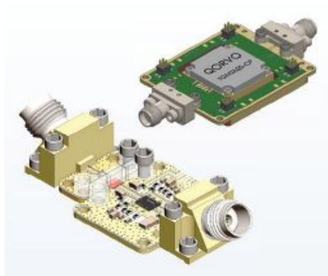

Drop-In Everything

- Over 6000 X-MWblocks
- SMT, DIE, Flip Chip, Die on Carrier, Flanged
- X-MWprobes to 100 GHz
- Solderless Interconnect

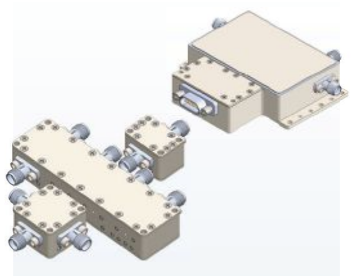

Connectorized & Hermetic Modules

- RF/Bias X-MWblocks
- Amps, filters, switches, DSAs, etc.
- Field Replaceable Connectors

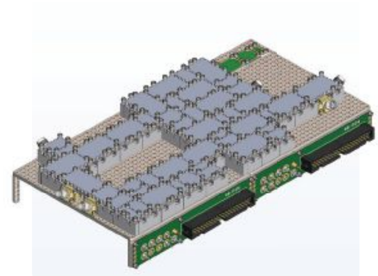

Quick-Turn Prototypes

- Complete Signal Chains
- Modular Walls & Lids
- RasPi Control

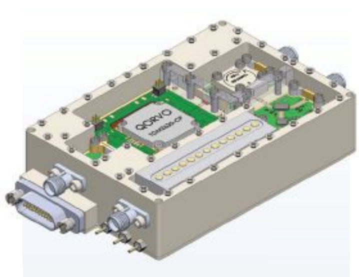

Integrated Microwave Assemblies

- Custom Designed IMAs
- TxRx Modules
- Synthesizers, LO Distribution

Benchtop Housing

- Quick-Turn Enclosed IMAs
- Versatile input/output options
- 2919 Format

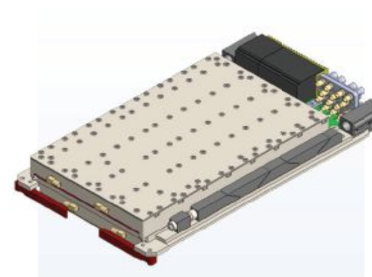

OpenVPX

- VITA 67.3 / SOSA Aligned
- 3U & 6U Card Assemblies
- Two RF Housings

Get a complete list of our X-MWblock drop-ins, connectorized modules, prototype plate assemblies and IMAs. Also find our brochures and tutorials for additional information at **quanticxmw.com**

IMS Booth 1251

Don't miss us.

Quantic™ X-Microwave

Microwave Journal

CONTENTS

May 2024
Vol. 67 • No. 5
5G/6G & IEEE MTT-S
IMS Show Issue
mwjournal.com

online spotlights

Look for this month's exclusive articles online at mwjournal.com

Time Travel

Cover Feature

Technical Features

127 5G 6G — SPECIAL FOCUS: 5G/6G

Special Report

Application Note

67 YEARS OF PUBLISHING EXCELLENCE

Miller MMIC is a global provider of RF semiconductor solutions with expertise in GaAs and GaN processes. We offer a diverse range of products tailored to various wireless applications. Our product lineup encompasses a wide array of offerings, including Low Noise Amplifiers, Distributed Amplifiers, Power Amplifiers, Driver Amplifiers, RF Switches, RF PIN Diode Switches, and numerous other voltage- and digitally-controllable RF components.

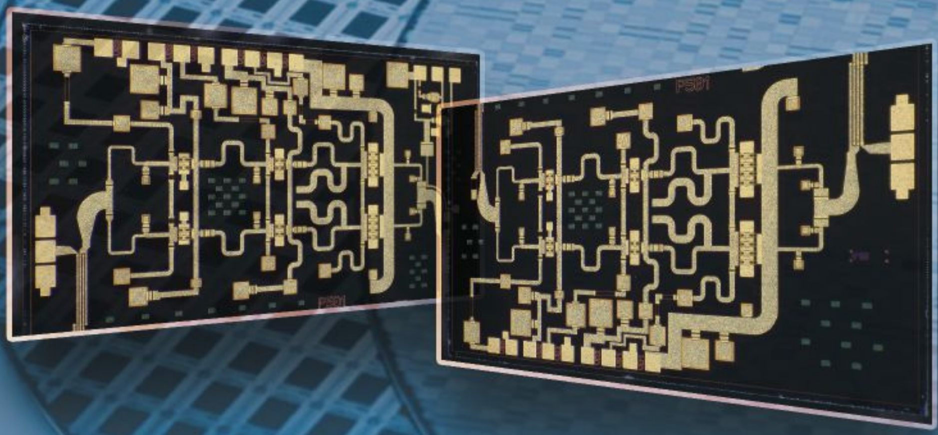

PN: MMW5FP

RF GaAs MMIC DC-67GHz

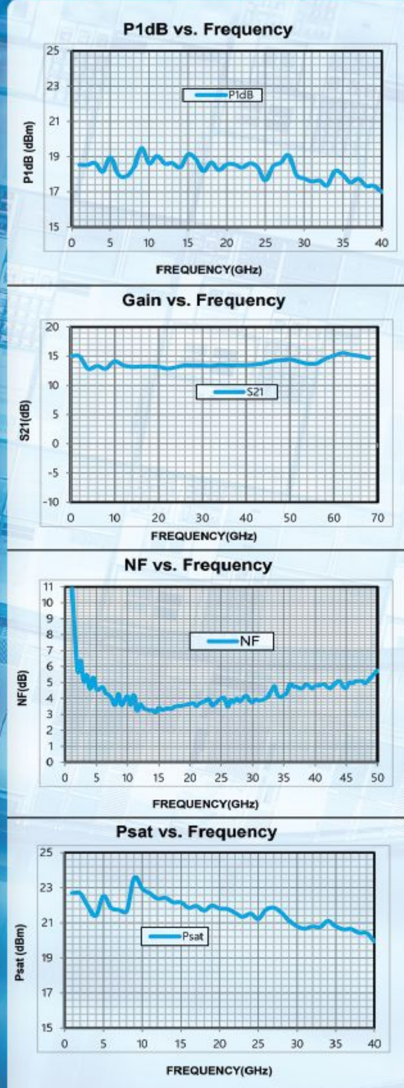

RF Distributed Low Noise Amplifiers

PN	Freq Low (GHz)	Freq High (GHz)	Gain (dB)	NF(dB)	P1dB (dBm)	Voltage (VDC)	Current (mA)	Package
MMW001T	DC	20.0	17~19	1~3.5	23 @ 10GHz	8.0	145	die
MMW4FP	DC	50.00	16.00	4.00	24.00	10	200	die
MMW507	0.20	22.0	14.0	4 - 6	28.0	10.0	350	die
MMW508	DC	30.0	14.0	2.5dB @ 15GHz	24.5	10.0	200	die
MMW509	30KHz	45.0	15.0		20.0	6.0	190	die
MMW510	DC	45.0	11.0	4.5	15.5	6.0	100	die
MMW510F	DC	30.00	20.00	2.50	22.00			die
MMW511	0.04	65.0	10.0	9.0	18.0	8.0	250	die
MMW512	DC	65.0	10.0	5.0	14.5	4.5	85	die
MMW5FN	DC	67.00	14.00	2.00	19.00	4.5	81	die
MMW5FP	DC	67.00	14.00	4.00	21.00	8	140	die
MMW011	DC	12.0	14.0		30.5	12.0	350	die

Low Noise Amplifiers

PN	Freq Low (GHz)	Freq High (GHz)	Gain (dB)	NF(dB)	P1dB (dBm)	Voltage (VDC)	Current (mA)	Package
MML040	6.0	18.0	24.0	1.5	14.0	5.0	35	die
MML058	1.0	18.0	15.0	1.7	17.0	5.0	35	die
MML063	18.0	40.0	11.0	2.9	15.0	5.0	52	die
MML080	0.8	18.0	16.5/15.5	1.9/1.7	18/17.5	5.0	65/40	die
MML081	2.0	18.0	25/23	1.0/1.0	16/9.5	5.0	37/24	die
MML083	0.1	20.0	23.0	1.6	11.0	5.0	58	die

RF Driver Amplifier

PN	Freq Low (GHz)	Freq High (GHz)	Gain (dB)	NF(dB)	P1dB (dBm)	Voltage (VDC)	Current (mA)	Package
MM3006	2.0	20.0	19.5	2.5	22.0	7.0	130	die
MM3014	6.0	20.0	15.0	-	19.5	5.0	107	die
MM3017T	17.0	43.0	25.0		22.0	5.0	140	die
MM3031T	20.0	43.0	20.0		24.0	5.0	480	die
MM3051	17.0	24.0	25.0	-	25.0	5.0	220	die
MM3058	18.0	40.0	20/19.5	2.5/2.3	16/14	5/4	69/52	die
MM3059	18.0	40.0	16/16	2.5/2.3	16/15	5/4	67/50	die

GaAs Medium Power Amplifier

PN	Freq Low (GHz)	Freq High (GHz)	Gain (dB)	P1dB (dBm)	Psat (dBm)	Voltage (VDC)	Current (mA)	Package
MMP107	17.0	21.0	19.0	30.0	30.0	6.0	400	die
MMP108	18.0	28.0	14.0	31.5	31.0	6.0	650	die
MMP111	26.0	34.0	25.5	33.5	33.5	6.0	1300	die
MMP112	2.0	6.0	20.0	31.5	32.0	8.0	365	die
MMP501	20.0	44.0	15.0	27 -- 32	29 - 34	5.0	1200	die
MMP502	18.0	47.0	14.0	28.0	30.0	5.0	1500	die

CALL US 1-833-2MILLER(264-5537)

WWW.MILLERMMIC.COM

sales@millermmic.com

support@millermmic.com

Microwave Journal

CONTENTS

mwjournal.com

Product Features

Tech Brief

Departments

Microwave Journal (USPS 396-250) (ISSN 0192-6225) is published monthly by Horizon House Publications Inc., 685 Canton St., Norwood, MA 02062. Periodicals postage paid at Norwood, MA 02062 and additional mailing offices.

POSTMASTER: Send address corrections to Microwave Journal, PO Box 1028, Lowell, MA 01853 or e-mail mwj@e-circ.net. com. Subscription information: (978) 671-0446. This journal is issued without charge upon written request to qualified persons working in the RF & microwave industry. Other subscriptions are: domestic, $130.00 per year, two-year subscriptions, $200.00; foreign, $225.00 per year, two-year subscriptions, $400.00; back issues (if available) and single copies, $20.00 domestic and $30.00 foreign. Claims for missing issues must be filed within 90 days of date of issue for complimentary replacement.

Posted under Canadian international publications mail agreement #PM40612608

STAFF

EXECUTIVE EDITORIAL OFFICE
685 Canton Street, Norwood, MA 02062
Tel: (781) 769-9750
FAX: (781) 769-5037
e-mail: mwj@mwjournal.com

EUROPEAN EDITORIAL OFFICE
16 Sussex Street, London SW1V 4RW, England
Tel: Editorial: +44 207 596 8730 Sales: +44 207 596 8740
FAX: +44 207 596 8749

SUBSCRIPTION SERVICES
Send subscription inquiries and address changes to:
Tel: (978) 671-0446
e-mail: mwj@e-circ.net

www.mwjournal.com

Printed in the USA

CONTENTS

IEEE MTT-S International Microwave Symposium & Exhibition

3H Communication Systems
P/N: 2X2CC5300-100-8AA
S/N: 8102-1762-03 Cage: 75ET3

3H Communication Systems
P/N: CC23435-T200-5KK
S/N: 2020-N005-2233-05

3H Communication Systems
TLC6500-100-9SS-X1 SN-53021
3H Communication Systems
TLC6500-100-9SS-X1 SN-53099

3H
TLC582-U80-9SS
2015-3055 S/N: 024

Microwave Journal ONLINE .COM

eLEARNING CENTER

Radar Evolution and Agile Filters
Sponsored by: Knowles Precision Devices 5/14

Improve Wireless RFFE Design with Highly Linear RF Switch for Interference and De-sensitivity Mitigation
Sponsored by: Menlo Micro 6/11

Catch *Frequency Matters*, the industry update from *Microwave Journal*,
microwavejournal.com/FrequencyMatters

WHITE PAPERS

ALTAIR — *Scalability of Full Wave and Asymptotic Solvers in Altair Feko*

ANALOG DEVICES — AHEAD OF WHAT'S POSSIBLE™ — *Radar Basics: How to Build a 24 GHz FMCW Radar System*

Anritsu — Advancing beyond — *Extended Reality (XR) Spreading in Business Field*

Quantic Croven — *Quartz Crystal Hermeticity and the Relationship to SC-cut Long Term Reliability*

Quantic Wenzel — *5 Critical Questions to Ask When Selecting Fixed-frequency Sources for Digitally Reprogrammable Multifunction AESA Systems*

Look for additional content from:

Anritsu — Advancing beyond
ERZIA
ROHDE&SCHWARZ — Make ideas real

Executive Interviews

Ian Dunn, CTO of **Spectrum Control**, talks about the company's heritage, its product portfolio and differentiators along with the future directions of the company.

Michael Cronin, VP of Sales Products at **TÜV Rheinland**, talks about the company's portfolio of services, the company's Northeast Technology and Innovation Center and the future directions of TÜV Rheinland.

Join Us Online

Follow us
@Pathindle
@MWJEric
@MWJEditor

Join us at the RF and Microwave Community

Become a fan at facebook.com/microwavejournal

Visit us @ mwjournal.com

1 MHz TO 50 GHz

Mesh Network Test Systems

Simulate Real-World Mesh Communication in Your Lab

- Port counts from 3 to N
- Independently controlled attenuation on every path
- Attenuation range up to 120 dB


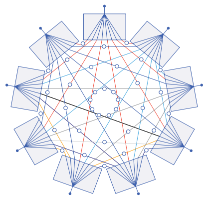

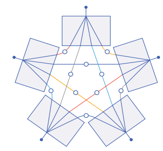

Ideal for testing receiver sensitivity, changes in range between devices, effects of interference on performance and more!

Common applications:

- R&D testing of wireless "smart" devices
- Bluetooth, Zigbee, Z-Wave, Wi-Fi, IoT
- Qualification / acceptance testing of military radios
- UHF / VHF band man-pack / vehicular systems
- PMR / TETRA

LEARN MORE

Mini-Circuits®

STAY CONNECTED TO COMING EVENTS

MARK YOUR CALENDAR

MAY

13-15
Space Tech Expo USA
Long Beach, Calif.
www.spacetechexpo.com

20-23
CS Mantech
Tucson, Ariz.
https://csmantech.org

JUNE

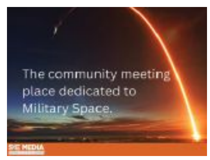

3-4
Future Military Space Technology USA
Los Angeles, Calif.
www.smgconferences.com/defence/northamerica/milspace-usa

10-12
MILSATCOM USA
Arlington, Va.
www.smgconferences.com/defence/northamerica/MilSatCom-USA

24-26
Sensors Converge
Santa Clara, Calif.
www.sensorsconverge.com

AUGUST

5-9
IEEE EMC + SIPI
Phoenix, Ariz.
https://emc2024.org

SEPTEMBER

22-27
EuMW 2024
Paris, France
www.eumweek.com

16-18
RFIC 2024
Washington, DC
https://rfic-ieee.org/

16-21
IMS2024
Washington, DC
https://ims-ieee.org

21
ARFTG-103
Washington, DC
https://arftg.org/103-conference/

Catch our exclusive conference information, news, social networking, photos, videos and more at mwjournal.com/ims2024

ONLINE PANEL SERIES

6/25

New Innovations in Power Amplifiers

Call for Papers Deadlines

7/1	IEEE MAPCON
7/7	IEEE HPEC
7/7	APMC

FOR DETAILS VISIT MWJOURNAL.COM/EVENTS

TIME TRAVEL

Eric Higham
Microwave Journal Technical Editor

DARPA: Born From a Surprise

The Time Travel feature has historically featured a person who was instrumental in the development of the electronics industry. As Washington, DC, prepares to host the International Microwave Symposium (IMS), we are spotlighting an agency that has been involved in much of the development of the electronics industry. Coincidentally, this agency, DARPA, was founded in February 1958, about six months before the first issue of Microwave Journal was published.

On October 4, 1957, the USSR successfully launched the first satellite into Earth orbit. The Sputnik launch came as a shock to U.S. experts and citizens who expected the U.S. would be the first to accomplish this scientific advancement. The launch also came during the Cold War era between the U.S. and the USSR and in addition to demonstrating technical superiority, it crystallized fears that the USSR could launch nuclear weapons that could reach any country in the world. In addition to kicking off the "space race," this "Sputnik surprise" triggered events that led to the formation of Advanced Research Projects Agency (ARPA). ARPA added a "D" to reflect the defense focus and contributions and became DARPA.

DARPA's stated mission is to invest in breakthrough technologies for national security. Despite a straightforward mission statement, DARPA's remit is both broad and well-funded, touching both commercial and defense applications with FY2024 funding levels expected to be slightly more than $4 billion.

The agency is credited with turning ideas about ballistic missile defense and space surveillance technologies into the reality of electronically-steered phased arrays in the early 1960s. DARPA funded the development of the first GaAs FET and then funding from the MIMIC program helped push GaAs technology from discrete devices to MMICs and helped to develop and establish the entire GaAs ecosystem from starting processes through to manufacturing and test. The significance of the "D" in DARPA's name was never more evident than with GaAs power amplifiers (PAs). Lower volume, high performance defense applications gladly used the new GaAs PAs while the supply chain evolved to the point where it could produce high yield, high performance, low-cost amplifiers that enabled the wireless revolution.

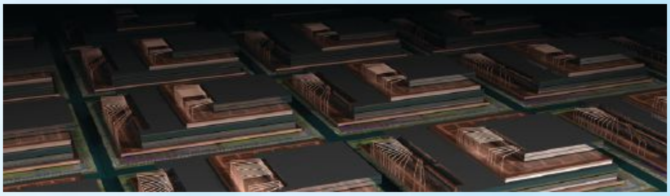

DARPA was the early driving force behind the development of GaN processes and products. Funding for this technology has produced a similar trajectory where the defense community was an early adopter of products that are widely used in commercial applications. DARPA looks to advance this technology through a program like NEXT that aims to develop nitride transistor technology to enable high speed PAs and high output DACs.

However, the interests of DARPA extend well beyond solid-state electronics and compound semiconductors. The agency claims at least some credit for developments ranging from Moderna's COVID-19 vaccine to weather satellites, GPS, drones, stealth technology, speech recognition, touchscreen displays, voice interfaces, the personal computer and the internet. A review of the DARPA website shows that their research activities come from six technical offices and they currently list 109 topics of interest. So, as we have our discussions about new products at IMS and perhaps look at old products, it is useful to remember that all the past, present and future products probably have been or will be touched by DARPA funding.

EXODUS ADVANCED COMMUNICATIONS

Powerful Solutions, Racked & Stacked Maximizing Performance

Model Number	Frequency Range	Rated Power Watts	Gain dB
10KHz-250MHz, Low Frequency Amplifiers			
AMP2080B	10kHz-250MHz	100	50
AMP2080C-1	10kHz-250MHz	150	52
AMP2080C	10kHz-250MHz	300	55
AMP2080D	10kHz-250MHz	600	58
80-1000MHz, VHF, UHF Range Amplifiers			
AMP2032	80-1000MHz	300	55
AMP2071-2	80-1000MHz	500	57
AMP2071A-LC	80-1000MHz	750	60
AMP2115-LC	80-1000MHz	1300	61
AMP2121-LC	80-1000MHz	2000	63
700MHz-6.0GHz, Broadband Amplifiers			
AMP2070C	0.7-6.0GHz	100	50
AMP2070A	1.0-6.0GHz	150	52
AMP2030-LC	1.0-6.0GHz	300	55
AMP2030-600-LC	1.0-6.0GHz	600	58
AMP2030D-LC	1.0-6.0GHz	750	59
AMP2030LC-1KW	1.0-6.0GHz	1000	60
2.0-8.0GHz, SC Band Amplifiers			
AMP2085-1	2.0-8.0GHz	120	51
AMP2085C	2.0-8.0GHz	200	53
AMP2085E-1LC	2.0-8.0GHz	250	54
AMP2085E	2.0-8.0GHz	400	56
6.0-18.0GHz, High Frequency Amplifiers			
AMP2118	6.0-18.0GHz	40	46
AMP2111	6.0-18.0GHz	50	47
AMP2033-LC	6.0-18.0GHz	100	50
AMP2065A-LC	6.0-18.0GHz	200	53
AMP2065B-LC	6.0-18.0GHz	300	55
AMP2065E-LC	6.0-18.0GHz	500	57
18-26.5GHz, K-Band, Millimeter Amplifiers			
AMP4032	18.0-26.5GHz	10	40
AMP4065LC-1	18.0-26.5GHz	20	43
AMP4065-LC	18.0-26.5GHz	40	46
AMP4065A-LC	18.0-26.5GHz	100	50
AMP4065B-LC	18.0-26.5GHz	200	53
26.5-40.0GHz, Ka-Band, Millimeter Amplifiers			
AMP4072	26.5-40.0GHz	10	40
AMP4066LC-1	26.5-40.0GHz	20	43
AMP4066-LC	26.5-40.0GHz	40	46
AMP4066A-LC	26.5-40.0GHz	100	50
AMP4066B-LC	26.5-40.0GHz	200	53
18.0-40.0GHz, Millimeter Amplifiers			
AMP2145A-LC	18.0-40.0GHz	10	40
AMP2145B-LC	18.0-40.0GHz	25	44
AMP2145C-LC	18.0-40.0GHz	50	47
40.0-50.0GHz, Q-Band, Millimeter Amplifiers			
AMP4076-1	40.0-50.0GHz	5	37
AMP4076A	40.0-50.0GHz	20	43
AMP4076B	40.0-50.0GHz	40	46
AMP4076C	40.0-50.0GHz	80	49

RF & Microwave Amplifiers

10KHz-75GHz

Amplifiers
CW & Pulse
Watts to KW

Versatile Across All Modulation Standards
Achieve Immediate Wide Bandwidth Access
Reliable and Durable
Powerful Precision with Class A/AB Linear Design

10KHz-250MHz
3000 Watts

800MHz-6.0GHz
1000 Watts

2.0-8.0GHz
500 Watts

3674 E. Sunset Road, Suite 100, Las Vegas, Nevada 89120 USA
Tel : 1-702-534-6564 Email : sales@exoduscomm.com

www.exoduscomm.com

Has Amplifier Performance or

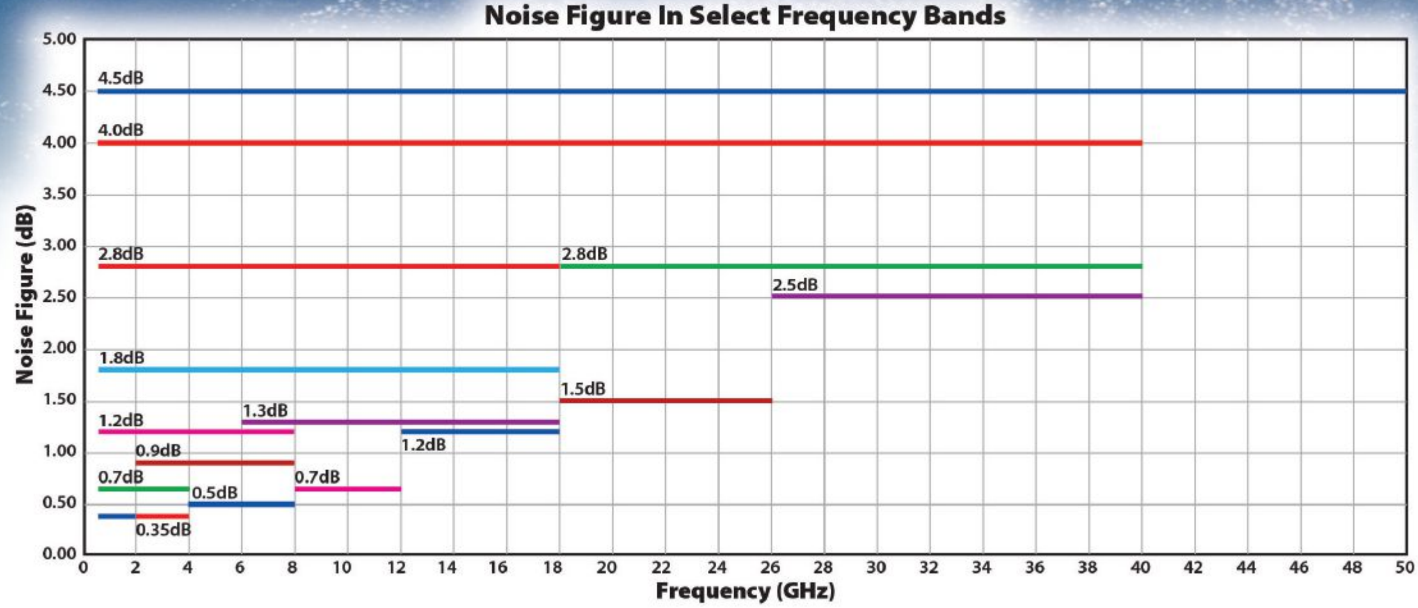


Delivery Stalled Your Program?
Features:
5 kHz to 50 GHz
Noise Figures:
from 0.35 dB @ 23ºC
from 10 K @ Cryogenic
P1 dB >+30 dBm
Up to 75 dB Gain
Input Power Limiter
Excellent Group Delay
Gain & Phase Matching
Temperature Compensation
Waveguide Connectors
Weather-Proof Enclosures
Visit us in Booth 512 at IMS 2024.
B&Z is the preferred source for
high performance amplifiers.
B&Z TECHNOLOGIES
INNOVATING TO EXCEL
www.bnztech.com

COVER FEATURE
INVITED PAPER

Full-Vehicle OTA Testing at the Core of the Connected Car (R)EVOLUTION

Benoit Derat, Bastian Balk and Jose M. Fortes
Rohde & Schwarz, Munich, Germany

Connectivity is at the core of the automotive technology revolution, which will enable not only self-driving cars but also new services and features. However, antennas interact with adjacent components and the performance of integrated car transceivers must be evaluated in situ. As a consequence, full-vehicle over-the-air (OTA) testing has become a subject of growing interest in the automotive industry. This article discusses the most recognized measurement methodologies, their implementation and the rationale behind the metrics of interest.

AUTONOMOUS, CONNECTED AND SHARED VEHICLES SHAPE EVOLUTION

A multi-dimensional technological evolution, or revolution, has moved the automotive industry forward in the past decade and is nowhere near completion. A major stir-up for the industry happened early in the 2010s when electric cars were introduced. These vehicles were powerful with enough battery autonomy to satisfy a significant segment of users. Reinforced by the fast-growing costs of fossil fuels and environmental concerns, this boosted the race towards carbon neutrality.

Several prominent advancements in connectivity and autonomous driving already impact the lives of consumers. When walking in San Francisco, it is not rare to see a car from a fully self-driving ride-hailing service, as shown in ***Figure 1***. Also, luxury cars already feature 31 in. 8K screens in response to the needs of premium customers who want flawless data quality. These examples of technical features may seem different, but they are correlated.

As cars become more autonomous, our needs stay the same. We connect to the internet, chat, watch videos, access data or simply entertain ourselves while our self-driving vehicle takes us to our destination. But, how does our vehicle get us to that destination safely? It relies on robust and intelligent sensing devices like radars and lidars, as well as high performance ground communication through cellular and non-cellular services, along with satellite links

Fig. 1 Waymo One Jaguar I-PACE in San Francisco.

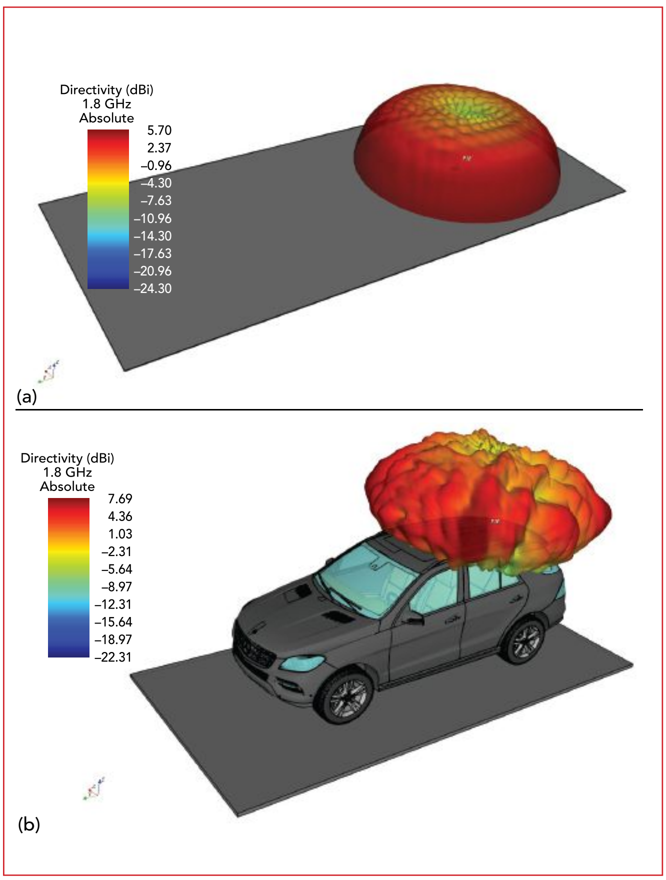

Fig. 2 (a) Shark fin antenna mounted on an ideal ground plane. (b) Shark fin antenna mounted on a vehicle.

for navigation and non-terrestrial network connectivity. Connectivity already plays a key role in road safety, with e-call functionality deployed and mandatory in multiple countries.

Connectivity occupies a vital role in the automotive revolution. High performance connectivity in vehicles is a differentiator, creating advantageous features for car makers. In the future, as the number of connected cars increases and embedded RF transceivers perform more safety-critical functions, high performance car connectivity will likely become a matter for network operators and regulators. As a result of this vision, industry efforts

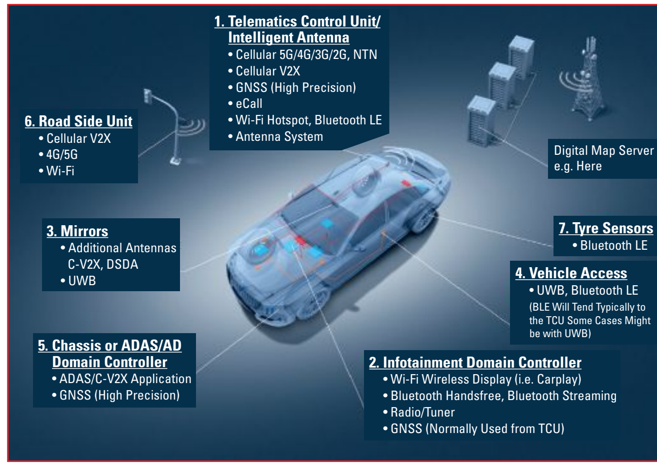

Fig. 3 Typical car connectivity module integration.

are underway to harmonize vehicle connectivity testing methodology that could be part of a homologation process, eventually. Demand for test equipment and solutions is increasing significantly to support these efforts. To address these issues, efforts have focused on vehicle-level OTA measurements in the past five years.

WHY FULL-VEHICLE OTA?

The antenna is a key component of every radio communication transceiver. Car antennas are more integrated, becoming almost invisible for aesthetics, theft prevention or mechanical robustness. Since the antenna radiates and receives electromagnetic energy, coupling mechanisms between the antenna and the rest of the car elements are an unavoidable consequence of tight integration. As a result, a car antenna cannot be designed or validated without considering the actual conditions. ***Figure 2a*** shows simulated directivity patterns for a typical shark fin antenna mounted on an ideal ground plane. ***Figure 2b*** shows the same antenna top-mounted on a commercial vehicle. Both simulations are far-field patterns at 1.8 GHz calculated with IMST EMPIRE XPU software.[1] The peak directivity increases from 5.7 to 7.3 dBi when the antenna is mounted on the roof of the car, indicating the impact of the car/antenna coupling.

This issue involves more than the modification of the radiation properties. Each car antenna is part of an RF system, so qualifying this system without the antenna provides an incomplete, imperfect picture. Conducted testing excludes the influence of coupling between the antenna and the RF boards. It affects the actual operation of the electronics, which typically sees a matched load from the instrumentation instead of the actual antenna impedance. As illustrated in ***Figure 3***, a car has multiple RF systems that perturbate each other and eventually degrade sensitivity. Similar to what the wireless industry adopted more than 20 years ago, major automotive industry stakeholders see OTA measurements in a controlled and repeatable chamber environment as the only approach to accurately evaluate embedded radio module connectivity performance and integration effects. As a benefit, OTA tests replace expensive proving ground tests.

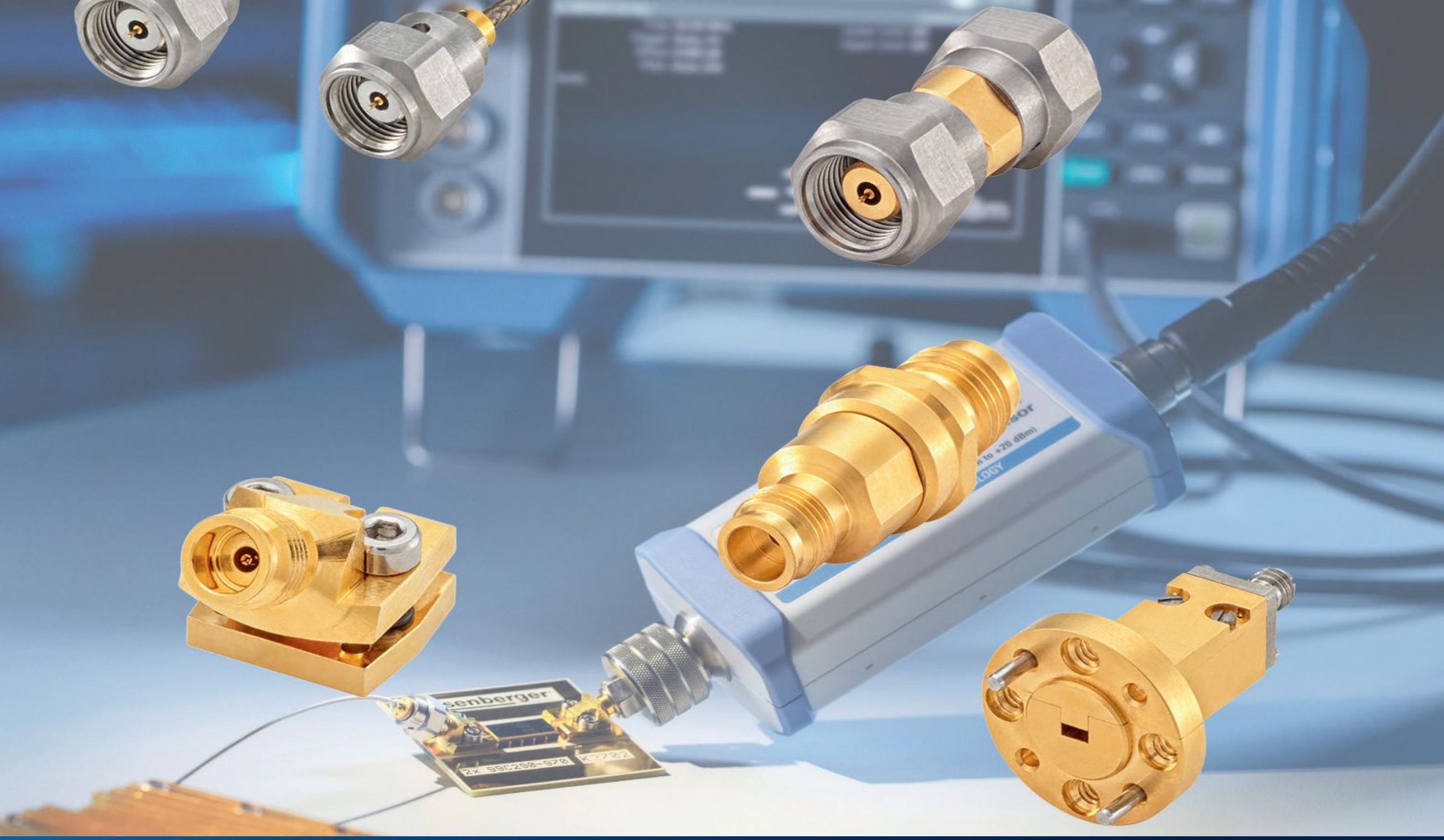

TEST & MEASUREMENT

Test, Measurement & Calibration

RF and microwave components from Rosenberger play a key role in a variety of test, measurement and calibration applications. RF high precision connectors, adaptors & devices, PCB connections, calibration kits, microwave test cables or VNA test port cables – the precision and quality of Rosenberger test and measurement products have been proven in various applications:

- Microwave measurements and VNA calibrations
- Lab testing, factory testing
- PCB connections
- Semiconductor test applications and high-speed digital testing
- Network testing
- Test and measurement equipment and devices

www.rosenberger.com

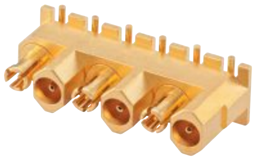

Rosenberger

A DE FACTO STANDARD?

Standards, technical specifications or test plans play a critical role in guaranteeing a consistent understanding of test methodologies and interpreting test data. Standards often originate from a growing market need, but long development times create situations where the technology precedes the standard. This describes the full-vehicle OTA measurement standards situation.

The landscape of testing guidances is not an open field, yet there is a dynamic in the industry to rapidly fill the gaps. As cars inherit the communication and localization functions supported by mobile phones, a cornerstone of full-vehicle OTA testing can be found in the CTIA "Certification Test Plan for Wireless Over-the-Air Performance."[2] CTIA has defined the key metrics characterizing OTA performance for wireless devices and put together proven methodologies to assess these metrics for all cellular and non-cellular technologies. CTIA test plans also define metrics and measurement procedures for standalone (GNSS) and assisted (A-GNSS) location-based services. Hardware and software measurement solutions that are compliant with CTIA test plans are state-of-the-art for OTA measurements. This is what all "active" system-level OTA measurements at the vehicle level required: system-level measurements including the transceiver, by opposition to the "passive" pure antenna measurements.

However, CTIA is primarily focused on wireless devices like smartphones, tablets and laptops. Additional considerations are required when measuring a device under test (DUT) as large as a car. These are currently not addressed by the CTIA "Test Plan for Wireless Over-the-Air Performance."

The 5G Automotive Association (5GAA) identified this lack of vehicle-level testing guidance and worked to produce the "Vehicular Antenna Test Methodology" (VATM) technical report published in August 2021.[3] Some of the key elements of this document include:

- Recommended test environments: Anechoic chamber, shielded chamber with a reflective ground plane or open area test sites
- Base methodology: Direct far-field probing or near-field measurements accompanied by near-field to far-field transformation with data measured with spherical, cylindrical or planar scanners with final results translated into spherical coordinates
- Key active OTA system-level metrics
- Required test volume, based on the maximum considered vehicle size and how to validate it using reference antennas
- Measurement methods, including options for conventional or combinational measurements and detailed procedures per wireless technology.

The CTIA "Certification Test Plan" and recommended practices from the 5GAA VATM precisely and thoroughly define how vehicle-level OTA testing should be performed

for accurate results. In the absence of a dedicated international standard, this combination of documents is being used as a de facto standard by automotive industry stakeholders to set the requirements of any new full-vehicle OTA test system.

However, China has recognized the strategic importance of defining procedures for full-vehicle OTA evaluations in the competitive race for connected and autonomous cars. In 2022, the National Technical Committee for Auto Standardization initiated a new work item for a local standard using the CTIA and 5GAA documents as input references.[4]

PRACTICAL IMPLEMENTATION OF VEHICLE OTA

Even though 5GAA describes alternative test sites, anechoic chamber environments are preferred for the reliability and repeatability of measurements. ***Figure 4*** illustrates a typical setup that meets 5GAA recommendations. In this type of anechoic chamber, the car under test is mounted on a pole rotating in azimuth at a distance from the floor. The measurement antenna is attached at the tip of a gantry arm, rotating in elevation. The combination of the two rotations provides a complete spherical scanning capability.

As recommended by the 5GAA VATM TR, the maximum elevation of the gantry, should be at least 120 degrees. To minimize test system size, anechoic chambers are designed so that the arm comes close to the floor absorbers at this maximum elevation. Lifting the car enables measurements down to this elevation angle with the exact height determined from the measurement range length. As an example, if the range length from the center coordinates at the base of the car to the tip of the measurement antenna is 6 m, then going down to 120 degree elevation requires a height of at least 6 m times cos(60 degrees), or 3 m.

Achieving the proper distance from the test probe to the absorbers may require additional height. Continuing the previous example and assuming that the test system measures down to 400 MHz, 1.5 m must be added to the previously calculated 3 m height. This means that the DUT has to be raised above the floor by about 4.5 m to provide absorber tips with enough distance at the maximum elevation range. The gantry also lifts similarly, as the center of rotation of the arm should remain in the same plane as the center of coordinates, the vehicle center projected to the turntable surface.

Measurements down to 120 degrees in elevation require specific care in DUT fixturing. A vehicle can

▲ **Fig. 4** **Full-vehicle OTA anechoic test environment.**

weigh several tons, so a large metal structure is required at the azimuth pole to position, lift and rotate the car. Metal creates scattering and perturbates measurements, so absorber panels typically hide the related structures. However, these panels create shadowing effects and absorb waves that should be measured. To reduce these effects, fixtures minimize the footprint extending beyond the vehicle. The 3D model in Figure 4 shows this approach with only small pieces of the fixture visible next to the wheels.

WHY MEASURE UNDER THE FLOOR?

Cars are used on the road, so it may appear absurd to measure the radiation patterns down to "30 degrees below the floor." This choice is justified by practical scenarios that are detailed in the 5GAA VATM. As one example, ***Figure 5*** shows communication with a mobile network. Evaluating the cellular propagation channels, the most significant angles of arrival linking a UE to a base station are from 60 to 90 degrees in elevation. However, because of ground reflections, signals from 90 to 120 degrees of elevation are also relevant in an anechoic environment, particularly to transceivers located on the sides of the car. The antenna radiation performance in those directions impacts connectivity and must be qualified.

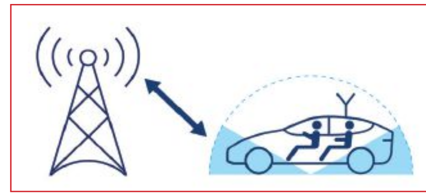

Fig. 5 **Angle of arrival for cellular technologies.**

Satellite communications present another interesting use case. The region of interest is in a cone looking at elevation angles towards the zenith (0 to 60 degrees), as waves are coming from the sky. However, good GNSS service performance requires a good signal-to-noise ratio, so measuring the spatial selectivity of the antennas and filtering out angles of arrival between 60 and 110 degrees is critical to minimize the power captured from poor-quality links coming at grazing angles. This is also addressed in the 5GAA VATM.

Addressing these considerations, the 5GAA VATM defines associated OTA metrics with the partial radiated power (PRP) or partial isotropic sensitivity (PIS). These quantities reflect the overall radiated power or sensitivity performance of the DUT in the relevant angular regions. As an example, PRP is calculated in ***Equation 1*** and ***Equation 2***:

$$PRP = \frac{\Delta\theta \cdot \Delta\phi}{4\pi} \cdot \left(\frac{cut_0 + cut_p}{2} + \sum_{i=1}^{p-1} cut_i \right) \quad (1)$$

$$cut_i = \sum_{j=0}^{q-1} \left[EIRP_\theta(\theta_i, \phi_j) + EIRP_\phi(\theta_i, \phi_j) \right] \cdot \sin\theta_i \quad (2)$$


MBT
Massachusetts Bay Technologies
Motivated by Performance, Focused on Reliability.®
A NAME YOU CAN TRUST WHEN THE CHIPS ARE DOWN
Our engineers are available to discuss your specific design and application requirements.
MBT's product line includes but is not limited to the following RF/Microwave semiconductor devices and Passive Products:
RF/MICROWAVE SEMICONDUCTOR DEVICES
Abrupt Tuning Varactors Diodes
Step Recovery/Multiplier Diodes
PIN/Beam Lead PIN/Limiter Diodes
Point Contact Diodes
Schottky Diodes
PASSIVE PRODUCTS
Thin Film Products
Chip Capacitors
Resistors
Single Layer Ceramic Capacitors
Spiral Inductors
PLEASE DOWNLOAD OUR CAPABILITIES BROCHURE TODAY AT WWW.MASSBAYTECH.COM
Visit MBT at IMS Booth #209
ITAR Registered International Traffic in Arms Regulations
ISO 9001:2015 CERTIFIED
378 Page St., Stoughton, MA 02072
Tel: 781-344-8809
Fax: 781-341-8177
sales@massbaytech.com
www.massbaytech.com

Where:

$i=0$ to p, is the index of an elevation cut in the EIRP patterns

cut_i results from discretized integration of the total EIRP including azimuth and elevation polarizations (θ, ϕ) in the θi-*plane*.

p and q are the total number for elevation and azimuth angle intervals, respectively. These are calculated based on the defined angle range of interest and the step size. The PRP is then the cumulated cut_i powers in the cuts where the elevation angles sweep through the angular region of interest. In the case of communicating to the mobile network, PRP and PIS, integrated through the 60 to 120 degree elevation region, would be the quantities of interest.

DEALING WITH LIMITED RANGE LENGTH

One of the concerns to address in full-vehicle OTA measurements is the size of the DUT. OTA quantities should be measured in the far-field. Far-field is, ideally, captured at infinity, but a practical and common approach is to select a measurement range length, *R*, greater than the Rayleigh or Fraunhofer distance (FHD). This reasonably approximates the far-field condition and is shown in ***Equation 3***:

$$R \geq \frac{2D^2}{\lambda} \tag{3}$$

Where:

D is the antenna radiation aperture

λ is the free-space wavelength.

However, except in canonical cases, the exact antenna aperture is not known a priori. Since antennas couple with nearby structures, the aperture will generally be larger than the antenna element itself. At a minimum, *D* will not be larger than the diameter of the minimum sphere encompassing the whole DUT. This is a workaround that can be used with compact devices like smartphones. The rationale behind the worst-case range length definition for CTIA OTA testing is based on considering *D* as the maximum DUT dimension. However, a large, high-end car with a 6 m length, supporting 5G NR FR1 communication up to 7.125 GHz returns a calculated *D* value of 6 m and an R of more than 1.7 km. Clearly, full-vehicle OTA testing requires more advanced considerations.

A car is a large device, but the integrated antennas are very localized. The car does not behave as one big antenna. Even though its structure couples to the radiated fields from the antenna elements, the currents spread over a limited region. As an example, the EMPIRE XPU simulation presented in ***Figure 6*** shows the magnitude of electric currents over the conducting car roof when the shark fin antenna from Figure 2a is excited with a 1.8 GHz signal. The amplitude decays quickly, down by 20 dB within 20 cm from the feed point, which is a little more than a wavelength. Standalone shark fin antenna evaluations typically use round metallic plates to simulate these close energy-coupling effects, but using size-


Anokiwave Is Now
qorvo
Always Connected
Anokiwave and Qorvo bring innovation and scale to SATCOM applications. Our system level support and broad portfolio of products are connecting the world through space.
Visit qorvo.com/go/satcom to see our complete portfolio for SATCOM.
© 04-2024 Qorvo US, Inc. | QORVO is a trademark of Qorvo US, Inc.

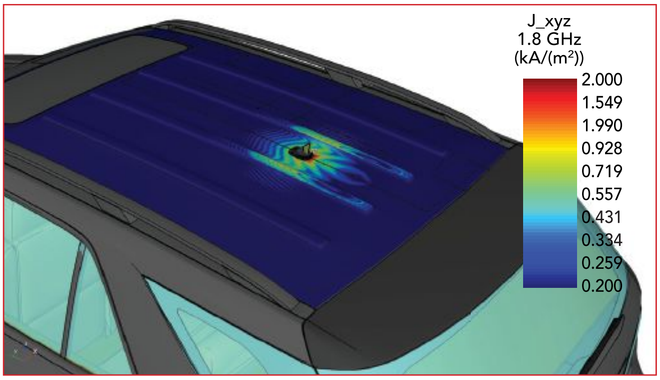

Fig. 6 Magnitude of electric currents at 1.8 GHz.

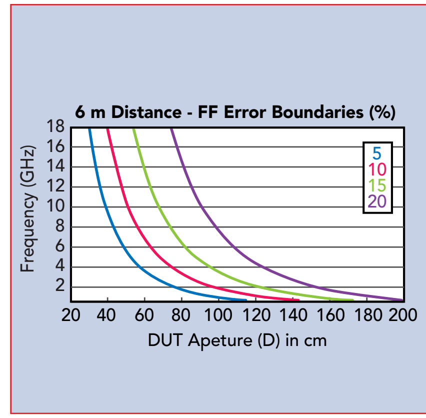

Fig. 7 Far-field error boundary isolines.

limited ground planes, typically a 1 m diameter disk, for measurements down to 600 MHz means only one wavelength radius at this frequency.

Also, as demonstrated in the past years, FHD may be overkill for certain OTA tests. If a certain error on the measured radiated metrics can be tolerated, then a shorter effective far-field distance can be used. Detailed considerations about this distance can be found in the related ANSI C63 white paper.[5] ***Figure 7*** continues the 6 m range length gantry system example and shows far-field error boundaries as a function of *D* and frequency. This plot shows that a 15 percent deviation, less than 0.7 dB, allows far-field OTA test antenna apertures as large as 75 cm at 8 GHz and 1.8 m at 500 MHz. Combining this finding with the considerations of Figure 6 gives confidence that 5GAA VATM-type ranges allow true far-field OTA measurements of vehicle-integrated transceivers.

When performing measurements at shorter range lengths, the offset between the center of radiation, typically at the antenna element and the center of the coordinate system must be considered. Ignoring this offset can result in large errors in the measured radiated quantities. To mitigate these effects, the car can be physically translated in the test environment by adding one or more linear axes at the turntable or processing the test signals for receive and transmit measurements.[6]

Another alternative from the 5GAA VATM to address the limited range length involves combining passive and active measurements.[3]

RF-LAMBDA

MADE IN USA

THE LEADER OF RF BROADBAND SOLUTIONS

EMC Broadband RF Power Amplifier

High Power Solid State

HUNDREDS IN STOCK

FAST SHIPPING

FREQUENCY UP TO 90GHZ

POWER UP TO 2KW CW

REMC06G18GG

6-18GHZ 300W

- AUTOMATIC BUILT IN SELF CALIBRATION AND BIAS ADJUSTMENT.
- OVER TEMPERATURE, CURRENT, INPUT POWER PROTECTION.
- VSWR MEASUREMENT AND OPEN CIRCUIT PROTECTION.
- USER FRIENDLY CONTROL INTERFACE.
- REMOTE ETHERNET CONTROL AND FIRMWARE UPDATE.
- HIGH POWER EFFICIENCY AND LIGHTWEIGHT.

RAMP42G47GA 42-47GHZ 8W

RAMP18G40GB-U 18-40G 20W

RAMP05M80GC 0.5-80GHZ

REMC02G06GE 2-6GHZ 500W

REMC08G11GE 8-11GHZ 400W

In this scenario, the fields radiated by the antennas in the DUT are first characterized in magnitude and phase with a vector network analyzer. Near-field to far-field processing is then applied to deduce the actual far-field directivity. Finally, an OTA test is run with the DUT in the same position, utilizing the same DUT antenna, but this time cabled to the transceiver and transmitting or receiving digitally-modulated signals. The setup change does not affect the propagation of electromagnetic fields from the measured scan, assumed to be in the near-field to the far-field region. The ratio of power in a given direction between the scanned sphere and a sphere at a larger distance obtained in the passive antenna test can be used to derive the actual far-field OTA values based on the near-field OTA scan.

CONCLUSION

Qualifying the connectivity performance of embedded car modules requires system-level OTA characterization that includes the vehicle. Without international standards covering these measurements, the 5GAA VATM TR has become the de facto standard, particularly to define test environments. Systems and software supporting CTIA's "Certification Test Plan for Wireless Over-the-Air Performance" are appropriate to execute the related measurements. This paper has provided some implementation details on the industry-preferred methodology using a large anechoic chamber, including a distributed-axis spherical scanner with an elevation range of up to 120 degrees. It has shown that full-vehicle far-field OTA tests can be made in compact 5GAA VATM-compatible environments. Finally, techniques were introduced to enable accurate measurements by mitigating the effects of limited measurement range length. ■

ACKNOWLEDGMENT

The authors would like to thank Winfried Simon at IMST GmbH for the vehicle antenna simulation and figure support using the EMPIRE XPU software.

References

1. A. Lauer, W. Simon and A. Wien, "XPU Technology for Fast and Efficient FDTD Simulations using Modern CPUs Cache Memory Bandwidth," *European Conference on Antennas and Propagation*, Vol. 13, No. 15, pp. 2584–2589, March 2015.
2. CTIA Certification Test Plan for Wireless Device Over-The-Air Performance V4.0.X, Web: https://ctiacertification.org/test-plans/.
3. 5GAA Technical Report, "Vehicular Antenna Test Methodology," Aug. 2021, Web: https://5gaa.org/vehicular-antenna-test-methodology/.
4. GB/T XXXX-XXXX draft standard, Road vehicles – RF Performance Requirements and Test Methods for Vehicle Antenna Systems, Jan. 24.
5. ANSI C63, Discussion on Measurement Test Distance for Determining EIRP or TRP of Active Antenna Systems, accepted for publication.
6. G. F. Hamberger, et al., "Correction of Over-the-air Transmit and Receive Wireless Device Performance Errors Due to Displaced Antenna Positions in the Measurement Coordinate System," *IEEE Trans. Antennas Propag.*, Vol. 68, No. 11, June 2020, pp. 7549–7554.

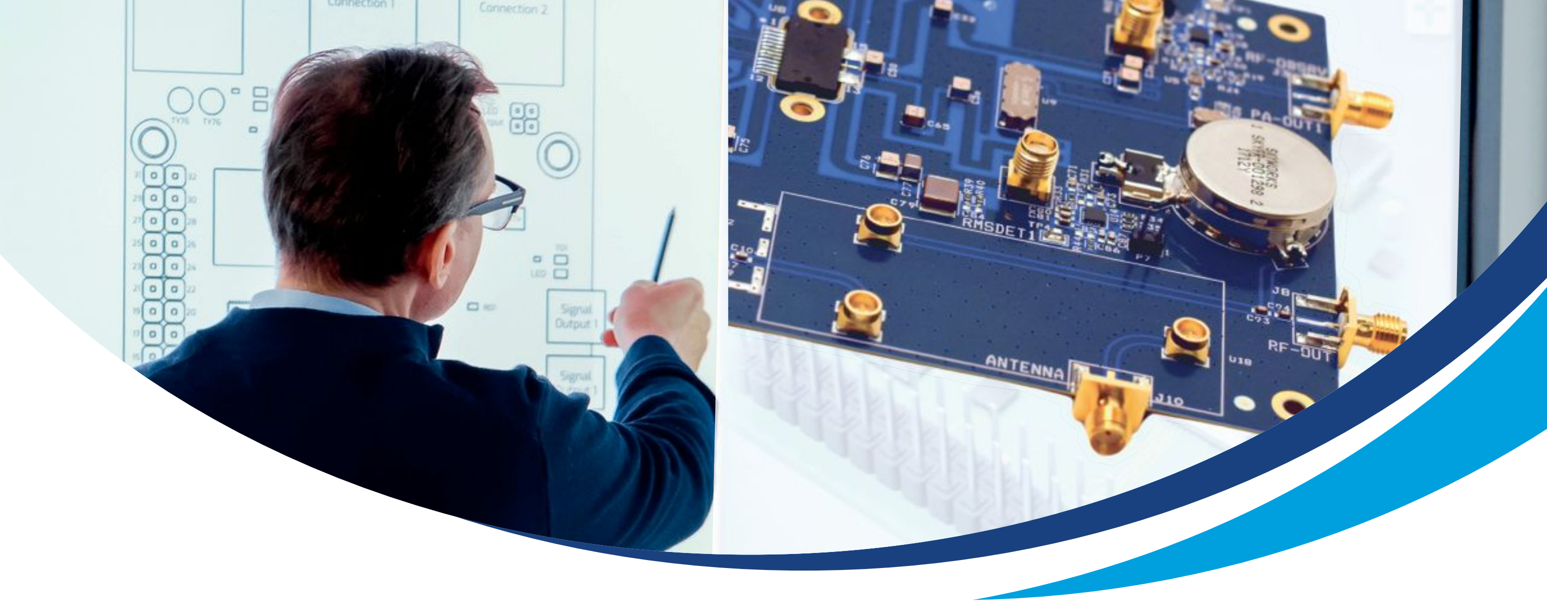
ANTENNA
RF-OUT

RF Amplifiers and Sub-Assemblies for Every Application

Delivery from Stock to 2 Weeks ARO from the catalog or built to your specifications!

- Competitive Pricing & Fast Delivery
- Military Reliability & Qualification
- Various Options: Temperature Compensation, Input Limiter Protection, Detectors/TTL & More
- Unconditionally Stable (100% tested)

ISO 9001:2000 and AS9100B CERTIFIED

OCTAVE BAND LOW NOISE AMPLIFIERS

Model No.	Freq (GHz)	Gain (dB) MIN	Noise Figure (dB)	Power-out @ P1-dB	3rd Order ICP	VSWR
CA01-2110	0.5-1.0	28	1.0 MAX, 0.7 TYP	+10 MIN	+20 dBm	2.0:1
CA12-2110	1.0-2.0	30	1.0 MAX, 0.7 TYP	+10 MIN	+20 dBm	2.0:1
CA24-2111	2.0-4.0	29	1.1 MAX, 0.95 TYP	+10 MIN	+20 dBm	2.0:1
CA48-2111	4.0-8.0	29	1.3 MAX, 1.0 TYP	+10 MIN	+20 dBm	2.0:1
CA812-3111	8.0-12.0	27	1.6 MAX, 1.4 TYP	+10 MIN	+20 dBm	2.0:1
CA1218-4111	12.0-18.0	25	1.9 MAX, 1.7 TYP	+10 MIN	+20 dBm	2.0:1
CA1826-2110	18.0-26.5	32	3.0 MAX, 2.5 TYP	+10 MIN	+20 dBm	2.0:1

NARROW BAND LOW NOISE AND MEDIUM POWER AMPLIFIERS

Model No.	Freq (GHz)	Gain (dB) MIN	Noise Figure (dB)	Power-out @ P1-dB	3rd Order ICP	VSWR
CA01-2111	0.4 - 0.5	28	0.6 MAX, 0.4 TYP	+10 MIN	+20 dBm	2.0:1
CA01-2113	0.8 - 1.0	28	0.6 MAX, 0.4 TYP	+10 MIN	+20 dBm	2.0:1
CA12-3117	1.2 - 1.6	25	0.6 MAX, 0.4 TYP	+10 MIN	+20 dBm	2.0:1
CA23-3111	2.2 - 2.4	30	0.6 MAX, 0.45 TYP	+10 MIN	+20 dBm	2.0:1
CA23-3116	2.7 - 2.9	29	0.7 MAX, 0.5 TYP	+10 MIN	+20 dBm	2.0:1
CA34-2110	3.7 - 4.2	28	1.0 MAX, 0.5 TYP	+10 MIN	+20 dBm	2.0:1
CA56-3110	5.4 - 5.9	40	1.0 MAX, 0.5 TYP	+10 MIN	+20 dBm	2.0:1
CA78-4110	7.25 - 7.75	32	1.2 MAX, 1.0 TYP	+10 MIN	+20 dBm	2.0:1
CA910-3110	9.0 - 10.6	25	1.4 MAX, 1.2 TYP	+10 MIN	+20 dBm	2.0:1
CA1315-3110	13.75 - 15.4	25	1.6 MAX, 1.4 TYP	+10 MIN	+20 dBm	2.0:1
CA12-3114	1.35 - 1.85	30	4.0 MAX, 3.0 TYP	+33 MIN	+41 dBm	2.0:1
CA34-6116	3.1 - 3.5	40	4.5 MAX, 3.5 TYP	+35 MIN	+43 dBm	2.0:1
CA56-5114	5.9 - 6.4	30	5.0 MAX, 4.0 TYP	+30 MIN	+40 dBm	2.0:1
CA812-6115	8.0 - 12.0	30	4.5 MAX, 3.5 TYP	+30 MIN	+40 dBm	2.0:1
CA812-6116	8.0 - 12.0	30	5.0 MAX, 4.0 TYP	+33 MIN	+41 dBm	2.0:1
CA1213-7110	12.2 - 13.25	28	6.0 MAX, 5.5 TYP	+33 MIN	+42 dBm	2.0:1
CA1415-7110	14.0 - 15.0	30	5.0 MAX, 4.0 TYP	+30 MIN	+40 dBm	2.0:1
CA1722-4110	17.0 - 22.0	25	3.5 MAX, 2.8 TYP	+21 MIN	+31 dBm	2.0:1

ULTRA-BROADBAND & MULTI-OCTAVE BAND AMPLIFIERS

Model No.	Freq (GHz)	Gain (dB) MIN	Noise Figure (dB)	Power-out @ P1-dB	3rd Order ICP	VSWR
CA0102-3111	0.1-2.0	28	1.6 Max, 1.2 TYP	+10 MIN	+20 dBm	2.0:1
CA0106-3111	0.1-6.0	28	1.9 Max, 1.5 TYP	+10 MIN	+20 dBm	2.0:1
CA0108-3110	0.1-8.0	26	2.2 Max, 1.8 TYP	+10 MIN	+20 dBm	2.0:1
CA0108-4112	0.1-8.0	32	3.0 MAX, 1.8 TYP	+22 MIN	+32 dBm	2.0:1
CA02-3112	0.5-2.0	36	4.5 MAX, 2.5 TYP	+30 MIN	+40 dBm	2.0:1
CA26-3110	2.0-6.0	26	2.0 MAX, 1.5 TYP	+10 MIN	+20 dBm	2.0:1
CA26-4114	2.0-6.0	22	5.0 MAX, 3.5 TYP	+30 MIN	+40 dBm	2.0:1
CA618-4112	6.0-18.0	25	5.0 MAX, 3.5 TYP	+23 MIN	+33 dBm	2.0:1
CA618-6114	6.0-18.0	35	5.0 MAX, 3.5 TYP	+30 MIN	+40 dBm	2.0:1
CA218-4116	2.0-18.0	30	3.5 MAX, 2.8 TYP	+10 MIN	+20 dBm	2.0:1
CA218-4110	2.0-18.0	30	5.0 MAX, 3.5 TYP	+20 MIN	+30 dBm	2.0:1
CA218-4112	2.0-18.0	29	5.0 MAX, 3.5 TYP	+24 MIN	+34 dBm	2.0:1

LIMITING AMPLIFIERS

Model No.	Freq (GHz)	Input Dynamic Range	Output Power Range Psat	Power Flatness dB	VSWR
CLA24-4001	2.0 - 4.0	-28 to +10 dBm	+7 to +11 dBm	+/- 1.5 MAX	2.0:1
CLA26-8001	2.0 - 6.0	-50 to +20 dBm	+14 to +18 dBm	+/- 1.5 MAX	2.0:1
CLA712-5001	7.0 - 12.4	-21 to +10 dBm	+14 to +19 dBm	+/- 1.5 MAX	2.0:1
CLA618-1201	6.0 - 18.0	-50 to +20 dBm	+14 to +19 dBm	+/- 1.5 MAX	2.0:1

AMPLIFIERS WITH INTEGRATED GAIN ATTENUATION

Model No.	Freq (GHz)	Gain (dB) MIN	Noise Figure (dB)	Power-out @ P1-dB	Gain Attenuation Range	VSWR
CA001-2511A	0.025-0.150	21	5.0 MAX, 3.5 TYP	+12 MIN	30 dB MIN	2.0:1
CA05-3110A	0.5-5.5	23	2.5 MAX, 1.5 TYP	+18 MIN	20 dB MIN	2.0:1
CA56-3110A	5.85-6.425	28	2.5 MAX, 1.5 TYP	+16 MIN	22 dB MIN	1.8:1
CA612-4110A	6.0-12.0	24	2.5 MAX, 1.5 TYP	+12 MIN	15 dB MIN	1.9:1
CA1315-4110A	13.75-15.4	25	2.2 MAX, 1.6 TYP	+16 MIN	20 dB MIN	1.8:1
CA1518-4110A	15.0-18.0	30	3.0 MAX, 2.0 TYP	+18 MIN	20 dB MIN	1.85:1

LOW FREQUENCY AMPLIFIERS

Model No.	Freq (GHz)	Gain (dB) MIN	Noise Figure dB	Power-out @ P1-dB	3rd Order ICP	VSWR
CA001-2110	0.01-0.10	18	4.0 MAX, 2.2 TYP	+10 MIN	+20 dBm	2.0:1
CA001-2211	0.04-0.15	24	3.5 MAX, 2.2 TYP	+13 MIN	+23 dBm	2.0:1
CA001-2215	0.04-0.15	23	4.0 MAX, 2.2 TYP	+23 MIN	+33 dBm	2.0:1
CA001-3113	0.01-1.0	28	4.0 MAX, 2.8 TYP	+17 MIN	+27 dBm	2.0:1
CA002-3114	0.01-2.0	27	4.0 MAX, 2.8 TYP	+20 MIN	+30 dBm	2.0:1
CA003-3116	0.01-3.0	18	4.0 MAX, 2.8 TYP	+25 MIN	+35 dBm	2.0:1
CA004-3112	0.01-4.0	32	4.0 MAX, 2.8 TYP	+15 MIN	+25 dBm	2.0:1

CIAO Wireless can easily modify any of its standard models to meet your "exact" requirements at the Catalog Pricing.

Visit our web site at www.ciaowireless.com for our complete product offering.

Ciao Wireless, Inc. 4000 Via Pescador, Camarillo, CA 93012

Tel (805) 389-3224 Fax (805) 389-3629 sales@ciaowireless.com

DARPA Aims to Develop AI, Autonomy Applications Warfighters Can Trust

An important goal of the Defense Advanced Research Projects Agency (DARPA) is developing artificial intelligence (AI) that is trustworthy for the Defense Department (DOD)—particularly for making life-or-death recommendations to warfighters, said Matt Turek, deputy director of DARPA's Information Innovation Office.

"AI, machine learning and autonomy are being used by about 70 percent of DARPA's programs in some form or another," Turek said at a recent Center for Strategic and International Studies event.

Another reason AI development is such a priority is to prevent an unexpected breakthrough in technology, or "strategic surprise," by adversaries who might also be developing advanced capabilities, he said, adding that DARPA also aims to create its own strategic surprise.

To accomplish those goals, DARPA is looking for transformative capabilities and ideas from industry and academia. One of the many ways the agency gets these capabilities and ideas is to hold various types of challenges where teams from the private sector can win prizes worth millions of dollars, he said.

An example of that is DARPA's Artificial Intelligence Cyber Challenge, which uses generative AI technologies, like large language models, to automatically find and fix vulnerabilities in open-source software, particularly software that underlies critical infrastructure. Large language models involve processing and manipulating human language to perform tasks such as secure computer coding, decision-making, speech recognition and making predictions.

Turek said a unique feature of this challenge is the partnership between DARPA and state-of-the-art large language model providers that are participating in the challenges, including Google, Microsoft, OpenAI and Anthropic. Most likely, large language model improvements will also benefit the commercial sector, as well as the DOD. An example of the use of autonomy and of AI that DARPA has been testing with the Air Force involves its F-16 fighter jets.

UAV (Source: U.S. Air Force)

Lower Tier Air and Missile Defense Sensor Detects and Engages Complex Target

Raytheon, an RTX business, recently announced that its Lower Tier Air and Missile Defense Sensor, (LTAMDS) continues to advance through its U.S. Army test program with another successful live fire event. Military leaders from seven nations were on-site to witness the radar's capabilities and performance first-hand.

This was the fourth live fire demonstration for the advanced, 360-degree radar known as LTAMDS. The series of exercises, increasing in complexity, effectively demonstrate the radar's performance and integration with the Integrated Battle Command System (IBCS). For this latest live fire, a cruise missile surrogate was launched, flying at high altitude, high speed and at a long range in an operational environment. LTAMDS acquired and tracked the target, passed track data to IBCS and LTAMDS guided a PAC-3 Missile Segment Enhancement missile to intercept.

"The advanced capabilities of LTAMDS outpace the global threats of today and tomorrow and allied forces are watching its progress intently," said Tom Laliberty, president of Land & Air Defense Systems at Raytheon. "The solid performance of the radar against these complex and realistic threats validates the radar's design and demonstrates how this capability will transform the air and missile defense mission."

LTAMDS (Source: RTX)

The program achieved significant developmental testing milestones in 2023, including the previous air breathing threat and ballistic missile live fires and the completion of CY23 contractor verification testing. Throughout, LTAMDS has met complex test objectives and demonstrated initial technical capability within its primary sector.

Six LTAMDS radars are currently progressing through full sector integration and test activities simultaneously at multiple government and Raytheon test sites. In 2024, rigorous testing will continue, leading up to fielding a 360-degree, full sector capability within the calendar year.

LTAMDS is the next generation air and missile defense radar for the U.S. Army. A 360-degree, active electronically scanned array radar, powered by Raytheon-manufactured GaN, LTAMDS provides dramatically more performance against the range of threats, from manned and unmanned aircraft to cruise missiles, ballistic missiles and hypersonics.

For More Information Visit mwjournal.com for more defense news.

XQ-58A EW Capabilities Demonstrated for USMC

Kratos Defense & Security Solutions, Inc. announced that Kratos Unmanned Systems Division has successfully demonstrated the ability of the XQ-58A to fly in concert with two F-35 aircraft and the ability to deliver an integrated electronic attack (EA) capability on the XQ-58A Valkyrie aircraft during a live flight test event at Eglin Air Force Base, Fla. The demonstration completes the first phase of the U.S. Marine Corps' Penetrating Affordable Autonomous Collaborative Killer – Portfolio (PAACK-P) program. Flight test support was provided by the 40th Flight Test Squadron, 96th Test Wing. All flight test objectives were successfully met.

The demonstration follows the award of a $22.9M "Phase 2" contract modification on December 4, 2023 for additional engineering development and flight test demonstrations, and marks a significant milestone in the PAACK-P program as the Headquarters Marine Corps Aviation Cunningham Group and Advanced Development Team, Marine Corps Warfighting Lab, the Office of the Undersecretary of Defense for Research and Engineering, the Naval Air Systems Command and Naval Air Warfare Center Aircraft Division AIRWorks continue to inform MQ-58B requirements for the Marine Air-Ground Task Force Unmanned Aerial System (UAS) Expeditionary (MUX) Tactical Aircraft for use in a suppression of enemy air defense role.


XQ-58A (Source: Kratos)

The XQ-58A's advanced EA payload autonomously detected, identified, and geolocated multiple tactically relevant targets of interest, transmitted emitter target track coordinates to collaborative assets and successfully presented non-kinetic electronic attack effects against multiple emitters. Flying since 2019, the Kratos XQ-58A Valkyrie is a high performance, runway-independent tactical UAV capable of long-range flights at high subsonic speeds. The Valkyrie can serve as a loyal wingman, conduct single UAS operations or operate in swarms. Combining affordability, survivability, long-range, high subsonic speeds, maneuverability and ability to carry flexible mission kit configurations and mix of lethal weapons from its internal bomb bay and wing stations, the XQ-58A provides unmatched operational flexibility at an affordable price for multiple DOD customers.


Reactel, Inc.
Reacting First to All Your Filter Needs.
Greetings from
WASHINGTON
"THE NATION'S CAPITAL"
Visit Reactel at Booth #814 at IMS2024 in Washington, DC and CAPITALIZE on over 45 years of filter-based engineering experience.
Reactel is the recognized source of filters, multiplexers and multifunction assemblies from DC to 67 GHz and offers solutions to your most challenging requirements.
I GOT PANTSED
DC
'24
AT IMS 2024
Get Pantsed at the Reactel Booth
Visit Booth #814, and Get Pantsed at IMS! Stop in for your photo-op in the famous Maryland Filter Guy's Pants! Enter our photo contest for a grand prize, but every visitor is a winner with giveaways, treats and more!
8031 Cessna Avenue • Gaithersburg, Maryland 20879 • (301) 519-3660 • reactel@reactel.com • reactel.com
Intertek
RoHS
RoHS Compliant
2002/95/EC
MADE IN MD
Since 1979

DC TO 50 GHz

MMIC Amplifiers

300+ Models Designed in House

Options for Every Requirement

CATV (75Ω)

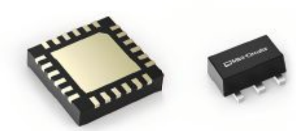

Supporting DOCSIS® 3.1 and 4.0 requirements

Dual Matched

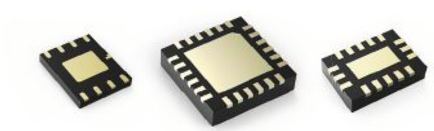

Save space in balanced and push-pull configurations

Hi-Rel

Rugged ceramic package meets MIL requirements for harsh operating conditions

High Linearity

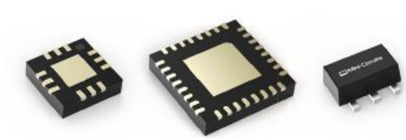

High dynamic range over wide bandwidths up to 45 GHz

Low Noise

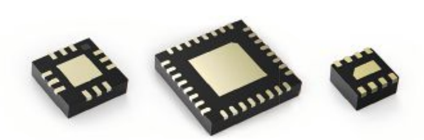

NF as low as 0.38 dB for sensitive receiver applications

Low Additive Phase Noise

As low as -173 dBc/Hz @ 10 kHz offset

RF Transistors

<1 dB NF with footprints as small as 1.18 x 1.42mm

Variable Gain

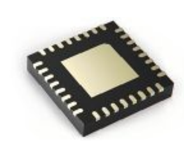

Up to 31.5 dB digital gain control

Wideband Gain Blocks

Flat gain for broadband and multi-band use

Mini-Circuits®

Global 5G Connections Surge to 1.76B, 66 Percent Growth YoY as North America Leads Charge

The wireless telecommunications industry witnessed a year of unprecedented growth and innovation, propelled by the unstoppable momentum of 5G technology. In 2023, adoption of 5G connections accelerated, reaching 1.76 billion globally by adding 700 million, according to 5G Americas and data from Omdia.

Chris Pearson, president of 5G Americas said, "The wireless telecommunications industry stands at the cusp of a new era, driven by innovation, collaboration and a shared vision for a connected future. With fixed wireless access continuing to drive consumer broadband demand, new technology milestones are advancing unparalleled connectivity experiences worldwide."

North America emerged as a trailblazer in 5G adoption, with connections in the region comprising 29 percent of all North American connections by the end of 2023. Notably, the region experienced a staggering 64 percent YoY growth in 5G connections, adding 77 million new connections to its network. By the end of 2023, North American 5G connections totaled 197 million.

Latin America also witnessed substantial progress in both 4G LTE and 5G connections, with LTE connections reaching 582 million by the close of 2023, adding 40 million new connections YoY. Moreover, the region embraced the 5G revolution, with 39 million 5G connections established by year-end, setting the stage for further expansion in the years to come.

Looking ahead, Omdia forecasts paint a picture of the telecommunications landscape we can expect to see throughout this decade. Global 5G connections are projected to skyrocket to 7.9 billion by 2028, with North America forecasted to boast an impressive 700 million 5G connections by the same year.

5G data traffic is expected to be 76 percent of all technology data traffic as it reaches a staggering 2.6 billion TB (or 2600 EB), with all technology data traffic reaching 3.4 billion TB (or 3400 EB) by 2028, reflecting the exponential growth trajectory of 5G connectivity.

While 5G technology continues to dominate headlines, the IoT ecosystem remains a vital component of the digital revolution. Currently, global IoT subscriptions stand at 3.1 billion, complemented by 6.6 billion smartphone subscriptions. Forecasts suggest that IoT subscriptions will reach 4.5 billion, while smartphone subscriptions will surge to 7.4 billion by 2026, highlighting the evolving nature of connectivity and the interconnectedness of our digital world.

Globally, the number of deployed 5G networks shows strength compared to 4G LTE deployments, and in the case of North America, almost matches 4G LTE networks deployed. Currently, there are 314 commercial 5G networks worldwide, and this number is anticipated to grow to 450 by 2025, reflecting significant investments in 5G infrastructure worldwide.

AiP Market Dynamics: Drivers and Challenges in 5G and 6G

Antenna-in-package (AiP) technology is essential for high frequency telecommunications, as it enables the integration of antennas with RF components directly into semiconductor packages, unlike traditional discrete antennas. This advancement, tailored for mmWave applications and potentially extending into the sub-THz spectrum for 6G, promises much smaller footprints and enhanced performance.

AiP technology continues to evolve as it drives toward higher frequencies. Design choices regarding types of antenna elements, substrate technology, materials and integration of passive devices are pivotal. Furthermore, the maturity of the supply chain and the manufacturing scalability are two key areas that should not be overlooked. These two factors frequently act as a bottleneck for the adoption of new technologies, given their correlation with the final product cost. Achieving affordability involves using cost-effective packaging materials and processes, along with miniaturization for seamless integration into consumer devices such as smartphones.

Achieving high performance requires the fabrication and integration of high gain, broadband mmWave antenna arrays, along with ensuring intra-system electromagnetic compatibility. Optimizing equivalent isotropic radiated power and ensuring signal and power integrity are crucial aspects as well. Integrating high-quality factor passives to co-design active mmWave front-end transceiver components further enhances performance, while reliability necessitates direct thermal passage from the chip to the exterior to dissipate heat from power amplifiers.

Scalability adds another layer of versatility, enabling the design of basic modules that can be upscaled to meet various applications with different power requirements. Addressing all these requirements is essential when designing an AiP module for high frequency communication devices.

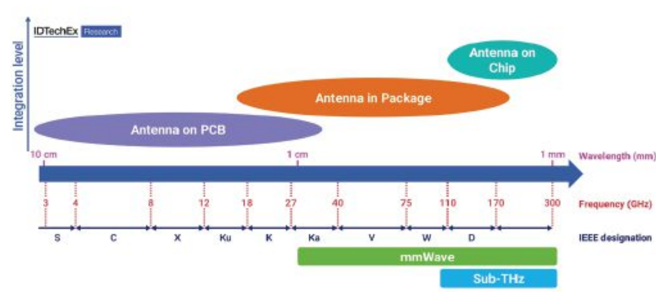

AiP (Source: IDTechEx)

For More Information Visit mwjournal.com for more commercial market news.

The AiP market is directly linked to the 5G mmWave and future 6G markets, as AiP is expected to be used in all 5G mmWave-based stations and 5G-enabled electronics like smartphones. While 5G technology is progressively being commercialized worldwide, the primary focus remains on mid-band (sub-6 GHz) deployments. IDTechEx reports that less than 10 percent of commercialized or pre-commercialized 5G services as of now are based on the mmWave frequency band. This is partly due to the challenges faced by mmWave deployment, as higher frequency signals are prone to attenuation in the air and are highly susceptible to obstacles in accordance with the laws of physics.

Telco operators prioritize creating cost-effective networks by maximizing coverage with minimal base stations. However, due to the shorter propagation distances of mmWave, approximately 10x more mmWave stations are required compared to 4G low/mid-band stations to cover the same area. As a result, national 5G coverage predominantly relies on low/mid-band and sub-6 GHz bands. IDTechEx anticipates that mmWave bands will mainly serve data-intensive hotspots like crowded stadiums, supporting critical applications such as streaming and uploading of high-definition videos.

Looking ahead, 6G, the next generation of telecommunication technology, promises even greater advancements than 5G mmWave. Operating beyond 100 GHz and toward the THz spectrum, 6G is expected to offer Tbps data rates, microsecond-level latency and extensive network dependability. Its capabilities extend beyond connectivity to areas such as energy harvesting, sensing, imaging and precise positioning. However, 6G will face greater challenges compared to 5G mmWave in both technology development and market penetration, given its even higher frequencies. Overcoming these hurdles will necessitate the development of innovative technological solutions, including advancements in packaging technologies for antennas to minimize signal transmission issues. Additionally, there is a crucial need for stronger market identification of future applications to drive the adoption of 6G technologies. This entails not only identifying killer applications but also fostering the ecosystem necessary for their successful implementation.

IDTechEx's market report, "Antenna-in-Package (AiP) for 5G and 6G 2024-2034: Technologies, Trends, Markets," delves into AiP technologies for 5G mmWave and 6G, focusing on various substrate types and packaging methods. It also explores antenna integration for beyond 100 GHz applications, showcasing case studies and addressing challenges. Drawing on IDTechEx's expertise, the report offers valuable insights into the evolving landscape of antenna packaging for future generations of wireless technology.

Nxbeam™

Ka / V / E - Band GaN MMIC Power

Ka

- NPA2001-DE | 26.5-29.5 GHz | 35 W
- NPA2002-DE | 27.0-30.0 GHz | 35 W
- NPA2003-DE | 27.5-31.0 GHz | 35 W
- NPA2004-DE | 25.0-28.5 GHz | 35 W
- NPA2020-DE | 24.0-25.0 GHz | 8 W
- NPA2030-DE | 27.5-31.0 GHz | 20 W
- NPA2040-DE | 27.5-31.0 GHz | 10 W

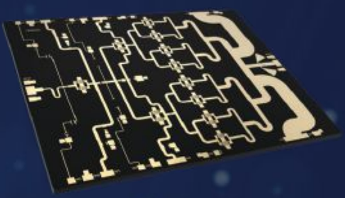

V

- NPA4000-DE | 47.0-52.0 GHz | 1.5 W
- NPA4010-DE | 47.0-52.0 GHz | 3.5 W

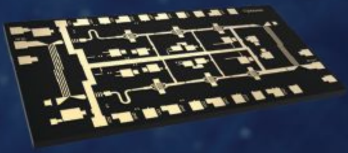

E

- NPA7000-DE | 65.0-76.0 GHz | 1 W
- NPA7010-DE | 71.0-76.0 GHz | 4 W*

* In Fabrication

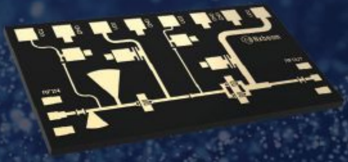

4388 Cerritos Avenue
Los Alamitos, CA 90720

www.nxbeam.com
info@nxbeam.com

Phone: 949-656-2883
info@nxbeam.com

Around the **Circuit**

Barbara Walsh, Multimedia Staff Editor

MERGERS & ACQUISITIONS

STI-CO® Industries LLC, a provider of RF antenna solutions, announced a strategic merger with **Communication Power Companies (CPC)**, an Addison Capital Partners portfolio company. CPC designs custom broadband power amplifiers for the defense and medical markets. STI-CO is a renowned antenna, filter and custom cable design company serving the defense, rail, homeland security and transportation markets.

GaAs Labs LLC announced the sale of its portfolio company, **Mission Microwave Technologies LLC**, a provider of GaN-based solid state power amplifiers and block up-converters, to the satellite communications market to an affiliate of **J.F. Lehman Company (JFLCO**). The long-standing partnership between industry veterans John and Susan Ocampo of GaAs Labs and the Mission team saw the company grow significantly as it expanded its portfolio of microwave and mmWave products to support critical ground-based, airborne, maritime and space-based applications for government and commercial customers. Utilizing its unique power combining technology and integrated systems design, Mission provides the industry's most efficient, lightweight and compact high-power systems.

Infinite Electronics, a global portfolio of leading in-stock connectivity solution brands, announced that it has signed a definitive agreement to sell its **KP Performance Antennas and RadioWaves** businesses to **Alive Telecommunications**, a global supplier of communications equipment, systems and services. The transaction was scheduled to close approximately on April 1, 2024.

VIAVI Solutions and **Spirent Communications plc**, a global provider of automated test and assurance solutions for networks, cybersecurity and positioning, announced an agreement on the terms of a cash offer for Spirent, which the Spirent board intends to unanimously recommend. Under the terms of the acquisition, Spirent Shareholders will receive 172.5 pence per Spirent share in cash (the acquisition price). Spirent Shareholders will also receive a special dividend of 2.5 pence per Spirent share in lieu of a final dividend for the year, which ended December 31, 2023.

COLLABORATIONS

Ansys announced a collaboration with **NVIDIA** to develop next-generation simulation solutions powered by accelerated computing and generative AI. The expanded collaboration will fuse cutting-edge technologies to advance 6G technologies, supercharge Ansys solvers via NVIDIA GPUs, integrate NVIDIA AI into Ansys software offerings, develop physics-based digital twins and customize large language models developed with NVIDIA AI foundry services. Ansys recently joined the AOUSD to strengthen data interoperability and deliver enhanced graphics and visual rendering to its portfolio. Ansys has already connected Ansys AVxcelerate Autonomy™ to NVIDIA DRIVE Sim, powered by the NVIDIA Omniverse platform, and plans to investigate additional integrations across the portfolio.

Mercury Mission Systems International SA announced that it will advance the manufacturing of defense technologies in Switzerland in collaboration with **Lockheed Martin**. This project is a direct result of the offset program between Lockheed Martin and the Swiss government as part of Switzerland's purchase of the F-35 Lightning II. Under two initial engineering development agreements, Mercury will begin manufacturing several embedded computing technologies at its production facility in Geneva.

Telesat and **ThinKom Solutions Inc.** announced an expanded development partnership to certify ThinKom's ThinAir® Ka2517 antenna for the Telesat Lightspeed low earth orbit (LEO) satellite network. The multi-year agreement calls for the organizations to cooperate on the integration and certification of the Ka2517 antenna with an airborne modem to enable communications across the Telesat Lightspeed Ka-Band LEO network. Telesat estimates that its enterprise-class constellation, paired with the Ka2517 antenna, will deliver over 1 Gbps to the aircraft. Telesat Lightspeed can dynamically allocate multiple Gbps of capacity to areas with high demand.

Teramount announced that it is collaborating with **GlobalFoundries (GF)** to address the challenge of connecting fibers to Silicon Photonics (SiPh) chips, to meet the ever-growing bandwidth demands and power challenges in datacom and telecom applications. As part of this collaboration, Teramount integrates its Universal Photonic Coupler solution with GF's 45CLO SiPh platform, GF Fotonix™, to provide a scalable fiber packaging solution to customers who want to utilize high speed optical connectivity for applications like AI/ML and data centers. This collaboration will enable deeper integration of optics into semiconductors through a variety of innovative packaging technologies which provide scalability of bandwidth, power and latency performance to future generations of advanced computing applications.

ACHIEVEMENTS

Analog Devices Inc. announced **U.S. Food and Drug Administration (FDA)** 510(k) clearance and the commercial launch of the Sensinel™ Cardiopulmonary Management (CPM) System. The compact, wearable device is a non-invasive, remote management system that captures cardiopulmonary measurements for chronic disease management, such as heart failure. It is the first FDA clearance the company has received in its 59-year

For More Information For up-to-date news briefs, visit mwjournal.com

history. More than 6 million Americans are living with heart failure today, and this number is estimated to rise to nearly 8 million by 2030. Heart failure currently costs Americans approximately $30 billion each year, and this is expected to rise to almost $70 billion by 2030.

Hughes Network Systems LLC announced that the **Republican Center of Space Communication (RCSC)**, a subsidiary of the Ministry of Digital Development, has chosen the Hughes JUPITER™ System ground platform to help close the digital divide in Kazakhstan. Hughes will supply JUPITER System equipment to more than 200 villages throughout the country, helping communities access broadband internet connectivity and e-government services through the Digital Kazakhstan program. The contract will be fulfilled through TIMIR LLP.

Flat panel satellite antenna company **Kymeta** announced the **U.S. Patent and Trademark Office** awarded Kymeta Corporation two U.S. patents. The first patent is related to the cooperation of a SD-WAN edge appliance and a satellite terminal, enabling users to engage in concurrent or switched satellite and cellular communications. The second patent is related to an electronically-steered array antenna operating across multiple satellite networks in multiple modes (e.g., concurrent mode, switched mode, etc.). These achievements demonstrate Kymeta's continued thought leadership in the marketplace as the satellite communications industry evolves into a multi-orbit, multi-network ecosystem.

CONTRACTS

Raytheon, an RTX business, was awarded a $1.2 billion contract to supply Germany with Patriot® air and missile defense systems. These new Patriot systems will augment Germany's existing air defense infrastructure. The scope of the contract includes the most current Patriot Configuration 3+ radars, launchers, command and control stations, associated spares and support. Patriot is the backbone of air defense for 19 countries, including Germany, the U.S. and Ukraine. The formidable, combat-proven performance of Patriot continues to demonstrate its effectiveness against the most advanced and complex threats.

Boeing received a $439.6 million contract to build the 12th Wideband Global SATCOM (WGS) communications satellite for **U.S. Space Force's Space Systems Command**. The WGS constellation delivers vital high-capacity, secure and resilient communications capabilities to the U.S. military and its allies. The WGS's responsive, steerable, high-capacity beams provide assured connectivity via the Protected Tactical Enterprise Service ground system and enhanced anti-jam communications by combining the U.S. military's jam-resistant Protected Tactical Waveform with antenna nulling in the Ka-Band.

Sivers Semiconductors AB announced that its subsidiary **Sivers Wireless** has signed a third product devel-

opment agreement with its lead **European Satellite Company**. This new contract, valued at USD $4,73 million, covers the development of next-generation, production-ready beamformer chipsets during 2024 and 2025. The agreement is expected to move to volume manufacturing in Q4 2025. These beamformers are advanced versions, with new features and capabilities, of the existing beamformers that were originally developed for this customer as a part of the first development agreement signed in December 2020 and are in mass production today.

PEOPLE

▲ *Rachel Pyles*

Ansys announced that finance veteran **Rachel Pyles** became the company's new chief financial officer. Pyles replaced Nicole Anasenes, who previously announced her planned departure from Ansys to focus on advisory and board work. Anasenes will remain with the company as a strategic adviser until June 2024 to ensure a smooth transition. Pyles joined Ansys in early 2023 as the vice president of strategic finance, running financial planning and analysis for the company. Prior to Ansys, she served in a number of finance, transformation and leadership roles at FIS, Worldpay and Vantiv.

REP APPOINTMENTS

EZ Form Cable announced the establishment of key partnerships with renowned manufacturing rep organizations, **Summit Technical Sales** for the Northern California territory and **Staffco** for the Midwest territory. These strategic alliances aim to bolster market presence for the full range of EZ Form Cable products across designated territories. The agreements solidify EZ Form Cable's commitment to delivering innovative cable solutions while expanding its footprint in the industry.

Richardson Electronics Ltd. announced a global distribution agreement with **Ideal Power** for products including the discrete B-TRAN™ device and SymCool™ power module. Ideal Power is pioneering the development and commercialization of the highly efficient and broadly patented B-TRAN™ bidirectional semiconductor power switch. Ideal Power utilizes an asset-light business model, leveraging the large investment already made in silicon processing, distribution, demand creation and support infrastructure. This business model allows the company to focus on further developing its disruptive B-TRAN™ technology while minimizing capital requirements.

INVITED PAPER

Waste Figure and Waste Factor: New Metrics for Evaluating Power Efficiency in Any Circuit or Cascade

Theodore (Ted) S. Rappaport, Mingjun Ying and Dipankar Shakya
NYU WIRELESS, Tandon School of Engineering, New York University, Brooklyn, N.Y.

Today, there is a great need for ensuring the energy-efficient design of circuits and systems, yet the electrical engineering field has lacked a clear, well-defined, unified key performance indicator (KPI) for quantifying the power efficiency of any device or cascade of devices or systems. The industry has such a metric for quantifying additive noise along a cascade and this is known as the noise factor (F) or noise figure (NF) when expressed in dB. This standardized approach to quantifying additive noise now dons the specification sheets of virtually all receiving devices or receivers and is used as a key figure of merit (FoM) in the research and design communities when creating new devices or exploring system concepts.

This article develops a FoM for the comparison of wasted power along a cascade. This new FoM, called the power waste factor, or simply the *waste factor* (W) or the *waste figure* (WF) expressed in dB, is derived using a similar mathematical modeling approach taken by Harald Friis in 1944 to create noise figure. This article will show that the waste figure is a useful FoM for comparing and contrasting the power efficiency of any circuit or cascade of circuits or systems. Just as noise figure characterizes the additive noise of a cascade, waste figure characterizes the additive wasted power along a cascade. Waste figure is a handy metric to determine and compare consumed power along a cascade and is useful in identifying design choices that optimize power consumption while providing a measure of the power efficiency of any circuit or cascade. In an era where energy efficiency is more important than ever, the waste factor and waste figure are new metrics for accomplishing power-efficient circuits and system designs. The waste factor (W), also called waste figure (WF) defined as WF (dB) = 10 log (W), merely requires knowledge of the device efficiency and device gain. Following the mathematical modeling approach taken by Harald Friis where he developed noise figure,[1] this article offers a standardized framework for evaluating power consumption in any wired or wireless device, system or network. This framework may have utility in standards bodies to reduce global power consumption.

The waste figure provides a simple analytical formulation and mathematical model for the additive power wasted along virtually any cascade. As shown here, W enables extremely general analysis, with application to circuits, transceivers, channels and

data centers. Virtually anything that forms a cascade of devices or systems for information flow may be characterized and quantified by W. Using the mathematical formulation of W in circuit and system analysis, it becomes possible to characterize specific power efficiency performance levels while gaining insight into design approaches that assure minimal power consumption. Furthermore, W allows a standardized way to interpret and analyze power consumption in any device or cascade, making it a powerful analysis tool as well as the basis of a learning model for artificial intelligence (AI) and machine learning (ML) design and control for optimized power efficiency. While some authors have recently applied the waste figure to analyze the power efficiency and to make design tradeoffs in unmanned aerial vehicle (UAV) cellular infrastructure systems,[2] millimeter wave wireless network[3] phase shifters in sub-THz phased arrays and data centers,[4] the waste figure remains relatively unknown and undiscovered. However, it offers a standard FoM for evaluating the power efficiency of any circuit or cascade.

This paper introduces the mathematical derivation of the waste figure and shows that its mathematical basis is strikingly similar to noise figure. The definition of waste figure is a simple and powerful metric based on the efficiency (η) and gain (G) of the various elements of a cascade. While the power efficiency may be referred to either the input or output signal power of the cascade, it is most sensible to consider the waste factor as related to the signal output power of a device or cascade, $P_{signal,out}$. The result of the waste figure for a cascade will be derived and it will be shown that the mathematical expressions for the waste figure of a cascaded system have a nearly identical form to Friis' original noise figure expression. The canonical results when deriving the waste figure for a passive load will be shown, which yields mathematically similar results as compared to the noise figure as well as key results when using W to analyze the power efficiency of a transmitter (TX)-receiver (RX) link with a lossy channel as part of the cascade. It will be shown that the waste figure may be used in circuit design to indicate the most power-efficient cascades while illuminating the most critical components that dominate power consumption and thus energy efficiency.

As shown subsequently, waste factor denotes the *total power consumed by a circuit or cascade*, divided by the *signal power out of the circuit or cascade*, and represents a new way to consider wasted power or power efficiency along a cascade. By definition, W is always greater than or equal to 1, where W=1 (WF=0 dB) denotes an optimally power-efficient circuit or cascade, where all the power consumed by the circuit or cascade is found to be in the usable signal output power. Conversely, if W equals infinity, it means there is no power output delivered from the cascade while power is being consumed (e.g., a dummy load). The article shows that waste factor is the inverse of power efficiency in standard passive circuit theory and the inverse of the original definition of total power added efficiency (PAE) for DC-powered amplifiers.[12] The waste factor may be used to readily quantify the total wasted power and efficiency of a cascade of matched, linear devices.

Examples will be shown to illustrate how waste figure can characterize the power efficiency of various types of cascades, including a cascade of a TX, a propagation channel and a RX, a homodyne transmitter, and even a data center (we show here how W offers improvement over a popular data center power efficiency metric). These examples allow engineers to make simple approximations regarding the impact and placement of power-efficient components in a radio network operating in a lossy channel. The virtue of using W is that a standard metric may now be used to demonstrate intuitive design choices. This will allow engineers to conduct power efficiency studies on a circuit or cascade, or any type of source-to-sink link.

FUNDAMENTALS OF NOISE FIGURE (NF) AND WASTE FIGURE (WF)

This section shows the duality between the derivations of noise figure (NF) and waste figure (WF), which are used to evaluate additive noise and additive wasted power in any circuit or cascade, respectively.

Noise Factor (F): Quantifying Additive Noise in Cascades

Noise factor (F) defines the additive noise along a cascade which causes degradation of SNR along the cascade. The noise factor, F, was defined by Harald Friis in 1944[1] as the ratio of the input SNR to output SNR, where $F=SNR_i/SNR_o$. When F is expressed in dB terms, it is referred to as the noise figure, where a value of 0 dB indicates that no added noise and no degradation in SNR occurs along a device or a cascade of devices. Friis' formula is widely used to calculate the overall F of cascaded devices, where each device has its own individual F and power gain, G. Once the total F is calculated for a cascade, it can be used to determine the overall noise power contribution of the entire cascade.

Friis was interested in modeling how the input noise level would be amplified and intensified in a receiver and created a mathematical model that considered the additional noise power contributed by components moving from the source (input) to the sink (detector). He was aware that there existed a nominal input thermal noise level to the cascade of *kTB* that could be measured as well as an output noise level that could be measured. Thermal white noise power is defined by: $N=kTB$, where *N* is the noise power available at the output of a thermal noise source, $k=1.380\times 10^{-23}$ J/K is Boltzmann's constant, *T* is the temperature in Kelvin and *B* is the noise bandwidth in Hz. At the input of a cascade, Friis was able to turn a signal on and off that could be added to the noise and detected at the output of the cascade. In this manner, he was able to adjust and measure the SNR at the input to the cascade relative to the output of the cascade. Since he had control of the cascade input signal power level and could measure the noise power at the output of the cascade relative to the signal and noise powers at the input, he defined noise figure relative to the input noise power of the cascade as shown in ***Equation 1***:

$$F = N_o/GN_i \tag{1}$$

From Equation 1, F for a cascaded system with matched loads is given by **Equation 2**, where the first component F_1 is closest to the source, (e.g., the antenna or front-end of a RX). Friis found Equation 2 simply by systematically applying Equation 1 at each successive stage in a cascade realizing that each component had output noise N_o which included an additive noise component related to F.

$$F = F_1 + \frac{(F_2 - 1)}{G_1} + \frac{(F_3 - 1)}{G_1 G_2} + \cdots + \frac{(F_N - 1)}{\Pi_{i=1}^{N-1} G_i} \tag{2}$$

In Equation 2, F_i represents the noise factor of the i_{th} device and

$$G_i = \frac{Output\ Power(P_{out})}{Input\ Power(P_{in})}$$

represents the power gain of the i_{th} device (linear, not in dB). For a given noise input power, N_i and noise output power, N_o, Friis showed that F (defined in Equation 1) was directly related to the additive noise contributed by the device or cascade alone as defined in **Equation 3**:

$$P_{additive-noise} = N_o - GN_i = FGN_i - GN_i$$
$$= (F-1)GN_i\,(\text{Watts}) \tag{3}$$

From Equation 3, it is clear that $(F-1)GN_i$ represents the additive noise power contributed by the component or cascade, above and beyond the input noise power and as referred to the input. F = 1 (0 dB) means there is no additional noise power contributed by the cascade other than what was applied to the input and then amplified with ideal noiseless amplifiers.

Waste Factor (W): A New Metric for the Analysis and Comparison of Power Efficiency

Waste factor (W) or waste figure (WF in dB) characterizes the power efficiency of a cascaded system by modeling the power wasted (e.g., power consumed but not delivered as output power) in each of the components along a cascade. Like the mathematical modeling method used by Friis to derive noise figure, the power wasted by a device or cascade may be analyzed by modeling the progressive useful signal power transferred along a cascade relative to the total power consumed by the components of the cascade. The derivation of the waste figure assumes that all power that is not transferred along the cascade as signal output is simply "wasted power" since such wasted power is not being passed along the cascade to the next stage as a useful signal.

This is a new way of defining power efficiency. In this way, it becomes clear that instead of additive noise being accumulated at each stage of a cascade as in noise figure, the amount of wasted power (e.g., power not delivered in the signal to the successive stage) from each of the components accumulates from the input to the output. Since it is easy and customary to measure the power consumption of an entire cascade of devices (e.g., the total power consumed by a system) and also easy to measure the signal power at the output in watts (e.g., $P_{out} = GP_{in}$), the waste factor is defined relative to the output of a device or cascade and is given by

Equation 4:

$$W = \frac{1}{\eta_w} = \frac{P_{consumed}}{P_{out}} = \frac{P_{non-signal} + P_{out}}{P_{out}} \quad (4)$$

Where:

η_w = *waste factor efficiency* and it equals 1/W

$P_{consumed}$ = total power consumed by the device or cascade

P_{out} = output signal power

$P_{non\text{-}signal}$ = total consumed power minus the signal power delivered to the output, which is the wasted power of the device.

As mentioned previously, the waste factor for an active component is the inverse of the total PAE, a key metric for assessing power amplifier efficiency as shown by A. A. Sweet.[12] The original PAE metric quantifies how effectively an RF amplifier with a DC power supply transforms the total consumed power, encompassing both the DC power supply and RF input power, into RF output power and is defined as[12]

$$PAE^{\#1} = \frac{P_{out}}{P_{consumed}} = \frac{P_{RF,out}}{(P_{DC} + P_{RF,in})}$$

Inspection of Equation 4 (also see Equation 11) shows $PAE^{\#1}$ is identical to the reciprocal of W. In 1993, Walker[13] introduced a second definition of PAE, given as

$$PAE^{\#2} = \frac{P_{RF,out} - P_{RF,in}}{P_{DC}}$$

which is now widely regarded as the industry standard for evaluating the efficiency of RF power amplifiers. It is easy to show from Equation 4 that W is related to $PAE^{\#2}$ such that

$$W = \frac{1}{PAE^{\#2}}\left[\left(1 + \frac{P_{RF,in}}{P_{DC}}\right)\left(1 - \frac{1}{G}\right)\right]$$

which is nearly identical to $PAE^{\#1}$ when gain is large.

Similar to how Friis defined noise figure as NF = $10\log_{10}$(F) (dB), the waste figure is defined as WF = $10\log_{10}$(W) (dB). It was shown[3,4,7,14] and derived previously that the waste factor of a cascade is expressed as ***Equation 5***:

$$W = \left(W_N + \frac{(W_{N-1} - 1)}{G_N} + \frac{(W_{N-2} - 1)}{G_N G_{N-1}} + \dots + \frac{(W_1 - 1)}{\Pi_{i=2}^{N} G_i} \right) \quad (5)$$

In Equation 5, W_i represents the waste factor of the i_{th} device and

$$G_i = \frac{Output\ Power(P_{out})}{Input\ Power(P_{in})}$$

represents the power gain of the i_{th} device (linear, not in dB) and the N_{th} device is the closest device to the information sink (e.g., the output of the cascade). Note the mathematical similarity between Equation 2 and Equation 5, except Equation 2 increases from source to sink and Equation 5 increases from sink to source.

For a given signal input power to a cascade, P_{in}, and cascade signal output power, P_{out}, W is a FoM that represents a measure of total additive power that is wasted (e.g., not part of the delivered signal power) at the output of a cascade. W quantifies the amount of consumed power that is wasted (e.g., consumed power that is not found in the output signal power) relative to the total signal power delivered at the output of the cascade, independent of the signal power applied at the input of the cascade (see Equations 8 and Equation 9). Thus, W defines a relationship between added wasted power of a device or cascade, vis à vis the delivered signal power in a similar way that Friis defined in Equation 3. This is shown in ***Equation 6***:

$$P_{wasted} = WP_{out} - GP_{in} = (W-1)GP_{in} = (W-1)P_{out}\,(Watts) \quad (6)$$

From Equation 6, it is clear that $(W - 1)P_{out}$ represents the total additive wasted power contributed by a component or by all the components within the cascade and is conveniently referred to the output. W=1 (0 dB) means there is no wasted power contributed by a component or by the cascade and the cascade has perfect 100 percent efficiency with all the power consumed by the cascade found in the output signal power. Similarly, W = infinity means all the power is wasted in the cascade, with no output signal power. Such formulation provides an intuitive way to understand power waste at each stage of the cascade and allows engineers to use W to compare the power efficiency of different devices and systems in a new way, just as noise figure did for noise analysis 80 years ago.

WASTE FACTOR DERIVATION: SUPERPOSITION FOR POWER CONSUMPTION

The mathematical basis of waste factor and waste figure was derived originally by Murdock and Rappaport[5,6,7,14] by noting that the power consumption of any device in a circuit or system may be decomposed into four distinct power consumption components which may be summed together to determine the total consumed power of any device or network. The four power components include (i) the signal path power delivered to the output by a device on the signal path within a circuit or cascade (e.g., the output signal power that is delivered to the sink), (ii) the power consumed by a device which is on the signal path (e.g., a component on the cascade), but which is not provided in the output signal path (this is called the additive "wasted" power of a component, since as described previously, the component is on the cascade but such power is not delivered to the output signal of the device), (iii) all other power that is consumed by components that are not on the signal path or which are not associated with a device on the signal-path cascade and (iv) the signal power delivered to the input of the device

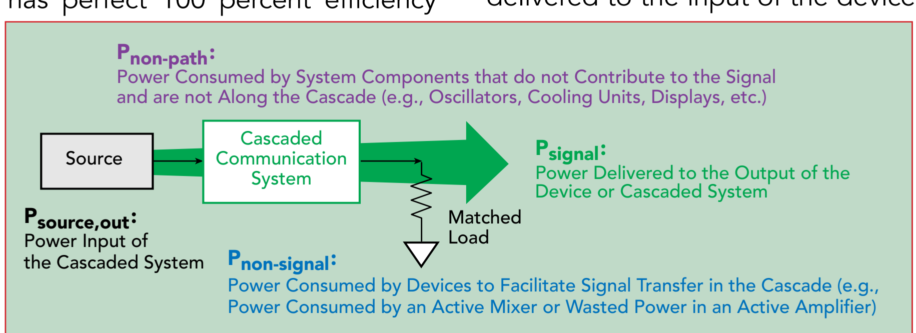

Fig. 1 Power decomposition of a cascaded communication system or device.[5-7]

TABLE 1

SUPERPOSITION OF POWER SOURCES IN ELECTRONIC NETWORK SYSTEMS

Type	Symbol	Description
Signal output power	P_{signal}	Power of signal delivered to the device/cascade output (e.g., power amplifier output delivered to a matched load).
Non-signal path power	$P_{non\text{-}signal}$	Power consumed by a device or circuit on the cascade path to facilitate signal transfer in the cascade (e.g., wasted power drawn by an active amplifier on the signal path).
Non-path power	$P_{non\text{-}path}$	Power consumption of components that do not contribute to the signal and are not along the signal path cascade (e.g., oscillators, displays, cooling elements, etc.).
Source power (Input signal power)	$P_{source,out}$	Power of the signal that comes from the output of the source and which is the input power signal of the device or cascaded communication system. At each step, this power coming in from the source is multiplied by the gain of the stages, yielding the signal power output, P_{signal}.

or cascade by a source that is connected to the input. ***Figure 1*** and ***Table 1*** describe the four types of power that make up any circuit or system.

The non-path powers are not considered in the derivation of waste figure since these components are not found in a cascade along a signal path, just as noise figure does not consider non-path components as noise contributors. However, the *total power consumption* of both the signal path and non-path components is easily found using W and the power components of Table 1 using upcoming Equation 9. While waste figure characterizes a device or cascade on a signal path, the basic principles of power superposition and waste factor may be useful in analyzing non-path wasted power and power consumption using similar mathematical models and new figures of merit. It may be that non-path powers include the quiescent power drain of cascaded components that are in a sleep/off state or for the case when impedances are high-Z or greatly mismatched. This remains an open area for definition and usage.

In the development of noise figure, the output power of the input source was due to thermal noise at the receiver input. For waste figure, the output power of a signal source is the signal input power to the cascade or device. When considering the four power sources of Table 1, it becomes clear that for any cascade or device along the signal path, which will be called a "system," the *total power consumed* by *just the system* carrying the signal ($P_{consumed}$), is equal to the total power consumed by the system, including the input signal power, minus the input signal power to the system, in order to refer W to the output of the system alone, regardless of input signal levels (assuming linearity). This is expressed in ***Equation 7***:

$$P_{consumed} - P_{source,out} = P_{system-added} + P_{non-signal} \quad (7)$$

where $P_{system\text{-}added}$ is the signal power added by the

system and the signal output power of the system is $P_{signal} = P_{source,out} + P_{system\text{-}added}$. From Equation 7, the total power consumption of the system along the signal path, independent of the input signal power, $P_{source,out}$, is given by the superposition of Equation 7 and is shown in ***Equation 8***:

$$\begin{aligned} P_{consumed} &= P_{system-added} + P_{non-signal} + P_{source,out} \\ &= P_{signal} - P_{source,out} + P_{non-signal} + P_{source,out} \\ &= P_{signal} + P_{non-signal} \\ &= P_{signal} W \end{aligned} \tag{8}$$

The use of W in Equation 6 and Equation 8 provides a convenient method to compute the total and wasted power consumed by a device or cascade. Using Equation 8 and then by including the non-path powers, $P_{non\text{-}path}$, contributed by all components that are off the signal cascade (such as displays, heat sinks, power supplies, etc.), the total power consumption of any system may be found as shown in ***Equation 9*** using superposition of all power types in Table 1:[7,14]

$$\begin{aligned} P_{consumed,total} &= P_{signal} + P_{non-signal} + P_{non-path} \\ &= P_{signal} W + P_{non-path} \end{aligned} \tag{9}$$

The only factors that must be known for every device on the signal path along the chain of a cascaded network are gain and efficiency. Gain has the standard definition for the signal path components in the cascade that carry information to later stages of the cascade and the efficiency is defined as the reciprocal of the waste factor (W) in Equation 4. These two formulations are shown in ***Equation 10***:

$$\begin{cases} Gain(G) = \dfrac{Output\ Power(P_{out})}{Input\ Power(P_{in})} \\ WF_{efficiency}(\eta_w) = \dfrac{1}{W} = \dfrac{P_{signal}}{P_{consumed}} \\ \qquad = \dfrac{P_{signal}}{P_{signal} + P_{non-signal}} \end{cases} \tag{10}$$

As noted earlier, the waste factor efficiency, η_w, as defined in Equation 4 and Equation 10, is the reciprocal of W. For passive devices, $1/W = \eta_w$ is identical to the traditional definition of efficiency when relating output power to input power $\left(\eta = \frac{\text{Power Output}}{\text{Power Input}}\right)$.

In the special case of active components powered by a DC source, W is equal to

$$\frac{P_{DC} + P_{source,out}}{P_{signal}}$$

which is equal to the reciprocal of $PAE^{\#1}$ [12] as shown in ***Equation 11*** from Equation 8:

$$\begin{aligned} W_{active} &= \frac{P_{consumed}}{P_{signal}} = \frac{P_{signal} + P_{non-signal}}{P_{signal}} = \\ &\frac{P_{signal} + (P_{DC} - P_{system-added})}{P_{signal}} = \\ &\frac{P_{signal} + P_{DC} - (P_{signal} - P_{source,out})}{P_{signal}} = \\ &\frac{P_{DC} + P_{source,out}}{P_{signal}} = \frac{1}{PAE^{\#1}} \end{aligned} \tag{11}$$

RF, microwave and circuit engineers characterize amplifiers using PAE.[10-13] While Equation 11 shows total PAE[12] ($PAE^{\#1}$) is the inverse of the waste factor for the case of an amplifier that uses a DC power supply, a more customary definition for PAE,[13]

$$PAE^{\#2} = \frac{P_{RF,out} - P_{RF,in}}{P_{DC}},$$

is easily shown to be related to W as:

$$W = \frac{1}{PAE^{\#2}}\left[\left(1 + \frac{P_{RF,in}}{P_{DC}}\right)\left(1 - \frac{1}{G}\right)\right],$$

which is nearly identical to Equation 11 when G is large. To consider the power wasted along a cascade of active devices, the reader can use Equation 5 which is proved in Equations 22 to 24 by simply using $W = \frac{1}{PAE^{\#1}}$ to characterize power efficiency and power consumption using the waste factor of a cascade, similar to how noise factor is used to quantify additive noise and SNR degradation for a cascade.

It should be clear that waste factor efficiency accounts for the proportion of signal power output when compared to the total power consumed, on the signal path cascade where the total power consumed includes both output signal power and all non-signal (e.g., wasted) power, independent of the input to the device or cascade. From Equations 4, 8 and 10, it can be seen from superposition that $P_{non\text{-}signal}$ (additive wasted power in a device or cascade) and the total power consumed by the device or cascade are related to W by ***Equation 12*** and ***Equation 13***:

$$\begin{aligned} P_{non-signal} &= P_{signal}\left(\frac{1}{\eta_w} - 1\right) \\ &= P_{signal}(W - 1) \end{aligned} \tag{12}$$

$$P_{consumed} = P_{signal} + P_{non-signal} = P_{signal}\left[1 + \left(\frac{1}{\eta_w} - 1\right)\right] = WP_{signal} \tag{13}$$

Fundamentally, Equation 4 and Equation 10 show that W is defined as the inverse of efficiency.[3-7] Defining the waste factor in this manner provides a FoM that may be used for any device or cascade and relates the waste factor to additive wasted power, just as noise figure did for additive noise power. This is shown in ***Equation 14***.

$$W = \frac{1}{\eta_w} = \frac{P_{consumed}}{P_{signal}} = \frac{P_{signal} + P_{non-signal}}{P_{signal}} = \frac{P_{delivered} + P_{wasted}}{P_{delivered}} \tag{14}$$

Because W characterizes the useful signal power delivered to the output of any device or cascade relative to the entire power consumed along the device or cascade, it is most sensibly calculated referred to the output. Employing the concept of waste factor allows one to quantify power dissipation within a device (e.g., wasted power, since some power is not contained in the signal that is carried forward) which from Equations 13 and 14 and Table 1 can be expressed in ***Equation 15***:

$$\begin{aligned} P_{wasted} &= P_{non-signal} = (W - 1)P_{signal} \\ &= (W - 1)GP_{source,out} \end{aligned} \tag{15}$$

It is clear from Equation 15 that the input power to the cascade, (e.g., $P_{source,out}$) is not required to be known when using W, since W is a characteristic of the cascade or circuit, unrelated to input or output signal powers, as the cascade is assumed to be linear and matched. When a device along the cascade is turned off (e.g., $P_{signal} = 0$ or $P_{source,out} = 0$), W is still defined for a device or cascade, just as Friis was able to turn off the input signal power and still define F for a cascade, even when $F = SNR_i/SNR_o$ was infinite or undefined.

The formulation of W for a cas-


RF EXCELLENCE.
MISSION-CRITICAL SUCCESS.
NIC
Innovative Solutions - DC-40GHz
Quick Prototype Delivery (3-4 wks)
Visit NIC's Booth #433 at IMS2024
LC Filters
Cavity Filters
Switched Filter Banks
Printed Filters
Ceramic & Crystal Filters • Space-Qualified Filters • Multiplexers • Integrated Assemblies
Radar | EW | Guidance & Navigation | Communications | GPS & Satellite
ISO 9001:2015
AS9100
CERTIFIED
NIC NETWORKS INTERNATIONAL CORPORATION
www.nickc.com
913.685.3400
15237 Broadmoor
Overland Park, KS
e-mail: sales@nickc.com

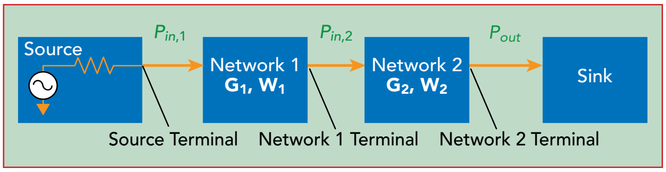

Fig. 2 A general cascaded communication system with a pair of devices.

caded system as shown in Equation 5 is proved using the simple cascade of two devices shown in ***Figure 2***.

Using Figure 2, the waste factor for the cascade signal path (where $P_{non\text{-}path}$ from auxiliary components is neglected since they are not on the cascade) can be calculated as illustrated using a cascade of two devices. First, the total power consumed at the output terminal of network 2 can be defined using Equation 4 or Equation 10 as shown in ***Equation 16***:

$$P_{consumed,2} = P_{delivered} + P_{wasted} = \mathbf{W}_{1,2} P_{out} \tag{16}$$

Then, the power consumed at the output terminal of network 1 can be defined in ***Equation 17***:

$$P_{consumed,1} = \mathbf{W}_1 P_{out,1} = \mathbf{W}_1 P_{in,2} \tag{17}$$

Here, $P_{consumed,1}$ denotes the total power consumption at the output terminal of device 1, which includes both the signal power applied to the input as well as the additional power consumed and contained in the signal that is transmitted to the subsequent device. It also includes the power wasted (e.g., not contained in the signal) by device 1, itself. When $P_{source,out}$ (the input signal power) is subtracted from the total consumed power using Equations 7, 16 and 17, the standalone power consumption of device 1 is defined by ***Equation 18***:

$$P_{consumed,Network-1} = \mathbf{W}_1 P_{in,2} - P_{in,1} \tag{18}$$

Applying the same approach to device 2, the standalone power consumption of device 2 is defined in ***Equation 19***:

$$P_{consumed,Network-2} = \mathbf{W}_2 P_{out} - P_{in,2} = \mathbf{W}_2 P_{signal} - P_{in,2} \tag{19}$$

Intuitively, the total power consumption of the cascaded system of the two devices is the sum of power consumed by each device alone and the power input to the system and this is shown in ***Equation 20***.

$$P_{total} = P_{in,1} + P_{consumed,Network-1} + P_{consumed,Network-2} \tag{20}$$

Also, the output signal power of the cascade is shown in ***Equation 21***:

$$P_{signal} = P_{out} = G_2 P_{in,2} \tag{21}$$

It follows from Equation 18 and Equation 19 that the total power consumption of the cascade can be shown in ***Equation 22***:

$$\begin{aligned} P_{total} &= P_{in,1} + P_{consumed,Network-1} + P_{consumed,Network-2} \\ &= (\mathbf{W}_1 - 1) P_{in,2} + \mathbf{W}_2 P_{signal} \\ &= \left(\mathbf{W}_2 + \frac{(\mathbf{W}_1 - 1)}{G_2} \right) P_{signal} \end{aligned} \tag{22}$$

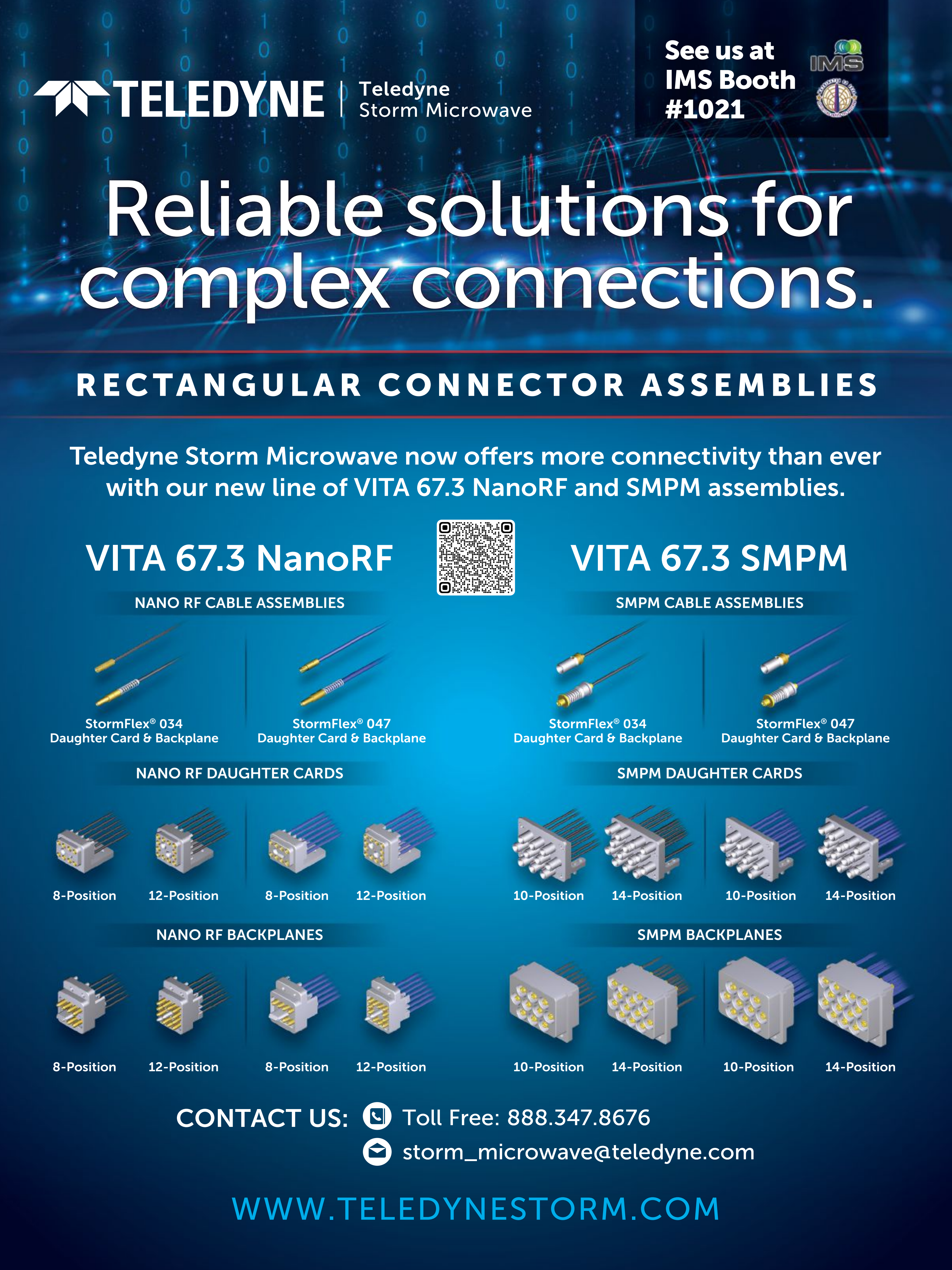
TELEDYNE | Teledyne Storm Microwave
See us at IMS Booth #1021
IMS
Reliable solutions for complex connections.
RECTANGULAR CONNECTOR ASSEMBLIES
Teledyne Storm Microwave now offers more connectivity than ever with our new line of VITA 67.3 NanoRF and SMPM assemblies.
VITA 67.3 NanoRF
VITA 67.3 SMPM
NANO RF CABLE ASSEMBLIES
StormFlex® 034 Daughter Card & Backplane
StormFlex® 047 Daughter Card & Backplane
SMPM CABLE ASSEMBLIES
StormFlex® 034 Daughter Card & Backplane
StormFlex® 047 Daughter Card & Backplane
NANO RF DAUGHTER CARDS
8-Position
12-Position
8-Position
12-Position
SMPM DAUGHTER CARDS
10-Position
14-Position
10-Position
14-Position
NANO RF BACKPLANES
8-Position
12-Position
8-Position
12-Position
SMPM BACKPLANES
10-Position
14-Position
10-Position
14-Position
CONTACT US:
Toll Free: 888.347.8676
storm_microwave@teledyne.com
WWW.TELEDYNESTORM.COM

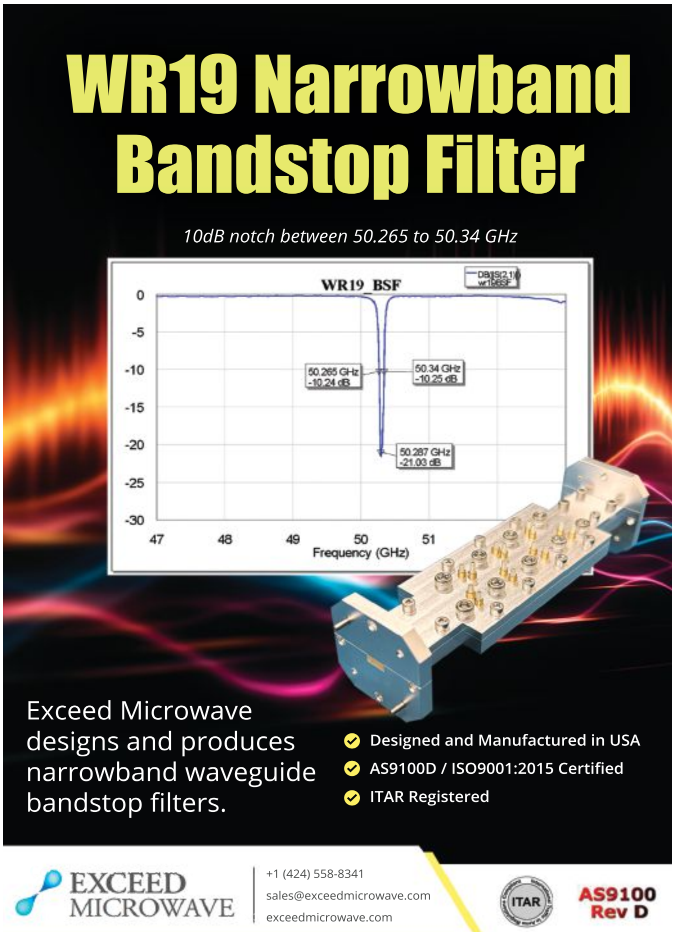

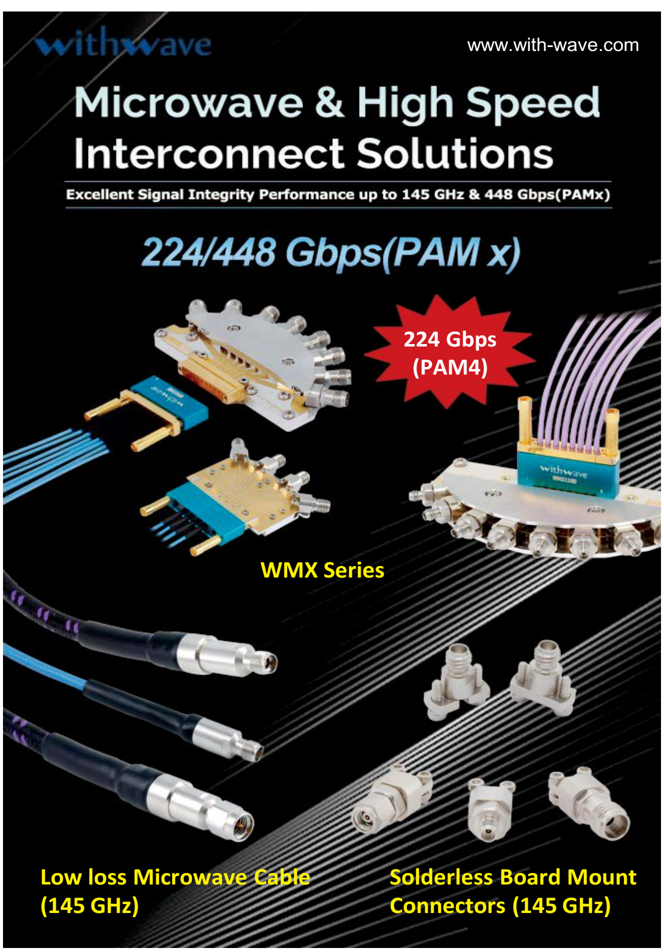

Since Equation 22 is of the same form as Equation 13 and Equation 8, the power waste factor for the cascaded system of Figure 2 is given by ***Equation 23***:

$$\mathbf{W_{1,2}} = \left(\mathbf{W_2} + \frac{(\mathbf{W_1} - 1)}{G_2}\right) \quad (23)$$

From Equation 23, W for a cascaded system with N devices may be generalized in ***Equation 24***:

$$W = W_N + \frac{(W_{N-1} - 1)}{G_N} + \frac{(W_{N-2} - 1)}{G_N G_{N-1}} + \cdots + \frac{(W_1 - 1)}{\Pi_{i=2}^{N} G_i} \quad (24)$$

Note the approach and mathematics are strikingly similar to the cascaded noise factor in Equation 2,[1] except W is referred to the output and is generally most impacted by the component closest to the *Nth* component closest to the sink.[5-7]

The wasted power of the cascade when there is a continual signal flow can be determined based on either the output power as in Equations 6, 8, 12 and 15 or based on the input source power and the gain of each stage as in ***Equation 25***, but a signal flow to the output is not required to define W.

$$P_{non-signal} = P_{wasted} = (W - 1)\Pi_{i=1}^{N} G_i P_{source,out} \quad (25)$$

In Equation 25, W is the waste factor for the entire cascade and G_i is the gain of i_{th} stage, with $i = 1$ denoting the stage closest to the source and *N* is the number of cascaded components.

HANDLING TIME-VARYING POWER STATES WHEN USING WASTE FACTOR

In a cascaded system, the components often exhibit dynamic behavior of varying power efficiency, leading to temporal variations in the waste factor. Amplifier efficiency levels may change above their quiescent power consumption levels over time when a signal of varying magnitude is applied or different devices, systems or chains are turned on and off at different times or for different functions to conserve power, etc. To account for these fluctuations, it is practical to calculate the average waste factor of each device over a designated time interval or averaged over all the finite power states. This can be mathematically described using the time average, which is simply the integral of the time-varying waste factor over an observation interval. Just like with the noise factor, a time-averaged waste factor may be used, denoted as $\overline{W}$ in ***Equation 26***:

$$\overline{W} = \frac{1}{T}\int_0^T W_t\,dt \text{ or } \overline{W} = \frac{1}{N}\sum_i^N W_i \quad (26)$$

Where:

T represents the selected period over which the average is taken, presumably over all operating states

W_t denotes the instantaneous waste factor at time t

W_i represents each of the finite number of power states

In this calculation, there are *N* states and the duration of each state is considered in the average. This formulation provides a time-averaged measure of the waste factor to capture an average value of the dynamic nature of the power consumption and efficiency. For on/off com-

ponents (e.g., amplifiers) with static/quiescent power, when a state is "off" during an observed epoch, the static power of such components may be treated as non-signal power ($P_{non\text{-}signal}$), although it may be more useful to consider these "turned-off" devices as contributing to non-path power rather than using Equation 26 since the "turned off" components do not carry signal power across a cascade when in the off state. This is an open research area ripe for discovery and definition of convention.

ANALOGIES BETWEEN WASTE FACTOR AND NOISE FACTOR

The analogous mathematical formulation of F and W is immediately apparent from the above text. However, there are important characteristics of each metric to keep in mind. Since noise figure is a measure of the additive noise from a source that results in the degradation of SNR caused by the components in a cascaded system, it quantifies the amount of total noise added to the signal referred to the input of the cascade. Therefore, F increases when observed from device 1 (closest to the source) to N (closest to the sink). On the other hand, W is a measure of the additive wasted power consumed by a cascaded system and quantifies the amount of power consumed and wasted by the cascade compared to the total signal power that is trans-

TABLE 2
WASTE FACTOR AND NOISE FACTOR COMPARISONS

Aspect	Waste Factor	Noise Factor
Definition	W: Indicates the amount of power wasted in a device or cascade when referred to the signal output power. η_w is the inverse of W, and is denoted as waste factor efficiency.	F: Indicates the amount of additive noise power from the device or cascade referred to as the input.
Reference port	Referenced to the output of a device or cascade.	Referenced to the input of a device or cascade.
Interpretation of value	W = 1 (WF = 0 dB) indicates all power consumed by a device or cascade is delivered as the signal output and no power is wasted. Greater W means greater additive power waste and less energy efficiency.	F = 1 (NF = 0 dB) indicates there is no additive noise in a device or cascade and there is no degradation in SNR at the output. Greater F means greater additive noise and SNR degradation.
Utility	Used to analyze the power consumed and wasted and overall power efficiency of cascaded networks and devices.	Widely used in industry to analyze and quantify the additive noise in cascaded networks and devices.
Application	For any cascaded linear system or electronic device with a source and a sink including channels of all types (not limited to receiver chains).	For any cascaded linear system or electronic device, primarily used in receiver chains.
Passive component	W is equal to the loss of the passive component or channel (W = L).	F is equal to the loss of the passive component (F = L).
Key observations	W of a cascade is generally dominated by W of the component closest to the sink. A high gain efficient amplifier at the cascade output maintains a small W and good power efficiency of entire cascade. When channel loss is greater than RX gain, channel loss dominates the system waste factor of the link. Increase RX gain and reduce TX W (e.g., increase TX WF efficiency) to overcome the power lost in the channel.	F of a cascade is generally dominated by F of the component closest to the source. A high gain LNA closest to the source (antenna) maintains a small F and little SNR degradation throughout the entire signal chain of a receiver.

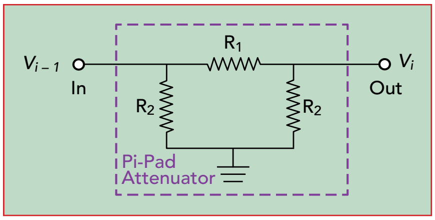

Fig. 3 **Passive attenuator circuit diagram.**

ported to the output. Since W is defined as the ratio of the total power consumed by the cascade to the signal output power, W is referred to the output and increases (e.g., efficiency decreases) when observed from device N (closest to the sink) to device 1 (closest to the source).

A larger value of W signifies more power wasted. The value of W is always equal to or greater than 1, with W = 1 signifying that all power supplied to a component or cascaded network is fully utilized in the signal output. This is the optimal condition with no power wasted. W equal to infinity indicates that no power is contributed to the signal output and all power is squandered (e.g., a perfect dummy load or a completely lossy channel). Some comparisons in the utility and scope of F and W in communication systems are summarized in ***Table 2***.

In conclusion, both F and W are useful in the analysis of communication systems. F is a well-established metric that provides a measure of the additive noise of a system and the degradation of the SNR. W is a new metric that provides a measure of the additive wasted power of a system and the energy efficiency of a system. Both metrics are important for circuits and communication systems, but as shown later in this article, W has further applications for understanding power efficiency in computing and processing, as well as communication systems. With the increasing importance of energy efficiency for our planet, W can be a useful metric for enabling the design of a wide range of greener systems.

APPLICATIONS OF WASTE FACTOR IN DEVICES AND SYSTEMS

Waste Factor for a Passive Device

Consider applying the waste factor to an attenuating stage like the passive attenuator shown in ***Figure 3***.

The gain of the attenuator is defined as the output power divided by the input power as shown in ***Equation 27***:

$$G_{atten} = \frac{P_{out}}{P_{in}} = \frac{V_i^2}{V_{i-1}^2} = L_{atten}^{-1} \quad (27)$$

Where:

V_{i-1} is the input voltage of the attenuator

V_i is the output voltage of this attenuator

L is the loss of this component (L > 1)

This assumes that the impedance at the input and the output of the attenuator are equal, which directly relates the power ratio to the square of the voltage ratio. Treating this attenuator as the i_{th} stage of the cascade, the output power is shown in ***Equation 28*** as:

$$P_{sig_i} = G_{atten} P_{sig_{i-1}} \quad (28)$$

The power wasted by the attenuator (e.g., not provided in the signal output) is defined in ***Equation 29***:

$$P_{non-sig_i} = P_{sig_{i-1}} - P_{sig_i} = (1 - G_{atten}) P_{sig_{i-1}} \quad (29)$$

Where:

P_{sig_i} is the total signal power delivered by the i_{th} stage to the $(i+1)_{th}$ stage

$P_{non-sig_i}$ is the signal power used by the i_{th} stage component but not delivered as signal power

Based on the definition of W in Equations 4, 10 or 14, W for a passive attenuator is computed in ***Equation 30*** as:

$$W_{atten} = \frac{P_{consumed}}{P_{signal,out}} = \frac{G_{atten} P_{sig_{i-1}} + (1 - G_{atten}) P_{sig_{i-1}}}{G_{atten} P_{sig_{i-1}}} = G_{atten}^{-1} = L_{atten} \quad (30)$$

Note the duality between attenuators using the waste factor and the noise factor. Waste factor, represented by $W_{atten} = L_{atten}$, quantifies the wasted power expended in the attenuator, while noise factor $F_{atten} = L_{atten}$ quantifies the degradation of the SNR due to additive noise.


There's nothing *Artificial* about our Intelligence.
Since 1961, Greenray Industries has been a preferred provider of precision, high performance reference sources to many of the world's leading military, defense and industrial manufacturers.
With a range of critical design innovations that enhance product performance and reliability, our quartz crystal oscillators help engineers realize their unique frequency control solutions.
On the ground, in the air – and beyond.
See what we've been up to >
GREENRAY

Waste Factor for a Communication Channel

In a communication system, the concept of waste factor (W) provides valuable insights into comprehensively understanding the power efficiency of the data transmission process through a lossy channel.[5-7] Any type of channel, whether wireless, wired, optical, etc., plays a vital role in the overall power efficiency of an end-to-end communication link. Consider a scenario where the power transmitted from the source is denoted as P_{TX} and the power received at the receiver is P_{RX}. Consider a lossy channel with a loss (e.g., L = 1/attenuation) given by ***Equation 31***:

$$L_{chan} = \frac{P_{TX}}{P_{RX}} \quad (31)$$

Also, the channel gain can be expressed as the reciprocal of loss as shown in ***Equation 32***:

$$G_{chan} = \frac{P_{RX}}{P_{TX}} = L^{-1}_{chan} \quad (32)$$

Assuming the i_{th} stage of a cascaded system represents the channel, then the signal power out of the channel, $P_{signal,i}$, is derived in ***Equation 33***:

$$P_{signal,i} = G_{chan} P_{signal,i-1} \quad (33)$$

Here $P_{signal,i-1}$ corresponds to the output power of the transmitter P_{TX}, $P_{signal,i}$ equates to the signal power out of the channel and is applied as input power at the receiver, P_{RX}. Consequently, the non-signal power $P_{non\text{-}signal,i}$ within the channel represents the amount of transmitted power not successfully received out of the channel (e.g., channel loss or path loss) which is additive wasted power of the channel which is a component of the cascade between source and sink and this can be formulated as ***Equation 34***:

$$P_{non\text{-}signal,i} = (1 - G_{chan}) P_{signal,i-1} \quad (34)$$

where $(1\text{-}G_{chan})$ quantifies the proportion of the signal power lost due to various factors such as attenuation, scattering and absorption. Multiplying $(1\text{-}G_{chan})$ by $P_{signal,i\text{-}1}$ yields the amount of power dissipated during transmission and is the power lost or wasted in the channel. The waste factor for the channel can readily be calculated using Equation 34 to get the results of ***Equation 35***:[5-7]

$$W_{chan} = \frac{P_{signal,i} + P_{non\text{-}signal,i}}{P_{signal,i}} = \frac{G_{chan} P_{signal,i-1} + (1 - G_{chan}) P_{signal,i-1}}{P_{signal,i}} = \frac{1}{G_{chan}} = L_{chan} \quad (35)$$

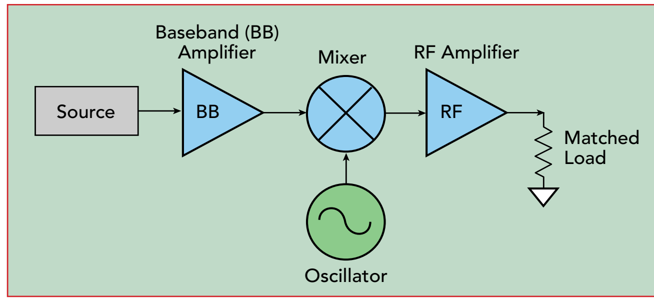

▲ **Fig. 4** **Homodyne transmitter with a matched load.**

Notably, unlike electrical devices, a wireless channel does not have a non-path power component ($P_{non\text{-}path}$), making it like a passive attenuator. Therefore, the waste factor for a channel (W_{chan}) is equivalent to that of a passive attenuator ($W_{chan}=L_{chan}$).

Waste Factor for a Homodyne Transmitter

The section presents a waste factor application example to compare two cascaded systems with different components. We compare the power efficiency of two different homodyne transmitters, each with matched load termination at the antenna. ***Figure 4*** shows the homodyne transmitter block diagram.

Table 3 illustrates the application of the waste factor (W) and the value of W for a cascade as described in Equation 5 and Equation 13 to evaluate the impact of overall energy efficiency using different components in a homodyne transmitter system.

Table 3 and Figure 4 are illustra-

TABLE 3 COMPARATIVE ANALYSIS OF W IN HOMODYNE TRANSMITTERS				
Example 1	**Component**	**Gain (Factor)**	**Efficiency (η_w)**	**W (WF)**
Case 1	RF amplifier	20 dB (100)	**52%**	**2.20 (3.42 dB)**
	Mixer	-6 dB (0.25)	25%	
	BB amplifier	13 dB (20)	14%	
Case 2	RF amplifier	20 dB (100)	**26%**	**4.12 (6.15 dB)**
	Mixer	-6 dB (0.25)	25%	
	BB amplifier	13 dB (20)	14%	
Example 2	**Component**	**Gain**	**Efficiency (η_w)**	**W (WF)**
Case 3	RF amplifier	20 dB (100)	30%	**3.39 (5.30 dB)**
	Mixer	-6 dB (0.25)	35%	
	BB amplifier	13 dB (20)	**52%**	
Case 4	RF amplifier	20 dB (100)	30%	**3.46 (5.39 dB)**
	Mixer	-6 dB (0.25)	35%	
	BB amplifier	13 dB (20)	**26%**	

tive for how to use W to characterize energy efficiency based on the selection of different components. Using Case 1 as an example, the waste factor of the homodyne transmitter based on component parameters in Table 3 is calculated using Equation 5 or Equation 24 and W = $1/\eta_w$:

$$W_{Case1} = \frac{1}{0.52} + \frac{(1/0.25 - 1)}{100} + \frac{(1/0.14 - 1)}{100 \times 0.25} = 2.20 = 3.42\,\text{dB}$$

Example 1 in Table 3 compares Case 1 and Case 2 to show how components with different efficiencies impact W of the cascade using Equation 5 or Equation 24. It can be seen that Case 1, with a more efficient RF amplifier, results in a lower W of 2.20 (3.42 dB), signifying better power efficiency and less wasted power than Case 2, which uses a less efficient RF amplifier and yields a larger W of 4.12 (6.15 dB) for the cascade. Example 1 shows that almost twice as much power is wasted in Case 2 (e.g., 6.15 dB – 3.42 dB = 2.73 dB) which is roughly the proportion of efficiencies of the two different final amplifiers. The above example shows that amplifier efficiency closest to the sink dominates the overall waste figure of the cascade.

In Example 2 of Table 3, Cases 3 and 4 are considered. Here, again, overall W, as computed in Equation 5 or Equation 24, is impacted by specific components, but for this example, we see that components farthest from the sink have much less impact on overall power efficiency. Case 3 shows how a baseband amplifier that is much more power efficient achieves only a slightly lower W of 3.39 (5.30 dB) compared to Case 4, which uses an identical RF amplifier but a much less efficient baseband amplifier. Case 4 has only 0.09 dB poorer energy efficiency with a W of 3.46 (5.39 dB). While these observations are intuitive, waste factor allows precise quantification and comparison.

These examples illustrate the importance of optimizing power efficiency in the components closest to the sink to reduce waste and enhance system efficiency. These examples also show how waste factor may assist researchers and engineers in creating energy-efficient component technologies and system designs.

Waste Factor for a Communication System with a Channel

Figure 5 shows a system with a channel that is easily treated as a cascaded system. Note that P_1 is the power from the *TX*, P_2 is the power out of the channel and into the *RX*, and W_{TX} and W_{RX} represent the waste factors of the TX cascade and RX cascade (not shown), respectively. Note that the channel may be wireless, wired, acoustical, optical, etc. and may have multiple users/links.

The total waste factor for the cascaded system, including the TX and RX components as well as the inherent loss of a channel, is defined as W_{sys}. Using Equation 5 or Equation 24, W_{sys} is given by ***Equation 36*** as:

$$W_{sys} = W_{RX} + \frac{(W_{chan} - 1)}{G_{RX}} + \frac{(W_{TX} - 1)}{G_{RX} G_{chan}} \quad (36)$$

From Equation 35, it is clear that $W_{chan} = L_{chan}$ and when the receiver gain, G_{RX}, is substantially less than the loss of the channel, L_{chan}, which is typical for wireless links, W_{sys} in Equation 36 then simplifies to ***Equation 37***:[5,6,7]

$$W_{sys} \approx \frac{L_{chan} \times W_{TX}}{G_{RX}} \quad (37)$$

Equation 37 implies that to achieve a smaller W_{sys} value, which is indicative of a more power-efficient end-to-end system, it is essential to have high-gain receivers, and transmitters with high power efficiency.

The key result of Equation 37 may be written in dB as ***Equation 38***:

$$WF_{sys}(dB) \approx L_{chan}(dB) + W_{TX}(dB) - G_{RX}(dB) \quad (38)$$

Equation 38 shows that the strategic configuration of power-efficient TX output components and high-gain receivers minimizes energy waste over any channel, optimizing the system energy efficiency. The simplicity of the system depicted in Figure 5 underscores the need for certain components to be properly designed for greater power efficiency to have the greatest impact on the overall minimization of power waste and offers a framework for understanding mobile system power consumption for individual users.

Now investigate how waste figure varies for different communication systems comprising a simplified TX, a lossy channel and a RX. The assessment considers the system architecture of Figure 5 while varying system gain and efficiency at each stage as shown in ***Table 4***. This comparison enables an intuitive understanding of how changes in system gain and efficiency impact the overall energy efficiency of the communication system in Figure 5.

The different cases in Table 4 illustrate that when the channel loss increases, as seen between Case

TABLE 4

COMPARATIVE ANALYSIS OF WASTE FIGURE IN FIGURE 5

Example 1	Component	Gain (dB)	W (η_w^{-1})	W_{sys} (dB)
Case 1	Transmitter	61	2	**13.27**
	Channel	-70	70 dB	
	Receiver	60	1.25	
Case 2	Transmitter	61	2	**23.03**
	Channel	-80	80 dB	
	Receiver	60	1.25	
Case 3	Transmitter	61	2	**23.01**
	Channel	-80	80 dB	
	Receiver	60	1	
Case 4	Transmitter	61	1	**20.00**
	Channel	-80	80 dB	
	Receiver	60	1	
Case 5	Transmitter	61	2	**13.22**
	Channel	-80	80 dB	
	Receiver	70	1	

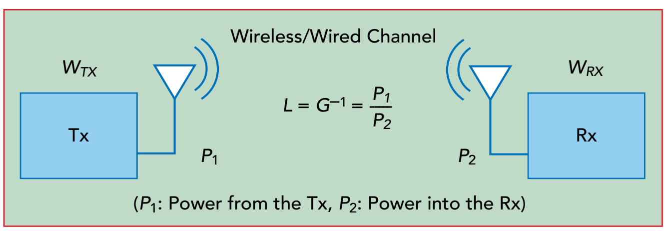

Fig. 5 **A communication system including a channel.**

1 and Case 2, the waste figure increases by a similar amount (e.g, the channel loss dominates power efficiency). Case 3 shows that making the RX more efficient (e.g., increasing its efficiency by 25% from 0.8 to 1), does not significantly affect the waste figure, reducing it by only 0.02 dB. However, in Case 4, when the TX efficiency is improved (e.g. doubled) from 0.5 to 1 with all other parameters the same as in Case 3, there is a noticeable decrease of 3 dB in the waste figure, which is equal to the increase in TX efficiency. This design saves half the consumed power for the same link quality. Case 5 uses the setup of Case 3 with the RX system gain increased from 60 to 70 dB. This saves much more power with the waste figure dropping by 10 dB. Comparing Case 5 and Case 3, Case 5 is vastly more energy efficient. By increasing the RX system gain, Case 5 needs only one-tenth the TX power compared to Case 3 for the same cascade output power. This efficiency is shown by a 10 dB reduction in the waste factor, indicating that Case 5 uses energy 10 times more effectively than Case 3.

The conclusion from these observations is that if a lower loss channel is not available, increasing the RX gain has a significant impact on reducing waste. Additionally, improving the efficiency of the TX is also a vital way to make the system more power efficient. The waste figure theory was first tested for the power consumption tradeoff between a single hop communication system versus a relay system, whereby operating regions were found that indicated which architecture was more power efficient to use for an end user.[7]

Waste Factor Applied to Data Centers

Data centers are one of the largest consumers of power today. The information technology (IT) field has established the power usage effectiveness (PUE) FoM.[8] Employing the PUE to determine the power usage of non-IT components in relation to servers in a data center offers a straightforward approach to associating non-IT power consumption with the power consumed by server operations.

The IT industry defines PUE as the ratio between the summation of the amount of energy consumed by IT equipment and the energy consumed by auxiliary equipment for data operations, compared to just the IT equipment energy usage. As shown in ***Equation 39***, the IT equipment includes networking equipment that is on the signal path, (e.g., switches, routers, firewalls, etc.) as well as components that do not transfer data but that are vital to data processing and thus may be considered as being on the cascade (using the waste factor model of Figure 1) but as not contributing (e.g., wasted power in the transport of information in servers, storage systems, etc.). The energy consumption of auxiliary equipment includes cooling, lighting and non-network devices that do not carry data center information, etc., and are similar to non-path components in the waste factor model (e.g. see Equation 9)[4,8]

$$PUE = \frac{\text{Total data center energy}}{\text{Total IT energy}} = \frac{P_{IT} + P_{aux}}{P_{IT}} \quad (39)$$

Since a data center provides information (e.g., data) from a source to a sink in its operation, the waste factor can be applied to gain new and vital insights to optimize the data center power efficiency. W can be applied to a data center if certain assumptions are made about how and where the signal power is transferred. Assuming that Equation 39 defines P_{IT} as the power consumed by the IT equipment, (e.g., signal path power and wasted power on the signal path) and P_{aux} is the auxiliary equipment power consumption, then Equation 39 may be recast in terms of W. This use of W considers only the powers consumed and delivered from a source to a sink within a data center while treating P_{aux} as off-path power that is not involved in the computation of W per Equation 9. Total data center power consumption is then computed through the sum of signal-path and non-path powers.

In the data transmission or processing within a data center, the major power consumption is attributed to servers, network switches

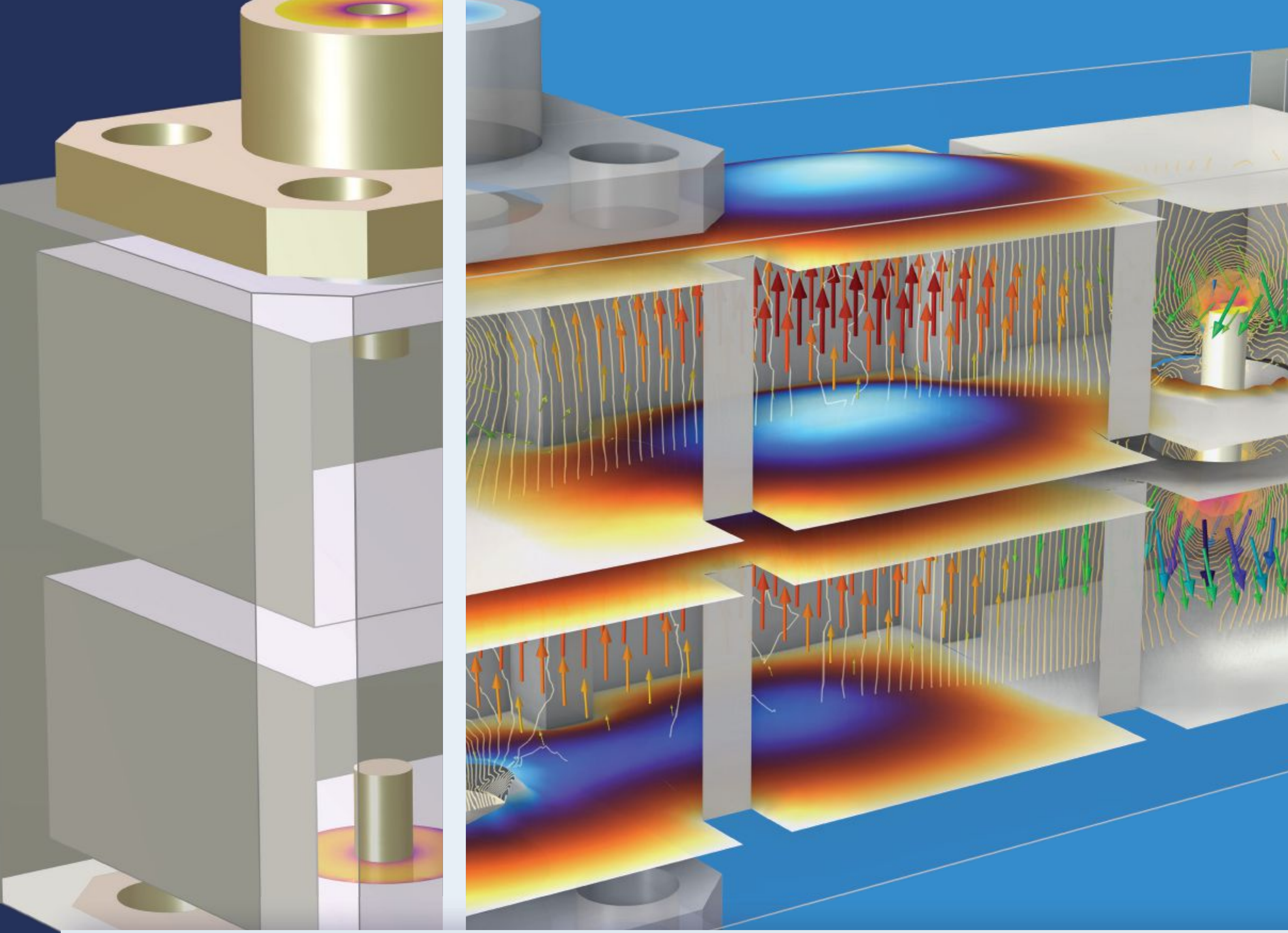

and computing equipment, while additional power consumption is associated with cooling systems, power distribution units (PDUs) and other auxiliary equipment. According to findings,[9] servers and networking equipment account for about 60 to 70 percent of the overall power consumption in a data center. Cooling systems contribute about 30 to 40 percent of the total power consumption, while the remainder is consumed by power distribution units (PDUs) and other auxiliary equipment.

To break down the information path power consumption of the data center, the total data center information path power consumption is modeled in ***Equation 40***:

$$P_{consumed} = P_{IT} = P_{info} + P_{non-info} \tag{40}$$

where P_{info} is the sum of all powers of each component that is used for carrying information or data in the system. The information path power is the network within the data center (e.g., P_{router}, P_{switch}, $P_{firewall}$) and other network equipment that carry information. This is similar to the previous definition of signal powers stemming from components on the cascade and it is defined in ***Equation 41***:

$$P_{info} = P_{router} + P_{switch} + P_{firewall} \tag{41}$$

and $P_{non\text{-}info}$ is defined as the power used by the other IT-critical components that process the data but that are not directly involved in data transmission (e.g., $P_{processor}$, P_{memory}, $P_{storage}$, P_{NIC}).This is similar to the previous definition of the non-signal or wasted power of cascaded signal path components. The power consumed by the non-info components is shown in ***Equation 42***:

$$P_{non-info} = P_{processor} + P_{memory} + P_{storage} + P_{NIC} \tag{42}$$

where NIC represents the network interface cards.

Using this dichotomy to represent a data center in terms of a fine-grain consideration of components, Equation 40 may be used to recast PUE, as defined in Equation 39, as ***Equation 43***:

$$PUE = \frac{P_{info} + P_{non-info} + P_{aux}}{P_{info} + P_{non-info}} \tag{43}$$

From Equation 39 and Equation 43, the data center's total IT power consumption (e.g., analogous to total power consumed by the cascade) can be rewritten in terms of PUE and the useful and wasted powers on the signal path as ***Equation 44***:

$$P_{IT} = \frac{P_{aux}}{PUE - 1} = P_{info} + P_{non-info} \tag{44}$$

Now, just as in previous sections, based on Equations 14, 43 and 44, the waste factor of the data center (ignoring auxiliary power similar to ignoring off-path power) can be defined as ***Equation 45***:

$$W = \eta_w^{-1} = \frac{P_{info} + P_{non-info}}{P_{info}} = \frac{P_{aux}}{P_{info}(PUE - 1)} \tag{45}$$

The total power consumption for the data center, like the approach in Equation 9, can then be calculated by considering the data center as a single system that has signal path components, with some that carry information and some that do not, as well as auxiliary non-path components. Using Equation 45, Equation 9 and the definition of PUE, the total consumed power is defined in ***Equation 46***:

$$\begin{aligned} P_{consumed,total} &= P_{info} W + P_{aux} = \frac{P_{aux}}{(PUE - 1)} + P_{aux} \\ &= P_{info} + P_{non-info} + P_{aux} \end{aligned} \tag{46}$$

The interpretation for W in Equation 46 is intuitive as it is for circuits or communication systems and relates W to PUE, an existing FoM in data centers. However, this interpretation requires a finer definition of components that map to Figure 1, and this approach enables a better understanding of the power efficiency of the data transport.

The example in ***Figure 6*** shows how waste figure applied to a data center provides a more detailed understanding of power efficiency compared to the commonly utilized PUE metric in data center evaluations. Consider two data centers with equal PUE values but with different architectures.

The example of Figure 6 assumes that Data Center A is a larger facility with more equipment and a higher

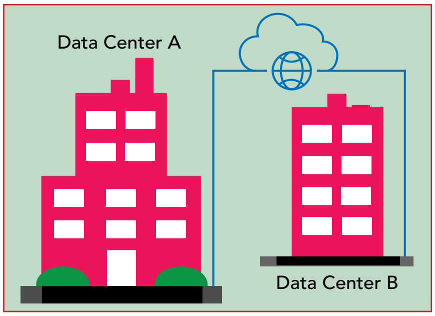

Fig. 6 Illustrative comparison of two data centers.

total energy consumption. Conversely, Data Center B is smaller and uses less total energy. Assuming both data centers have identical PUEs and comparing total energy use, it might seem that Data Center B is more efficient. However, PUE, like waste factor, is designed to determine relative or proportionate energy efficiency without respect to actual consumption levels.[8,9] Waste factor, with its focus on power wasted on the path that transfers data, provides a better measure of the power efficiency of these two data centers since their ultimate mission is to transfer data in a network. ***Table 5*** shows a comparison of the power consumption on PUE for both data centers.

For Data Center A, the power allocation is as follows: $P_{info,A}$ = 140 kWh for information transmission, $P_{non\text{-}info,A}$ = 40 kWh for non-data transmission components and $P_{aux,A}$ = 150 kWh for auxiliary equipment. In comparison, consider Data Center B, which allocates $P_{info,B}$ = 60 kWh of power for information transmission components, $P_{non\text{-}info,B}$ = 30 kWh for non-data transmission components and $P_{aux,B}$ = 75 kWh for auxiliary equipment. This example has been specifically chosen to ensure the PUE values for each data center are identical (e.g., PUE would indicate they are equally energy efficient).

$$PUE_A = \frac{P_{info\_A} + P_{non\text{-}info\_A} + P_{aux\_A}}{P_{info\_A} + P_{non\text{-}info\_A}} = \frac{140 + 40 + 150}{140 + 40} \approx 1.833$$

$$PUE_B = \frac{P_{info\_B} + P_{non\text{-}info\_B} + P_{aux\_B}}{P_{info\_B} + P_{non\text{-}info\_B}} = \frac{60 + 30 + 75}{60 + 30} \approx 1.833$$

where PUE_A and PUE_B denote the PUE of Data Center A and Data Center B, respectively.

Now, using Equation 45, W for the data centers can be calculated:

$$W_A = \frac{P_{aux\_A}}{P_{info\_A}(PUE_A - 1)} = \frac{150}{140(1.833 - 1)} \approx 1.286$$

$$W_B = \frac{P_{aux\_B}}{P_{info\_B}(PUE_B - 1)} = \frac{75}{60(1.833 - 1)} \approx 1.5$$

By evaluating the waste factors, W_A and W_B, it is apparent that Data Center A is about 20 percent more efficient in its energy use in transporting data, even though both have identical PUEs. This efficiency is measured by comparing the amount of power used directly for carrying and processing information in the system to the overall power consumption. The PUE metric, although standard in the industry, does not capture the detailed energy usage of specific equipment and their relative power waste along the signal path, which is the ultimate job of a data center. It is worth noting that this result is somewhat analogous in Reference 3 where wider bandwidth THz channels are more power efficient on a per bit basis than narrower millimeter wave channels. The waste factor offers a more detailed perspective by considering the function and efficiency of individual components, which may be defined with their own W values. This analysis demonstrates the potential benefits of adopting the waste factor as a metric for evaluating energy efficiency in complex infrastructures such as data centers. Utilizing W as an efficiency metric can provide new insights into optimizing power consumption across various systems involving a source and a sink.

CONCLUSIONS AND FUTURE DIRECTIONS

The waste factor (W) or waste figure (WF in dB) is a new figure of merit for quantifying power efficiency and offers a useful advancement in the field of electrical engineering and system design. By providing a standardized metric for power con-

TABLE 5

DATA CENTER POWER CONSUMPTION AND PUE COMPARISON WITH W

Data Center	P_{info} (kWh)	$P_{non\text{-}info}$ (kWh)	P_{aux} (kWh)	PUE	W
A	140	40	150	1.833	1.286
B	60	30	75	1.833	1.5

sumption, it becomes possible for designers and researchers to have a common approach to quantifying power efficiency. This article has shown how the mathematical formulation is similar to the historical approach used to create the noise factor (F), yet W has much broader applications to systems of all types. The waste factor enables electrical engineers and circuit designers to quantify and minimize power waste in any circuity or cascade of devices or systems. This paper has demonstrated the foundational principles of the waste factor, its mathematical derivation and its practical applications across various scenarios, including passive devices, wireless channels, communication systems and data centers. More applications are possible.

Waste factor provides an intuitive understanding and mathematical formulation of power consumption within cascaded systems and allows for the optimization of designs in a manner that was previously challenging due to the lack of a unified metric. Moreover, the application of waste factor in emerging and critical areas such as UAV cellular infrastructure, millimeter wave wireless networks and data centers underscores its versatility and relevance in contemporary engineering challenges. As the demand for energy-efficient solutions continues to grow, the waste factor offers promise as a standard analysis tool for enabling green communications and sustainable technology development. Its adoption as an industry standard could drive significant improvements in the energy efficiency of future electronic devices and systems. The waste factor not only complements existing metrics such as the total PAE in amplifier design or PUE in data center design but also enriches the toolkit available to engineers for designing systems that are not only high-performing but also environmentally responsible. Future work may open new areas of application of the waste factor in both academic research and industry practice with the development of standardized measurement and reporting guidelines and applications of waste factor to other types of systems or devices. Additionally, further exploration of potential applications, such as in the use of AI and ML algorithms for power-efficient design, could lead to more innovative solutions and advancements in energy efficiency. ■

ACKNOWLEDGMENTS

The authors thank Nicola Piovesan, Antonio De Domenico and Prof. Hamed Rahmani for useful discussions, feedback and suggestions.

References

1. H. T. Friis, "Noise Figures of Radio Receivers," *Proc. IRE*, Vol. 32, No. 7, pp. 419–422, 1944.
2. Y. Xing, F. Hsieh, A. Ghosh and T. S. Rappaport, "High Altitude Platform Stations (HAPS): Architecture and System Performance," in *2021 IEEE 93rd Vehicular Technology Conference (VTC-Spring)*, April 2021, pp. 1–6.
3. O. Kanhere, H. Poddar, Y. Xing, D. Shakya, S. Ju and T. S. Rappaport, "A Power Efficiency Metric for Comparing Energy Consumption in Future Wireless Networks in the Millimeter Wave and Terahertz Bands," *IEEE Wirel. Commun.*, Vol. 29, No. 6, pp. 56–63, 2022.
4. M. Ying, D. Shakya, H. Poddar and T. S. Rappaport, "Waste Factor: A New Metric for Evaluating Power Efficiency in any Cascade," *IEEE Global Communications Conference*, Kuala Lumpur, Malaysia, Dec. 2023, pp. 1–6.
5. T. S. Rappaport, J. N. Murdock and F. Gutierrez, "State of the Art in 60-GHz Integrated Circuits and Systems for Wireless Communications," *Proc. IEEE*, Vol. 99, No. 8, pp. 1390–1436, 2011.
6. J. N. Murdock and T. S. Rappaport, "Consumption factor: A Figure of Merit for Power Consumption and Energy Efficiency in Broadband Wireless Communications," *IEEE GLOBECOM Workshops*, pp. 1393–1398, 2011.
7. J. N. Murdock and T. S. Rappaport, "Consumption Factor and Power-efficiency Factor: A Theory for Evaluating the Energy Efficiency of Cascaded Communication Systems," *IEEE J. Sel. Areas Commun.*, Vol. 32, No. 2, pp. 221–236, 2014.
8. M. Dayarathna, Y. Wen and R. Fan, "Data Center Energy Consumption Modeling: A Survey," *IEEE Commun. Surv. Tutorials*, Vol. 18, No. 1, pp. 732–794, 2016.
9. L. A. Barroso and U. Holzle, "The Case for Energy-proportional Computing," *Computer*, Vol. 40, No. 12, pp. 33–37, 2007.
10. S. Lucyszyn, "Power-added Efficiency Errors with RF Power Amplifiers," *International Journal of Electronics*, Vol. 82, No. 3, pp. 303–312, 1997.
11. M. Steer, "Microwave and RF Design V: Amplifiers and Oscillators," 3rd ed., Vol. 5, *NC State University*, 2019.
12. A. A. Sweet, "MIC & MMIC Amplifier and Oscillator Circuit Design," *Artech House*, 1990.
13. L. B. J. Walker, "High-Power GaAs FET Amplifiers." *Artech House*, 1993.
14. T. S. Rappaport, "Waste Figure (W): A Figure of Merit for the Power-efficient ("Green") Engineering of Any Device or Cascade of Circuits or Systems," ITU Webinar, Feb. 20, 2024, https://www.itu.int/en/journal/j-fet/webinars/20240220/Pages/default.aspx.

INVITED PAPER

Implementing Automation in Microwave System Testing

Brad Cole and Roy Zohrabian
ATE Systems, N. Billerica, Mass.

The growing demand and complexity of advanced microwave systems are changing the paradigms of microwave system production, especially for array-based radar and communication systems. One of the key outcomes of this paradigm shift is that OPEX and the time required for testing modern microwave systems are tracking with the increased complexity of these systems. Previously, long calibration times for S-parameters, power and noise, as well as error-prone and time-consuming and labor-intensive testing, did not dominate microwave system costs. However, time and expense have now become a major hurdle for production testing in many system applications. Much of that time and expense is spent during test equipment calibration and test system setup. This article explores trends in advanced microwave system production, focusing on system quality and performance testing. It introduces how advanced automation and calibration technologies can reduce time, enhance reliability, repeatability and accuracy, along with minimizing operator error in microwave system testing.

HOW RADAR AND COMMUNICATION TECHNOLOGY TRENDS IMPACT MICROWAVE TEST

Radar and communications antenna systems have become indispensable for military, government, public safety, civilian and industrial applications. Wireless communication, sensing and networking are now ubiquitous. This popularity and increased adoption have increased competition and the rate of innovation and advancement. These wireless communication and sensing systems have seen a shift toward higher frequencies, larger operating bandwidths, direct digital synthesis/conversion and the development of advanced/active antenna systems (AAS). Evolution in wireless communication and sensing has been instrumental in enhancing the performance of these systems and enabling new techniques that provide superior utility for various applications.

However, these advancements bring an increase in complexity, especially with the move to higher frequencies and bandwidths, along with increased system port counts to enable advanced beamforming and MIMO functionality. These design and production issues have largely been addressed, but some challenges remain. These remaining challenges revolve around calibration times for S-parameters, power and noise, as well as minimizing human error during the fixturing and interconnect process.

Current test system calibration and setup procedures for wireless applications support the cost and yield expectations of the business model for those applications. However, with pressure on government and capital expenditures, coupled with a desire to reduce design cycles in all applications, system testing is under more scrutiny. Many emerging wireless communication and sensing systems have tens of ports and a single interconnect misalignment or calibration mishap can result in failures. This concern is exacerbated as wireless systems evolve to be more complex, have more ports and operate at higher frequencies and greater bandwidths.

Electronic calibration (eCal) technology was developed to help minimize user calibration error, reduce calibration time and enhance calibration repeatability. However,

HYPERLABS™

Innovation at Hyperspeed since 1992

KEEP YOUR EYES WIDE OPEN: DESIGNS FOR HIGH-SPEED DATA

HL5897 Linear Amp (63 GHz)

- Exceptionally flat bandwidth (48 kHz to 63 GHz)
- 14 dB gain
- Optimized as data driver
- 112 Gbps PAM4 signaling
- Small form factor
- Single 6 V power supply

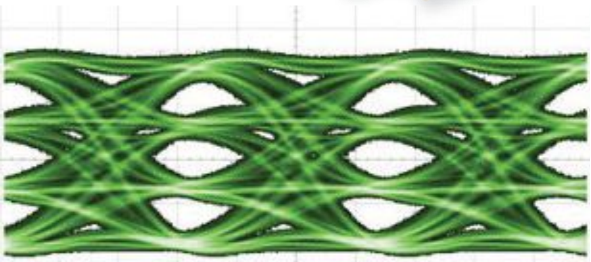

NEW: HL9469 Pick-off Tee

- Ultra-broadband (DC to 110 GHz)
- Suitable for 224 Gbps PAM4
- Available in matched pairs

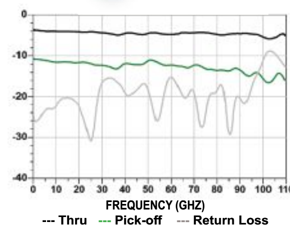

NEW: HL9429 Attenuators

- Ultra-broadband (DC to 110 GHz)
- Exceptional price for performance
- 3, 6, and 10 dB options available

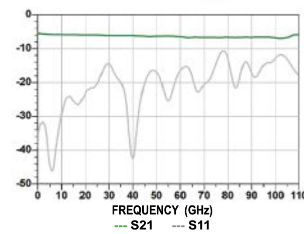

ULTRA-BROADBAND PARTS FOR 112 & 224 GBPS PAM4 APPLICATIONS

HL9409 BALUN (500 kHz-100 GHz)

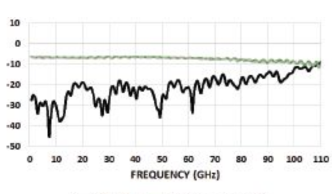

HL9449 BIAS TEE (160 kHz-110 GHz)

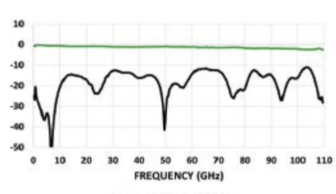

HL9439 DC BLOCK (160 kHz-110 GHz)

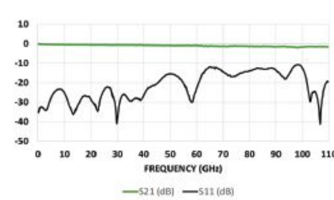

Also Available:

- **HL9479 2-Way Power Divider** from DC to 110 GHz (3 dB)
- **New HL942x Inverters** from 150 kHz up to 100 GHz (3 dB)
- **New HL952x Terminations** up to 110 GHz
- **HL945x Transition Time Converters** up to 50 GHz (7 ps)

Visit our website for baluns, pick-off tees, power dividers, risetime filters, DC blocks, amplifiers, and more!

PUT HYPERLABS IN YOUR LAB

ULTRA-BROADBAND

We offer some of the broadest band components on the market.

Our engineers are constantly working on new designs and expanding our product line.

Components that are "invisible" with regards to bandwidth roll-off and jitter performance keep pulse and eye fidelity at their best.

We design our products specifically to achieve these goals over the broadest band possible.

DEMOS AVAILABLE

Demos are in stock for most offerings, and we will get them in your lab quickly for a "hands on" evaluation.

CUSTOM DESIGNS

Don't see exactly what you need? Our engineers may be able to help.

Many of our products can be modified or adapted to your specific needs quickly and with low minimum order quantities.

HL OREGON
13830 SW Rawhide Ct.
Beaverton, OR 97008

HL COLORADO
315 W South Boulder Rd.
Suite 206
Louisville, CO 80027

www.hyperlabs.com

the technology was not designed to tackle emerging systems with high port-counts. eCal improves calibration standards for S-parameter testing but different standards and methods are often needed for power and noise testing calibrations. A power sensor is needed for power calibrations and these sensors must be metrology grade and each port that needs power calibration must be tested. Similarly, additional noise calibration features, like a noise source or the ability to present a desired characteristic impedance are required to extract noise parameters.

Traditionally, S-parameter, power and noise calibrations were performed separately. These calibrations often required separate test setups, standards and interconnects. This creates a challenge in harmonizing test results, often requiring different personnel addressing test devices, test equipment and data.

A significant factor causing test setup errors is connecting, disconnecting and cycling the interconnects. Threaded coaxial connectors are the most common RF test interconnect method and these connector types require precise torque for proper RF connection. They are reliable and repeatable if connected to specifications, but variations in torque and threading techniques can lead to interconnect electrical performance variations. A big issue with threaded interconnects is the time required to make the connection and the possibility of improper torque. Many systems now use non-threaded coaxial interconnects like probe systems and blind mate connectors. Probe systems require precise positioners and this becomes a challenge with the number of ports requiring testing in emerging systems. Hence, automation and fixturing become important to efficiently probe-test high port-count systems.

Blind mate connectors, often regarded as unreliable with poor repeatability, are now incorporated because of their rapid connect/disconnect capabilities and small profile. The small connector profile enables smaller pitches and higher connector densities for high port-count systems. A drawback of the blind mate connectors is connector alignment during insertion has a significant impact on the electrical performance of the connector. Blind mate connectors can have comparable performance and be as reliable and repeatable as threaded connectors if they are inserted with the proper alignment and force. However, this is difficult to do consistently without automation.

EMBRACING AUTOMATION TO ADDRESS SYSTEM TEST CHALLENGES

A solution to these test challenges involves automated systems that minimize operator error, shorten calibration times, enhance calibration repeatability and accelerate test fixturing and interconnect while improving repeatability and reliability. This implies a fully-automated calibration system handling large multi-port devices under test (DUTs) and test equipment, automated fixturing and interconnect systems. This system could also include robotics for handling and alignment. While such a system is possible, a more economical, faster and simpler solution may be a modular system with custom components to accommodate specific DUT requirements. The diversity of DUT needs, manufacturing processes and additional test criteria prioritize customized fixture and handling features and automation that reduces test time and enhances reliability. These advantages may offset the cost of customization. Properly designed automation systems can dramatically enhance testing throughput and reduce the cost per test.

The Next Stage of Microwave Test Calibration

Reducing interconnect cycling during the calibration process, especially with vector network analyzers (VNAs), is a key enabler for automated RF testing. Traditionally, RF calibration of VNAs requires connecting calibration standards to the appropriate DUT and VNA ports, often in sequence, which minimizes operator error and improves software control. eCal, a two-decade-old advancement of this calibration technique,

incorporates calibration standards into a unit that includes some electronic control, software and data allowing for coordination with a VNA. An eCal, which must be factory-calibrated periodically, communicates data from various calibration states to the VNA. The eCal switches between standards, meaning the operator only needs to connect and disconnect the eCal module for the calibration and then connect the test cables to the DUT. eCal systems are typically only used for S-parameter calibration. ***Figure 1*** shows an example of an inline calibration module.

Fig. 1 **Single-path inline calibration module.**

There are several methods to automate RF calibration. Robotic systems can properly connect and disconnect calibration standards, including an eCal, and then connect cables to the DUT. High RF port counts would require a very sophisticated robotic system and this would not eliminate the potential for interconnect cycling error. In addition, the test system would still change as the calibration connections and test leads were cycled.

To minimize these concerns, the DUT must have a single connection and the calibration standards must connect directly to the test equipment. This approach requires an integrated calibration system or a standalone calibration system that accommodates a sufficiently high port-count and allows the test signals to pass through the calibration standard. This would require one connection between the DUT and the calibration system and one connection between the calibration system and the VNA. This inline calibration feature has many advantages, including reducing the chance of operator error by reducing the number of connections between the calibration system and the DUT. This stage could be automated, further reducing handling and interconnect errors.

An inline calibration system for systems with many ports may be costly and complex. Cost and complexity can be reduced with a solution consisting of a modular approach with small single-port or multi-port inline calibration units. These units can provide the required calibration standards for the DUT and test equipment port-count needs. More compact and modular inline calibration units can be placed close to the DUT ports, reducing the interconnect length between the two systems. For example, an inline calibration unit can be placed on the coaxial interconnect of a probe system. Probe heads are typically characterized from the interconnect to the probe tip and this de-embedded data can be programmed into the VNA. An inline calibration unit at the coaxial port of the probe head allows for calibration to the probe tip and the probe can be arranged for ease and speed of testing. Compact and modular inline calibration devices also enable direct connection to DUT ports without additional support or fixturing. This, in turn, enables very compact automated systems with short interconnects.

The next evolution of this calibration technique is to include power sensing and a noise source in the inline calibration system. This would allow for small-signal S-parameters, power and noise calibration and testing to be done with one setup. It would also eliminate the need to cycle interconnects with the DUT. This technique would harmonize the results of small-signal S-parameters and large signal power measurements. Since the test equipment and DUT will see impedance standards, the corrected noise figure can easily be determined from the extracted noise parameters. The corrected noise figure is more useful than the nominal scalar noise figure that is typically measured. Extracting the noise figure with known and variable source impedance results in a source-pull noise figure and a noise parameter plot. This plot includes

GaAs-Based Q/V/E-Band Solutions from Altum RF

Altum RF's lineup of broadband Q/V/E-band low-noise and medium-power amplifiers enable next-generation technology and high-capacity networks. Applications include test and measurement, SATCOM, and point-to-point wireless communication for 5G and 6G networks. These high-frequency amplifiers use advanced GaAs technology, which delivers low noise figure and linear amplification with less signal distortion at medium power.

Part Number	Frequency Range (GHz)	Gain (dB)	OP1dB (dBm)	NF (dB)	Package
ARF1208	37 – 59	26.5	16.5	2.5	Bare Die
ARF1207	57- 71	24	23	5	Bare Die
ARF1206	71 - 86	20	12	2.5 at 71 GHz 3.5 at 86 GHz	Bare Die
ARF1303	DC - 60	15	21	3.5 at 20 GHz 4.8 at 40 GHz	Bare Die

LEARN MORE AT BOOTH 510 AT IMS2004 & ALTUMRF.COM

INFO@ALTUMRF.COM | +31 (0) 40 2390 888 | TWINNING CENTER, DE ZAALE 11, 5612 AJ EINDHOVEN, THE NETHERLANDS the nominal noise figure, along with noise figure performance in response to a varying source impedance. This plot allows the user to determine DUT sensitivity varying antenna impedance and this can be valuable for active/advanced antenna systems.

Including S-parameters, power and noise into a single inline calibration standard in the test leads between the DUT and test equipment helps eliminate interconnect error and could dramatically decrease the calibration and testing time per DUT. In some cases, S-parameter, power and noise calibration testing are done at different test stations by different operators or as part of a series of calibrations and tests. An inline calibration unit with S-parameter, power and noise calibration and testing features would allow these tests to be done in a single location and under virtually the same conditions. This can help eliminate testing variances that could cause false failures or false passes for DUTs by establishing a consistent baseline that eliminates the need to account for different test stations, operators or the time required to perform traditional multi-domain testing.

Automation Accelerates Test and Eliminates Operator Error

The next challenge is automating part and material handling, along with interconnect. These are two separate challenges that have many closely related dependencies. How a part or material is handled and how accurately it can be placed influences the required tolerances of an automated interconnect system. Generalized robotic systems that use artificial intelligence and machine learning systems to ensure accurate and reliable connections over a wide range of tolerances are possible. However, these systems are costly and require substantial development resources and a long development cycle. For many applications, it may be more efficient to use a precision part or material handling system that uses alignment features like a cassette or plate. Alignment features for part handling simplify the robotic system so that it only needs to consider a range of tolerances along specific axes. In robotics applications, limiting the number of axes of movement results in simpler and less costly developments. Single-axis robotic systems can be easily developed to accommodate tolerances as low as 10s of micrometers. Greater precision can be achieved at higher costs and development time. ***Figure 2*** shows an example of an automated fixture with robotic interconnect and handling features for a high frequency module that includes thermal environmental controls.

Robotic interconnect systems for coaxial interconnect can solve the challenges of reliability and repeatability in blind mate connectors. These systems are well-suited to probe technologies like probe heads and pogo pins or pogo probes. Practical tests have demonstrated that robotic systems can achieve similar, or better, levels of repeatability and reliability with blind mate coaxial connectors when compared with precision-threaded coaxial connectors installed by an experienced operator. ***Figure 3*** shows the setup for this experiment. The vectorial differences of the S-parameters are captured using this test setup and compared over frequency. After a reference measurement is made, the connection is cycled and another set of measurements is made. The process was repeated for 200 cycles and the complex difference is then computed and the magnitude, in dB, of that complex difference is analyzed. ***Figure 4*** shows the S-parameter results.

A repeatability value of -50 dB

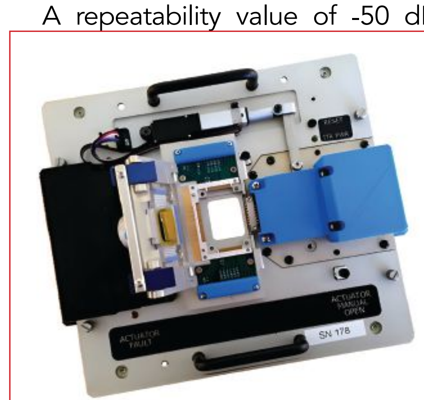

Fig. 2 **Automated fixture with robotic interconnect and handling features.** ***Source:*** **ATE Systems Inc.**

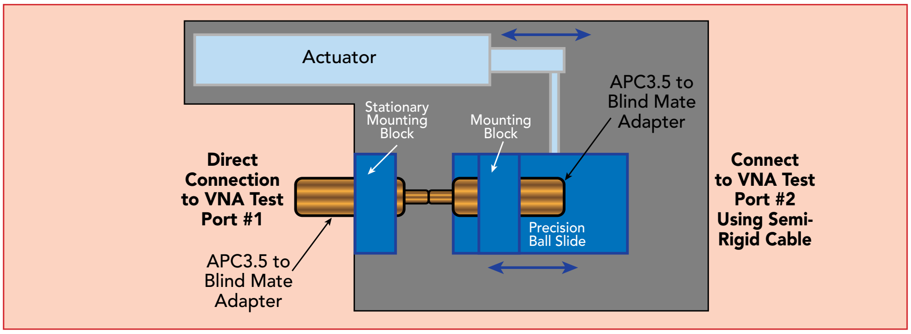

Fig. 3 Test setup using a robotic actuator.

is generally acceptable and comparable with threaded coaxial connectors of a comparable size and engagement method. This metric is possible using a robotic interconnect technique with blind mate connectors. The data from this experiment showed a worst-case repeatability better than -60 dB and a worst-case transmission phase repeatability of 0.17 degrees. To achieve this level of reliability and repeatability using automation requires precision alignment in all axes, including depth of insertion and insertion force. Performing such a feat over many cycles is typically challenging, if not impossible, for a human operator.

A complete fixture for communi-

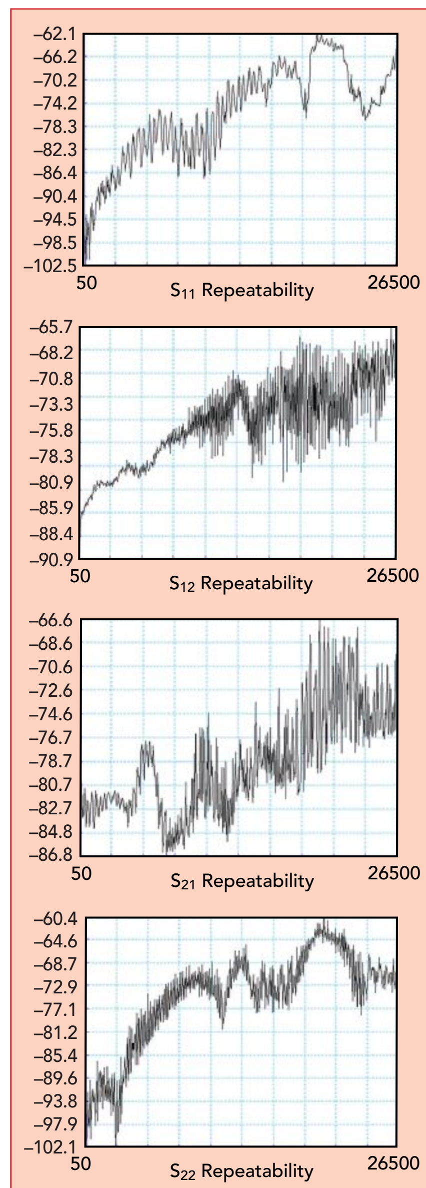

Fig. 4 S-parameter repeatability results.

cations and radar/sensing systems requires more than RF interconnects. These systems typically require interconnects for digital I/O, DC/AC power, bias voltages and currents, analog I/O and potentially, other test ports and features. All these electrical stimuli and signals, along with thermal and other environmental conditions must be accounted for during testing. In many cases, the DUTs require shielding, depending on the proximity of other test systems, production equipment and electrical systems that could interfere with the quality and repeatability of the testing.

DESIGNING FOR INLINE CALIBRATION AND TEST AUTOMATION

With automated fixturing and interconnect engagement complementing inline calibration technology, it is possible to design completely automated test systems with optimally-designed cable management, shielding and environmental controls that ensure the desired testing environment to a high level of reliability and repeatability. Achieving the same performance and capability from a test system that relies on human operators would be much more difficult. The automated system minimizes the interconnect lengths between the test equipment and the DUT. This is critical for the dynamic range of high frequency test systems that have high conductive and dielectric losses in coaxial transmission lines.

However, some considerations must be addressed to enable a high degree of automation. With inline calibration technology available, test designers must include APIs and other software tools for inline calibration in the test process programming. While this will likely involve a learning curve, it should not be significantly different from the learning curve associated with an eCal system. A custom automated test rack and fixture with robotic handling and interconnect for a microwave radar board is shown in ***Figure 5***. The key interconnect and calibration elements are in a shielding box that enhances the overall test fidelity in noisy production and test environments.

The most cost- and time-efficient approach to automated part/material handling and interconnect would include a custom test fixture that enables automatic interconnect engagement. Such a system would

Fig. 5 Automated test rack and fixture with robotic handling and interconnect. *Source:* ATE Systems Inc.

benefit from a precision-machined housing as the carrier for the interconnect. To minimize interconnect tolerances for laminated parts such as PCBs, the carrier must include some type of precision guides for surface-mount connectors that are "floated" during the reflow process. Achieving a tolerance of a few thousandths of an inch in the DUT interconnect position requires precision alignment throughout the production process. If these features are not already included, they must be developed. Though modern blind mate interconnects, such as G3PO, can have pitches on the order of tens of millimeters, it may be necessary to increase the pitch of the connector ports to allow them to comply with the robotic interconnect engagement system requirements. With these constraints, it is advisable to consider automated testing during the part and material development process to minimize the automated system development effort, cost and time.

CONCLUSION

The accelerating advancement of communications and sensing/radar technology, along with the heightened pressures this evolution is placing on production tests, are strengthening the argument for additional automation in RF calibration and testing. There are clear advantages to automating RF communication and sensing calibration and testing for many applications where test throughput and yield are critical metrics. The value of test automation increases with the value of the DUT, as errors during calibration and testing can result in parts being passed or failed at much higher rates with human operators than with properly designed automation. Though systems that are complex enough to warrant this degree of automation have traditionally been used only for military, government, space and aerospace applications, there is a growing need for enhanced testing automation for New Space communication and sensing systems and AAS applications, such as satellite-to-user terminals and 5G/6G communications. ■

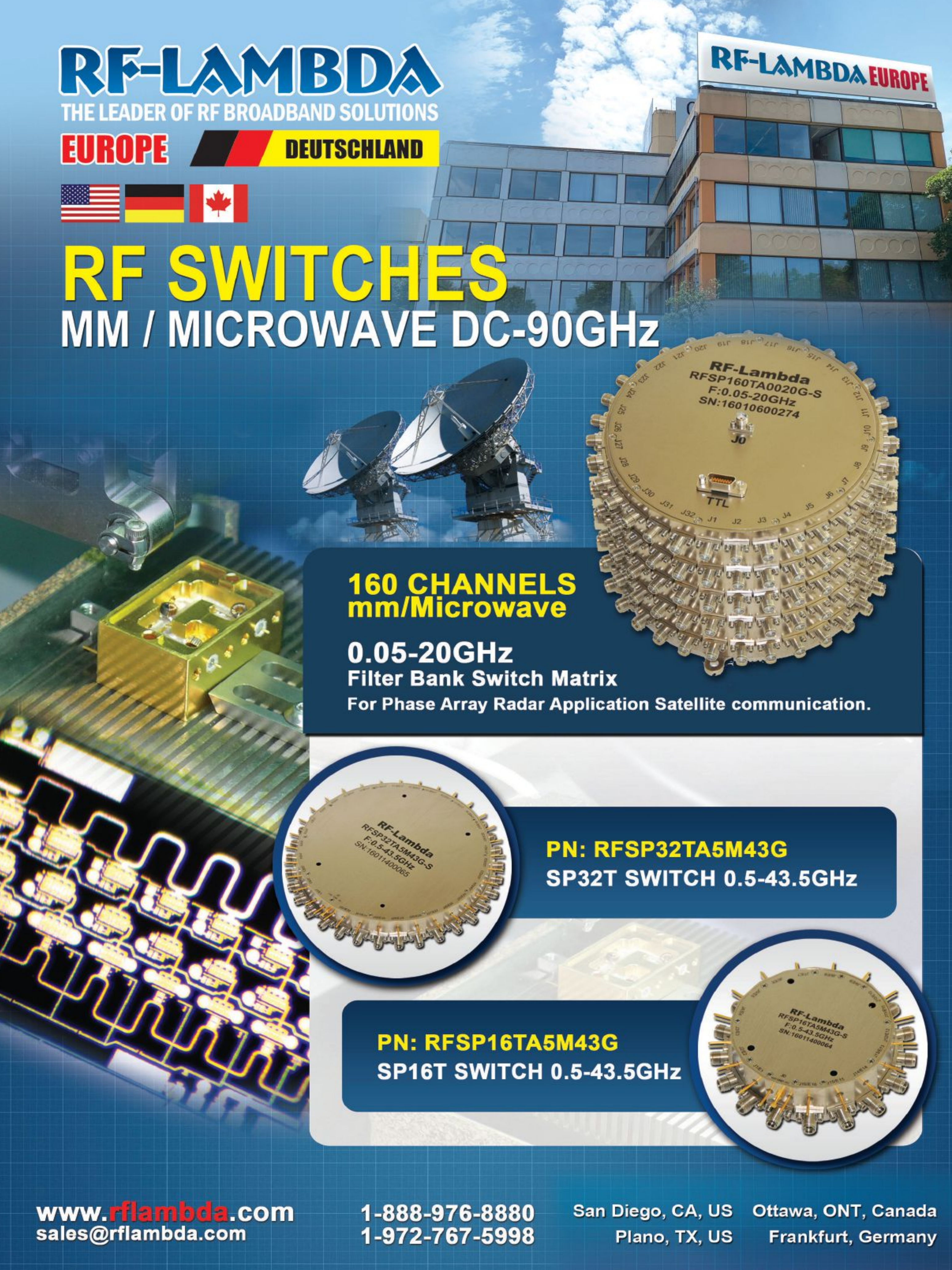
RF-LAMBDA
THE LEADER OF RF BROADBAND SOLUTIONS
EUROPE
DEUTSCHLAND
RF-LAMBDA EUROPE
RF SWITCHES
MM / MICROWAVE DC-90GHz
RF-Lambda
RFSP160TA0020G-S
F:0.05-20GHz
SN:16010600274
J0
TTL
160 CHANNELS
mm/Microwave
0.05-20GHz
Filter Bank Switch Matrix
For Phase Array Radar Application Satellite communication.
RF-Lambda
RFSP32TA5M43G-S
F:0.5-43.5GHz
SN:16011400065
PN: RFSP32TA5M43G
SP32T SWITCH 0.5-43.5GHz
RF-Lambda
RFSP16TA5M43G-S
F:0.5-43.5GHz
SN:16011400064
PN: RFSP16TA5M43G
SP16T SWITCH 0.5-43.5GHz
www.rflambda.com
sales@rflambda.com
1-888-976-8880
1-972-767-5998
San Diego, CA, US
Plano, TX, US
Ottawa, ONT, Canada
Frankfurt, Germany

Emerging Microwave Heating Applications Incorporate Solid-State Semiconductors

John Lee
RFHIC, Gwacheon, South Korea

The concept of using RF energy to heat materials is not new. Bell Telephone Laboratories was issued a patent in 1937 that addressed an invention that would uniformly heat a mass through dielectric loss in response to a high-power RF signal.[1] This method, called dielectric heating, has proven useful for materials that are poor electrical conductors. A similar technique, called induction heating, is used in materials that are good electrical conductors.

In induction heating, an electromagnetic (EM) field created by an RF source excites electrical currents in the material that lie within the EM field of the inductor. Because the material will have resistance, these currents heat the object. The amount of heat generated depends on the magnitude of the induced currents, the resistance of the material and the duration of the magnetic field.

In dielectric heating, materials with poor electrical conduction are placed in a varying RF EM field. Typically, these systems will have two metal plates that serve as electrodes and the material between these two plates forms a capacitor. The heat results from electrical losses in the dielectric material forming the capacitor. The advantage of dielectric heating is that the dielectric is uniform, resulting in uniform heating throughout the object. In the specific case of materials containing water, the RF generator creates an alternating electric field between the two electrodes. The polar water molecules in the material will reorient in response to the varying polarity of the electric field and the friction resulting from this molecular movement results in heat. This is the basis for the microwave oven, which was developed just after World War II in 1945.

Given the heritage of industrial RF heating applications and microwave ovens, these early models derived the RF energy required for heating from tube-based sources. Tubes will generate the necessary RF power, but they have disadvantages. The tubes are physically large, meaning single application points for the heating systems. EM wave interference can easily lead to hot and cold spots within the heating chamber as waves interfere constructively and destructively. The tubes typically operate from extremely high voltages and the tube is an emissive technology, meaning that an electron beam is generated from the source and amplified, limiting the lifespan of the tube. As these applications evolve, vacuum tubes are still widely used as power sources, but


TEMPERATURE CONTROLLED
Trexon brands offer a variety of cryogenic connectivity solutions. Milli-Kelvin specified superconducting and standard cables and cable assemblies, connectors, high density connectors, adaptors, hermetic adaptors, attenuators, hardware and sticks/inserts.
TREXON
Designed for Durability. Engineered for Excellence.

solid-state solutions are emerging as competitive alternatives.

Solid-state semiconductor devices alleviate many of the issues of vacuum tubes in RF energy applications. The devices themselves are small and voltages can be much lower. This means an RF heating device can have multiple application points within the heating chamber. This provides a much more uniform heating environment. Unlike the tubes, solid-state devices can be set to intermediate output powers and these power levels can change over time and in response to sensor feedback to provide an optimized heating profile. Most importantly, the lifespan of a solid-state source is measured in years and not cycles.

While consumer-grade microwave ovens remain the most attractive applications because of the volume of the opportunity, less cost-sensitive industrial applications are proving to be early adopters of solid-state technology for RF heating. The performance of GaN devices, particularly power density, in RF heating applications is giving this technology a competitive edge. Solid-state technology, in general and particularly GaN technology, is enabling new RF heating applications and new performance standards in existing RF heating applications.

One of these applications is pyrolysis. Pyrolysis is the process of heating an organic material, typically in the absence of oxygen, to temperatures above the decomposition temperature of the material. At these temperatures, chemical bonds in the molecules of the material will break and the fragments usually become smaller molecules. This is the process used to produce charcoal from wood and it has been in use for quite some time. Ancient Egyptians are believed to have obtained embalming fluid from the pyrolysis of wood.[2] New applications of this process and how GaN is enabling these new developments are leading to exciting and innovative opportunities.

Marine vessels, particularly cruise ships, generate a lot of carbon-based waste. A 2022 article in Reuters estimates that a typical cruise ship will generate more than one ton of solid waste every day that it sails.[3] With cruising exceeding pre-pandemic levels and new ships getting even larger, this problem will only get worse. While cruise ships are the most obvious example of this issue, it exists in all marine vessels.

THE PATH FORWARD

Vow, a Norwegian company devoted to converting biomass and waste into other resources and alternative energy sources, has partnered with RFHIC through their subsidiary, Scanship. The purpose of this partnership is to develop an innovative, microwave-assisted pyrolysis (MAP) system for waste management. The centerpiece of the pyrolysis system is RFHIC's 30 kW, GaN solid-state microwave generator system. The RIK0930K-40TG is a full rack-mount system operating from 900 to 930 MHz with eight solid-state power amplifier (SSPA) shelves, a

0.6~7.25GHz

High Accuracy Butler Matrices

NEW

ONE MODEL COVER 5G NR(FR1) / WiFi 6E Freq. Bands

Excellent Phase Accuracy & Amplitude Unbalance

Low VSWR / Low I.L. / High Isolation

Good Stability & Repeatability

P / N	Structure	Freq. Range (GHz)	VSWR Max. (:1)	Insertion Loss* Max. (dB)	Amplitude Unbal. Max. (dB)	Amplitude Flatness Max. (dB)	Phase Accuracy Max. (Deg.)	Isolation Min. (dB)
SA-07-4B006073	4x4	0.617-0.96	1.4	8.2	±1.1	±0.8	±11	17
		1.427-2.69	1.5	8.7	±1	±1	±10	14
		3.3-5	1.5	9.2	±1	±1	±12	14
		5.15-7.25	1.6	9.8	±1.1	±1.1	±12	13
SA-07-8B006073	8x8	0.617-0.96	1.4	12	±1.5	±1.4	±13	17
		1.427-2.69	1.5	13.2	±1.4	±1.6	±12	14
		3.3-5	1.5	14.6	±1.4	±1.6	±14	14
		5.15-7.25	1.6	15.9	±1.5	±1.7	±14	13

*Theoretical Insertion Loss Included

— Typical Test Curve** —

SA-07-4B006073

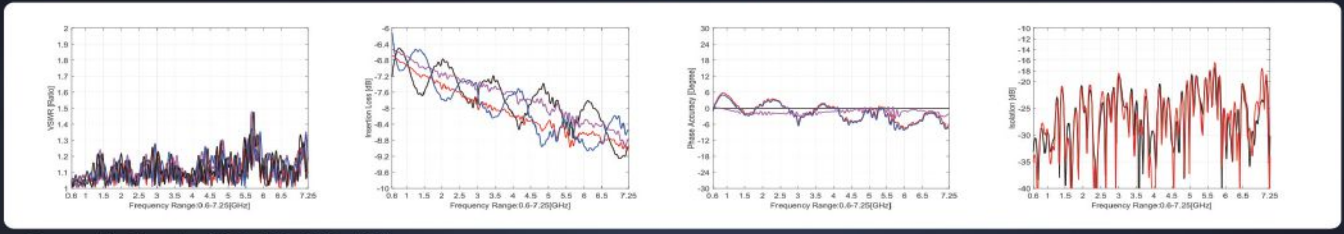

**Corresponding Channels: A1B1、A1B2、A1B3、A1B4

More Information-
Scan the QR Code

MIcable Inc.
www.micable.cn sales@micable.cn +86-591-87382856

Fig. 1 **RFHIC RIK0930K-40TG 30 kW system.**

Fig. 2 **Royal Caribbean's Icon of the Seas.**

power supply unit, a main control unit and a WR975 waveguide output port. The rack-mounted system is shown in ***Figure 1***.

In addition to cruise ships, Scanship also addresses aquaculture and land-based industrial industries. In the cruise segment, Scanship has ongoing deliveries of waste systems for a total of 31 cruise ships that have entered service since 2017. As an evolution of the technology, Scanship has developed a MAP system, using the techniques previously described to convert carbon-based waste into valuable biofuels and energy. Scanship's system, incorporating the RFHIC microwave generator, has recently been installed on the Icon of the Seas. This ship, shown in ***Figure 2,*** accommodates 7600 passengers and the

Fig. 3 **(a) Overview of Scanship's MAP system. (b) The MAP system chamber. (c) Biochar produced from the MAP system.**

total capacity reaches nearly 10,000 when the crew is included. With occupancy reaching these levels, the efficiency and capacity of the waste management system becomes of paramount concern.

THE MICROWAVE-ASSISTED PYROLYSIS SYSTEM

A functional diagram of the MAP system is shown in ***Figure 3a***. This system is part of the complete ship waste management system. Biowaste is collected and converted into pellets, as shown in the upper left corner of the diagram in Figure 3a. From here, the pellets flow into the reactor where the RFHIC microwave generator enables the pyrolysis process. Out of the reactor comes biochar, a valuable biofuel with many industrial uses. Additionally, residual gases that are formed during the process are converted into electricity or steam for further use. The leftover biochar is available to be used in many useful applications. The actual Scanship system, containing the RFHIC microwave generator is shown in ***Figure 3b*** and the leftover biochar is shown in ***Figure 3c***.

MAP System Challenges

In the initial phases of developing their MAP system, Scanship tried using magnetrons as the components for microwave generation. However, they encountered the following challenges:

Inconsistent and non-uniform heating patterns: Magnetrons have inherent issues with providing a stable source of microwave power because of their difficulty in providing a stable frequency signal. Factors such as temperature fluctuations, wear and tear from prolonged use and variations in power supply can cause unexpected shifts in magnetron frequencies. Additionally, due to their fixed resonant structure, magnetrons provide limited control over both frequency and phase.

In the initial versions of Scan-

ship's MAP system, the magnetrons not only failed to uniformly heat the organic waste, but they also inflicted damage to delicate components caused by the constantly shifting magnetron frequencies. In particular, the spurious harmonics caused electric discharges, which continuously damaged the windows of the pyrolysis chamber. In addition to creating system damage, these discharges adversely affected the quality of the biochar and renewable gas produced.

High failure rate over time: Magnetrons typically have short lifespans, lasting from 4000 to 6000 hours of operation. In addition to their limited lifespan, the magnetrons operate at extremely high voltages, often reaching up to 20,000 volts. Because of these factors, users frequently found themselves replacing malfunctioning magnetron units, as well as associated components like circulators, diodes and launchers.

The need for frequent replacements not only escalated operating expenditures, but it also partially offset the magnetron cost savings. In addition, Scanship's MAP systems are designed to be most useful when the cruise ship is at sea, during a voyage. A failure of magnetron units in the pyrolysis system meant that all operations would come to a halt until the components could be replaced on land. This interruption would result in the ship using backup systems and this reduces efficiency and increases operating costs. An image of a failed magnetron from a MAP system is shown in ***Figure 4.***

THE SOLUTION: REPLACE THE MAGNETRONS

RFHIC was able to solve the issues Scanship was having with the magnetrons by replacing them with the RFHIC RIK0930K-40TG microwave generator that uses GaN-on-SiC solid-state technology for RF power amplification. This system offers 30 kW of output power over the 900 to 930 MHz frequency range. The RF PAs in the RIK0930K-40TG use RFHIC's internal GaN-on-SiC

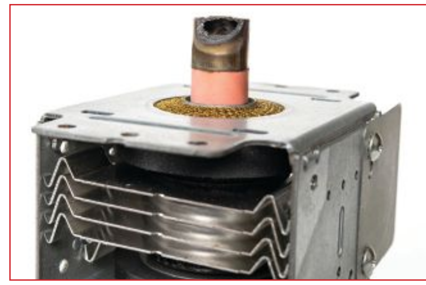

▲ Fig. 4 **High voltage magnetron failure.**

process. The system comes fully equipped with a three-phase 380 VAC power supply unit, a control module and eight SSPA shelves. ***Figure 5*** shows RFHIC's microwave generator installed into Scanship's MAP system.

In addition to the other benefits mentioned, RFHIC's RIK0930K-40TG provides precise digital control of both frequency and phase. This is a feature that cannot be matched by magnetrons and this allows the Scanship MAP system to adjust the operating environment depending on the composition of the organic waste. The microwave

generator also achieved more uniform and consistent heating patterns, allowing the pyrolysis system to process higher volumes of waste in a shorter time. These added features are enabled by RFHIC's software. ***Figure 6*** shows a representative display of the software used with the microwave generator that is part of Scanship's MAP system.

The RIK0930K-40TG operates at 50 V, which is much less than the magnetron-based systems that it replaces. It boasts an average lifetime of around 50,000 to 100,000 hours. Each of the eight PA shelves incorporates a redundancy feature to ensure a smooth and gradual decline in performance. In the event of a malfunction occurring in one or two shelves, the microwave generator will continue to function correctly until those shelves can be replaced. The generator is also equipped with hot-swappable power supply units which allows the users to replace any failed packs even while operating.

Fig. 5 RIK0930K-40TG mounted in the ship.

Fig. 6 Control software for the microwave generator.

THE KEY BENEFITS OF RFHIC'S SOLID-STATE GAN TECHNOLOGY

Consistent and Uniform Heating Patterns

RFHIC's GaN-based solid-state microwave generator produces uniform and consistent heating patterns. This feature is essential to enabling the pyrolysis process and

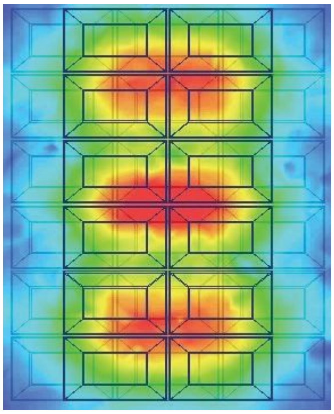

Fig. 7 Microwave heat distribution model.

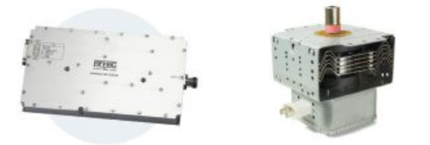

	GaN Solid-State MW	Magnetron
Average Lifetime	50,000 - 100,000 Hrs	4,000 - 6,000 Hrs
OPEX Cost	Low	High

Fig. 8 GaN comparison to magnetrons.

effectively heating the carbon-based waste produced onboard. ***Figure 7*** shows the heat distribution model at 915 MHz and 30 kW of output power.

The GaN-based generator maintains much better frequency stability than the magnetron-based microwave generator. This prevents the unexpected damage to connected components including chamber windows that the magnetrons caused. As a result, these improvements in microwave generation enable higher yields of biochar and renewable gas from the system using GaN PAs. The microwave pyrolysis process described in this article can be used to produce various types of renewable gasses, including hydrogen, syngas and more.

Increased System Lifetimes and Stability

As mentioned, solid-state amplifiers have much better lifetimes than tube-based amplifiers. This is certainly the case for RFHIC's GaN solid-state microwave generator. ***Figure 8*** shows a quantitative comparison of the lifetimes, along with the qualitative comparison of OPEX for the RFHIC solid-state solution versus the magnetron that was previously used in this application.

In addition to the performance and cost advantages, the built-in redundancy feature that the size and weight of the GaN amplifiers allow the microwave generator to continue operating in case one of the PA shelves fails. This adds flexibility in both system design and operation. This feature significantly reduces system malfunctions, which further reduces maintenance and operating costs.

A SUSTAINABLE FUTURE IN MICROWAVE PYROLYSIS

The collaboration between RFHIC and Scanship represents a significant step forward in waste management. With RFHIC's GaN-on-SiC solid-state microwave technology, Scanship has been able to overcome the limitations of conventional magnetron systems, paving the way for more effective and environmentally friendly waste conversion processes. As the world continues to seek cleaner and more sustainable waste treatment solutions, GaN and solid-state microwave technology serve as a compelling enabler for a greener future. ■

References

1. J. G. Chaffee, U.S. Patent US2147689A, Web: patents.google.com/patent/US2147689.
2. J. Koller, U. Baumer, Y. Kaup, M. Schmid and U. Weser, Ulrich, "Analysis of a Pharaonic Embalming Tar," *Nature*, October 2003, 425 (6960): 784. doi:10.1038/425784a. ISSN 1476-4687.
3. C. Palmer, "Cruise Industry Faces Choppy Seas as It Tries to Clean Up Its Act on Climate," *Reuters*, July 2022, Web: reuters.com/business/sustainable-business/cruise-industry-faces-choppy-seas-it-tries-clean-up-its-act-climate-2022-07-27/.

Solutions That Are Above and Beyond

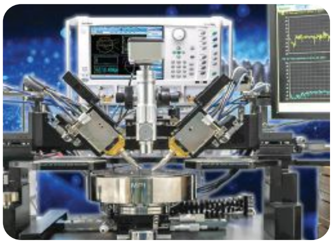

4-Port VectorStar 220 GHz
ME7838x

Single Sweep 4-port, 70 kHz to 220 GHz VNA/SPA with Differential Probes

Building on more than 40 years of design experience, Anritsu has broken the millimeter-wave barrier with the VectorStar ME7838x series VNA/SPA. RF and microwave engineers now have access to a powerful measurement tool for performance analysis of devices ranging from transistors in an on-wafer environment to communication systems.

Rubidium™
MG362x1A

The Source of Purity, Power, and Stability Up to 70/72 GHz

Signal purity, output power, and frequency stability are essential distinguishing characteristics of a high-frequency microwave signal generator. The Rubidium MG362x1A signal generator product line is built to deliver outstanding signal purity and frequency stability across a broad frequency range, even at high output power levels.

Power Master™ MA245xxA
Spectrum Master™ MS2760A

USB-powered mmWave Analyzers

The ultraportable Power Master MA245xxA is a power analyzer that provides simple, numeric and frequency selective average RF power measurements from 9 kHz up to 110 GHz and power range coverage as low as –90 dBm.

The Spectrum Master MS276xA (9 kHz to 170 GHz) provides a unique insight into FMCW radars. The zero span display enables the measurement of pulsed signals in time domain for pulse width and pulse flatness measurements. The small form factor of these ultraportable analyzers eliminate the need for test port cables, enhancing accuracy and ease of use.

Thin Film Fabrication

Custom Substrate Fabrication

The Anritsu Microelectronics Fabrication Center Build-to-Print Thin Film Substrate Services helps customers actualize their thin film substrate designs, from the initial low volume prototyping design phase to full-on high-volume manufacturing. Our Quality Assurance Program is ISO9001 certified, ITAR/ROHS/REACH compliant, and meets most existing military and aerospace requirements. Our inspections meet MIL-STD-883 for 100% visual inspections and MIL-STD-105D Level II sampling for final QA inspection.
Visit: www.anritsu.com/en-us/thin-film-microelectronic-assembly

Precision RF and Microwave Components to 110 GHz

41W Series
Fixed Attenuators
Metrology grade calibration and characterization for precision measurements

W241A
Power Splitter
Symmetrical two-resistor design accurately divides orientation-specific signals

W255MF
Bias Tee
Low insertion loss and very high return loss – ideal to bias Optical Modulators and Broadband Data Drivers

MN25110A
Directional Coupler
10 dB coupling for best repeatability and performance

W240A
Power Divider
Symmetrical three-resistor design accurately divides or combines signals

W252FM
Kelvin Bias Tee
Excellent DC and RF performance eliminates DC biasing errors

Anritsu
Advancing beyond

Discover how you can achieve measurement confidence with Anritsu.
Learn more at **www.anritsu.com/test-measurement**
Visit our booth at IMS

INVITED PAPER

Selecting the Best ADC for Radar Phased Array Applications: Part 2

Benjamin Annino
Analog Devices, Wilmington, Mass.

Many papers discuss the system trade-offs and relative merits of digital, RF and hybrid beamforming.[1] Building on prior work, this article uses RF-to-ADC cascade modeling to show dynamic range (linearity and noise) and sample rate trade-offs versus DC power consumption in a multichannel system with varying channel summation in both the RF and digital realms. The optimal selection of sample rate, ADC effective number of bits (ENOB) and RF versus digital channel combining is weighed against DC power consumption. The popular Schreier and Walden ADC figures of merit (FOMs) are proposed as extensible to a multichannel system to express a single system FOM portraying optimal dynamic range normalized for DC power considerations. The article has two parts: Part 1, published in the January 2024 edition of *Microwave Journal*, explains the method of modeling the system and Part 2 analyzes the results and draws conclusions from system FOMs.

SYSTEM MODELING RESULTS

The system model results presented in the following plots consist of the attributes and swept variables shown in ***Table 1***.

Sweeping RF Channel Summation

The examples in this section use a subarray size of 64 channels. The horizontal axis in these plots shows the model swept from an all-digital summation on the left (64-channel digital sum, no RF sums) to an all-RF summation on the right (no digital sum, 64-channel RF sum). In between is a blend of digital and analog channel summations, referred to as hybrid beamforming with the RF channel summation increasing from left to right along the x-axis.

Figure 1 shows the system sensitivity versus the number of RF channels summed while ADC ENOB is varied. ***Figure 2*** shows the system spurious-free dynamic range (SFDR) versus the number of RF channels summed while ADC ENOB is varied and ***Figure 3*** shows the system DC power per element versus the number of RF channels summed with the same variation in ADC ENOB. The problem is that viewing sensitivity, SFDR and DC power results individually does not indicate if it is good or bad because performance is portrayed separately from power. For example, maximum SFDR at the lowest possible DC power consumption is the goal, but what configuration of ADC ENOB and RF-to-digital combining is best? The next section is a more useful apples-to-apples comparison, as the results show per-

TABLE 1

MODEL RESULTS

Merit Attribute	*Swept Variables*
SFDR	ADC ENOB; Blend of RF sum to digital sum, always totaling 64
Sensitivity	
DC Power/Channel	

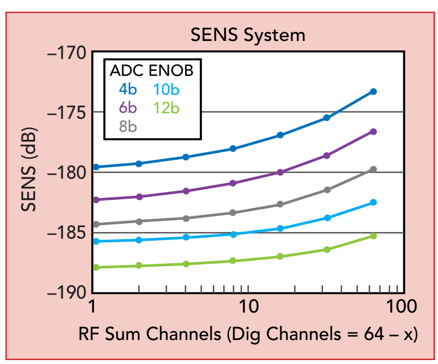

Fig. 1 System sensitivity versus the number of RF channels summed.

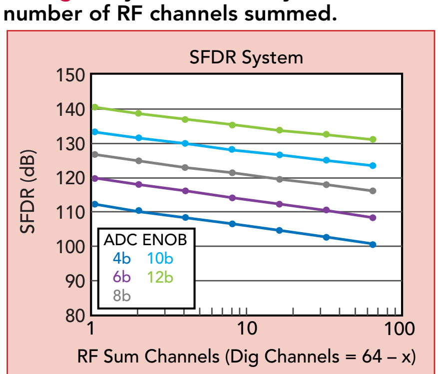

Fig. 2 System SFDR versus the number of RF channels summed.

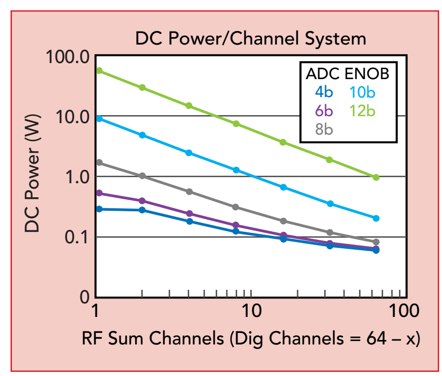

Fig. 3 Overall DC system power per element versus the number of RF channels summed.

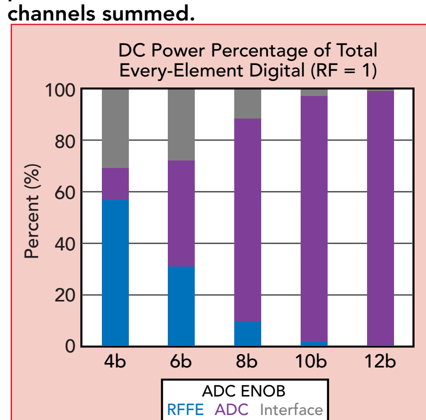

Fig. 4 DC system power from RFFE, ADC and digital summation when every element is digital.

Take Control.

Choose Powerfilm surface mount resistives from Inmet by Spectrum Control for your next RF-to-mmWave project.

- Best-in-class passive resistive components for high-frequency (1 to 50 GHz) and high-power (1 to 1000 W) applications
- Alumina, BeO, and AIN substrate options
- Control signal levels and improve impedance matching, and variable-level control
- MIL-PRF-55342, MIL-PRF-55182, MIL-PRF-8833

We will work with your team to determine the right match for your design.

Ask about the Powerfilm SMT attenuator design kit.

SPECTRUM CONTROL

RFMW®

RFMW.com/powerfilm

Visit us at IMS IMS

RFMW booth 1029; **Spectrum Control** booth 208 formance with the dynamic range normalized for DC power consumption.

Sweeping ADC ENOB

The plots in this section show the results of sweeping ADC ENOB for combinations of beamforming architectures. Trends in DC power and performance (SFDR and SENS) are analyzed as these parameters are swept. The figures in this section show the relative percentage of power consumed by the RF front-end (RFFE), ADC and the digital summation/interface. ***Figure 4*** represents the digital beamforming case, where every element is digital. ***Figure 5*** shows the same results for a hybrid system architecture that sums 16 RF channels and ***Figure 6*** shows the results for a large RF subarray that uses hybrid beamforming with 64 RF channels summed.

Unsurprisingly, the results show that the contribution of the digital interface and summation functions become more important as the number of digital elements increases. Figure 4 shows a large proportion of the overall power consumption can be attributed to the digital interface at the lower bit resolution values, but this decreases rapidly as bit resolution increases. However, for systems with higher RF channel summations, the digital interface is less significant. Another trend is that the RFFE is dominant at low ADC bit resolutions, but the ADC is dominant at high ADC bit resolutions. These plots show the big impact ADC ENOB and the RF-to-digital channel summation ratio have on DC power consumption.

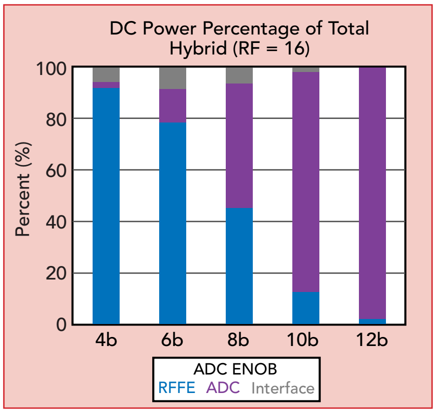

Fig. 5 DC system power from RFFE, ADC and digital summation for a medium-sized RF subarray.

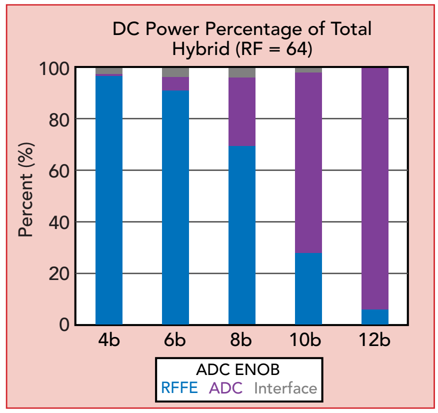

Fig. 6 DC system power from RFFE, ADC and digital summation for a large RF subarray.

Normalizing SFDR and Sensitivity

Next, the relative merits of SFDR and sensitivity are normalized for DC power/channel. This analysis is performed for different ADC ENOB and RF-to-digital channel summation schemes. ***Table 2*** lists the swept variables and markers on each trace for the plots in this section.

The plots of sensitivity (Figure 1), SFDR (Figure 2) and DC power versus RF-to-digital channel summation (Figure 3) are rearranged to better visualize performance trends

TABLE 2
AGGREGATED RESULTS COMPARISON

Attribute	Swept Variable	Markers on Each Trace
SFDR; sensitivity	DC power/channel Blend of RF-to-digital sum, always total = 64	ENOB increasing left to right 4b to 12b by 2b
SFDR; sensitivity	DC power/channel ADC ENOB	Blend of RF: digital sum, total = 64. 64:1 all-RF sum on left, going 32:2, 16:4, 8:8, 4:16, 2:32, ending 1:64 all-digital on right

when normalized for DC power. ***Figure 7*** and ***Figure 8*** show SFDR and sensitivity versus DC power for a few fixed RF-to-digital summation examples. The discrete bit resolution values are shown on the RF = 1 curve and the variation in ENOB along the curves remains the same for the other RF channel summation curves.

Figure 9 and ***Figure 10*** show the same underlying data arranged a bit differently. In this case, the traces represent ENOB values from 4 to 12. On each curve, the RF-to-digital summation varies along the trace, ranging from an all-RF sum as the first point on the left of the curve to an all-digital sum on the right of each curve. The advantage of presenting the data in this format is that performance versus DC power conclusions can now be drawn from the plots.

Table 3 summarizes the conclusions from the plots. In general, for the same SFDR and sensitivity, hybrid beamforming systems em-

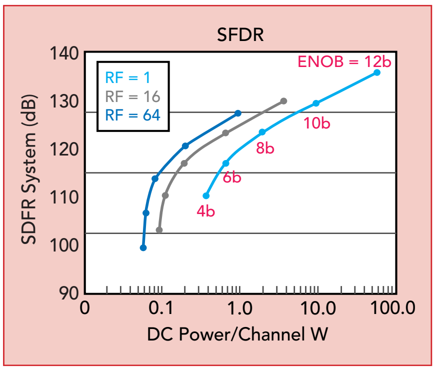

Fig. 7 SFDR versus DC power/channel for different RF-to-digital summations.

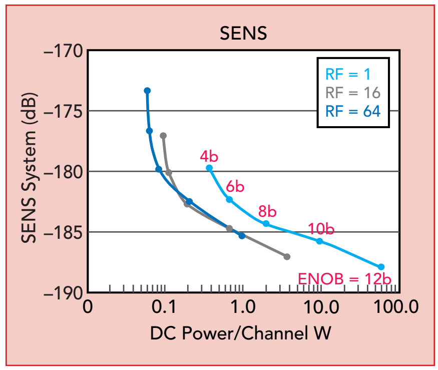

Fig. 8 Sensitivity versus DC power/channel for different RF-to-digital summations.

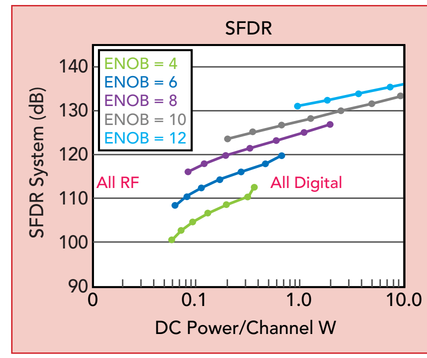

Fig. 9 SFDR versus DC power/channel.

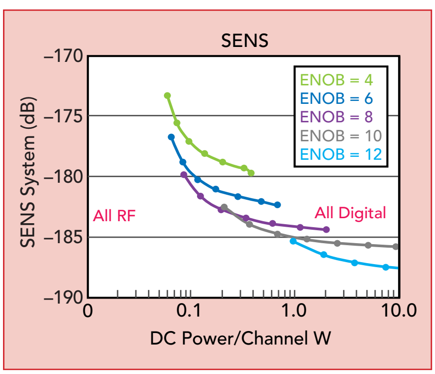

Fig. 10 Sensitivity versus DC power/channel.

TABLE 3

CONCLUSIONS FROM PLOTS

Topic	Observation	Why?	Conclusion
Best RF: digital summation?	Increasing RF sum is beneficial in reducing system DC power for the same SFDR and SENS	Fewer ADCs and lower linearity are needed at RFFE (lower DC power)	Use the highest possible RF summation that meets beam-related objectives. There is a rapid benefit with RF subarray sizes of RF = 2 to 16, but this slows with a subarray with RF > 16
Best ADC ENOB?	SFDR and SENS versus DC power improves rapidly going from ENOB = 4 to 8, then slows	Knee in Figure 7 to Figure 10	ENOB = 6 to 8 offers the best performance versus DC power value

ploying a blend of RF and digital beamforming require an ADC with a higher ENOB versus an all-digital solution. However, these hybrid systems are more power efficient. The plots show a performance sweet spot when SFDR, sensitivity and DC power consumption are evaluated together. Diminishing returns exist as ENOB improves beyond the knee of the curves and values deteriorate fast as ENOB degrades from the knee. Is an all-digital solution better in any of these situations? From a dynamic range efficiency perspective where DC power is handicapped, no. The benefits of an all-digital solution occur in software-defined beamforming flexibility and adaptability but these benefits come at the expense of increased power consumption.

TABLE 4

SOME COMMON OBJECTIVES

Must-Have Objective	Trade-Off	RF: Dig Sum	ADC ENOB	SFDR (dB 1 Hz)	SENS (dBm 1 Hz)	DC Power/ Channel (W)
All-digital beamforming	High DC power	1:64	8.2	127	–185	2
All-digital beamforming < 1 W/channel	Degraded SFDR and SENS	1:64	7.2	124	–184	1
All-digital beamforming ~ 0.25 W/ channel	Much degraded SFDR and SENS	1:64	4	112	–180	0.28
Lowest power	Much degraded SFDR and SENS; Combo of RF and digital BF	64:1 64:1 64:1	4 6 8	101 109 116	–173 –177 –180	0.057 0.061* 0.080
Best possible SFDR and sensitivity at 1 W/channel	Combo of RF and digital BF	64:1 16:4 2:32	12 10.5 8	131 128 125	-185 -185 -184	1 1 1

Table 4 provides a comparison of example scenarios with each having a different design priority. There is no single configuration that satisfies all the requirement scenarios. Different system objectives drive different performance priorities that force performance trade-offs with other attributes.

*Slightly higher, but better value

Table 5 shows a popular ADC ENOB = 8 example assuming practical IF bandwidths. A designer must pay attention to the signal level at the ADC, as the linearity of most ADCs degrades approaching full-scale input. The optimal RF operating level at the ADC increases as processing bandwidth increases. The ADC cannot be operated to full scale, in practice. In Table 5, it is important to note the limitation of the ADC input power and how it varies with IF bandwidth.

EVALUATING SYSTEM RESULTS

It is proposed that the Walden and Schreier ADC FOMs can be used to develop system FOMs to compare performance versus power trade-offs for RF-to-ADC cascades. The goal is to sweep parameters and spot the best value performance normalized for DC power at the system level. In this analysis, the FOMs are presented while:

- Varying RF-to-digital summation, ranging from all-digital to all-RF
- Varying ADC ENOB, linearity and DC power.

The migration from the ADC FOMs to the proposed ADC system FOMs is shown in *Table 6*. The proposed ADC system FOM based on the Walden ADC FOM is unchanged. The Schreier FOM can be modified by swapping SFDR for signal-to-noise and distortion ratio (SNDR) to make an FOM that reflects two-tone linearity performance.


cādence®
Heterogeneous Innovation
Cadence high-frequency design solutions allow you to tackle challenging RF to millimeter wave (mmWave) front-end components and wireless subsystems from concept through signoff in silicon radio frequency integrated circuits (RFICs), III-V compound semiconductors, PCBs, and multi-technology modules. Our leading AI-enabled computational software helps you bring multi-fabric systems to market faster.
Visit Us at IMS in Booth 1321!

TABLE 5

REPRESENTATIVE RESULTS WITH ACTUAL PROCESSING BANDWIDTHS

IF Bandwidth (Processing BW)	RF: Dig Sum	ADC ENOB	SFDR (dB)	SENS (dBm)	RF Input Level for SFDR (dBm)	Pre-ADC Signal Gain (dB)	RF Input Level to ADC (dBm)	DC Power/ Channel (W)
1 MHz	1:64	8.2	87	–125	–37	15	–22	2
10 MHz		8.2	81	–115	–34		–19	
100 MHz		8.2	74	–105	–30		–15	
1 GHz		8.2	67	–95	–27		–12	
1 MHz	4:16	8.2	84	–124	–40	20	–20	0.6
10 MHz		8.2	77	–114	–37		–17	
100 MHz		8.2	71	–104	–34		–14	
1 GHz		8.2	64	–94	–30		–10	

Using these proposed ADC system FOMs and the relationships shown in ***Equation (1)***:

$$SNR_{system} = NSD_{system,input} - Full\ Scale_{system,input} + 10Log(F_{s,Nyq}/2) \quad (1)$$

Where:

$NSD_{system,input}$ = -174 dBm/Hz + NF

SFDR (dB) = 2/3 (IIP3 (dBm) – Sensitivity (dBm))

Sensitivity (dBm) = -174 dBm/Hz + NF + 10Log(IFBW)

T = 290 K

$Full\ Scale_{system,input}$ = input-referenced full scale.

With these assumptions, ***Figure 11*** shows the proposed ADC system FOM developed from the Walden FOM where a lower reading is better per the analysis in Table 6. ***Figure 12*** shows the proposed ADC system FOM developed from the Schreier FOM where a higher reading is better. Both plots show the system FOM plotted versus the RF-to-digital sum ratio.

The phrase "best value" is meant in the sense of best performance for a given DC power consumption. The derived FOMs assist in drawing conclusions about this best value because they normalize performance against DC power consumption. Sensitivity observations are drawn from the Walden-based system FOM in Figure 11 and SFDR observations are drawn from the Schreier-based FOM in Figure 12. ***Table 7*** contains some summary observations for both performance metrics.

CONCLUSION

Performance-critical applications like phased array radar deployments strive to find the optimal balance of sample rate, dynamic range and DC power. Overprioritizing any one of these parameters will result in a suboptimal and possibly bad solution. The era of 20 GSPS to 100+ GSPS ADC sampling is here, but higher sampling comes with a cost for DC power consumption and dynamic range (ENOB), the other two critical performance attributes in the FOM triad. High sample rates are not a design miracle, but a chosen prioritization of sample rate at the expense of higher DC power and lower ENOB. In many cases, the optimal ADC for a phased array system will prioritize dynamic range and DC power, with a sample rate just high enough for frequency planning efficiency and oversampling gain.

High dynamic range, high sample rate data converters with ENOB ~8 are popular choices for phased array radar applications because they


MIL-PRF-83446
MIL-PRF-27
MIL-PRF-39010
MIL-PRF-15305
Custom Designs
In-House Test Lab
MIL-STD-1553
MIL-STD-202
MIL-STD-981
HIGH RELIABILITY.
HIGH PERFORMANCE.
EXTREMELY RUGGED.
The iNRCORE Family of Brands work together to deliver exceptionally reliable electronic components that enable power and signal in the most extreme environments. Whether catalog or custom, our components deliver.
iNRCORE
Family of Brands
www.inrcore.com/brands/ (215) 781-6400
ISO 13485 CERTIFIED
ISO 9001 CERTIFIED
AS9100 CERTIFIED
ITAR
iNRCORE
GOWANDA
TTE
RCD
DYCO
VANGUARD ELECTRONICS
BICRON
Our Products
Broadband Conicals
Chip Inductors
Military QPL Inductors
Ethernet Transformers
Transceiver Modules
RF Filters
EMI/RFI Filters
Capacitors
Resistors
Custom Magnetics
JOIN US AT:
IMS 2024
June 16 - 21, 2024
Booth# 2031

TABLE 6
ADC VS. SYSTEM FOM

	ADC FOMs	ADC System FOM (Proposed)	Units	What's Good?
Walden	$FOM_W = \frac{Power}{2^{ENOB} \times f_{s,Nyq}}$ →	Same	$\left(\frac{fJ}{conv-step}\right)$	Lower is better
	$ENOB = \frac{SNDR - 1.76}{6}$	$ENOB_{system} = \frac{SNR_{system} - 1.76}{6}$		
Schreier	$FOM_S = SNDR + 10Log\left[\frac{f_{s,Nyq}/2}{Power}\right] dB$	$FOM_S = SFDR + 10Log\left[\frac{f_{s,Nyq}/2}{Power}\right] dB$	dB	Higher is better

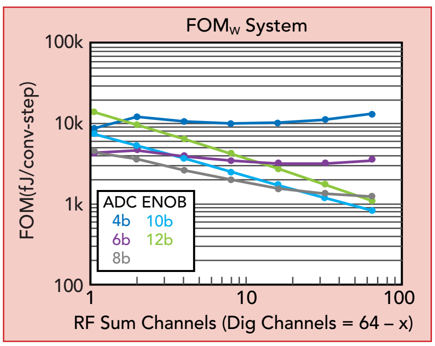

▲ **Fig. 11** **Proposed Walden-based system FOM (lower is better).**

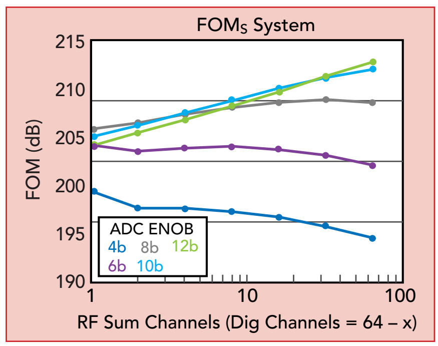

▲ **Fig. 12** **Proposed Schreier-based system FOM (higher is better).**

offer the best compromise between dynamic range and DC power. However, designers should be careful how SNDR (ENOB) is defined and make sure to consider two-tone intermodulation performance with SNDR. Phased array radar ADCs also need high linearity with IP3 requirements typically greater than 22 dBm. When evaluating SNDR, know whether it includes interleave spurs and make sure spectral regions are not cherry-picked.

A system must have a significant

INSULATED WIRE INCORPORATED

Our Re-Flex™ Cables really have the competition bent out of shape...

...because It's cool to be RE-FLEXible

IW's Re-Flex Cables were designed to offer a highly flexible alternative to standard semi-rigid & conformable cables.

IW's unique laminate dielectric, combined with a tin/alloy plated outer braid provide a double shielded, low loss, re-formable cable that eliminates the failure mode of traditional semi-rigid & conformable cables.

Industry standard line sizes provide a range of interconnect options including SMA, TNC, N-type, 3.5mm, 2.92mm, 1.85mm, GPO™ & GPPO™, with standard length SMA male/male assemblies available from 2", in stock.

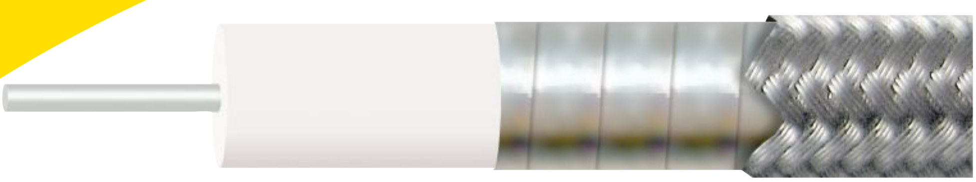

Impedence:	50 Ω	**RF leakage:**	Equivalent to semi-rigid cable
Time delay:	1.4 ns/ft	**Temp range:**	-55˚C to 165˚C
Cut off frequency:	62 GHz for RF 085 34 GHz for RF 141	**Bend radius:**	1/16 inch for RF 085 1/8 inch for RF 141

AS9100 Rev D and ISO9001:2015 certified.

SEE US AT AOC EUROPE
May 13-15
Oslo, Norway
BOOTH B64

SEE US AT IMS 2024
June 18-20
Walter E. Washington Convention Center
Washington, D.C
BOOTH 1312

SCAN THIS CODE
TO FIND OUT HOW YOU CAN GET CONNECTED

We're how the microwave industry **gets connected!**

www.insulatedwire.com
t + 1 631 4724070
e sales@insulatedwire.com

TABLE 7

SUMMARY OBSERVATIONS

Topic	Observations
Sensitivity	The best sensitivity for DC power value occurs at high ADC ENOB (8 to 12) and high RF sum levels.
	ENOB ~6 has merit at low RF sums where the systems are all or mostly digital but decreasing the ENOB value to 4 to 5 is generally worse.
SFDR	SFDR for DC power value is the same for ENOB 6 to 12 when using an all-digital beamforming network. As the dynamic range increases, DC power increases, offsetting each other and holding the FOM constant.
	The best SFDR performance for DC power value occurs at ENOB 8 to 12 and the highest possible RF sum.
	ENOB = 6 is okay in an all-digital network, but when the RF sum increases to 2 or higher, ENOB 8 to 12 is a better solution.
	Over the RF sum range 2 to 8, ENOB 8 to 12 has equal merit.
	At RF sum = 16 and above, ENOB 8 fades in preference and ENOB 10 to 12 is the best choice.
	Worse than the sensitivity case, ENOB = 4 to 5 is always bad for SFDR and it has the worst value of any scenario.

mission-critical requirement to justify the use of high dynamic range, all-digital beamforming because this architecture comes at a steep DC power penalty. The arrays with the best balance of performance and DC power use a hybrid scheme, which is a combination of RF beamforming in subarrays that feed distributed DAC/ADC nodes that use digital beamforming. If beam attributes allow it, a small subarray of RF beamforming in front of each ADC helps improve performance and lowers DC power. RF beamforming is highly recommended for improving SFDR and sensitivity at lower DC power and providing blocker mitigation using beam null steering. Extra power is consumed to achieve the software-defined adaptability of fully digital beamforming.

Over the next five to 10 years, all-digital phased arrays will increase their technology readiness and viability at increasingly better performance. To enable this evolution, new state-of-the-art ADCs will put a greater emphasis on reducing DC power while maintaining sample rate and ENOB. ADC sample rate capability will continue to push higher, but these developments may benefit wideband applications, like electronic warfare, more than phased array applications. The phased array market will determine a sample rate sweet spot, perhaps in the 10 to 20 GSPS range, then the market winners will provide the best ENOB at the lowest power. ■

Reference

1. P. Saha, "A Quantitative Analysis of the Power Advantage of Hybrid Beamforming for Multibeam Phased Array Receivers," *Analog Devices, Inc.*

Microwave Journal

5G/6G SPECIAL**FOCUS**

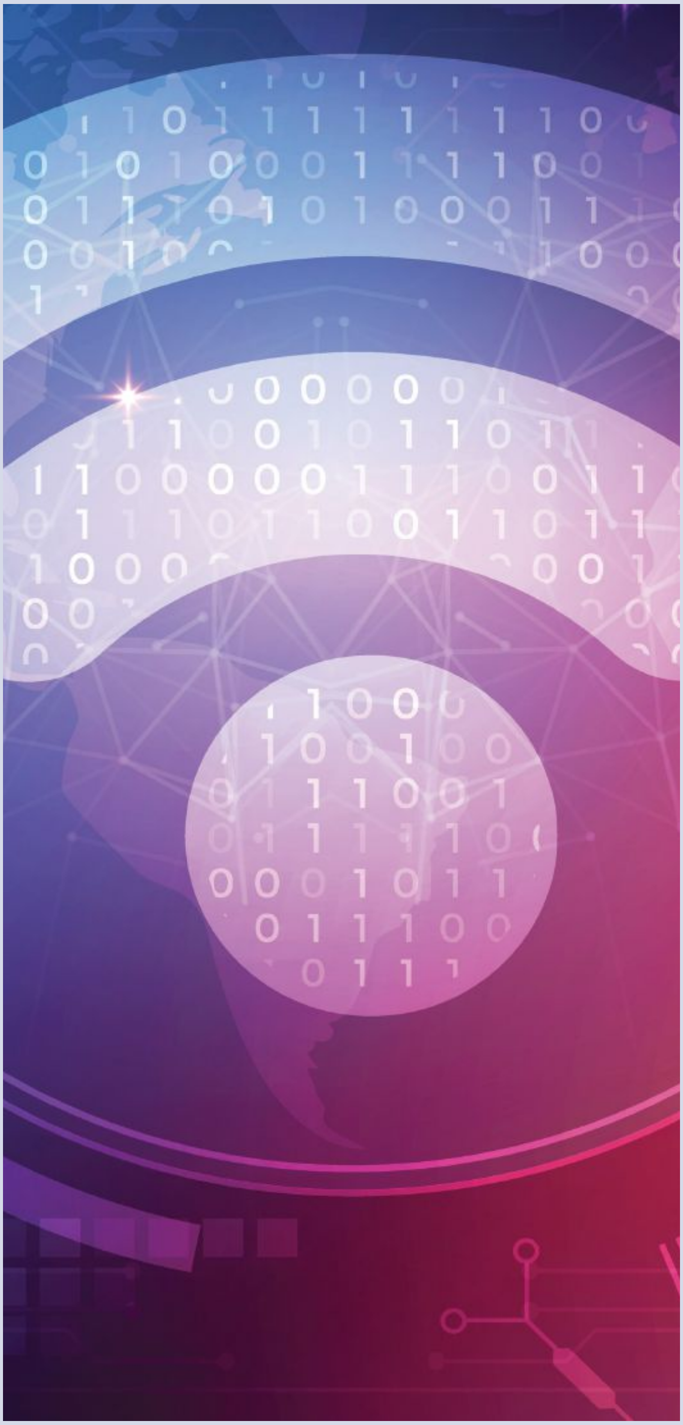

Cover Feature

Perspective

Special Report

Technical Feature

Product Features

Tech Brief

Departments

STAFF

Group Director: Carl Sheffres
Associate Publisher: Michael Hallman
Media Director: Patrick Hindle
Brand & Content Director: Jennifer DiMarco
Technical Editor: Eric Higham
Associate Technical Editor: Cliff Drubin
Editorial & Media Specialist: Kelley Roche
Associate Editor: Kaitlyn Joyner
Multimedia Staff Editor: Barbara Walsh
Electronic Marketing Manager: Chris Stanfa
Senior Digital Content Specialist: Lauren Tully
Digital Content Specialist: Vincent Carrabino
Director of Production & Distribution: Edward Kiessling
Art Director: Janice Levenson
Graphic Designer: Ann Pierce

EUROPE
Office Manager: Nina Plesu

CORPORATE STAFF
CEO: William M. Bazzy
President: Ivar Bazzy
Vice President: Jared Bazzy

Beyond the Bench: Adapting Test and Measurement for 6G in the Age of AI

Vincent Kotzsch
NI, Emerson Test & Measurement, Austin, Texas

As the telecommunications landscape gears up for the advent of 6G technology, the role of artificial intelligence (AI) becomes increasingly indispensable, bringing with it immense opportunity for innovation as well as major challenges for the wireless industry. On one hand, AI promises to usher in an era of improved mobile network efficiency. However, testing AI-integrated devices requires new testing methodologies that push the boundaries of measurement science. On the other hand, as devices continue to increase in complexity, meeting time-to-market, quality and cost objectives will become increasingly complex. In this space, AI can help acquire more actionable insights from measurement data to help make business decisions. This strategic embrace of AI not only ensures seamless integration into the dynamic wireless landscape but also lays the foundation for future breakthroughs, propelling the industry toward a future defined by innovation and excellence.

UNDERSTANDING THE INTERSECTION BETWEEN AI AND 6G TEST

The convergence of AI and testing unfolds through a multifaceted lens, encompassing diverse applications and transformative potentials. However, there are two main use cases driving change in the industry. First, generative AI begins to emerge as a tool for accelerating design workflows, optimizing time-to-market and minimizing operating costs. Second, wireless industry players are increasingly integrating AI into their products, leading to an increased device under test (DUT) complexity requiring new testing methodologies.

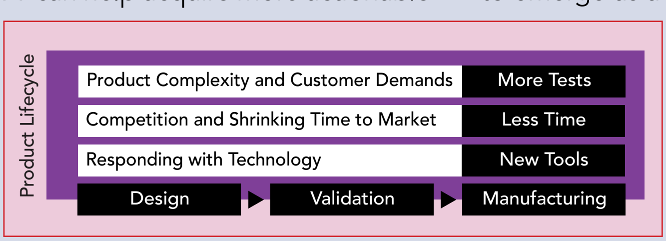

Fig. 1 **Product development life cycle.**

LEVERAGING GENERATIVE AI TO BOOST PRODUCTIVITY

As of 2024, wireless connectivity has become ubiquitous, reaching most households and mobile devices worldwide. This widespread adoption signals a shift in industry dynamics from a primary focus on revenue growth to one centered on profitability and optimization. This transition towards optimization has propelled discussions surrounding the integration of AI in 6G wireless technology as industries seek to enhance efficiency and maximize returns in this mature market landscape. In the context of test and measurement, AI-driven solutions offer unparalleled opportunities for streamlining workflows, optimizing resource allocation and enhancing overall operational efficiency. ***Figure 1*** shows a product life cycle flow, including some of the compounding and conflicting issues that pressure this product cycle.

57% Fear their production processes are outdated and cannot keep up with new business and technology trends

46% Say they will lose market share within two years unless they make significant changes to product lifecycle processes.

Fig. 2 **Findings from an NI 2022 research report.**

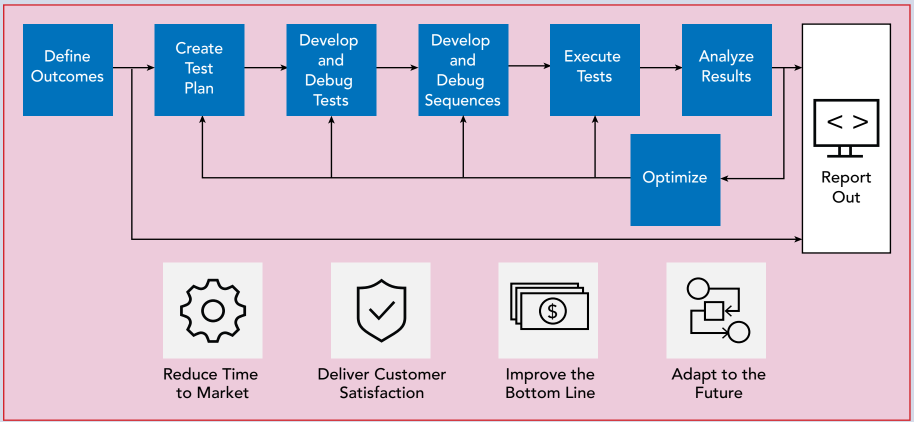

Fig. 3 **Simplified device characterization and validation workflow.**

The integration of generative AI into design workflows marks a transformative leap for the industry. By leveraging AI-driven insights derived from measurement data, businesses can unlock unprecedented levels of productivity and competitiveness. Generative AI algorithms play a crucial role in optimizing the design of intricate antenna systems, enabling rapid prototyping and iterative refinement to meet stringent performance requirements. The need to realize these benefits is becoming much more concrete, as evidenced by the data points shown in ***Figure 2***. These two results come from internal NI research conducted in partnership with the research division of the Financial Times Group.[1]

This strategic convergence not only expedites design workflows but also empowers engineers and designers to innovate. In sectors like the semiconductor industry, AI-driven design tools revolutionize chip layout optimization, yielding higher performance and energy efficiency while shortening design cycles. Ultimately, the integration of AI into design processes presents unparalleled opportunities for enhancing productivity, efficiency and innovation, propelling industries toward sustained growth and competitiveness in the dynamic landscape of wireless technology.

A CASE FOR IMPLEMENTING AI IN SEMICONDUCTOR WORKFLOWS

Figure 3 shows a simplified rendition of the workflow involved in characterizing and validating a device. The process typically commences with defining the desired outcomes, which may stem from various sources such as design specifications, product requirements or cost and time constraints. Engineers then translate these requirements into a comprehensive test plan encompassing all necessary tests to evaluate the device against the specified criteria. Subsequently, they develop and refine the tests, striving for maximum automation. This phase often consumes the most amount of test time.

Following test development, engineers execute the tests on multiple devices to assess individual performance and device-to-device variations. The results are then meticulously analyzed and reported with room for refinement or optimization of tests and sequences as needed. Depending on the complexity of the device, this process may extend from weeks to months, exerting pressure to expedite it to accelerate revenue generation.

By leveraging state-of-the-art software and hardware tools, like NI's LabVIEW and TestStand, organizations can significantly boost engineering efficiency within each step of the process. NI has developed a prototype of a significantly optimized workflow driven by generative AI. This approach utilizes an AI infrastructure with a chat interface to autonomously generate tests and sequences based on given requirements and datasheets. Automating this segment alone could slash the time required for design characterization from weeks to days. The integration of tools like generative AI marks another significant leap forward, promising to expedite time-to-market, reduce operating costs, enhance leverage and promote reusability.

AI-EMBEDDED DEVICES INTRODUCE A NEW LEVEL OF COMPLEXITY

The integration of AI into 6G wireless products ushers in a new era of complexity and innovation. Unlike their traditional counterparts, AI-enhanced DUTs present a host of unique challenges that demand innovative solutions to guarantee both performance benefits and trustworthiness. For instance, in telecommunications, AI-driven network optimization algorithms are deployed to enhance spectral efficiency and minimize interference, thereby elevating overall network performance and user experience. This widespread adoption of AI underscores the pressing need for the test and measurement industry to evolve and craft specialized solutions tailored to the testing requirements of AI-enhanced DUTs, ensuring seamless integration and optimal performance in real-world scenarios.

As the industry gears up for the era of 6G and beyond, complexity reaches unprecedented levels as devices integrate advanced functionalities and AI-driven intelligence. The dominance of software components over hardware further amplifies the demand for frequent testing to maintain reliability amidst rapid software evolution. The integration of AI exacerbates this complexity, necessitating rigorous evaluation to guarantee safety and trustworthiness. Given the pivotal role of these devices across industries, en-

Data	Test	AI to Test AI
• Sufficient Data Quality and Quantity • Organization, Management, Labeling, and Pre-Processing Tools	• Scenario-Based, End-to-End Test • Cyber-Physical Test Leveraging SIL, MIL, and HIL Approach Based on Real-World Scenarios	• Reduce and Manage Complexity of Test • Hyper-Automation of Improvements to the Model and Training Data

Fig. 4 **Embedded, trustworthy AI in 6G.**

suring quality remains paramount, prompting new test challenges like efficiently sourcing (the right) data, setting up accurate scenarios for test and managing the "infinite test space." Some details of these challenges are shown in ***Figure 4***.

While the technology of AI applied to wireless is new and with many challenges, addressing them allows the wireless industry to effectively harness the transformative power of embedded AI. In applications where spectrum, energy and chip real estate are both finite and valuable resources, AI can help optimize them in next-generation wireless devices. This helps pave the way for enhanced performance, reliability and efficiency in future wireless networks.

SOURCING DATA EFFICIENTLY: BALANCING QUANTITY AND QUALITY

The integration of AI into test and measurement processes stands at the forefront of a transformative era, poised to redefine industry standards and methodologies. This is particularly true in the realm of 6G wireless and beyond. This strategic embrace of AI not only ensures seamless integration into the dynamic wireless landscape but also lays the foundation for future breakthroughs, propelling the industry toward a future defined by innovation and excellence.

AI algorithms are poised to play a pivotal role in revolutionizing test management processes, automating scenario selection, optimizing test coverage and mitigating the complexities associated with diverse use cases and edge conditions. However, testing AI devices in the context of 6G applications presents formidable challenges, particularly in the critical phase of AI model training. This phase, essential for creating robust and reliable AI models, encompasses three main steps: model design, training and validation. While synthetic training data generated through simulation tools offer some utility, the accuracy of this training data hinges on the fidelity of the simulation models. In contrast, real-world training datasets, acquired under authentic channel conditions, offer superior quality but are inherently more challenging to obtain due to the specialized hardware and software required for data recording. Striking a balance between these considerations is essential to ensuring the robustness and reliability of AI models tailored for 6G applications.

SCENARIO-BASED TESTING: THE FUTURE FOR AI-EMBEDDED DUTS

Traditional stimulus-response testing systems fall short when it comes to validating embedded AI devices. The challenge lies in the unpredictable nature of machine learning-trained systems, which may exhibit unexpected behavior across a broad spectrum of test scenarios. Unlike traditional algorithms, embedded AI models can be highly sensitive to environmental factors and system configurations, making it challenging to identify relevant stimulus signals. To address this, scenario-based test systems offer a viable alternative, abstracting different test conditions into easily understandable scenarios with predefined parameters and outcomes. These scenarios are then dissected into concrete test cases for comprehensive evaluation. Despite the potential complexity of scenario selection, leveraging smart techniques enables the identification of pertinent scenarios, ensuring thorough testing of AI devices in the wireless space. As the wireless landscape continues to evolve, scenario-based testing is a promising approach to efficiently validate the performance and reliability of embedded AI technologies.

MANAGING THE INFINITE TEST SPACE

The "infinite test space" refers to the vast array of potential scenarios and conditions that an AI system may encounter in real-world applications. Unlike traditional software testing, where inputs and outputs can be exhaustively enumerated, AI systems are trained on data and may exhibit unexpected behaviors when faced with novel situations. This means that testing AI involves grappling with an expansive and often unpredictable range of circumstances, making it impractical to test every possible scenario. Hierarchical scenario descriptions, coupled with smart scenario reduction techniques, are needed to manage the complexity of the test and measurement process while maintaining the test coverage and ensuring the reliability and robustness of an AI-enhanced DUT.

IMPLICATIONS FOR FUTURE 5G & BEYOND DEPLOYMENTS

The integration of AI into wireless applications represents a pivotal advancement, with discussions around its role in future standards gaining momentum. Notably, the 3rd Generation Partnership Project (3GPP) is actively exploring AI's integration into the forthcoming 5G Advanced and 6G standards, a topic of significant interest in Release 18 and 19 discussions. This strategic embrace of AI is not merely speculative but grounded in pragmatic considerations, driven by the imperative to enhance profitability within the wireless industry. Given the scarcity of resources such as spectrum, size constraints and power consumption concerns, even marginal improvements facilitated by AI can yield substantial cost savings. AI holds the potential to unlock significant gains across various fronts, including spectral efficiency, interference reduction, chip size optimization and power consumption, thereby reshaping the landscape of wireless technology. ***Figure 5*** shows a base station tower and sectors, along

Fig. 5 **Wireless base station tower, sectors and backhaul installation.**

with wireless backhaul links, as an example of a network that can benefit from AI integration.

While AI's current application primarily targets higher network layers, its potential extends to lower layers of the protocol stack, presenting a burgeoning trend in 6G discourse. Research endeavors are actively exploring the integration of AI into lower layers, recognizing its capacity to improve spectrum and energy efficiency as well as performance. However, to realize the promise of embedded AI within wireless networks, several prerequisites must be met. These include access to a sufficient quality and quantity of training data, the development of test systems capable of emulating real-world scenarios and the implementation of robust methodologies for navigating the infinite array of testing scenarios.

THE BOTTOM LINE: AI WILL REVOLUTIONIZE THE WIRELESS SECTOR

The integration of AI into the physical layer of 6G devices represents a monumental leap in wireless communication technology, promising to unlock new possibilities and transform industries. However, with great innovation come significant new challenges, particularly in the realm of testing. The industry must proactively address the test implications of AI integration to ensure that 6G devices deliver on their promises of ultra-low latency, reliability, energy and spectrum efficiency, massive connectivity and blistering data rates.

As we move closer to the era of 6G, collaboration, standardization and the development of AI-powered testing solutions will be critical. Establishing industry-wide standards for testing 6G devices with embedded AI is paramount. These standards should encompass AI algorithms, AI training and corresponding data, as well as performance metrics and testing methodologies, to ensure consistency and reliability. Collaboration among device manufacturers, network operators and AI experts is essential to address the challenges of AI integration. Sharing best practices and insights can lead to more robust testing methodologies, as well as ensuring interoperability with optimum performance. By addressing these challenges head-on, we can help ensure that AI-integrated 6G devices operate flawlessly, ushering in a new era of connectivity. ■

Reference

1. INSIGHTS.NI.COM/DESIGNED-TO-PERFORM/

Artificial Intelligence In 6G: More Than Large-Language Models

Roger Nichols
Keysight

The late 2022 launch of OpenAI's ChatGPT and subsequent enhancements through GPT-4, changed the world's perception of the maturity and potential of artificial intelligence (AI). Governments are now writing regulations, industry is developing technology and business models and academics are probing the latest research topics. Driven by a chatbot built on a large-language model (LLM) created by the transformer architecture, this tidal wave of activity is hiding many practical AI developments that are more relevant to radio systems in mobile wireless.

As early as 2019, the ITU-T's Network 2030 Focus Group (FG Network-2030)[1] highlighted the necessity of AI from the physical to the application layer of the 6th generation of wireless networks to accommodate the demands of realizing their vision. Thus, the 6G vision has always included AI as a fundamental building block and tool. However, LLM's AI models, trained on the vast database of text on the global internet, are not the solution for overcoming many technical challenges in wireless communications. Since FG Network-2030, there have been myriad journal articles, research papers, technical demonstrations, early standards work and commercial solutions illustrating that the intensity of this work is focused on machine learning (ML) unrelated to LLMs. In most cases, language models will not be adequate for wireless and particularly radio technology. Instead, they will require models trained on other sources of data such as radio I/Q pairs, signaling traffic or user (payload) data.

ML-based optimization is the subject of research and development at all layers of the wireless network. Allow me to examine just a snapshot of the work closest to the physical layer. This includes AI as applied to the "air interface." An excellent early overview[2] delineated novel concepts using ML to:


TIMES
MICROWAVE SYSTEMS
AN AMPHENOL COMPANY
LMR®
CABLES • CONNECTORS • TOOLS • ASSEMBLIES
The Tower
King!
The LMR® cable solution from Times Microwave Systems offers a complete line of highly flexible, rugged, low-loss braided cables with the fastest, easiest connector installation available.
LMR cables provide superior performance compared to RG and competing coaxial cables of similar size.
• Flexible, rugged, low loss coaxial cable
• Compatible with Advantage® EZ Connectors, LMR® Tools & Accessories
• UV Resistant, Fire Retardant
• Manufactured in the U.S.A
LMR® 195
LMR® 240
LMR® 400
LMR® 600
Competing cables do not provide the flexibility and ease of termination as Times Microwave LMR® cables do
Competing cables may lack UV resistance
With superior performance, reliability, and durability, LMR® coaxial cable assemblies always rise to the top of the tower
Competing coaxial cables don't reach the top with their high loss and poor quality cable
LMR® Original
See you at the IMS 2024 Show: Booth #1004
LMR® is a registered trademark of Times Microwave Systems

- Create custom waveform and modulation optimized for transceiver hardware and real-time channel conditions
- Design and train transceivers themselves based on use-case specifics
- Allow these capabilities to moot PHY- and MAC-layer standards themselves by standardizing only how ML would be implemented for such bespoke and real-time determination of the air interface
- Take steps towards semantic communications rather than optimizing only how to transmit bits.

A panel of experts in 2021[3] were asked if AI was already used in contemporary commercial wireless and the answer was a resounding "yes." AI was already being used in 4G and 5G applications including traffic load balancing and signaling optimization, MIMO precoding algorithms, energy-use management and network planning. The intent is to expand the use of ML to drive improvements in system behavior that have become so complex that conventional solutions are constrained by their deterministic one-size-fits-all mathematical models.

For ML to drive large-scale reliable and viable improvements in performance, quality of service and even quality of experience, the challenges we must address fall into three categories:

Known weaknesses: The October 2021 issue of IEEE Spectrum[4] featured a cover asking: "Why is AI so Dumb?" Charles Q. Choi's article therein described seven "ways AI's fail." These included brittleness, embedded bias, catastrophic forgetting and perhaps the most challenging issue: a lack of both "explainability" and "common sense." I have read about recent progress in addressing the former but neural-network ML suffers from a lack of explainability when answers are "right" or "wrong." From an engineering perspective, understanding the "whys" is essential to reliable and viable solutions. One can see "common sense" manifest daily in the inanity of AI-generated news articles and some of the false and ridiculous answers to questions posed to LLMs.

Data and model validation: Training AI models requires tremendous amounts of data that fits the balance of being "random enough" (unbiased, uncorrelated) while also being "appropriate enough" (relevant to solving the problem at hand). Clean and controlled training data has thus become a premium commodity. While LLMs can capitalize on the vastness of internet data, data for solving more specific technical systems issues is less plentiful and often private and proprietary. These two words are operative in the implications of how the data can be used. And, once a dataset is available, how does one know whether it is adequate, appropriate, unbiased and secure? Once a model is trained, designers learn that the model itself requires continuous improvements and thus, model validation has become a critical step.

Standards: Perhaps the most relevant work for wireless is in 3GPP.[5] 3GPP started AI standardization discussions as early as Release-17 with RAN3 initial study items[6] related to data collection and focusing on energy saving, load balancing and mobility optimization. RAN1, in Release-18, added an extensive study item on using ML for improving channel-state information, beam management and positioning accuracy. Work has progressed to multiple normative work items in 3GPP as part of Release-19, now underway.

This all must happen in the context of governments developing associated policies related to AI technology. Related headlines include European Parliament's landmark law[7] related to proper use, security and consumer recourse, the U.S. Executive Order on AI Safety and Security[8] and the subsequent founding of the U.S. AI Safety Institute.[9] Much of this policy work is focused on the impact of LLMs on the internet and other media as well as on the security of critical communications and compute infrastructure. We can expect impacts on the deeper technical uses of AI in unpredictable ways.

For radio engineers, we are already seeing new approaches to using AI to not only manage wireless communications but even do some designing. Rather than becoming cynical or worried, I view these as technical challenges characteristic of any advance in technology that our engineering community has put to good use time and again. I have seen the interesting results of ML-designed filters and antennas and, while not always practical, they change one's perspective as to how to meet the demanding key performance indicators of our industry. In a demanding technical environment like radio systems and wireless communications networks, there is much work ahead of us to not only validate models and datasets but also to validate and improve the results of the AI-optimized behavior and designs themselves. The combination of conventional and AI-enabled means of such measurement is an intriguing and exciting area of development and I am looking forward to working to make the most of this technology. ■

References

1. Focus Group on Technologies for Network 2030, Web: www.itu.int/pub/t-fg-net2030.
2. J. Hoydis, F. A. Aoudia, A. Valcarce and H. Viswanathan, "Toward a 6G AI-native Air Interface," *IEEE Commun. Mag.*, Vol. 59, No. 5, pp. 76–81, May 2021.
3. "Exploring the Role of AI in Wireless ," Keysight, 2022, Web: www.youtube.com/watch?v=DW0iZyXcDr8.
4. "The Turbulent Past and Uncertain Future of Artificial Intelligence," IEEE Spectrum, Sept. 2021, Web: spectrum.ieee.org/magazine/2021/october.
5. Finding AI in 3GPP, 3GPP, August 2022, Web: www.3gpp.org/technologies/finding-ai-in-3gpp.
6. "Study on Enhancement for Data Collection for NR and ENDC," 3GPP, Web: portal.3gpp.org/desktopmodules/Specifications/SpecificationDetails.aspx?specificationId=3817.
7. "Artificial Intelligence Act: MEPs Adopt Landmark Law," European Parliament, March 2024, Web: www.europarl.europa.eu/news/en/press-room/20240308IPR19015/artificial-intelligence-act-meps-adopt-landmark-law.
8. "Executive Order on the Safe, Secure, and Trustworthy Development and Use of Artificial Intelligence," The White House, Oct.2023, Web: www.whitehouse.gov/briefing-room/presidential-actions/2023/10/30/executive-order-on-the-safe-secure-and-trustworthy-development-and-use-of-artificial-intelligence/.
9. U.S. AI Safety Institute, Web: www.nist.gov/artificial-intelligence/artificial-intelligence-safety-institute.

The Emergence of mmWave Applications Drives Interconnection Development

Pasternack, an Infinite Brand
Irvine, Calif.

In recent years, a surge of new applications, along with legacy applications, are utilizing the mmWave frequencies. This has been enabled by the availability of lower-cost mmWave semiconductors and the advent of active/advanced antenna system (AAS) technologies for communications and sensing that are viable for consumer, commercial and industrial applications. The expansion of mmWave technology and applications is generating new challenges with production tests. Traditional mmWave test methods have been based on labor-intensive manual techniques that require relatively long unit test times. These new applications are creating substantial pressure for modern mmWave production and quality tests to be performed faster and at lower costs. This is causing a shift in the style of interconnect used for testing and the need for greater levels of automation.

INCREASING AVAILABILITY OF MMWAVE TECHNOLOGY

Before the 2000s, the opportunities for mmWave technology were primarily in defense, government or aerospace applications. Some satellite communications (satcom) applications, like satellite television and marine or aerospace communication platforms, used mmWave, but terrestrial wireless communications applications were still in their infancy. During this era, 2G cellular speeds were a fraction of a megabit per second (Mbps).

After the turn of the century, consumer, commercial and industrial wireless communication solutions started gaining traction and automotive radar operating in the 24 GHz band became available. Early mmWave automotive radars still operate in the 24.0 to 24.25 GHz industrial, scientific and medical (ISM) band, which is sometimes referred to as narrowband (NB). The NB automotive radar application is limited in use due to the narrow bandwidth but is still viable for automotive emergency braking and adaptive cruise control. Despite the NB nature of 24 GHz automotive applications, the mmWave spectrum is characterized by wider bandwidth channels and backhaul applications make use of this feature in unlicensed and licensed bands.

Despite several applications, much of this early hardware was manufactured in small batches using manual fabrication, assembly and testing techniques. As the industry exited the 2000s, mass manufacturing of mmWave chipsets and integrated circuits (ICs) started becoming more commonplace. Developments enabled cheaper and more accessible 24 GHz automotive radars that were far less expensive than the previous mmWave technology that, largely, served defense and government satcom applications.

In 2009, the WiGig Alliance introduced WiGig, which was designed to operate in the 60 GHz band. This technology was intended as a wireless standard to replace cable in home theater and wireless docking for mobile device applications. These applications started becoming popular with the advent of the smartphone and 3G. WiGig was subsequently absorbed into the Wi-Fi Alliance and while there were limited launches of WiGig hardware and 60 GHz Wi-Fi routers, the standard did not experience commercial success. Wi-Fi efforts are now directed toward lower frequency IEEE 802.11ax (Wi-Fi 6) and emerging Wi-Fi 7 applications. One of the culprits for this lack of commercial success was likely the higher cost of 60 GHz WiGig chipsets. The high cost of the chipsets discouraged designers from integrating 60 GHz

Wi-Fi features into user devices. ***Figure 1*** shows an E-Band radio block diagram and the need for high performance, high frequency, cost-effective RF components is clear.

In the early 2010s, Ku-Band ICs became more readily available and the race toward low earth orbit (LEO) satellite constellations for global broadband began. As Ka-Band satcom networks became more prevalent, investment and interest in Ka-Band satellite constellations and ground terminals for commercial applications increased. During this period, mmWave frequencies emerged as a key enabler for the 5G vision.

The development of phased array antennas and antenna array-related technologies has been a big factor in making mmWave wireless applications attractive for consumer, commercial and industrial applications. These technologies and architectures require more RF paths, but these paths operate at lower RF powers. This approach provides advantages compared to traditional architectures that rely on one high-power mmWave signal path. Lower-power ICs provide the desired result in conjunction with beamforming architectures that utilize antenna drivers. MIMO methods complement beamforming architecture to enable smaller, more compact mmWave antenna systems. This approach also benefits from the smaller physical sizes of mmWave antenna elements.

After 2015, the 3GPP standard adopted mmWave spectrum use and Ka-Band satcom chipsets became more widely available. In addition to wireless mobile communications, fixed-wireless access (FWA) and other satellite broadband applications that make use of mmWave frequencies have emerged. Now, a host of mmWave applications, such as 5G, satcom, Wi-Fi and 77 GHz automotive radar, incorporate mmWave frequencies and components. There is a broad portfolio of applications and use cases that are benefiting from the heavy investment into mmWave chipsets and other technologies. ***Figure 2*** shows a 77 GHz radar block diagram.

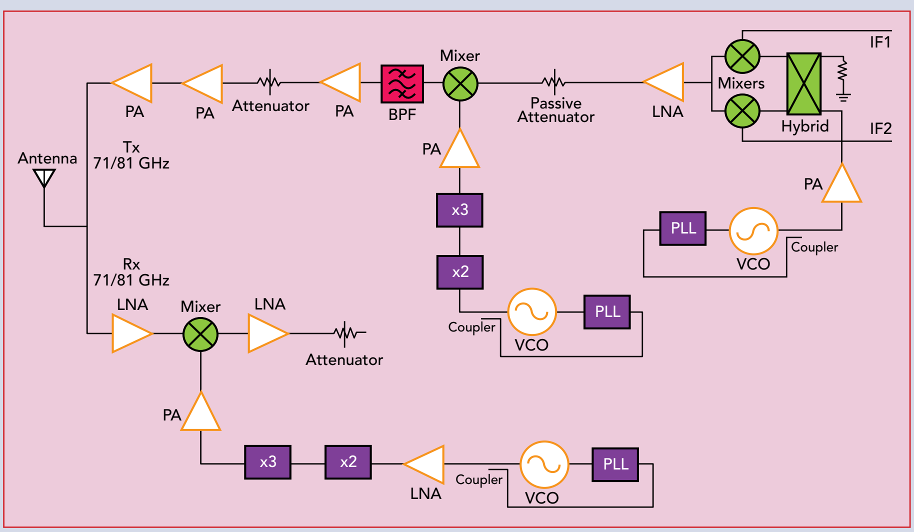

Fig. 1 **71/81 GHz E-Band radio block diagram. *Source:* Pasternack.**

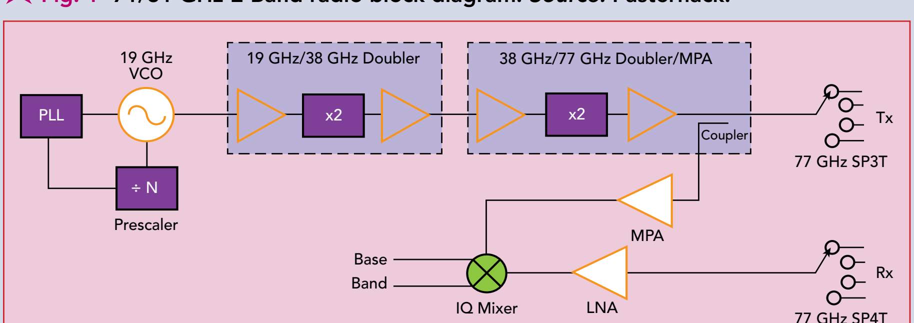

Fig. 2 **77 GHz automotive radar front-end block diagram. *Source:* Pasternack.**

MMWAVE TRENDS INFLUENCE RF INTERCONNECT

As described, the emergence of mmWave technology in non-government applications is happening quickly. The rapid adoption of mmWave technologies into these applications relies heavily on the development of mmWave chipsets and advances in computing and simulation software. However, the mmWave interconnect ecosystem, which has been in place for decades in response to existing government and satcom requirements, is evolving to meet the needs of these new mmWave applications.

To enable these emerging mmWave applications, interconnect density is increasing, along with operating frequencies. Supporting these trends is necessary to meet the performance requirements of mmWave antenna array applications and AAS systems that have many more signal paths than legacy mmWave systems. As described, the signal paths in these new architectures are at lower power levels than single-path systems. This enables semiconductor technologies, like silicon, GaAs, InP and GaN to provide the required performance.

An important performance consideration in these applications is thermal dissipation. Conduction and dielectric losses are a function of frequency, meaning intrinsic losses in a signal path are much higher for mmWave frequencies. Using multiple signal paths decreases the power and dissipation in each path. This makes it possible to use a distributed thermal management approach in an mmWave system design that accommodates the increased number of signal paths. This approach avoids a high concentration of thermal energy in a small region and minimizes the thermal design challenges.

In addition to an increase in the interconnect volume for devices and systems, mmWave interconnects require better tolerances to ensure proper connection. The operation of a transmission line and the interaction of electromagnetic

Fig. 3 **Manual test probe positioner.**

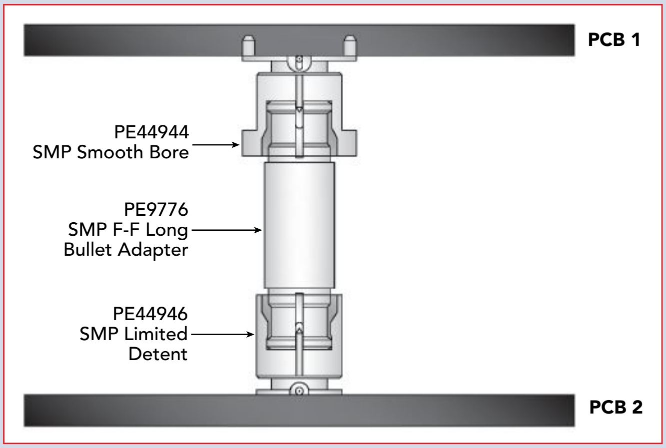

Fig. 4 **Blind mate coaxial interconnect.**

waves within a transmission medium is a function of frequency. This means that the required surface finish, feature tolerances and size of the transmission lines scale with frequency. At higher frequencies, better finishes, machining and tolerances on coaxial alignment result in the lowest loss and VSWR, along with the best conformability for the coaxial cable assembly.

Higher frequency interconnects must also have better overall alignment tolerances than lower frequency cables to ensure optimal performance. For instance, the wavelength of a 500 MHz signal is roughly 600 mm, a 50 GHz signal is 6 mm and a 150 GHz signal is 2 mm. As a rule of thumb, it is recommended to keep feature resolution and tolerances below one-tenth of a wavelength and ideally below one-twentieth of the highest operating wavelength. For the 500 MHz feature resolution just described, tolerances should be below 60 mm and ideally, below 30 mm. At 50 GHz, the resolution/tolerances should be below 600 μm and ideally below 300 μm.

Within an RF module and an AAS, it is possible to use planar transmission lines, vias, high frequency mezzanine connectors, solderable coaxial cables and other high-density, board-to-board and cable-to-board interconnects that present a relatively small pitch and profile. However, for test and measurement applications, like prototyping and quality control, the types of interconnects just described are not generally viable. With mmWave technology being used in more and higher volume applications, long, manual processes for prototyping and quality testing do not support the time and cost requirements. The result is a growing use of spring probes (pogo pins), coaxial spring probes and blind mate connectors, as opposed to the legacy standard threaded coaxial connectors and solderable coaxial cable interconnects. ***Figure 3*** shows a manual test probe positioner and ground-signal-ground probe with a 2.92 mm coaxial connector interface that may be used for mmWave test applications.

RF port counts are increasing rapidly. Systems that have traditionally incorporated roughly one to four ports are now routinely incorporating 64 or more ports. This increases the urgency of finding smaller, lower-pitch, high performance interconnects for mmWave applications. In many cases, flexible coaxial cable assemblies that are commonly used in test and measurement applications to accommodate various devices under test and test setups are not adequate for mmWave applications. Rigid and semi-rigid coaxial cable assemblies tend to have lower losses and better VSWR than comparable flexible coaxial cables. However, skilled technicians must shape rigid and semi-rigid coaxial cables to properly install these interconnects. Flexible coaxial assemblies only require a technician to push-fit or properly thread and torque a threaded coaxial connector. These assemblies do, however, require some attention to ensure minimal deflection of the flex cable during operation or between calibrations. Rigid and semi-rigid coaxial cable assemblies generally cannot be reworked and should be formed and left in place. Using these cables requires some planning, along with adequate tools and expertise in the laboratory or test floor to properly form and install the connectors. ***Figure 4*** shows a blind mate coaxial connector that uses a bullet adapter to connect between two PCBs.

Another solution is to use probes and precision positioners to make RF connections for prototype and verification/quality testing. Using probe interconnects in this way requires planning and design to ensure that there are enough test points for the RF paths. This test setup requires complex probe heads and precision positioning to connect every test point properly and reliably. These tests may require several to thousands of test cycles, depending on the device or system under test. In some cases, it may be necessary to probe multiple sides of a device or system simultaneously. As an example, many transmit-receive modules for AAS applications are fabricated on planar laminates or ceramic boards where the routing may only allow probe test points to be on the top and bottom. This requires dual-sided probing to access all test points and typical probe stations/probe positioners are designed to probe only a single side. This may require a custom probe station or precision probe positioner. ***Figure 5*** shows a blind mate connector operating from DC to 22 GHz that can be used in these applications.

AUTOMATION IS INCREASINGLY CRUCIAL

There is a shift away from high-mix, low volume mmWave devices and systems to much higher volume production. Part of this volume increase has been enabled by greater levels of integration of mmWave technology.

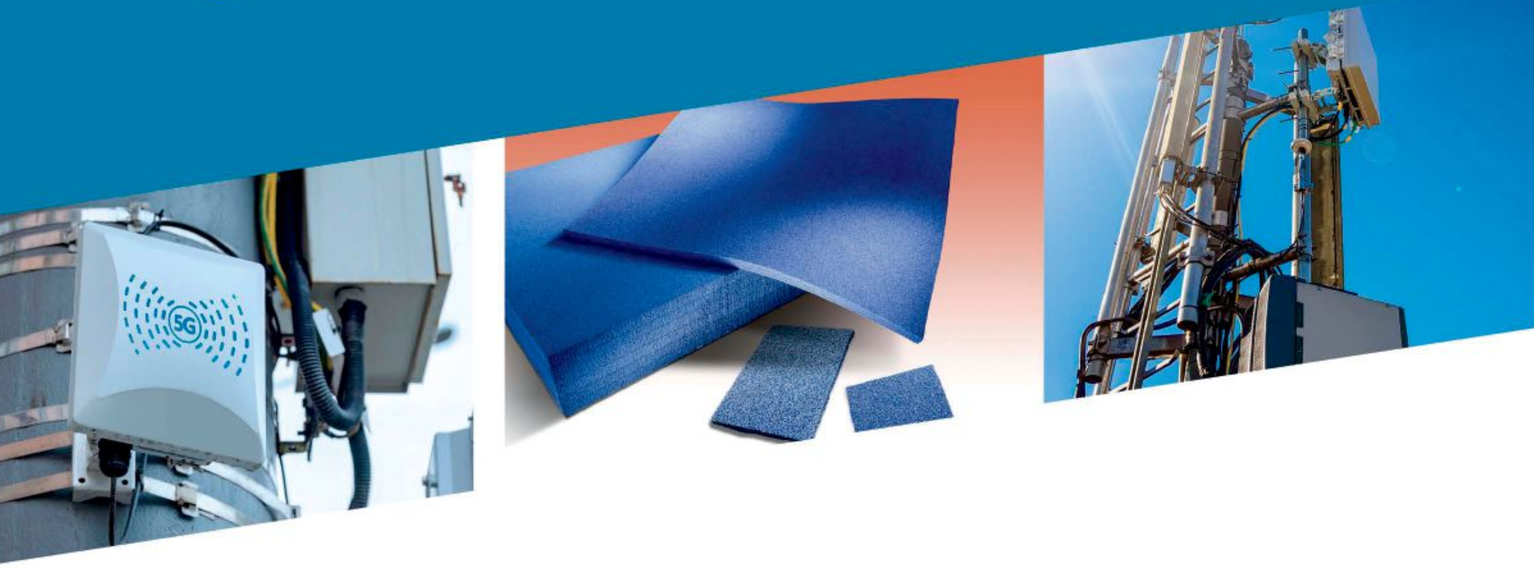
5G

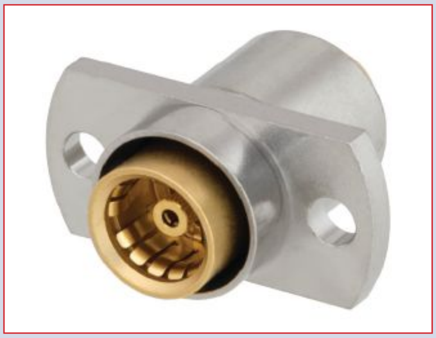

Fig. 5 **Pasternack BMA connector.**

Chipsets and ICs with more integrated features are available but there also has been a shift toward more automation and less manual manufacturing, assembly and testing. Automating manufacturing and assembly of RF parts has been an ongoing advancement for decades and automation in this area leverages many of the technologies used for high speed digital and computing systems. However, automation of both prototype and laboratory RF testing and quality/verification testing of mmWave components and systems has lagged other automation implementations that have realized lower costs and higher volumes.

Initial applications have not lent themselves to automating mmWave tests. Government and defense agencies have dominated these applications and they can accommodate the costs and yields of manual and time-consuming mmWave test strategies. Until the recent upticks in volume and cost concerns, there has not been substantial pressure to develop lower-cost, faster and more automated solutions. Additionally, government and defense users may be more willing to sacrifice repeatability and cost in the products to meet stringent standards and performance requirements.

Technologies like electronic calibration (e-Cal) have been instrumental in making typical small-signal RF testing more repeatable and reliable. However, these technologies still require interconnect cycling between calibrations. Greater emphasis on the repeatability, accuracy and reliability of mmWave test systems necessitates more automation and less manual effort in moving mmWave devices and systems between calibration and various test setups. Beyond small-signal S-parameter testing, there is also a need for large-signal S-parameters and power, impedance (load-pull) and/or noise testing measurements in many mmWave systems, especially TR modules and other active RF devices and systems. Traditional quality/verification testing of mmWave devices and systems usually involves the use of various test stations or lines. Naturally, having to disconnect, transport and reconnect a device or system under test in a different location, even within the same facility, can result in test variations and changes. Consistency and repeatability concerns resulting from the various test domains of a given device or system under test make harmonizing the results of these test domains difficult, if not impossible. ***Figure 6*** shows a precision-calibrated noise source module with 2.92 mm coaxial connector interfaces that may be part of an mmWave test setup.

Fig. 6 **Calibrated noise source module.**

Making the test setup flexible enough to perform all the necessary quality/verification tests minimizes data repeatability concerns. It also results in higher test throughput and fewer steps with less manual intervention. As an example, this approach might allow small-signal and large-signal S-parameters for a transmitter module to be measured and the data harmonized without substantial manipulation. This would provide a more complete analysis of the overall transmitter behavior for sensing or communications applications.

Another outcome of additional automation, especially with interconnect, is a dramatic increase in connection repeatability when compared to manual insertion and connection. Though the repeatability of properly torqued threaded coaxial connectors by a skilled technician may be very high, the repeatability of blind mate connectors and other insertion methods is less so. The speed of mating and occupied space advantages of blind mate connections may outweigh repeatability concerns. The optimum solution is to enhance the repeatability of blind mate connections with robotic connection cycling instead of human operators. A robotic insertion system will likely ensure much better repeatability than human operators for spring probes and blind mate connections. The goal would be to achieve the same repeatability as threaded coaxial connectors. Using spring probes and blind mate connectors with automation can also reduce the overall test time and may reduce the test system footprint as robotic systems can be designed that require less area than human operators need. Faster interconnect speeds could result in higher throughput that would lower test costs and increase the ROI of what are becoming increasingly expensive test and measurement systems for emerging high port count mmWave systems.

CONCLUSION

For decades, mmWave technology was relegated to defense, aerospace, space and some backhaul communications applications. To support the insatiable demand for data consumption, along with mitigating spectrum clutter concerns in the sub-6 GHz telecom spectrum, applications are moving to higher frequencies. The advent of mmWave 5G applications has renewed interest in consumer, commercial and industrial mmWave communications and sensing. This interest is being kindled into a roaring flame with many new non-government mmWave applications emerging and evolving. Some of these applications include 5G FR2, 802.11ay from 57 to 64 GHz, automotive radar from 77 to 81 GHz, mmWave imaging/radar for security and machine learning and new space communication and sensing. Each of these new applications needs a robust supply chain of interconnect options and will benefit from more automated manufacturing and testing approaches. ■

Dielectric Varactor

Tecdia's SMT analog varactors, made with unique voltage controlled dielectrics, are designed for controlling impedance inside analog phase shifters operational up to 100GHz.

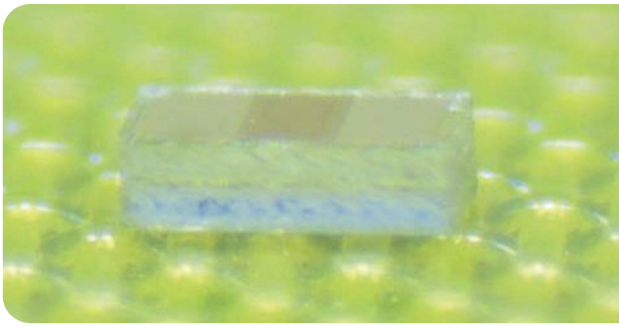

- Low ESR
- High Linearity
- Microsecond Switching Speed
- 0V Capacitance of 0.1pF or more
- 0201 SMT Solderable Form Factor

Applications

- Tunable Phase Shifters
- Tunable Matching Networks
- Tunable Filters
- Beamforming
- Voltage Controlled Oscillators

Final Markets

5G Backhaul and Small Cell
24GHz ~ 86GHz

Low Earth Orbit
26 ~ 40GHz

Radar
3GHz ~ 6GHz &
8GHz ~ 12GHz

Let's do this.

TECDIA Inc.
TEL +1-408-748-0100
FAX +1-408-748-0111
Email sales@tecdia.com

Website : us.tecdia.com

Paving the Way to Terabit Wireless Telecommunications

Dr. John Howard, Rana Barsbai and Steve Jalil
Electromagnetic Technology Industries, Inc., Boonton, N.J.

WIRELESS TECHNOLOGY TODAY

Today, data has become a major part of the digital existence. The demand for faster, more reliable and ubiquitous connectivity has reached unprecedented heights. The U.S., home to around 144,000 to 145,000 telecom towers, stands at the forefront of this digital revolution. These towers have long been the backbone of communication networks, facilitating both fixed and mobile communications. However, now the FCC proposes the national fixed broadband standard requiring 100 Mbps for download speeds and 20 Mbps for upload speeds. To support that standard and to continue to enable the demands of ubiquitous connectivity, data throughput speeds must increase. There are various methods to increase wireless telecommunications data throughput speeds and this section will address several of these techniques.

More Channel Bandwidth

It is well known that as the channel bandwidth increases, the data throughput speeds in bits per second also increase. Unfortunately, an increase in bandwidth also increases the effects of noise. For a constant power output, this increase in noise acts to reduce the signal-to-noise ratio (SNR). This, in turn, reduces the modulation index, which reduces the data throughput speed. The net effect is to reduce the spectral efficiency, meaning the increase in data throughput speed is substantially lower than the bandwidth increase would imply. The noise power is determined by the formula in ***Equation 1***.

$$N=KTB \qquad (1)$$

Where:
N = Noise power (W)
K = Boltzmann's constant = 1.381×10^{-23} W/Hz/K
T = 290 K at room temperature
B = RF carrier bandwidth (Hz)

Incorporate mmWaves

Frequencies from 30 to 300 GHz are considered mmWaves. In 5G telecommunications technology, mmWaves are employed to provide high data rates and low latency in wireless communication systems. However, mmWave signals have propagation limitations; they are more susceptible to atmospheric absorption and scattering[1] and obstacles like buildings and foliage can disrupt propagation. To compensate for these limitations, networks typically use higher transmission powers and this introduces more noise. In these noisy channel environments, whether the noise is caused by atmospheric absorption, scattering, reflections or if signal sidelobes are interfering, this noise will impair the ability to increase data throughput speeds.

Adding to the challenges, absorption plus scattering caused by hydrometeors[2,3] in the transmission medium depolarizes the transmitted radiation. This effect may severely limit system performance, particularly in the case where two orthogonal polarizations are used as separate communication channels. ***Figure 1*** shows a plot of the atmospheric attenuation of RF signals and how this attenuation changes with frequency for various rainfall rates. This shows the effect of absorption and scattering on RF signals in varying rain conditions and the substantial increase in loss per km for the mmWave frequency range is clear.

Increase Modulation Indices

Higher modulation indices, like 64-QAM, 256-QAM or 1024-QAM,

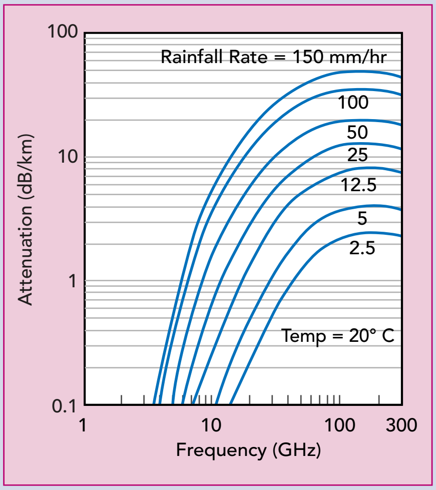

▲ Fig. 1 **RF signal atmospheric attenuation versus frequency.**

increase data throughput speeds but these modulation indices require high SNRs to reap a substantial benefit from the increase in modulation complexity.[4] ***Table 1*** shows an example of SNR requirements for different modulation schemes and coding rates. In addition to the atmospheric attenuation of the RF signal, there will also be spreading loss with distance that will depend on the geometry of the transmit/receive antenna array. The effect of these losses will be to reduce the received signal while the interfering noise increases, reducing the SNR. This will decrease the modulation index of the system, reducing the data throughput speeds.

Implement MU-MIMO

Multi-user MIMO (MU-MIMO) is like troposcatter diversity. This technique permits separate data streams to propagate in parallel. Using multiple data streams increases the data throughput speeds with the increase dependent on channel conditions.

Creating multiple antenna beams to transmit multiple data streams means that only a portion of the full phased array antenna is used for each beam.[5] This reduces the EIRP of each beam of the communication link. This reduction in antenna gain reduces the SNR and this will reduce the modulation index and decrease the data throughput speeds. These efforts can quickly create a law of diminishing returns situation. Conceptually, the gain reduction experienced with multiple beams from a MU-MIMO antenna system is shown in ***Figure 2***.

A SOLUTION

The four methods to increase data throughput are all currently in use and enable higher data throughput rates. However, as demonstrated, there are challenges associated with each method. This section provides an alternative solution that avoids or minimizes these challenges. The previous analysis showed that even though an increase in bandwidth increases the throughput speeds, it also increases the noise. As a result, the modulation index decreases to keep the link closed and this reduced spectral efficiency partially negates the benefit of larger bandwidth for data throughput speeds.

The alternative solution that is being developed maintains the same bandwidth in a sector but repeats this bandwidth multiple times within the sector. The bandwidth reuse scheme behaves similarly to an increase in bandwidth, but it does not increase the noise of each of the beams. The net effect is higher data throughput speeds and higher spectral efficiency. ***Figure 3*** shows a rendering of the four-beam radiation pattern in azimuth and ***Figure 4*** shows the simple architecture of this MIMO beamforming network.

Electromagnetics Technology Industries (ETI) has built and deployed this four-beam MIMO beamforming network. The system uses a 20 MHz channel in a 120-degree sector to provide an average of 28 Mbps data speed in an urban environment. By implementing the four-beam architecture shown in Figure 4 in the same 120-degree sector and repeating the same 20 MHz bandwidth for each beam, data speeds increased by a factor of 10.[6] The results of the existing network and the ETI network are presented in ***Figure 5***.

Earlier, the article discussed the signal propagation challenges for signals in the mmWave frequency range. The reason for going to mmWave frequencies was to access wider bandwidth channels to obtain higher data rates, but the bandwidth reuse architecture obviates this need. The ETI system addresses the signal propagation issues by using frequencies below 10 GHz. This earlier section also discussed how absorption plus scattering could depolarize orthogonal transmission signals. U.S. patent 10,141,640 B2

TABLE 1

SNR REQUIREMENTS FOR DIFFERENT MODULATION SCHEMES AND CODING RATES

REQUIRED BASEBAND SNR
SNR REQUIREMENTS VS. CODING RATE AND MODULATION SCHEME

Modulation	Code Rate	SNR (dB)
QPSK	1/8	-5.1
	1/5	-2.9
	1/4	-1.7
	1/3	-1.0
	1/2	2.0
	2/3	4.3
	3/4	5.5
	4/5	6.2
16-QAM	1/2	7.9
	2/3	11.3
	3/4	12.2
	4/5	12.8
64-QAM	2/3	15.3
	3/4	17.5
	4/5	18.6

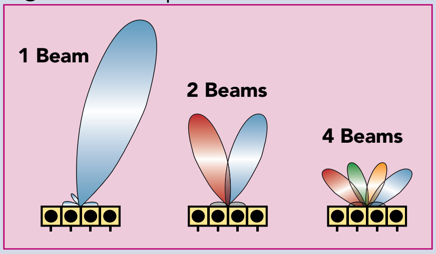

Fig. 2 Gain reduction in MU-MIMO system.

Fig. 3 Rendering of a simple four-beam azimuth pattern.

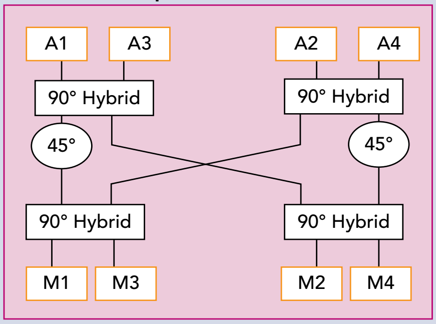

Fig. 4 Four-beam MIMO beamforming network.

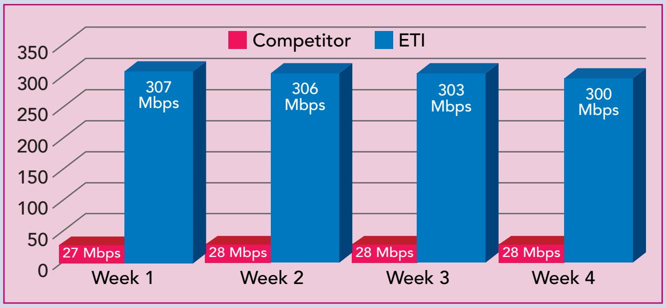

Fig. 5 ETI four-beam system speeds versus the original network speeds.

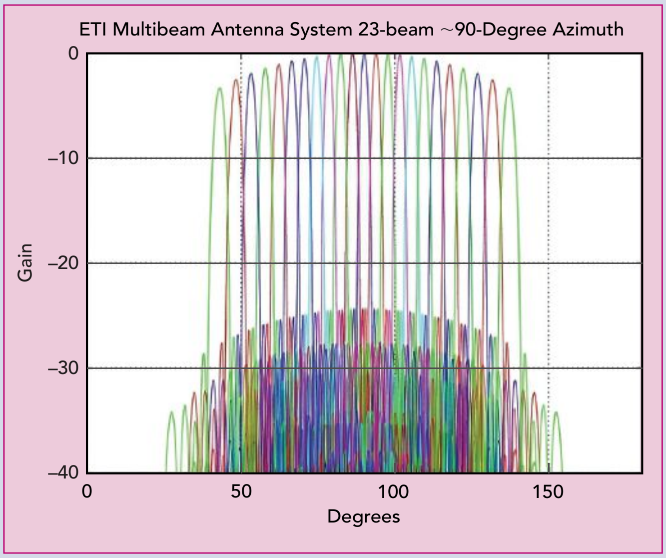

Fig. 6 23-beam ETI antenna system with 90-degree azimuth coverage.

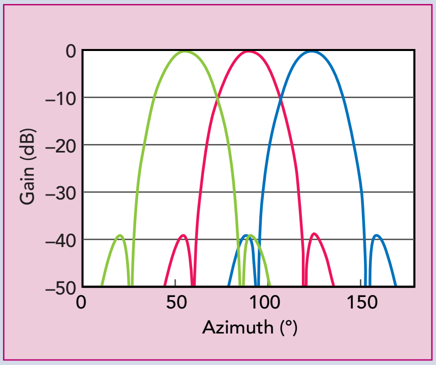

Fig. 7 Sidelobe reduction techniques.

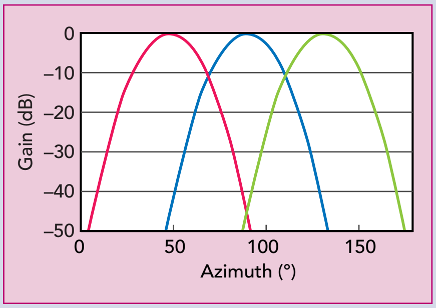

Fig. 8 Improved sidelobe reduction technique.

discusses MIMO dual-polarization scenarios and these ideas are fundamental to the ETI architecture.[7]

Higher modulation indices were shown to increase data throughput speeds, but this increase came with the requirement of higher system SNR values. Achieving these higher SNRs requires higher gain antennas and multiple, narrow beams. Passive and active beamforming networks in azimuth and elevation can easily enable the antenna gain and beam characteristics necessary to support the higher modulation indices.

Finally, the MU-MIMO section presented a method to increase data throughput speeds with multiple bit streams transmitted by an antenna array capable of generating multiple simultaneous beams. When the antenna array generates multiple beams, the gain of each beam is reduced from the gain that would result if all the antenna array radiators were used to produce a single beam. To increase antenna beam gain, beam shaping networks can be added to the beamforming networks mentioned previously.

Figure 6 shows a gain plot for a 23-beam ETI antenna system in a 90-degree azimuth sector. As the plot shows, the sidelobe levels are more than 25 dB from the main lobe as it is steered in its azimuth angle. Figure 6 also shows the gain reduction at the edges of the 90-degree scan from broadside. This gain reduction as the beam is scanned from broadside can be corrected by proprietary and patented techniques.

Figure 7 shows the results of implementing these proprietary and patented techniques. From the results, we see that the sidelobe levels have been reduced to more than 38 dB below the main lobe with constant beamwidth. These sidelobe levels remain roughly constant as the antenna is scanned along its azimuth angle.

Figure 8 shows a second technique that reduces sidelobe levels even more. In this case, the sidelobes are more than 50 dB below the main lobe. Using this technique maintains this sidelobe reduction performance over an even broader azimuth scan angle. The results of Figure 7 and Figure 8 raise the possibility of using these techniques to improve antenna performance enough to increase the modulation index and improve data throughput rates.

TERABIT WIRELESS SOLUTIONS

Enhancing the performance of wireless networks involves increasing the capacity and data throughput speeds provided by wireless base station antennas. This can be done with multiple radiating lobes in both azimuth and elevation to effectively cover a designated geographic volume. Using the proprietary and patented sidelobe reduction techniques described earlier, along with the antenna architecture that the article describes, allows for modulation indices of 256-QAM and 1024-QAM. These techniques, along with repeating the full bandwidth in each beam, can help achieve higher capacity and data throughput speeds. ***Figure 9*** shows a rendering of the radiation pattern

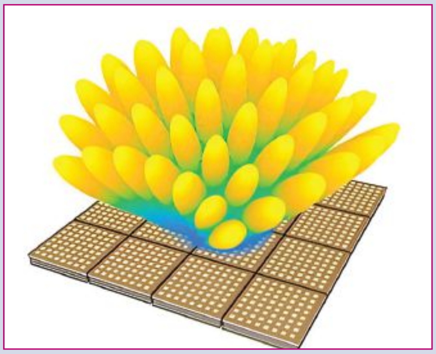

Fig. 9 Phased array with multiple beams in azimuth and elevation. *Source:* courtesy of DARPA.

of an antenna system that employs beamforming in the azimuth and elevation directions.

Examples of the Technology

Traditional macrocell tower deployments use three 120-degree sectors. This first example uses three antennas and each antenna has 24 radios. ***Figure 10*** shows a drawing of the tower that supports the antenna and radio infrastructure at a wireless base station.

Figure 11 shows the concept of the radios housed inside a tower for a three-antenna system. For the data results that follow, the radios generate four beams in azimuth and six beams in elevation.

Table 2 shows the maximum speeds available for various channel sizes using 1024-QAM modulation and ***Table 3*** shows the same data for 256-QAM modulation.

The number of radios per antenna can change based on the number of beams that are required. In the following example, the network again has three antennas, but in this case, each antenna has 32 radios. The deployment is the same as shown in Figure 11, but the radios provide four beams in azimuth and eight beams in elevation.

Table 4 shows the maximum speeds available for various channel sizes using 1024-QAM modulation in this new radio configuration and ***Table 5*** shows the same data for 256-QAM modulation.

The practical implications of the architecture are interesting. A network using this architecture with the 32-radio configuration, 1024-QAM modulation and 80 MHz channel bandwidth will provide an aggregate speed of 18.4 Tbps from only 120 telecom towers. To put this into perspective, a geographical area of 348 square miles, roughly the size of Lehigh County in Pennsylvania, can distribute 128.4 Mbps to 143,000 households from these 120 towers. This is without factoring in a contention ratio, but this service still fulfills the U.S. requirements for broadband.

Fig. 10 Mounting configuration for three-sector base station.

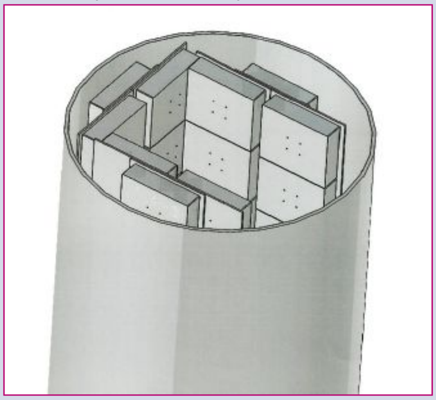

Fig. 11 Radios housed inside the tower.

TABLE 2

MAXIMUM SPEEDS FOR 1024-QAM MODULATION, 24-RADIO CONFIGURATION

Channel Size (MHz)	Total Maximum Speed (Gbps)
80	115
40	57
20	28

TABLE 3

MAXIMUM SPEEDS FOR 256-QAM MODULATION, 24-RADIO CONFIGURATION

Channel Size (MHz)	Total Maximum Speed (Gbps)
80	92
40	46
20	23

TABLE 4

MAXIMUM SPEEDS FOR 1024-QAM MODULATION, 32-RADIO CONFIGURATION

Channel Size (MHz)	Total Maximum Speed (Gbps)
80	153
40	76
20	38

TABLE 5

MAXIMUM SPEEDS FOR 256-QAM MODULATION, 32-RADIO CONFIGURATION

Channel Size (MHz)	Total Maximum Speed (Gbps)
80	122
40	61
20	30

CONCLUSION

This article has compared various methods currently used throughout the industry to increase data throughput speeds. Each one of these methods has advantages and disadvantages. To minimize the disadvantages of these techniques, the article has also presented a simple solution based on a cascadable radio architecture that uses passive beamforming networks, along with proprietary and patented antenna sidelobe techniques. Results show that data throughput speeds, even in simple cases, can increase substantially. The benefit of this technique is it enables operators to meet emerging broadband requirements more readily. In the words of Leonardo da Vinci, "Simplicity is the ultimate sophistication." ■

References

1. H.C. Van de Hulst, "Light-scattering by Small Particles," *New York: Wiley*, 1957, pp. 28–36.
2. J. Howard and N.A. Mathews, "Crosspolarisation of Microwaves due to Rain on a Satellite to Earth Path," *IEEE Trans. Antennas and Propagate*, Vol. AP 27, No. 6, November 1979, pp. 890–891.
3. G. Brussaard, "A Meteorological Model for Rain-Induced Crosspolarisation," *IEEE Trans. Antennas and Propagate*, Vol. AP 24, No. 1, January 1979, pp. 5–11.
4. Dr. O. Werther and R. Minihold, "LTE: System Specifications and Their Impact on RF & Base Band Circuits," *Rohde & Schwarz Application Note*, 2013.
5. E. Björnson, "Basics of Antennas and Beamforming-Massive MIMO Networks," 2018, Web: https://www.youtube.com/watch?v=xGkyZw98Tug.
6. J. Howard, "World's First Wireless Fiber," *The North Jersey IEEE MTT/AP Societies 37th Annual Symposium and Mini-Show,* October 4, 2023.
7. J. Howard, "Isolation of Polarizations in Multi-Polarized Scanning Phased Array Antennas," *US 10, 141, 640 B2*, 27, November 2018.

MMWAVE FILTERS

LTCC Meets 5G

The World's Widest Selection

- Band pass filters optimized for n257, n258, n260 and n261 5G bands
- Low pass filters with passbands up to 32 GHz
- High pass filters with f_{co} up to 57 GHz
- Rejection up to 100+ dB
- Proprietary material systems and distributed topologies
- Pick-and-place standard case styles

Mini-Circuits®

Python Package Controls AWG DDS Multi-Tone Generation

Spectrum Instrumentation
Grosshansdorf, Germany

Spectrum Instrumentation released a new direct digital synthesis (DDS) firmware option for the company's range of versatile 16-bit arbitrary waveform generators (AWGs). The AWGs offer output rates of up to 1.25 GSPS and bandwidths of up to 400 MHz. The option allows users to define 23 DDS cores per AWG that can be routed to the hardware output channels. Each DDS core can be programmed for frequency, amplitude, phase, frequency slope and amplitude slope. This enables control of lasers through acousto-optic deflectors and acousto-optic modulators, as is often used in quantum experiments, with just a few simple commands. Using the abstraction layer of the new Python package makes programming the AWG hardware and the DDS mode extremely easy. A DDS example with 16 superimposed sine waves on one channel and the FFT is shown in ***Figure 1***.

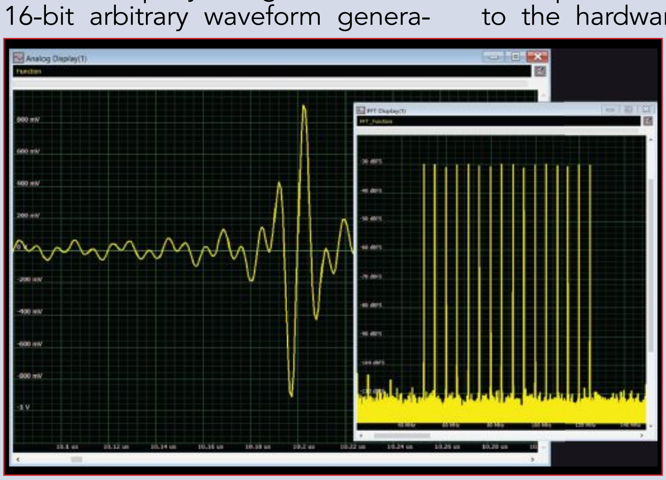

Fig. 1 **16 superimposed sine waves and the FFT.**

DIRECT DIGITAL SYNTHESIS

DDS is a method for generating arbitrary periodic waves from a single, fixed-frequency reference clock. It is a technique widely used in a variety of signal-generation applications. The DDS functionality implemented on Spectrum's AWGs is based on the principle of adding multiple DDS cores to generate a multi-carrier (multi-tone) signal, with each carrier having a well-defined frequency, amplitude and phase.

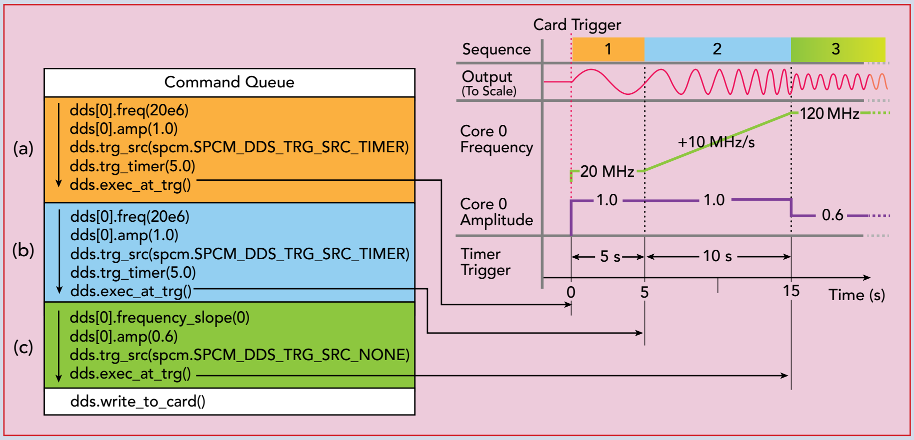

Fig. 2 DDS command block and response.

```
# Fast DMA mode with a timer of 100 ms as trigger source
dds.data_transfer_mode(spcm.SPCM_DDS_DTM_DMA)
dds.trg_src(spcm.SPCM_DDS_TRG_SRC_TIMER)
dds.trg_timer(0.1)

# define the starting frequency of 100 MHz
dds[0].amp(0.5)        # 50% output amplitude
dds[0].freq(100e6)     # 100 MHz signal frequency
dds.exec_at_trg()

# s-form slope in 7 steps (22 MHz change in 700 ms)
for sub_ramp in [10e6, 20e6, 40e6, 80e6, 40e6, 20e6, 10e6]:
    dds[0].frequency_slope(sub_ramp)
    dds.exec_at_trg()

# final frequency 122 MHz
dds[0].frequency_slope(0)
dds[0].freq(122e6)
dds.exec_at_trg()

# writing the whole setup to the card
dds.write_to_card()
```

Fig. 3 DDS command script.

DDS Mode Application Examples

For years, Spectrum AWGs have been successfully used worldwide in pioneering quantum research experiments. The flexibility and fast streaming mode of the AWGs enables data to be streamed straight from a GPU and allows the control of qubits directly from a PC. While using an AWG in this way offers full control of the generated waveforms, large amounts of data need to be calculated. This slows the critical decision-making loop. In contrast, using the versatile multi-tone DDS functionality greatly reduces the amount of data that must be transferred, while still maintaining full control. All the key functionality required for quantum research is built in. With just a single command, users can apply intrinsic dynamic linear slope functions to produce extremely smooth changes to frequency and amplitude. Only a few Python commands are necessary to generate a sine wave, shown in the top block on the left of ***Figure 2***, ramp up the frequency, shown in the middle block, and reduce the amplitude, shown in the bottom block.

The DDS option provides an easy and programmable way for users to produce trains of waveforms, frequency sweeps or finely-tunable references of various frequencies and profiles. Applications that require the fast frequency switching and fine frequency tuning that DDS offers are widespread. They can be found in industrial, medical and imaging systems, network analysis or even communication technology, where data is encoded using phase and frequency modulation on a carrier.

PYTHON PACKAGE FOR EASY CONTROL OF DDS

The Python package is available through GitHub with a single pip command. It allows full control of all current Spectrum hardware, including digitizers, AWGs, digital I/O cards and options, including the DDS option. Generating a single 100 MHz sine wave requires five DDS-specific single-line commands as follows:

dds.reset()

dds[0].amp(0.5) # 50% output amplitude

dds[0].freq(100e6) # 100 MHz signal frequency

dds.exec_at_trg()

dds.write_to_card()

In total, there are more than 10 different core-related functions, as well as more than 30 general functions, realized inside the Python DDS class. This allows users to read all the internal parameters and read back all the possible DDS settings.

10 Million DDS Commands Per Second

The DDS commands can be sent using an extremely fast DMA mode into the 4 GB sample memory of the AWG. This fast transfer mode allows more advanced DDS functions that are not implemented in firmware as intrinsic functions to be performed. These include:

- S-shaped frequency/amplitude slopes consisting of multiple linear slope commands.
- Custom frequency/amplitude slopes consisting of multiple linear slope commands
- AM modulation consisting of multiple amplitude change commands
- FM modulation consisting of multiple frequency change commands
- FSK modulation consisting of multiple frequency change commands.

A simple s-shaped frequency slope can be achieved by using multiple intrinsic linear frequency slope functions. The example in ***Figure 3*** defines a command timer of 100 ms

Fig. 4 **Examples of the 66xx AWG series.**

to generate an s-form slope in seven steps where each step is 100 ms. The slope goes from 100 to 122 MHz.

Availability and Software Integration

The DDS option is available for the full range of M4i.66xx PCIe cards, M4x.66xx PXIe modules, portable LXI/Ethernet DN2.66x units and multi-channel desktop LXI/Ethernet DN6.66xx products. All previously purchased 66xx-series products can be equipped with the new firmware option by simply performing a firmware update. Besides the high-level Python package, programming can be done using the existing driver SDKs that are included in the delivery. Examples are available for C, C++, JAVA, C#, MATLAB, LabVIEW and many more.

One Python Package for All Spectrum Products

The high-level, object-oriented Python package not only supports the DDS mode, but it also supports all current Spectrum products and nearly all product features and operating modes. This includes digitizer, AWG, synchronization, single-shot mode, continuous FIFO acquisition, averaging modes, pulse generator and DDS options, along with many more. More than 30 examples and detailed documentation are available on how to use the package. Spectrum is constantly improving Python support and continues to add new examples and new features. All 23 of the 66xx AWG series, some of which are shown in ***Figure 4***, can be used with the DDS option.

VENDOR**VIEW**

Spectrum Instrumentation
Grosshansdorf, Germany
www.spectrum-instrumentation.com

MMIC Filter Design Goes Mainstream with Web-Based Design Tools

Marki Microwave
Morgan Hill, Calif.

Size, weight and power (SWaP) are key considerations in the component selection process for RF systems. MMIC processes have a proven track record as the technology platform for high performance components throughout the various sub-blocks in the RF signal chain. However, MMIC technology has become a viable option for high volume filter development only recently. This is largely due to the growing importance of size reduction.

In an ideal world, filters would be selected early in the system design phase. These filters can be commercial off-the-shelf solutions and in some cases, frequency plans can be changed to accommodate filters available in the market. Unfortunately, due to the presence of unexpected spurious products that may only present themselves during testing, a real-world receiver will also have several "oh no" filters. The job of these filters is to suppress these unexpected tones. For projects where time to market is key, this presents a problem as these filters will be custom designs that require engineering and manufacturing lead-times. For this reason, modern custom filter designs must be fast-turn designs that are right the first time.

In recent years, Marki Microwave has developed a novel design flow for MMIC filter design including standard response types (bandpass, highpass and lowpass) as well as some more advanced concepts like notch, reflectionless and configurable filters. Marki Microwave's proprietary design flow has demonstrated a high level of agreement between initial simulations and measured results, leading to first-pass design success for custom filter solutions. This enables rapid filter development and reduced cycle times. Due to the inherent advantages of the MMIC platform, these solutions are repeatable from unit to unit and wafer to wafer and are scalable to high volume.

RECENT MMIC FILTER DEVELOPMENTS

MMIC is well suited not only for common filter response types but also for more advanced concepts. Marki Microwave recently released a family of varactor diode tunable filters that allow users to create bandpass filters with variable center frequencies and percent bandwidths through independent analog tuning of the highpass and lowpass sides. This makes them well-suited for adaptive filtering applications such as LO tracking. These impedance-insensitive filters utilize a balanced design to feature low return loss in both the passband and stopband. ***Table 1*** shows the performance results.

Figure 1 demonstrates the tuning capability of Marki Microwave's MFBT-00003PSM, which features a wide center frequency tuning range of 8 to 30 GHz. The top chart in Figure 1 shows the MFBT-00003PSM sweeping lowpass and the bottom chart shows the MFBT-00003PSM sweeping highpass.

TABLE 1
MMIC TUNABLE FILTER RESULTS

	Center Frequency, f_c	3 dBc Passband	Tuning Voltage	Package
MFBT-00001PSM	3.5 to 9.5 GHz	3 to 10 GHz	0 to 16 V	4x4 mm QFN
MFBT-00002PSM	5.5 to 15.5 GHz	4.5 to 16.5 GHz	0 to 16 V	4x4 mm QFN
MFBT-00003PSM	10 to 26 GHz	8 to 30 GHz	0 to 16 V	4x4 mm QFN

FILTER DESIGN TOOLS & PRODIGY™ FILTER DESIGNER

Figure 2 shows several filter design tools that Marki Microwave hosts on its website to enable the development of accurate fast-turn solutions:

LC Filter Design Tool: Uses a lumped element model to calculate LC filter circuit values for lowpass, highpass and bandpass responses, using either Chebyshev, Elliptic, Butterworth, Bessel or Legendre filter topologies. It is a great tool to see whether a filter is theoretically possible. If a filter cannot be realized using this tool, it is unlikely that it is a realizable filter.

Microstrip Filter Tool: Provides an ideal design of a distributed-element microstrip filter. This tool allows you to design on various dielectric substrates, using Chebyshev or Butterworth filter types, to get a first approximation of a filter design. This demonstrates what is

possible, but results should be verified and optimized in 3D EM simulations.

Prodigy Filter Designer: Custom filter solutions often need to be developed quickly to prevent delays. The standard filter development flow is an iterative process between a customer and manufacturer on filter specification negotiations and system validation that can take weeks. Marki Microwave developed Prodigy Filter Designer to streamline the development flow for system designers and reduce time to market.

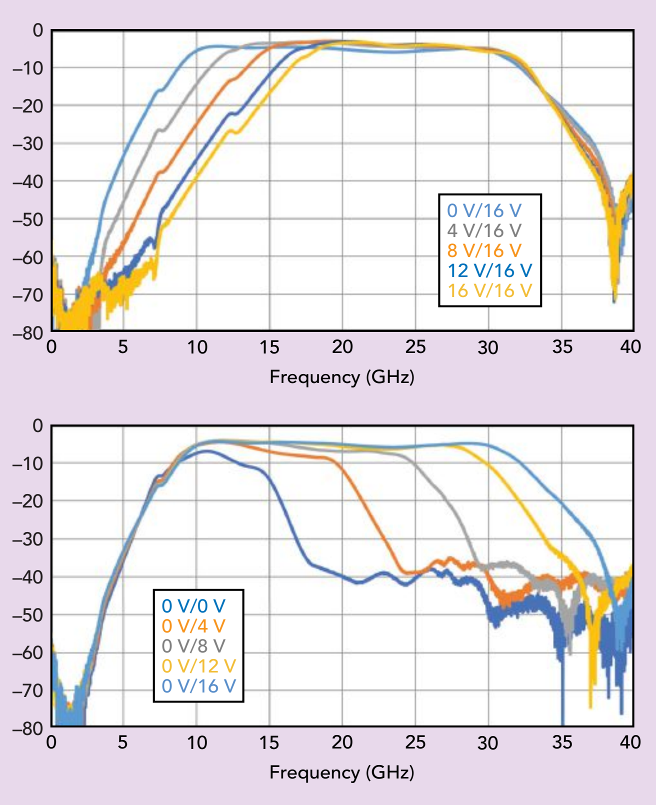

Fig. 1 **MFBT-00003PSM insertion loss.**

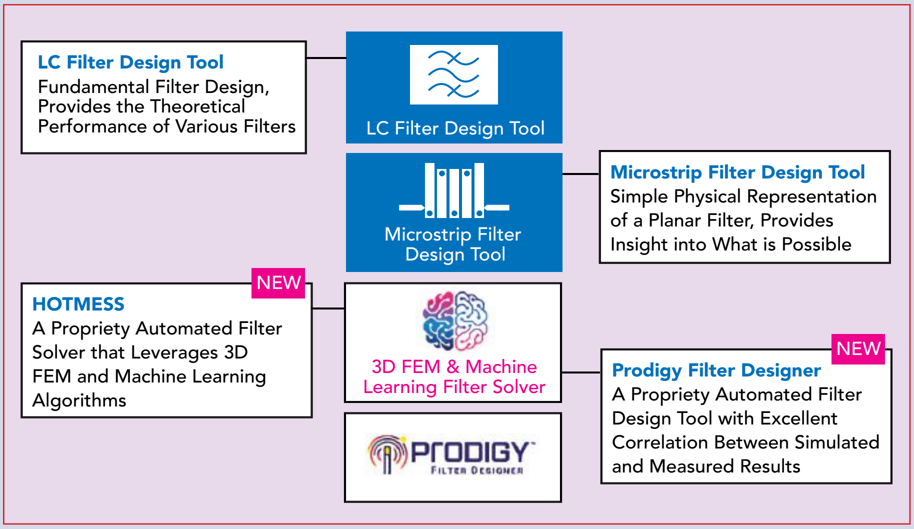

Fig. 2 **Marki Microwave's web-based filter design tools.**

WHAT IS PRODIGY?

The LC Filter Design Tool and Microstrip Filter Design Tools can be thought of as calculators to see what is theoretically possible, whereas Prodigy Filter Designer is a MMIC filter design tool that produces a real FEM-designed filter with known design variables and size. It uses machine learning to calculate real S-parameters nearly instantaneously, including all the 3D effects like metal loss, parasitics, cross-coupling, etc. Prodigy is powered by HFSS optimization through microwave element surrogate simulation (HOTMESS), which is Marki Microwave's proprietary automated 3D FEM solver. HOTMESS generates a set of 3D FEM-validated S-parameters, including the physical layout of the filter. Marki Microwave uses HOTMESS to create databases of known good filters by filter type and filter topology. This is the foundation of the Prodigy Filter Designer. Prodigy takes the known good filter designs and uses machine learning algorithms to interpolate between these points to design a filter based on customer inputs. This idea is shown, conceptually, in ***Figure 3***.

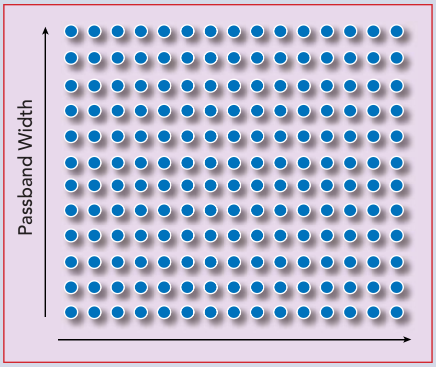

Fig. 3 **Matrix of known good filter designs generated by HOTMESS.**

Users can select the filter best suited to their specific requirements and input desired center frequency and percent bandwidth from the growing list of topologies. The S-parameter file and die dimensions of their filter are instantly provided from these inputs. Designers can then take that S-parameter file and validate the design in their system. Prodigy essentially pushes the iterative process of specification negotiation to the customer without having to involve a Marki engineer, saving weeks in the process. Once they are happy with a design, Marki's engineers take it from there. If a customer desires a filter to be packaged into a surface-mount package, Marki's engineers can take their filter design, apply packaging effects and send back a validated set of S-parameters.

Currently, Prodigy can be used to design bandpass filters and it will continue to grow as more topologies and filter response types are added. Prodigy Filter Designer is currently available on www.markimicrowave.com.

VENDORVIEW

Marki Microwave
Morgan Hill, Calif.
www.markimicrowave.com

Bootstrap Oscillator Delivers Exceptional Phase Noise Performance

The Quantic Wenzel bootstrap oscillator is a cutting-edge frequency control and timing solution designed for applications requiring ultra-low phase noise performance and low g-sensitivity in harsh environments. Operating between 80 MHz and 130 MHz, the bootstrap oscillator uses two phase-locked oven-controlled crystal oscillators (OCXOs) of the same frequency. The innovative technology cancels vibration-induced phase noise by mechanically and electrically aligning the oscillators. The result is a highly stable oscillator assembly with exceptional low g-sensitivity.

PERFORMANCE CHARACTERISTICS

- **Frequency Range:** Covering any fixed frequency between 80 MHz and 130 MHz, the oscillator provides versatility for diverse applications.
- **Phase Noise Performance:** With a static phase noise of -188 dBc/Hz and dynamic phase noise of -165 dBc/Hz, the oscillator ensures precision in signal generation.
- **Vibration Compensation:** Offered in active and passive versions, the oscillator exhibits a sensitivity of 5 x 10^{-11}/g below 300 Hz offsets and 5 x 10^{-12}/g above 300 Hz offsets with vibration isolation.
- **Size and Housing:** Housed in a 5.86 x 3.7 x 1.18 in. machined case, the oscillator meets space constraints in airborne, mobile and shipboard environments.
- **Aging Stability:** The bootstrap oscillator maintains reliability over time, with a typical aging rate of ±1 x 10^{-6} in the first year after 30 days of continuous operation.
- **Power Supply Stability:** An internal voltage regulator enhances power supply line rejection, contributing to stable and reliable operation.

Established in 1978, Quantic Wenzel is a pioneer in ultra-low phase frequency control and timing solutions. The portfolio extends to advanced frequency sources and integrated microwave assemblies reaching 30 GHz and beyond. These products find applications in mission-critical military, space and commercial environments, delivering reliable performance in extreme conditions.

Quantic Wenzel
Austin, Texas
quanticwenzel.com

COMPLETE ANTENNA MEASUREMENT CHAMBER SOLUTION

Copper Mountain Technologies' has partnered with Milli-Box and Eravant to offer a complete antenna measurement chamber solution. It is a turnkey system for customers needing to make far-field antenna measurements above 18 GHz. The over-the-air (OTA) antenna measurement chamber solution features a wide array of configurations depending on the user's anechoic chamber requirements, antenna size, desired frequency range and antenna positioner functionality. The result is an affordable and smaller than traditional chamber testing solution. Learn more now!

Copper Mountain Technologies
www.coppermountaintech.com

5G LOW NOISE AMPLIFIER

Experience unmatched power and precision with Fairview Microwave's compact, coaxial 0.7 dB NF low noise amplifier, tailored to cover pivotal 5G frequency bands. With an operating range from 600 MHz to 4.2 GHz, our low noise amplifier is a connectorized medium power version with SMA connectors that is rated at 17 dBm, has a 21 dB typical gain and is available for same-day shipping. Find additional specs and data sheets for FMAM1079 at fairviewmicrowave.com.

Fairview Microwave
www.fairviewmicrowave.com

OMT

The OMT is a bi-directional device which allows signals to be sent from, or received at, the rectangular ports via an antenna supporting dual polarisation (at the common port). With models available from 33 to 220 GHz Flann's full-band OMTs offer the high performance demanded by today's communication systems in which good polarisation purity and isolation are paramount. These instruments have two rectangular ports on adjacent faces and a common circular port.

Flann Microwave
www.flann.com

RACK-MOUNT ATTENUATOR

Model 50PA-1019-XX is a 19 in. rack-mount attenuator assembly containing 50 Ω solid-state step attenuators. The number of attenuators can be selected from 1 to 8 attenuators. The attenuators have an attenuation range of 0 to 63 dB by 1 dB steps and operate at 100 MHz to 40 GHz. It is available with SMA female connectors. This attenuator assembly can be remotely controlled via an Ethernet connection or a serial connection.

JFW Industries
www.jfwindustries.com

6G SUB-THZ REFERENCE ARCHITECTURE

NI's 6G Sub-THz Reference Architecture brings D-Band measurement capability with PXI vector signal transceivers and Virginia Diodes (VDI) frequency extensions. With support for Tx and Rx power, power and flatness calibration, up to 4 GHz instantaneous bandwidth and real-time data streaming with an FPGA coprocessor, this solution delivers a high-level starting point for configuring 6G sub-THz research, prototyping and validation applications while enabling real-world communication system prototyping and validation.

National Instruments (NI)
www.ni.com

NEX10 5G TERMINATION

Pasternack's precision-engineered terminations with a NEX10 connectorized design is crafted for seamless operation up to 6 GHz. With a 50 Ω impedance and a maximum input power rating of 5 W, this termination has an aluminum body and is designed to withstand temperatures between -40°C and +75°C. Ideal for telecommunications, broadcast and aerospace applications, these terminations ensure reliable signal modulation and termination. Download data sheets and shop for PE6TR1160 at our website.

Pasternack
www.pasternack.com.

SOLID-STATE SWITCHES

Quantic PMI's portfolio of RF and microwave, solid-state switches that range up to 70 GHz. Features include ultra-broadband performance, ultra-high isolation, low loss, ultra-high speed, ultra-low power consumption, SPST - SP64T, reflective or absorptive available. Options include ultra-low video transient models, high input power models, custom package or form factor can be supplied (usually without a NRE charge), hermetic sealing, military or space screening, amplitude and phase matching. Form, fit and function designs our specialty. COTS availability!

Quantic PMI
www.quanticpmi.com

WIRELESS INSITE®

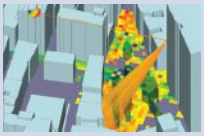

The ability to control the EM propagation environment is an important area of 6G research. Remcom's Wireless InSite® supports the simulation of RF interactions with engineered electromagnetic surfaces (EES), allowing modeling of passive metasurfaces designed to optimize wireless communication coverage by manipulating how signals propagate through a scene. Wireless InSite's ray-tracing and EM path processing calculations enable the prediction of reflections, transmissions and diffractions that interact with EES placed within office buildings and urban areas.

Remcom
www.remcom.com

CERAMIC METALLIZATION OPTIONS

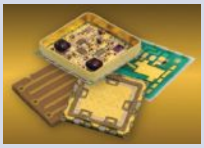

Remtec Inc. (Canton, Mass.) offers a newly expanded range of metalized thick film ceramic substrate material options – including Alumina, BeO, BTO, Silicon Nitride and AIN. Combined with advanced and proprietary screen printing, etching and plating capabilities – such as plated copper (PCTF®) and direct bonded copper (DBC) -- Remtec is uniquely positioned to be the design and production arm for customers requiring single or multilayer ceramic circuits for SMT modules, hybrid integrated

circuits, integrated passives devices, antenna arrays, filters, comb generators, as well as optoelectronic and sensor applications. Contact Remtec's Business Development Manager to arrange a free, thick-film capabilities presentation.
Remtec Inc.
www.remtec.com

THERMAL POWER SENSOR

VENDORVIEW

Discover the R&S®NRP170TWG(N) thermal power sensor, the market's only NMI-traceable power sensor for precise D-Band measurements, covering 110 to 170 GHz. Engineered for simplicity and top performance, it integrates into any setup. Moreover, with fast, accurate and stable readings, as well as USB/LAN connectivity, it provides capabilities essential for 6G R&D and advanced radar applications, allowing you to measure power with confidence and exceed expectations.

Rohde & Schwarz GmbH & Co. KG
www.rohde-schwarz.com

ULTRA-LOW PHASE NOISE FREQUENCY SYNTHESIZERS

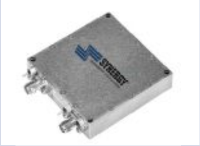

The KSSLO series of ultra-low noise frequency synthesizers offer unmatched phase noise performance in a variety of frequency bandwidths operating in frequency range 1 and 2 allocations in 5G and 6G NR systems and supporting test equipment applications. These products are user programmable for dynamic selection of desired TX and or RX channel bandwidths within the desired FR allocation, phase lock to the available external master reference of the user system requirement and have extremely low latency due to the wide loop bandwidth, which also allows for wideband frequency modulation. Frequency selection is by three-wire SPI control. Phase noise within the wide loop bandwidth is typically as low as -116 dBc/Hz at 10 KHz and 100 kHz offset from the selected frequency when operating at 26 GHz. The product is housed in industry standard 1.25 × 1.25 × 0.5 in. package. The operating temperature range is from -40°C to +65°C.
Synergy
www.synergymwave.com

ACE9600 ADVANCED CHANNEL EMULATOR

A major design challenge for 5G non-terrestrial networks is the proper evaluation of electromagnetic and environmental effects on the signal path, including noise, Doppler shift, latency and multi-path and fading within a laboratory environment. The explosive growth of low earth orbit satellites has intensified the need for a flexible, COTS satellite link emulation system such as the ACE9600 to emulate the wireless path before satellite deployment. Visit booth 704 at IMS2024 for additional information.
Wireless Telecom Group
www.wirelesstelecomgroup.com

CERNEX, Inc. & CernexWave

5G Ready SUB-SIX,Ka-Band&V-Band

- 5G AMPLIFIERS FOR BASE STATIONS WITH MULTICHANNELS(10-100W) 0.6-2.7GHz,2.7-6GHz,0.5-6GHz,6-8GHz 24-29GHz,64-71GHz
- ATTENUATORS
- ANTENNAS
- BANDPASS FILTERS
- BIAS TEE
- CABLE ASSEMBLIES/ CONNECTORS
- COUPLERS
- CONVERTERS
- DETECTORS
- DIPLEXERS
- FREQUENCY MULTIPLIERS/ DIVIDERS
- ISOLATORS/CIRCULATORS
- LMITERS
- MIXERS
- PHASE SHIFTERS
- POWER COMBINERS/DIVIDERS EQUALIZERS
- RADIOS
- SOURCES
- SUB-SYSTEMS
- SWITCHES
- TERMINATIONS/LOADS
- TRANSITIONS/ADAPTERS
- WAVEGUIDE PRODUCTS

Add:1710 Zanker Road Suite 103,San Jose, CA 95112

Tel: (408) 541-9226 Fax:(408) 541-9229

www.cernex.com www.cernexwave.com E mail: sales@cernex .com

High-Power Analyzers Enable Millimeter Wave Testing

Signal Hound
Battle Ground, Wash.

Signal Hound's SM435 series spectrum analyzers and monitoring receivers are powerful and accurate test and measurement tools that are designed with premium components. A philosophy of innovation inspires all the product designs at Signal Hound and these latest high frequency analyzers provide all the performance and precision needed for diverse uses across a wide variety of applications. Long known for reliable and efficient test and measurement equipment, Signal Hound has applied their brand of innovation and quality to the latest high-powered devices in the product portfolio. The SM435B and SM435C combine extended frequency range, real-time operation and extremely low phase noise into an accessible device that enables spectrum analysis into the mmWave space.

The SM435B is a high performance 43.5 GHz spectrum analyzer and monitoring receiver with 110 dB of dynamic range and 1 THz/sec sweep speeds. It offers 160 MHz instantaneous bandwidth (IBW) calibrated I/Q capture available through block transfer of a two-second I/Q buffer over USB 3.0 to the PC. The phase noise of the SM435B rivals even the most expensive spectrum analyzers on the market. This device utilizes a sub-octave preselector that enables exceptional sweep speed performance from the device. It features outstanding dynamic range that has been optimized across the entire frequency band. This feature is achieved with special high-linearity amplifiers having a flat noise figure over 10 dB of gain adjustment. The SM435B excels at a broad range of RF test and measurement applications that include EMC pre-compliance, phase noise characterization, wireless signal characterization, calibration, manufacturing test and more. It is an exceptional product that provides access to higher frequency analysis capabilities to a broad range of engineers and technicians. ***Figure 1*** shows the SM435B analyzer.

▲ **Fig. 1** **SM435B real-time spectrum analyzer.**

To enhance the capabilities of the SM435 series, Signal Hound also offers the network-capable SM435C. Utilizing all the performance specifications of the SM435B, this spectrum analyzer adds a 10 Gigabit Ethernet SFP+ port, making it an attractive companion for remotely located RF data analysis. This feature is especially useful for off-site device control applications like streaming RF data back to a system via ethernet and spectrum monitoring in remote areas. Remote interface and control capabilities are facilitated using SCPI-compatible commands. These devices can be remotely operated by sending SCPI commands through a TCP/IP link. The SM435C software can connect and interface through any VISA implementation or any programming language that allows for SOCKET programming. In practical use case scenarios, SM series products have been utilized in nationwide spectrum monitoring systems and possess the performance capabilities to

Fig. 2 **SM435C real-time spectrum analyzer with 10 GbE.**

meet the demands of ongoing field use. Factor in the desire to reduce the size, weight, power and cost in the RF space and the SM435 series products become much more effective and attractive as a field companion. ***Figure 2*** shows the SM435C in a laboratory setting.

Both the SM435B and SM435C are available with an Option-80 configuration. This option replaces the front panel 10 MHz output with 800 MHz of IF bandwidth selectable from 24 to 43.5 GHz and centered at 1.5 GHz. With Option-80 installed, users can switch modes between spectrum analysis and mmWave down-conversion.

Critical performance standards differentiate superior RF tools from low-grade products. Sweep speed is one of those standards. The SM435B and SM435C offer exceptional sweep speeds to enable real-time data when it is needed most. This component of analysis is important in many applications but essential for spectrum monitoring. Certain situations require broad frequency sweeps while searching for a variety of signal characteristics. The SM435 series analyzers offer a 1 THz/sec sweep speed at any of its resolution bandwidth settings greater than or equal to 30 kHz. Covering 1 to 43.5 GHz in just 20 milliseconds allows for a constant sweep of the airwaves. This is due to a very agile local oscillator in the devices. With a sustained 1 THz/sec sweep speed, these powerful spectrum analyzers can monitor a 2 GHz span with a 100 percent probability of intercept for signals lasting two milliseconds or longer.

Next-generation uses for signal analysis and monitoring systems are ever-expanding. The boundaries of performance continue to be pushed. Signal Hound develops high performance products to keep up with the demand for the powerful tools required for this wide-ranging industry. Providing innovative tools for RF professionals around the globe is an ongoing pursuit for the company. Beginning with the award-winning BB60 series and now with the SM435B and SM435C, engineers, technicians and others have access to devices to assist in further exploration of the RF spectrum in standard as well as developing frequency ranges.

To learn more about the SM435B and SM435C real-time spectrum analyzers and monitoring receivers, visit the Signal Hound website.

Signal Hound
Battle Ground, Wash.
signalhound.com


WE TAKE
YOU WHERE
OTHERS CAN'T
208 M MILES
FARTHEST ERZIA MODULE FROM EARTH
With a space legacy that spans over 20 years, ERZIA is the partner to turn to when your missions aim for other worlds.
ERZIA
ERZIA
WE TAKE YOU FURTHER
ERZIA.COM
RF & MICROWAVE | AMPLIFIERS | SWITCHES | MIXERS | FILTERS | CUSTOM INTEGRATED ASSEMBLIES
IMS
SEE YOU AT IMS | 16-21 JUNE 2024, WASHINGTON, DC | BOOTH 428

Rotary Joints Deliver High Power to 170 GHz

Eravant, formerly Sage Millimeter Inc.
Torrance, Calif.

Antennas with rotary joints are widely used in radar systems to scan targets, in ground stations to track satellites and in radio telescopes to scan the sky. For optimum system performance, the rotary joints should minimize amplitude and phase variations when rotated. Eravant has developed an updated series of rotary joints operating over full waveguide bands from 50 to 170 GHz. An example of one of these rotary joints is shown in ***Figure 1***. With over 360 degrees of rotation, members of the SAN series of rotary joints limit variations to as little as 0.2 dB in amplitude and 2.0 degrees in phase, as shown in ***Table 1***.

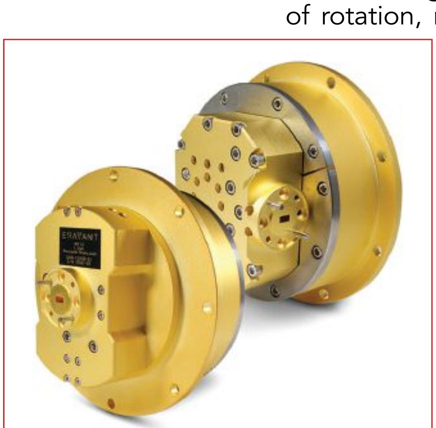

Fig. 1 **Rotary joint.**

A variety of rotary joints have been developed over the years, with a relatively small set of design strategies prevailing due to their consistently favorable results. One such design approach uses the TE-01 propagation mode to pass signals through circular waveguides positioned along the axis of the rotary joint. The TE-01 mode concentrates electromagnetic energy away from the waveguide wall. It also supports higher power levels than other waveguide modes without generating longitudinal currents on waveguide surfaces. By avoiding longitudinal currents, TE-01-based rotary joints do not require electrical continuity between the rotating and stationary waveguides. The non-contacting electrical interfaces provide low insertion loss, good impedance matching and excellent amplitude and phase stability.

The SAN series of rotary joints incorporates the TE-01 design approach and combines it with an improved mode converter design. The mode converter employs an eight-way signal divider/combiner network that feeds a circular array of rectangular waveguide ports surrounding a circular waveguide section, as shown in ***Figure 2***. The symmetry of the mode converter suppresses unwanted propagation modes and limits the distortion of electromagnetic fields within the circular waveguide, enabling good impedance matching and avoiding spurious resonances.

The signal divider/combiner in the mode converter is similar to discrete waveguide

TABLE 1

SAN SERIES HIGH-POWER ROTARY JOINTS

Model	Frequency Range (GHz)	Configuration	Insertion Loss (dB)	Loss Variation (dB)	Phase Variation (°)
SAN-06I06I-S1	110 to 170	In-Line	2.5	0.4	4.0
SAN-06I06R-S1	110 to 170	L-Style	2.3	0.4	3.5
SAN-06R06I-S1	110 to 170	L-Reverse	2.3	0.4	3.5
SAN-06R06R-S1	110 to 170	U-Style	2.3	0.4	3.5
SAN-10I10I-S1	75 to 110	In-Line	2.0	0.2	3.0
SAN-10I10R-S1	75 to 110	L-Style	1.7	0.2	2.5
SAN-10R10I-S1	75 to 110	L-Reverse	1.7	0.2	2.5
SAN-10R10R-S1	75 to 110	U-Style	1.7	0.2	2.5
SAN-12I12I-S1	60 to 90	In-Line	1.7	0.2	3.0
SAN-12I12R-S1	60 to 90	L-Style	1.5	0.2	2.5
SAN-12R12I-S1	60 to 90	L-Reverse	1.5	0.2	2.5
SAN-12R12R-S1	60 to 90	U-Style	1.5	0.2	2.5
SAN-15I15I-S1	50 to 75	In-Line	1.5	0.2	2.5
SAN-15I15R-S1	50 to 75	L-Style	1.2	0.2	2.0
SAN-15R15I-S1	50 to 75	L-Reverse	1.2	0.2	2.0
SAN-15R15R-S1	50 to 75	U-Style	1.2	0.2	2.0

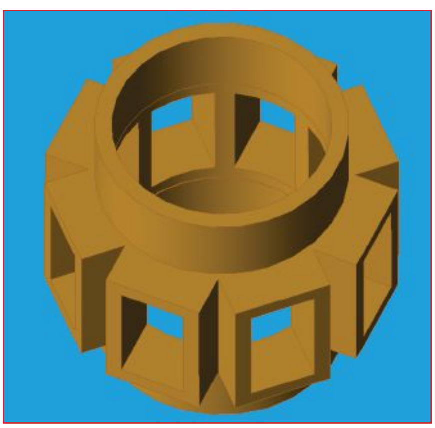

Fig. 2 **Eight-way signal divider/ combiner network.**

feed networks that are often used at lower frequencies. The improved waveguide network is machined into a solid block of metal that surrounds the circular waveguide, avoiding the cost and the difficulty of connecting multiple waveguide sections. Additionally, the solid-block network is easily adapted to different waveguide bands by mechanically scaling the structure.

Configuration options for the rotary joints include an in-line arrangement for both ports (I/I). Other configurations include the L-style (I/R), the reversed L-style (R/I) and the U-style (R/R). L-style rotary joints have one right-angle waveguide port mounted on the rotating end of the assembly. Reversed L-style models have one right-angle port mounted on the stationary end. U-style rotary joints have right-angle ports on both ends. The right-angle waveguide ports are oriented with their E-plane perpendicular to the axis of rotation.

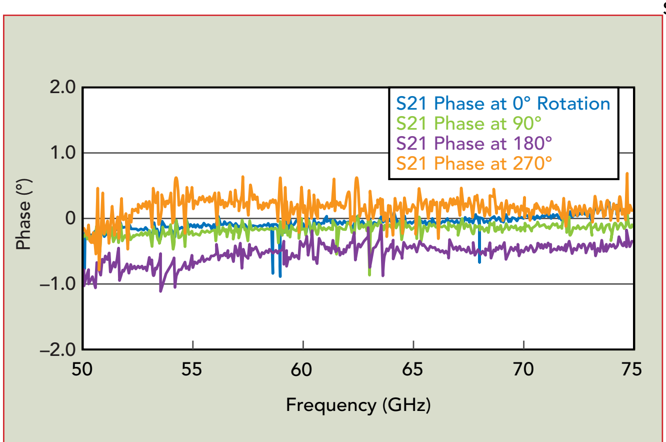

Fig. 3 **V-Band phase performance.**

All the rotary joints can handle up to 250 W of RF power while rotating at 60 RPM or more. They are constructed from stainless steel and gold-plated aluminum with UG-385/U or UG-387/U anti-cocking flanges on the waveguide ports. Typical mid-band insertion loss ranges from 1.2 dB for V-Band models up to 2.5 dB for W-Band versions. For V-Band models, the minimum return loss is 12 dB and the maximum insertion loss is 3.0 dB from 50 to 75 GHz. Phase variation over 360 degrees of rotation is typically within ± 1.0 degree for V-Band models, as shown in ***Figure 3***. This level of phase control is roughly equivalent to maintaining 0.001 in. of end-to-end stability, indicating the level of mechanical precision built into the rotary joints.

For WR06 versions of the rotary joints, the circular mounting flange on the stationary side measures 2.5 in. in diameter while the rotating side of the assembly is 2.0 in. in diameter. For the WR10, WR12 and WR15 models, the mounting flange on the stationary side is 3.25 in. in diameter while the rotating side of the assembly is 2.75 in. in diameter. The temperature range of the rotary joints is -40°C to +85°C with an environmental rating of IP40 to reject foreign objects larger than 1 mm.

The rotary joints complement a wide selection of antennas and accessories offered by Eravant, including reflector antennas and lens-correct horn antennas that are often found in scanning radar systems, satellite-tracking communication links and mobile communication systems. In a common radar application, a rotary joint is combined with a high-sensitivity Doppler radar sensor, a rotating servo mechanism and a suitable antenna to scan the terrain and detect moving objects such as personnel, drones and low-flying aircraft. For additional information see eravant.com/products/antenna-feeds/waveguide-rotary-joints.

VENDORVIEW

Eravant
Formerly Sage Millimeter Inc.
Torrance, Calif.
www.eravant.com

Low-Cost Programmable Waveguide Attenuator

Flann Microwave
Bodmin, U.K.

Being able to change the signal power of an RF system is a fundamental need. There are many reasons why it is preferable to attenuate the signal close to the source. When developing and testing a new product, it is often useful to bring the input power up slowly to avoid damage and to ensure proper characterization. When a vector network analyzer is calibrated, an absolute standard such as a TRL offset enables accurate results. When the transmission medium is waveguide, power levels may be controlled with a waveguide attenuator.

The industry standard defines an attenuation value as a ratio of the input power to the output power, expressed in decibels (dB). However, to fully specify an attenuator, the user must understand the specific requirements of the application. Some of the specifications will involve determining:

- Fixed or variable attenuation
- Maximum attenuation range and insertion loss
- Power level
- Frequency range
- Attenuation accuracy
- Phase change.

These specific requirements are combined with requirements for cost, quantity, size, mass, environment, integration and control to determine the most appropriate waveguide attenuator solutions for a particular application.

Fig. 1 **Examples of Flann Microwave rotary vane attenuators.**

The mix of waveguide solutions reflects the market segmentation. Automatic test and programmability have become important test attributes, driven by factors such as the growth in data traffic, more sophisticated testing equipment with closed-loop feedback, manufacturing advances, evolving digital control in IoT applications and advances in design tools such as finite element modeling analysis. These test and measurement applications are likely to use variable attenuators for the continuous attenuation that they can offer.

Flann Microwave believes that future market growth for products will come from ATE applications and competitive pricing. Flann offers standard rotary vane attenuators that deliver high accuracy over a full waveguide band. They have a flat attenuation profile versus frequency and have attenuation ranges from 0 dB up to 60 dB. This style of attenuator comes in various forms with both manual and programmable versions for ATE applications. Some examples of these attenuators are shown in ***Figure 1***.

Figure 2 shows a plot of attenuation versus frequency for the 29625-03 attenuator shown as the first device in Figure 1. This device operates in the WR-06 waveguide frequency band with a flat attenuation response over this 110 to 170 GHz range. The Flann rotary vane attenuator family is capable of operating up to 500 GHz.

While this family of attenuators offers excellent performance, some applications may require a smaller size with a device that is less costly and easier to manufacture. For these applications, Flann provides a basic variable attenuator. These designs are easy to manufacture, compact and low-cost de-

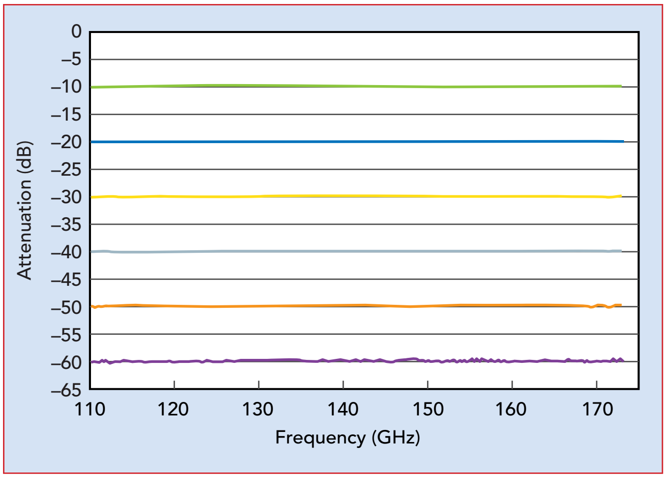

Fig. 2 **Flann 29625 programmable rotary vane attenuator.**

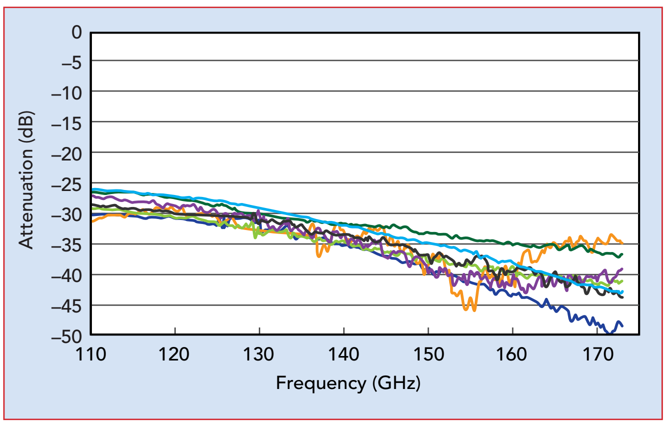

Fig. 3 **Flann 29020 low-cost calibrated manual variable attenuator.**

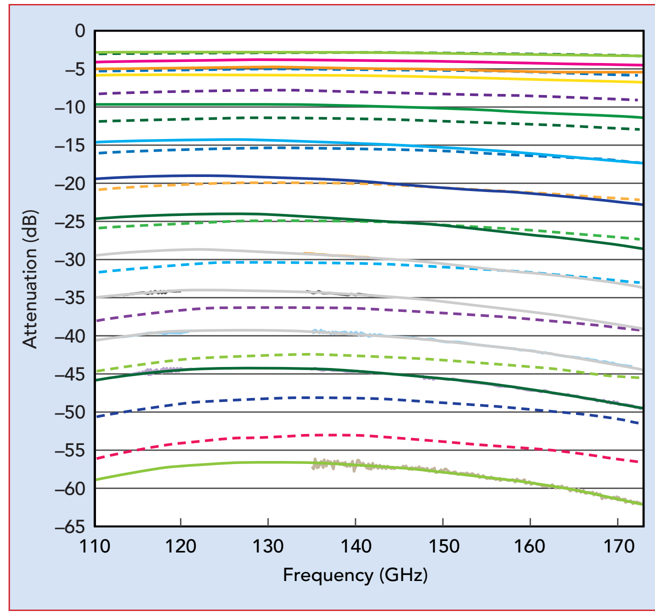

Fig. 4 **Measured values (solid) overlaid with modeled (dashed) values.**

TABLE 1

ATTENUATOR SPECIFICATIONS

Attenuation (dB)	-3	-4	-5	-6	-11	-16	-21	-26	-31	-37	-42	-47	-59
± Variation (%)	8.2	8.4	8.7	9.2	9.2	9.3	9.5	8.6	8.0	6.7	6.1	5.7	5.1
± Variation (dB)	0.26	0.36	0.46	0.59	0.98	1.48	2.00	2.27	2.49	2.46	2.54	2.70	3.00

vices. The trade-off with these devices is an attenuation range of 0 to 25 dB or 30 dB and 40 to 60 percent attenuation variation with frequency, along with a simple lookup table that varies for every frequency for calibration.

The performance of one of these basic attenuators is shown in ***Figure 3***. This attenuator is shown in the middle of Figure 1. The attenuation flatness and accuracy show the performance trade-offs made to reduce size and cost. While this performance is not sufficient for ATE applications, these attenuators are good solutions to improve mismatches or in "level set" applications requiring only a single frequency with calibration lookup tables.

The applications for this low-cost family are also limited by the method of changing attenuation. Historically, devices of this type have used a manual micrometer to adjust attenuation. Automating the attenuation process requires a compact actuator that would be of comparable size to the attenuator. The cost and size of these actuators have been prohibitive, but suitable actuators are becoming available and Flann is re-evaluating the design approach.

Introducing a product suitable for high performance ATE applications meant minimizing the disadvantages while maintaining the advantages of the low-cost versions. To achieve this, Flann designed programable/remote attenuation control from a PC using a USB interface with power. The attenuation range was increased to 50 dB and the attenuation flatness was improved to ±10 percent. All this was accomplished with an eye toward reduced size and moderate cost targets.

Flann's new design uses an improved RF design and an absorbing material, coupled with a compact actuator. The design relies on a thorough understanding of EM waves, aided by FEM software analysis. ***Figure 4*** shows dashed lines that represent modeled results along with the measured data represented by the solid lines. The attenuator can be seen to the far right of Figure 1.

Combining the RF design with an actuator having a 5 μm resolution enables the specifications shown in ***Table 1***. In addition to the performance, the design uses an element that is entirely retracted from the waveguide at the minimum attenuation value. This ensures that the insertion loss of the device is the only insertion loss of the waveguide as this will be an important advantage as frequencies go higher.

Flann Microwave
Bodmin, U.K.
https://flann.com

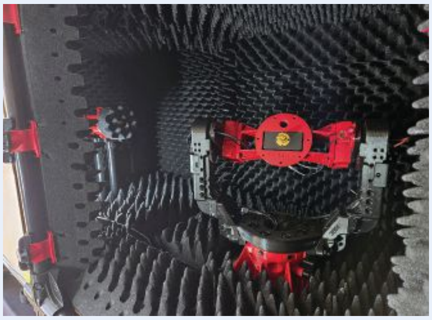

OTA Your Way

MilliBox has expanded its antenna test systems capabilities for mmWave and sub-THz OTA measurement. The original MBX02, comprising a four-foot benchtop anechoic chamber plus a GIM01 3D positioner, has been augmented with many product variants. The MBX0x series with 24 in. cubes reaches up to 2 m in far field and the MBX3x series with 30 in. cube units reaches up to 3 m. The GIM04 positioner series is now the MilliBox standard HV positioner. It is available in four sizes with options like X-Pol: a third-axis motorized polarization controller. Alternatively, the GIM05 series offers a 3-axis spherical roll positioner for wider unobstructed fields of view and native spherical data captures. The cross-compatibility and modularity of these components allow for the creation of highly integrated setups for every need and budget.

MBX32E is a complete solution, featuring an MBX32 chamber and a GIM04-300E, which mounts sub-THz compact Tx and Rx frequency extenders close to the measurement points. Mounting the frequency extenders onboard the 3D positioner minimizes wiring issues for frequencies above 60 GHz.

MBX33R is an accessorized version of the MBX33 chamber with a GIM04-300X 3-axis positioner. It features a target wall with up to nine fixed or moving trihedral corner reflectors. The LIN04 accessory is a programmable linear actuator mount for oscillating radar targets. This setup is developed for mmWave and sub-THz radar performance testing and used during the R&D phase or production calibration.

Construction modularity, software flexibility and overall affordability have anchored MilliBox in a market segment between DIY and full built-in solutions. When the effort of preparing for a test is many times higher than executing it, MilliBox brings a new criticality to the word accessibility: your setup is at your fingertips, always ready when you need it.

MilliBox
San Jose, Calif.
www.millibox.org
millibox@milliwavess.com

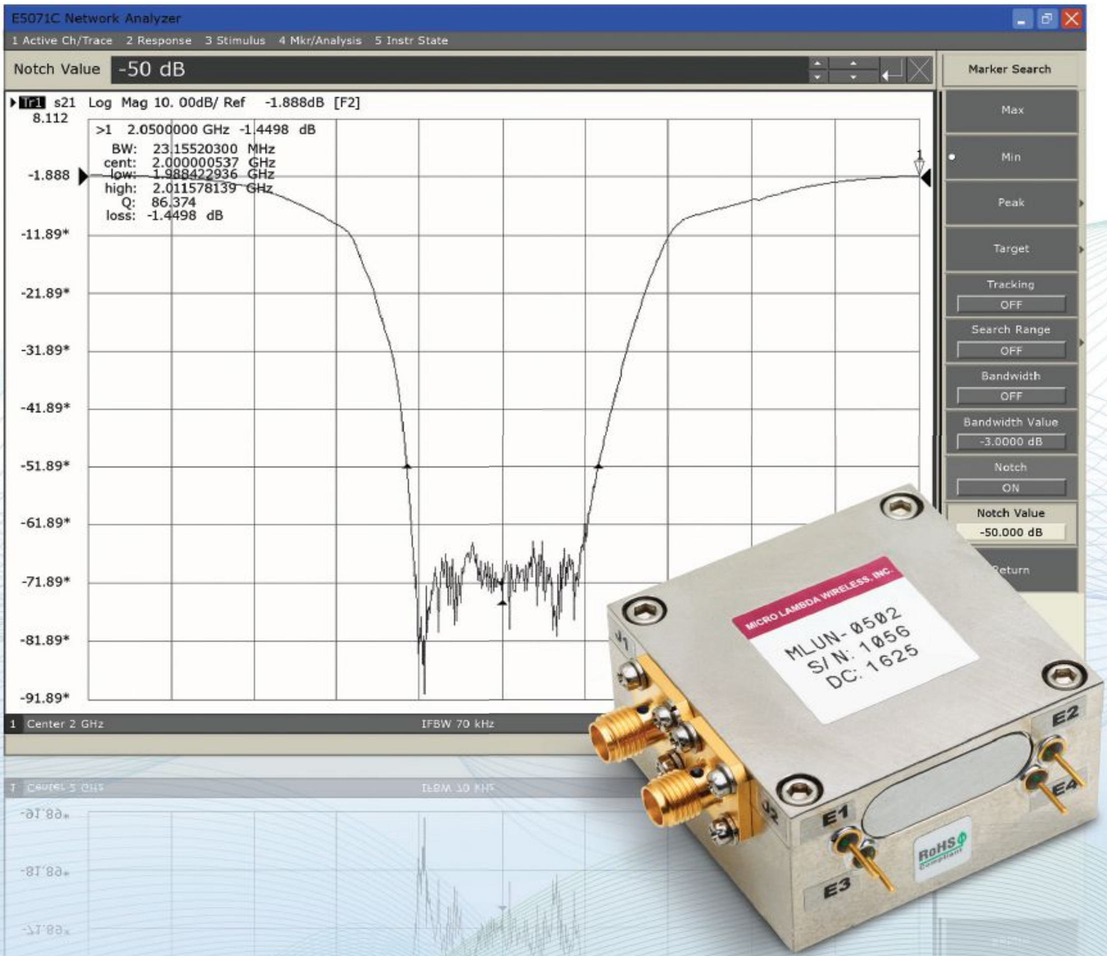

"Ultra-Notch" YIG-Tuned Bandreject Filters

50 dB Notch depths at 500 MHz
60 dB Notch depths at 2 GHz

Industry Leading Performance!

MLUN-Series "Ultra-Notch" Yig-Tuned Bandreject Filters with 50 dB notch depths at 500 MHz and 60 dB notch depths starting at 2 GHz. Standard models cover the 500 MHz to 2 GHz, 2 to 6 GHz, 6 to 18 GHz and 2 to 18 GHz. Customer specified tuning ranges can be supplied on special order.

Standard model operates over the 0° to +65°C temperature range, with Military versions covering -40° to 85°C are available. Al units are available with Analog, 12 bit TTL and 16 bit serial drivers.

Applications include test instruments, wide band receivers, telecom, satcom and military applications.

For more information contact Micro Lambda Wireless.

www.microlambdawireless.com

Micro Lambda is a ISO 9001:2015 Registered Company

MICRO LAMBDA WIRELESS, INC.

"Look to the leader in YIG-Technology"

46515 Landing Parkway, Fremont CA 94538 • (510) 770-9221 • sales@microlambdawireless.com

IMS2024 General Chairs' Welcome

Scott Barker and Sanjay Raman

It is our great honor to welcome you to Washington, DC. The last time the IEEE MTT-S International Microwave Symposium (IMS) was held in the U.S. capital was 1980! Much has changed since then for both IMS and DC, while some of the best parts of both are alive and well. In 1980 there were ~1500 attendees, 160 papers and 123 exhibitors; today IMS has grown to ~10,000 attendees, ~350 papers and ~550 exhibitors. Both the Automatic Radio Frequency Techniques Group (ARFTG), first co-located with IMS in 1979, and the Radio Frequency Integrated Circuits Symposium (RFIC), initially launched as the IEEE Microwave and Millimeter-Wave Monolithic Circuit Symposium in 1982, are still vibrant components of Microwave Week. The Washington, DC, region is home to many high technology companies, major aerospace and defense firms, government science and technology agencies and national laboratories, including the U.S. Army and Navy Research Labs, and the National Institutes of Standards and Technology.

The area around the Walter E. Washington Convention Center, including Penn Quarter, Chinatown and the Shaw district, is one of the most dynamic parts of the city with a phenomenal restaurant and bar scene, and within 10 blocks of the White House and the National Mall. Washington, DC, boasts the greatest number of completely free museums — there are over 40 museums and attractions in Washington, DC, that can be visited without charge, including the 17 museums and galleries that together comprise the Smithsonian Institution. It is quite convenient to get around the city and the region using DC's extensive Metro system, which also connects directly to Reagan National Airport (DCA) and Dulles International Airport (IAD).

The IMS2024 program is built around thematic areas that highlight the symposium's focus on "Capitalizing Across the Spectrum." In addition to showcasing a broad spectrum of engaging technical topics, IMS2024 will celebrate the diversity of contributions, talents and accomplishments across our community's "human spectrum" throughout the week. Moreover, the major technical themes of the conference will emphasize the role our host city of Washington, DC, has played in supporting the use and management of the RF-to-THz spectrum, including: Systems and Applications, Aerospace and Security, Spectrum Coexistence and Sustainability, each as thematic days, and Emerging Technologies and Directions. The Future Directions theme for this year's IMS is Wireless Power Transfer, with a bootcamp, workshops and collection of special, focus and panel sessions on this emerging topic area. On Wednesday, we will also be co-locating with the industry-focused FutureG Summit, which we are jointly sponsoring with the IEEE MTT, Antennas & Propagation, Communications and Photonics Societies. We are also continuing forward several industry engagement efforts introduced in recent years, including the industry showcase session immediately before the Monday plenary session, best industry paper awards and session keynotes. This year features the Startup Pavilion on the exhibit floor, featuring 12+ early stage RF/microwave companies, mentoring and networking opportunities and a pitch competition.

In addition, we are emphasizing Diversity, Equity, Inclusion and Belonging, cutting across all aspects of the symposium. This effort starts with the creation of a new Executive Committee level position – the Outreach and Inclusion Chair. We have also started collecting additional optional demographic information from our attendees so that we are able to understand and appreciate the great diversity that already exists within our community, as well as identify those areas where we need to be more inclusive. In addition, we have updated our selection processes to ensure that our conference events are representative of the diversity of our community. We hope this effort will continue into the future so that IMS will continue to lead the way as the premier international microwave conference!

We are thrilled to welcome you to IMS2024 in Washington, DC, for Microwave Week, June 16-21, 2024. Attendees will have another opportunity to experience IMS in the capital of the U.S., as IMS will return to Washington, DC, in 2029! ■

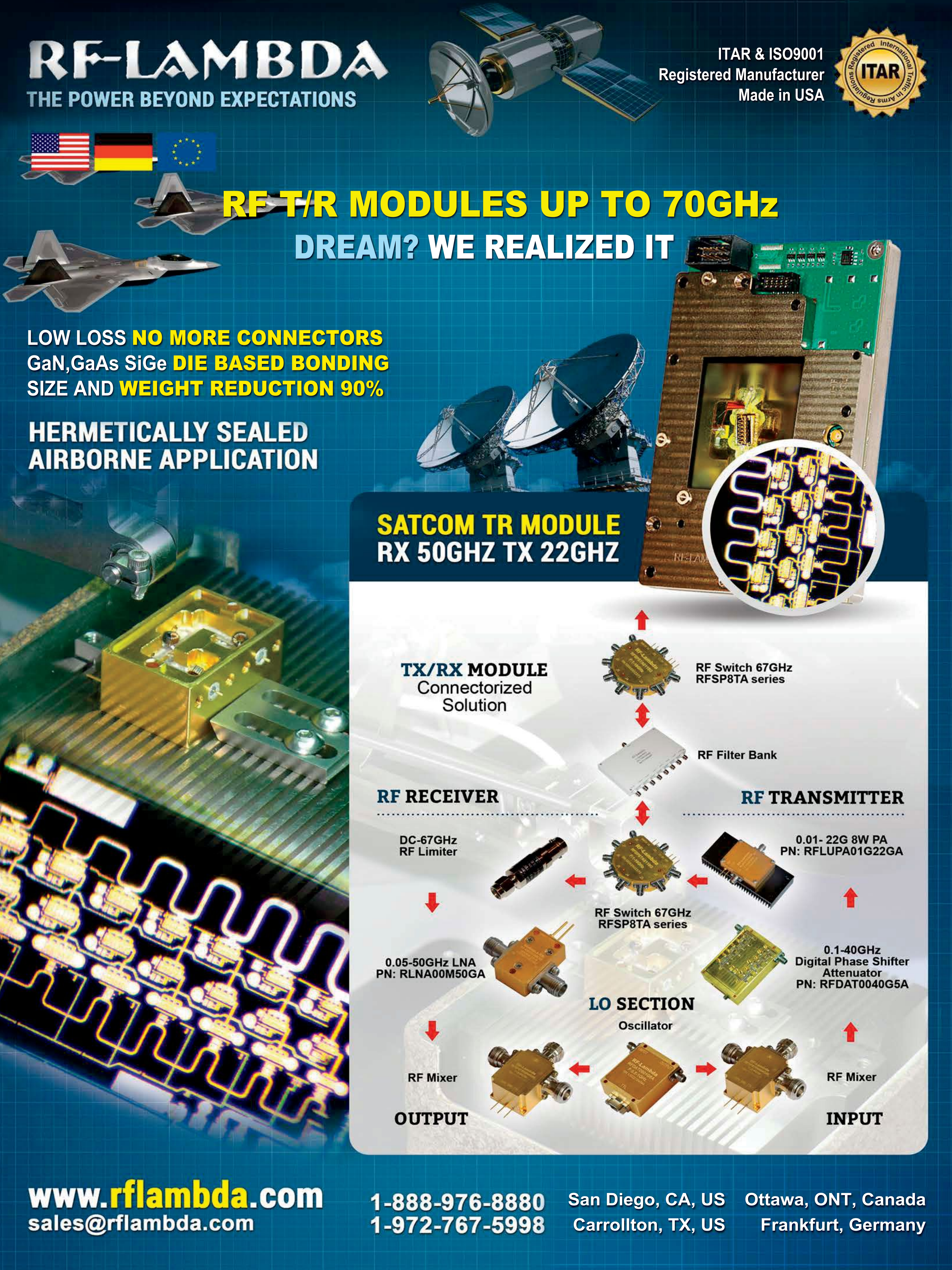
RF-LAMBDA
THE POWER BEYOND EXPECTATIONS
ITAR & ISO9001
Registered Manufacturer
Made in USA
ITAR
Registered International Traffic in Arms Regulations
RF T/R MODULES UP TO 70GHz
DREAM? WE REALIZED IT
LOW LOSS NO MORE CONNECTORS
GaN,GaAs SiGe DIE BASED BONDING
SIZE AND WEIGHT REDUCTION 90%
HERMETICALLY SEALED
AIRBORNE APPLICATION
SATCOM TR MODULE
RX 50GHZ TX 22GHZ
TX/RX MODULE
Connectorized
Solution
RF Switch 67GHz
RFSP8TA series
RF Filter Bank
RF RECEIVER
RF TRANSMITTER
DC-67GHz
RF Limiter
0.01- 22G 8W PA
PN: RFLUPA01G22GA
RF Switch 67GHz
RFSP8TA series
0.05-50GHz LNA
PN: RLNA00M50GA
0.1-40GHz
Digital Phase Shifter
Attenuator
PN: RFDAT0040G5A
LO SECTION
Oscillator
RF Mixer
RF Mixer
OUTPUT
INPUT
www.rflambda.com
sales@rflambda.com
1-888-976-8880
1-972-767-5998
San Diego, CA, US
Carrollton, TX, US
Ottawa, ONT, Canada
Frankfurt, Germany

RFIC'24 Overview

Danilo Manstretta
RFIC 2024 General Chair, University of Pavia, Pavia, Italy

On behalf of the Executive and Steering Committees, I would like to cordially invite you all to the 2024 IEEE Radio Frequency Integrated Circuits (RFIC'24) Symposium. The IEEE RFIC Symposium is the premier annual forum focused on presenting the latest breakthroughs and research results in all areas related to RF, mmWave and wireless ICs. The RFIC Symposium, combined with the International Microwave Symposium (IMS), ARFTG and the Industry Exhibition, form "IMS Week," the world's largest RF and microwave technical meeting of the year.

Building on the remarkable success of RFIC'23 in San Diego, which drew over 900 attendees, this year RFIC'24 promises an even more significant impact. Set to take place at the Walter E. Washington Convention Center, nestled in the heart of Washington, DC, from Sunday morning, June 16, through Tuesday night, June 18, the event anticipates a substantial increase in attendance.

The RFIC'24 will feature a rich educational program on Sunday, June 16, followed by the Plenary Session, a welcome reception and the Symposium Showcase, all on Sunday night. The RFIC technical sessions will be held on Monday and Tuesday in three parallel tracks. These sessions will cover several technical areas, including power amplifiers, RF front-ends, oscillators, frequency synthesizers, device modeling, packaging and testing technologies. Exciting developments in artificial intelligence/machine learning applied to RF circuits, D-Band circuits, 3D ICs and interconnects, wireline, optical, quantum computing and mixed-signal circuits, as well as imaging, spectroscopy and sensing circuits at RF through THz frequencies, will be explored. The scope of the conference includes innovations in IC and system architectures, usage models, calibration techniques and integration approaches, fostering collaboration between researchers and practicing engineers on the frontier of RFICs and systems to the benefit of all.

RFIC'24's Sunday program is mainly devoted to educational events, with 13 RFIC-focused workshops and one technical lecture. The workshops cover a wide range of advanced topics in RFIC technology. The technical lecture will be delivered by Prof. Ali Hajimiri of Caltech on "Noise in Oscillators: from Understanding to Design." This 80-minute lecture begins by exploring the evolution of noise from device and external sources to phase noise. A time-varying phase noise model is developed, with a discussion on its complexities and the insights it provides for designing voltage-controlled oscillators (VCOs). The lecture also examines the application of this model to different types of oscillators, including LC and ring VCOs, and its alignment with the broader context of frequency generation.

Following the full day of Sunday workshops, the RFIC Plenary Session will be held in the evening beginning with conference highlights, the presentation of the Student Paper Awards and the Industry Best Paper Awards. The RFIC'24 Plenary Session will conclude with two visionary plenary talks: "The 6G Network at the Center" by Peter Vetter, President of Nokia's Bell Labs Core Research; and "CMOS Technology Evolution for Revolutionary Impact" by Prof. Tsu-Jae King Liu Dean of the College of Engineering of UC Berkeley. Immediately after the Plenary Session, the RFIC Reception and Symposium Showcase will follow, with highlights from our industry showcase and student paper finalists in an engaging social and technical event supported by RFIC'24 corporate sponsors. The showcase will provide authors the opportunity to demonstrate their work in a lab-like environment for close-up discussions.

On Monday and Tuesday, RFIC will offer multiple tracks of technical paper presentations and will offer panel sessions during the lunch breaks. Monday's panel is titled "RF and Microwave League of Champions." Rather than a traditional panel, it will be a quiz show pitting a team of academics against a team of industry veterans to answer technical riddles sourced from RF and microwave history. Each team will comprise three members who will answer as a team on questions about RF/microwave theory, circuits and systems. This event will be an entertaining diversion from the typical technical panel and hopefully a great deal of fun for participants. The audience is invited to participate and support their favorite team. Tuesday's RFIC/IMS joint panel will discuss "AI in RFIC: Opportunities, Threats, and Limitations." The use of AI has become one of the hottest and most controversial discussion topics of the moment. A panel of experts from both academia and industry will debate on the opportunities and the potential threats posed by AI and how this pervasive technology will transform our industry. Following the success of its first edition in 2023, RFIC'24 will again feature a "chip chatting" session dedicated to students. It will offer a unique opportunity for students to meet and interact with industry leaders and learn about exciting technology trends and potential opportunities for their future careers. All parties are welcome to stay chip chatting at the RFIC nacho station with free food and drinks. Visit the RFIC'24 website (http://rfic-ieee.org/) for more details and updates. ■

2~6GHz 100W GaN Power Amplifier

New

- **High Power** Psat 49/50 dBm
  P1dB 46/47 dBm (Min/Typ.)
- **High OIP3** 50/53 dBm (Min/Typ.)
- **Low Harmonic(2nd/3rd)** -20/-25 dBc (Typ.)
- **Low Spurious** -70 dBc (Typ.)
- **Low VSWR** 1.5:1 (Typ.)
- **High Efficiency** 20% (Typ.)

MPAR-020060S50 is a 2~6GHz 100W GaN amplifier with state-of-the-art GaN design technology. It has higher saturation output power while keeping higher P1dB and better linearity.

The built-in control, monitoring and protection functions are offered. It is designed for high power CW & pulse system applications, such as 5G, LTE, WIFI and other related system module & EMC test.

★ Custom designs are available

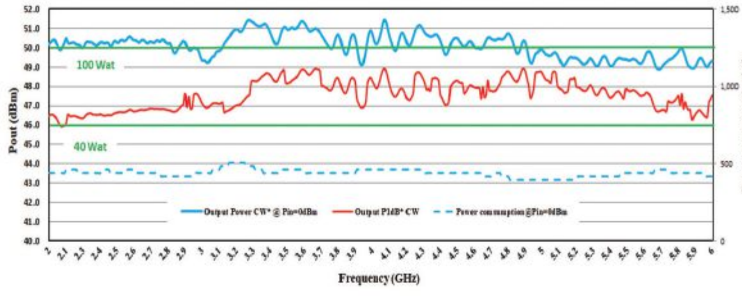

Pout@ Pin=0dBm & P1dB (CW, Load VSWR≤1.2, 25℃)

More Information-
Scan the QR Code

MIcable Inc.

www.micable.cn sales@micable.cn +86-591-87382856

2024 Spring/Summer ARFTG Microwave Measurement Conference

Dominique Schreurs, Marco Spirito, Mauro Marchetti and Dennis Lewis

We welcome you at the 103rd ARFTG Microwave Measurement Conference on June 21, 2024! The conference theme is "Advanced measurement techniques for next-G communication systems." Papers that will be presented cover topics such as measurements for 6G and Future-G systems, mmWave and sub-THz measurements, characterization of material properties and advances in linear and nonlinear measurements. Oral technical sessions are presented in a single-track format. Extended breaks combine an exhibition and interactive forum, which provides networking opportunities with vendors and colleagues, whether researcher or practitioner.

The conference is preceded by Users' Forums focusing on nonlinear vector network analyzer and on-wafer measurements held on Thursday, June 20. ARFTG is also co-sponsoring joint workshops with IMS, which are scheduled on 16-17 June.

If you have an interest in measurements from 1 kHz to 1 THz and beyond, be sure to add the 103rd ARFTG Conference to your plans in Washington, DC, this June. You will find our atmosphere to be informal and friendly. For further details regarding the conference as well as the ARFTG programs for students, visit www.arftg.org.

The IMS2024 Exhibition

Carl Sheffres
Horizon House Publications, Inc.

The IEEE International Microwave Symposium (IMS) features the largest exhibition in our industry, showcasing the world's leading suppliers of products and services. Exhibition visitors will have the opportunity to see and experience the latest technologies and innovations available for all of your design requirements. There will be live demonstrations, new product launches and plenty of networking.

IMS2023 in San Diego was a great success, with nearly 550 companies exhibiting in 867 booth spaces. We expect the IMS2024 exhibition to exceed even those lofty numbers, as IMS visits the Walter E. Washington Convention Center in the nation's capital for the first time in its history. The Mid-Atlantic region boasts many RF/microwave companies, so the event should attract a large audience of industry professionals.

The exhibition will take place in halls A and B of the convention center. Exhibition hours are Tuesday, 18 June, from 09:30 to 17:00; Wednesday, 19 June, from 09:30 to 18:00; and Thursday 20 June from 09:30 to 15:00. Registration will be in the main lobby, convenient to both the exhibition and conference meeting rooms. Coffee will be served on the exhibition floor each morning and Tuesday and Wednesday afternoons. "Sweet Treat Tuesday" has become a welcome staple of the exhibition on Tuesday afternoon, providing all attendees with an afternoon indulgence.

The annual "Industry Reception" will take place on Wednesday, from 17:00 to 18:00 featuring food and beverages in the aisles and at participating exhibitors' booths. Wednesday is also the day for free exhibition registration.

Exhibition attendees are encouraged to visit the XMA-sponsored "game zone" where they can compete to win prizes or just take a break. Relaxation and recharge can also be found in the three networking lounges spread throughout the halls, once again sponsored by Analog Devices.

The "Startup Pavilion" is a new addition for IMS2024. This area will feature emerging companies on the exhibition floor and in the MicroApps Theater, where they will present their technologies and participate in panel sessions. Come listen to and speak with these entrepreneurs to find out what's driving their growth strategies and what emerging markets they are leveraging.

In addition to the startup sessions, the MicroApps Theater will host more than 60 presentations from exhibitors, along with the second annual "Executive Forum," featuring Corporate Sponsors, including Raytheon, and other invited industry experts. The 2023 session proved to be standing room only, so arrive early.

The IMS exhibition is the place to find new ideas, make new relationships and reunite with old friends and colleagues. There are only two industry events that serve the international RF/microwave community and IMS is one of them. Come to Washington, DC, in June and experience all that the IMS exhibition has to offer. ■

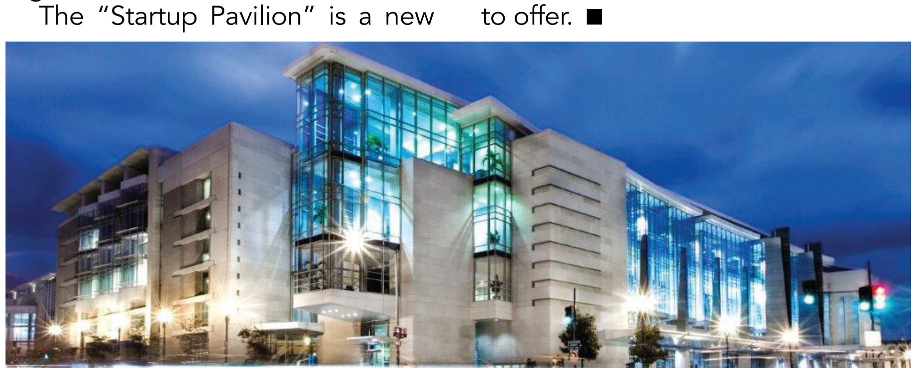

3H Communication Systems
Filters
VENDORVIEW

3H Communication Systems product offering includes filter products from DC to 50 GHz. These filters offer custom designed high performance filters in the smallest packages on the market today. 3H filter products support military, space and commercial applications. 3H's new VHF/UHF, 8-channel multiplexer with bidirectional coupler ports offers a frequency range from 5 MHz to 2.0 GHz with low passband insertion loss and sharp co-channel isolation and is available in leadless surface mount application as well as other mounting options and meets Mil-Std-202 conditions.
www.3hcommunicationsystems.com

Aaronia AG
SPECTRAN®
VENDORVIEW

SPECTRAN® V6 5G has been specially developed for monitoring the FR1 and FR2 bands in 5G networks. With a scanning speed of more than 3 THz/s (equivalent to 6 GHz in less than 2 ms), even the shortest signal interference or power degradation is detected. Due to its weight and dimensions, the V6 5G is ideal for measurements in the field and in the laboratory. Its price/performance ratio and the number of additional functions available are second to none.
www.aaronia.com

ACE/Accurate Circuit Engineering
Prototype PCBs

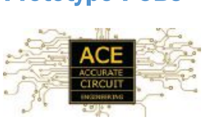

ACE is MIL-PRF-31032 and MIL-PRF-55110 certified up to 32 layers, and can build up to 50+ layers. We are leading experts in RF, hybrid PTFE/FR4 and antenna/microwave technologies.
www.ace-pcb.com

Agile Microwave Technology Inc.
Broadband Low Noise Amplifier

AgileMwT's broadband low noise amplifier with 10 W pulsed 4 W CW RF limiter medium power amplifier operating from 0.1 to 20 GHz is offered in a compact Module configuration. AMT-A0580 provides P1db of +24 dBm typical with 3 dB typical NF, flat small signal gain of 33 dB typical, flat gain with VSWR of 1.8:1 typical. Family of these LNAs are competitively priced and ship from stock or short lead time. AgileMwT offers great value with most innovative designs in the industry.
www.agilemwt.com

Altum RF
Low Noise Amplifier Die

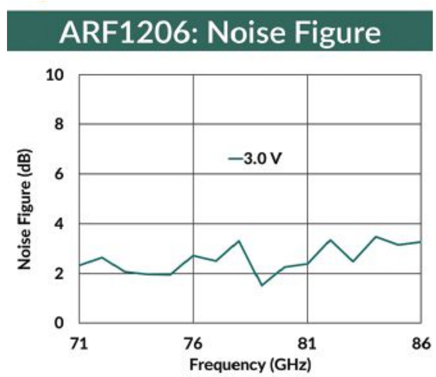

Altum RF's ARF1206 is a low noise amplifier die for E-Band applications. With 20 dB typical gain and 2.5 dB noise figure at 71 GHz and 3.5 dB noise figure at 86 GHz, it is suitable for a variety of demanding telecommunication and sensing applications. The part is pre-matched to 50 Ω and is ESD protected to simplify handling and assembly. The part is RoHS compliant and built with the latest manufacturing techniques to optimize for reliability and quality control.
www.altumrf.com

Analog Devices
Wideband Multichannel RF Digitizers
VENDORVIEW

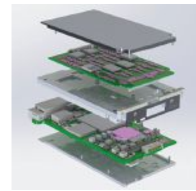

Analog Devices' ADSY1100-series is a family of wideband multichannel RF digitizers in a 3UVPX SOSA™-aligned format. The system is built around ADI's next generation "Apollo" MXFE™ product (AD9084) featuring DAC sample rates up to 28 GSPS and ADC sample rates up to 20 GSPS in a 4 Tx/4 Rx configuration. ADSY1100's Integrated digital signal processing reduces system power consumption, while the integrated RF tuner reduces end system size and complexity.
www.analog.com

Anoison Electronics
Torque Wrench

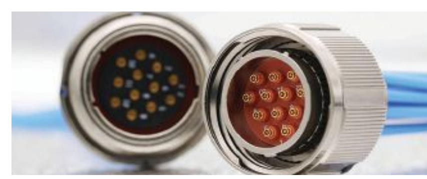

Anoison's innovative product meets the twenty-first-century need for proper torque in VNA connectors and adapters. The Micro-NMD is a smaller profile NMD interface connector used for VNA test cables and VNA port protection adapters. Its hex 17 mm size makes it a perfect fit for the new Micro-NMD construction. With the increasing demand for smaller NMD connectors in the marketplace, tools like torque wrenches are also needed to effectively use them.
www.anoison.com

Anokiwave is Now Qorvo
MARCOM ICs
VENDORVIEW

Together Anokiwave and Qorvo provide the most capable components for high performing X-Band radars. Silicon quad core beamforming ICs feature selectable dual Rx beam to support monopulse or dual polarization operation. GaN T/R FEMs with a range of transmit

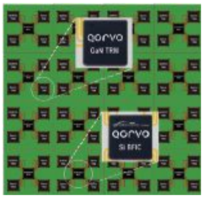

output powers complement and interface directly with the beamformer ICs. Independent phase/amplitude setting at each element is achieved through direct SPI control. These ICs are widely proven in military and commercial platforms and are available today with short lead time.
www.anokiwave.com

Cadence
Computational Software

Cadence enables engineers to drastically reduce turnaround times for product development of the RF to mmWave components and integrated systems for 5G/6G, radar and other wireless applications. Leading AI-enabled computational software supports next-generation design, analysis and front-to-back workflows for III-V, silicon and multifabric heterogenous integration.
www.cadence.com

Cernexwave
CFA Series Fixed Attenuators
VENDORVIEW

CernexWave's CFA Series Fixed Attenuators are offered with an attenuation of 1 to 60 dB and over 30 different waveguide bands from 1 to 500 GHz or coaxial versions from DC to 110 GHz in a variety of bandwidths. They can be customized to handle power levels from 0.5 W to 4 kW CW with natural, forced air or oil cooled designs. Our Model CFA350D030815780-01 has a frequency range of 3.5 to 8.2 GHz with an average power handling capability of 780 W and 13 kW peak.
www.cernexwave.com

Ciao Wireless Inc.
Amplifiers

Standard models include units with instantaneous bandwidths covering 10 MHz to 6.0 GHz and 24 to 43 GHz (designs for 52 GHz available), to support both the uplink/downlink bands for 5G NR. Designs are available with O/P levels up to +33 dBm P1 dBPT and functions including detectors, switched/RF bypass (TTL), variable gain (digital and VVA) or full rack-mount with Ethernet control. Multiple gain levels from 10 dB and up are available, typical noise figures in the 3.0 to 5.0 dB range.
www.ciaowireless.com

Communications & Power Industries LLC
X-Band Solid-State Transmitter
VENDORVIEW

CPI Electron Device Business' VSX3696ON is an air-cooled 1.0 kW X-Band solid-state transmitter optimized for pulsed radars. X-Band solid-state power transmitters are efficient, high-power and compact with proven GaN transistor technology. CPI EDB's VSX3696ON solid-state power amplifier is rugged, reliable designed for airborne applications. The VSX3696ON solid-state transmitter is designed for use in radar applications and covers the 9.1 to 10.0 GHz frequency band. This amplifier utilizes GaN transistors to provide high gain, high efficiency and excellent pulse fidelity. The result is excellent AM/PM, phase-noise and spectral regrowth performance.
www.cpii.com

Conduct RF
D38999 Cable Assemblies with Choice of Connectors

As a cable assembly company first, Conduct RF offers a unique solution to your supply chain requirements for D38999 assemblies. First, they make their own cable. It offers industry leading performance, and it's always in stock. Second, they're configuration and assembly experts with years of experience. Finally, they're capable of terminating to all of the industry standard brands of D38999 connectors. This means, complete capability to deliver quickly, and to the highest quality standards possible. Look for them at IMS '24.
www.conductrf.com

COMSOL Inc.
COMSOL Multiphysics®

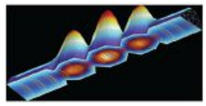

The COMSOL Multiphysics® modeling and simulation software is used in all fields of engineering, manufacturing and scientific research to simulate designs, devices and processes. The platform includes workspaces for multiphysics and single-physics modeling, building and maintaining custom simulation apps and model and app management. The apps can be compiled into standalone apps via COMSOL Compiler™. Add-on modules provide specialized functionality for investigating new wireless technologies; virtually testing and optimizing designs of devices such as antennas, waveguides and filters; and more.
www.comsol.com

Copper Mountain Technologies
Complete Antenna Measurement Chamber Solution
VENDORVIEW

Copper Mountain Technologies' has partnered with MilliBox and Eravant to offer a complete antenna measurement chamber solution. It is a turnkey system for customers needing to make far-field antenna measurements above 18 GHz. The over-the-air (OTA) antenna measurement chamber solution features a wide array of configurations depending on the user's anechoic chamber requirements, antenna size, desired frequency range and antenna positioner functionality. The result is an affordable and smaller than traditional chamber testing solution.
www.coppermountaintech.com

Crane Aerospace & Electronics
Space Qualified Products

Crane designs and manufactures high performance space qualified passive products for defense and commercial satellite customers. We can readily meet your specific space program needs with a selection of pre-qualified products that provide proven high-reliability design, shorter delivery and reduced costs. Products include power dividers, directional couplers, mixers, modulators, iso-dividers/combiners and beamformers.
www.craneae.com

Empower RF
S-Band GaN Pulsed Amplifier for Radar
VENDORVIEW

The Model 2239 is a compact, rugged pulsed amplifier delivering 1000 W peak power between 2.9 to 3.5 GHz. Ideal for S-Band radar systems, it handles pulse widths from 1 to 500 μs and duty cycles up to 20 percent. Longer pulses allowed at derated power. Utilizing GaN technology, the 2240 achieves high power and efficiency in an air-cooled 3U package. Suitable for 19-in. rack-mount or benchtop use, remote control and diagnostics are accessible via Ethernet with a web browser or M2M interface.
www.empowerrf.com

Eravant
Frequency Extenders
VENDORVIEW

Frequency-extendable vector network analyzers (VNAs) are increasingly vital for measuring components and antennas at mmWave and sub-THz frequencies. The STO series of

transmit/receive frequency extenders support bi-directional VNA measurements covering waveguide bands from 50 to 330 GHz. Internal frequency multipliers generate higher frequency RF and LO signals from lower frequency outputs provided by the VNA. Sensitive downconverters and effective noise filters yield dynamic range as high as 120 dB. Accessories include Proxi-Flange™ contactless waveguide adapters that eliminate the need for waveguide screws during tests.
www.eravant.com

ERZIA
Wideband Amplifier

Break through the bandwidth barrier with this wideband amplifier from ERZIA that operates at up to 20 GHz while providing an output power of 42 dBm and a gain of 51 dB. The compact, lightweight aluminum housing features multiple mounting options, making it ideal for a variety of demanding applications.
www.erzia.com

EZ Form Cable
Cables and Connectors

EZ Form Cable, a Trexon company, is an AS9100D certified manufacturer of coaxial cable, coaxial cable assemblies, RF connectors and coaxial delay lines. EZ Form's RF, microwave and mmWave transmission line solutions offer proven performance for critical applications in military/aerospace, cryo/quantum computing, telecommunications, medical, instrumentation and test.
www.ezform.com

Flann Microwave
Motorised Linear Attenuator

As the requirement for automated test equipment grows, we have re-evaluated our offering to accommodate our customers' needs. What Flann has achieved is a compact, programmable attenuator at a lower cost than our RVAs. It also boasts an impressive 0 to 50 dB range with an improved ± 10 percent attenuation flatness across the whole waveguide band, along with a high return loss.
www.flann.com

Garlock
WavePro®

WavePro® is a ceramic-filled PTFE dielectric, engineered for use in antennas, lenses and discrete components including phase shifters, couplers and more for RF and mmWave applications. Its precise formulation provides a low loss factor and superior mechanical and thermal stability. It exhibits minimal phase shift with frequency and temperature, and its highly consistent characteristics within and across panels improve quality control and result in higher production yields. WavePro® is an excellent choice for reliable, high performance wireless applications up to 80 GHz.
www.waveproantenna.com

Hasco

Low Loss Flexible Cable Series

VENDORVIEW

The HLL150A low loss flexible cable series provided by HASCO are armored phase stable against flexure, rated up to 40 GHz and are available in a variety of RF connectors and custom lengths designed for production and testing environments. This new series of low loss flexible cables expands HASCO's growing selection of low loss, phase stable, conformable, ruggedized and low PIM cable assemblies that are in stock and ready to ship daily.

www.hasco-inc.com

Dual Directional Coupler

Model WMHPDDC-80-1000M-40dB-N from Werbel Microwave is a dual directional coupler covering 80 MHz to 1 GHz. This model features 40 dB coupling factor in both forward and reverse. Ships with N Female connectors at all ports. Custom configurations of dB values and connector types are available. Forward and reverse coupled outputs are independently isolated, which means that a mismatch on one coupled port will not affect the other. This is useful in amplifier power monitoring applications where a good VSWR cannot always be guaranteed at the detector input.

www.werbelmicrowave.com

Herotek

Limiter

Herotek offers a wide range of high-power limiters. Model LS00105P200A is a 200 W CW limiter operating from 10 MHz to 500 MHz with 1 kW peak, 1 microsecond pulse width limiting protection. It has a low insertion loss of 0.8 dB and 2.2:1 VSWR with typical leakage of +20 dBm at 200 W CW input. This limiter has built-in input and output DC blocks. It comes in a hermetically sealed package with removable connectors for drop-in assembly and designed for both military and commercial applications.

www.herotek.com

HYPERLABS

Ultra-Broadband Test and Measurement Components

HYPERLABS is a leading provider of high performance, ultra-broadband test and measurement components including 63 GHz linear amplifiers. Designed to drive data in 224 Gbps applications, HYPERLABS components offer industry-best bandwidth to maintain optimized eye patterns. Since 1992, HYPERLABS has built a reputation as an industry leader in broadband component designs including baluns, bias tees, DC blocks, power dividers, and more. Visit HYPERLABS at IMS booth 1749.

www.hyperlabs.com

Insulated Wire Inc.

Ultra Low-Loss Coaxial Cables and Assemblies

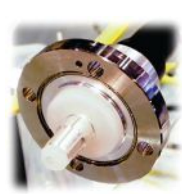

Insulated Wire Inc. manufactures a broad range of ultra low-loss coaxial cable and assemblies operating to 110 GHz. Our unique laminated EPTFE dielectric provides exceptional attenuation performance, which translates to excellent power handling, a requirement for various commercial and military applications. Primary high-power cable types are 2801, rated at 1.9 kW at 1 GHz, 4806 able to handle 3.2 kW 1 GHz and our 7506, which offers 10 kW at 1 GHz capability. Interfaces available include C, SC, LC, HN, 7/16, 1 5/8 in. and 7/8 in. EIA flanges.

www.insulatedwire.com

Ironwave Technologies

Non-Blocking Switch Matrix

Ironwave Technologies company introduces Mu-del Electronics' 16 × 64 non-blocking switch matrix, 16MDMS-2600-64NB/49. Designed for top performance and versatility, this solid-state switch matrix offers outstanding features and benefits for a wide range of applications. Offering touchscreen and remote interfacing with a frequency range of

20 MH to 6000 MHz, 16 inputs and 64 outputs, this switching matrix is designed to serve a wide variety of applications. This switch matrix also features 45 dBm minimum isolation and unity gain with a flatness of ±3 dB.

www.iwtllc.com

JFW Industries

Benchtop Attenuator

VENDORVIEW

Model 50BA-048-95 is a 50 Ω benchtop attenuator assembly containing two solid-state step attenuators. The attenuators have attenuation range of 0 to 95 dB by 1 dB steps and operate from 200 MHz to 8.4 GHz. The attenuator can be controlled manually or remotely. Its current attenuation setting is displayed on the front panel.

www.jfwindustries.com

JQL Technologies Corp.

Isolators & Circulators

VENDORVIEW

JQL continues to expand their product base through innovation and launched

a unique design of coaxial isolator and circulator in the frequency 27 to 31 GHz. This design has an integral housing with connectors. This device has extremely low insertion loss over the broad band, stable over temperature range and almost zero RF leakage, makes it ideal for applications such as space, airborne terminals, man-pack radios and satcom-on-the-move.
www.jqltechnologies.com

KR Electronics
Positive Train Control Bandpass Filters for Railroad Industry

NIC's positive train control filter series, designed for the railway industry, plays a critical role in minimizing RF interference between ITC and ACSES bands within the frequency range of 160 to 460 MHz. These IP54 and IP67 rated filters feature N Type connections and handle up to 100 Watts CW power. They are available for quick turn delivery, ensuring reliable railway communication. Please stop by Booth #433 for additional information.
www.krfilters.com

Kratos General Microwave
mmWave Control Components and Integrated Assemblies

General Microwave Corporation is a key partner with major OEMs and primes, having been chosen for our broad and comprehensive understanding of mmWave technologies. We offer catalog mmWave phase and amplitude control modules, which includes IQ modulators, phase shifters, switches, attenuators, as well as custom integrated assemblies operating in the 18 to 50 GHz frequency range. If it's a catalog unit or a highly customized mmWave assembly designed specifically for your high performance system needs, contact General Microwave.
www.kratosmed.com

Krytar
Butler Matrices
VENDORVIEW

The new Krytar butler matrix family uses Krytar's high performance 90- and 180-degree hybrid couplers providing superior phase accuracy, amplitude imbalance, stability, high isolation, low insertion loss and VSWR and repeatability. Offering coverage of multiple microwave bands, from 0.5 to 40 GHz, a Krytar butler matrix is the ideal choice for antenna array beamforming, 5G NR testing, mmWave testing, MIMO testing, multipath simulation and performance evaluation and many other applications.
www.krytar.com

KVG Quartz Crystal Technology GmbH
New Website With Outstanding Products

Superior products deserve superior presentation: KVG's new website presents their highly stable products with best phase noise on the market. The newest high-end product of KVG is the high performance 100 MHz oscillator O-22-ELPN with extraordinary low phase noise of -140 dBc/Hz at 100 Hz and -190 dBc/Hz noise floor. Visit our website and learn more about KVG and our products.
www.kvg-gmbh.com

LadyBug Technologies
New Power Sensor Options
VENDORVIEW

LadyBug Technologies' LB5900 series power sensors with LAN and PoE capabilities offer fast, accurate and traceable measurements. Covering frequencies from 4 kHz to 75 GHz and featuring triggering and other advanced functions, these sensors are

well-suited for tower, satcom and manufacturing test applications. Security options such as military, which prevent storage of information in the sensor, and for applications that require storage of settings or data within the sensor, Option SAN that securely erases stored data upon command.
www.ladybug-tech.com

Logus Microwave
SPDT Manual Toggle Coaxial Switches

High reliability for your RF/microwave requirements: SOC12EMT performs from DC to 18 GHz with a VSWR of 1.5:1 maximum, insertion loss of 0.5 dB maximum isolation of 60 dB minimum SOC12EKT performs from DC to 40 GHz with a VSWR of 2.0:1 maximum, insertion loss of 0.9 dB maximum and isolation of 50 dB minimum. Small quantities are available from stock.
www.logus.com

LPKF
Direct PCB Laser Processing Systems

The latest LPKF ProtoLaser systems provide direct laser processing for flexible, rigid-flex and rigid RF/microwave materials. Advantages of the laser technology includes rapid metal removal for fine pitch traces/spacing, pristine drilling and cut quality, controlled laser pocket or channel engraving and user adjustable settings for new materials variations. Sophisticated software allows development and on-demand production within your lab creating precision devices in only minutes.
www.lpkfusa.com

Marki Microwave
Surface-Mount MMIC Tunable Filter
VENDORVIEW

The MFBT-00003PSM is a surface-mount MMIC tunable filter for adaptive filtering applications. It offers separate lowpass and highpass tuning capability, allowing users to

create bandpass filters with variable center frequencies and percent bandwidths. Performance features include low return loss in both the passband and stopband, low insertion loss and high stopband rejection, and high IP3 relative to other tunable filters. Available as a 4x4 mm plastic QFN, it is suited to replace much larger switched filter banks.
www.markimicrowave.com

Maury Microwave
Characterization Solutions, Components and Services

Our mission is to give our customers confidence in their RF through THz measurements and models. We accomplish this by providing best-in-class and fully-proven characterization solutions, components and services. We help the world's leading manufacturers in the wireless technology chain build better products and bring them to market faster. Visit Maury Microwave at IMS2024, booth #704.
www.maurymw.com

MIcable Inc.
Wideband High Accuracy Butler Matrices
VENDORVIEW

MIcable 0.6~7.25 / 0.6~5 / 2.4~7.25 / 24~43 GHz 4×4 and 8×8 wideband high accuracy butler matrices can transfer the signal reciprocally from any of 4 or 8 ports to any of the other 4 or 8 ports. They have unbelievable super excellent phase accuracy, amplitude balance, stability and repeatability over very wide bandwidth. These advantages make them ideal for 5G, Wi-Fi 6E/Wi-Fi 7, MIMO testing, signal multipath simulation, antenna array beamforming and IoT, etc.

Cryogenic Component Solutions

MIcable cryogenic product series provides complete connection solutions for cryogenic applications such as quantum computers. The products mainly include cryogenic cable assemblies, coaxial adapters and fixed attenuators. The components have the advantages of small size for high-density arrangement, hermetic seal feature for avoiding air inflow and gas leakage, low heat conductivity for minimizing inflow of the heat from the high temperature end, as well as excellent electrical performance and high working frequency up to 18 GHz.
www.micable.cn

Mician GmbH
µWave Wizard™ Filter Workbench

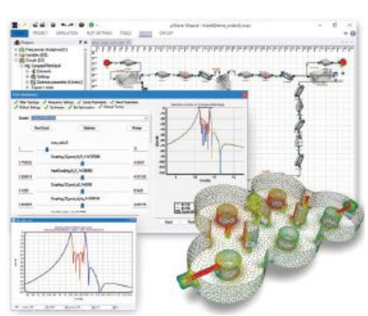

Filter Workbench is a powerful quasi-automated filter synthesis add-on to Mician's renowned µWave Wizard™ product line. Tailored to assist users in designing and optimizing microwave filters of moderate relative bandwidth, Filter Workbench centers around a user-generated coupling matrix as input. Its intuitive user interface accommodates a diverse range of filter topologies, from simple waveguide iris filters to intricate cross-coupled combline filters. As a result, Filter Workbench provides a complete schematic layout with tiered subcircuits, and associated goal functions based on filter specifications.
www.mician.com

Millibox

Affordable sub-THz OTA Test Setups to 330 GHz

MilliBox, the leader in benchtop mmWave OTA test systems, has integrated Eravant's frequency extenders into a complete solution. The new MBX32E allows OTA testing up to 330 GHz, where coax cabling becomes impractical. The test setup includes a benchtop anechoic chamber, a programmable 3D positioner and a pair of STO-series compact frequency extenders mounted to the positioner and probe. This combination is ideal for 6G and sub-THz applications.

www.millibox.org

Mini-Circuits

VENDORVIEW

Coaxial Filter Passes

Mini-Circuits' model ZVBP-40600-K1+ is a coaxial cavity bandpass filter with low loss passband of 37.7 to 43.5 GHz. Typical passband insertion loss is 1.8 dB with typical passband return loss of 18 dB. Lower stopband rejection is typically 88 dB from DC to 36.6 GHz while upper stopband rejection is typically 79 dB from 44.6 to 55.0 GHz. The RoHS-compliant 50 Ω filter is well suited for cellular 5G n259 and n260 bands and is equipped with 2.92 mm female coaxial connectors.

Surface-Mount Filter

Mini-Circuits' model WSBP-26G+ is a substrate-integrated-waveguide (SIW) bandpass filter with passband of 25 to 27 GHz. Passband insertion loss is typically 2.3 dB while passband return loss is typically 12.0 dB. Stopband rejection is typically 41 dB or better from DC to 23 GHz and typically 35 dB from 31 to 32 GHz. Suitable for 5G n258 band applications, the 50 Ω surface-mount filter measures 1.20 × 0.210 × 0.015 in. (30.54 × 5.33 × 0.38 mm) and weighs 0.35 g.

Signal Generator

Mini-Circuits' model SSG-44G-RC is a versatile signal generator that provides CW and pulsed outputs (as narrow as 0.5 μs) from 100 MHz to 44 GHz. It offers signal levels from -40 to +17 dBm at a 2.92 mm female output connector and can operate in swept frequency and frequency hopped modes. Typical harmonic levels are -30 dBc, with typical spurious content of -40 dBc. The compact signal generator, which can be controlled via USB or Ethernet bus, includes full software support.

Variable-Gain Amplifier

Mini-Circuits' model ZVA-18443VG+ is a coaxial amplifier with adjustable gain range of 30 to 47 dB from 18.0 to 43.5 GHz. Featuring 2.92 mm female input and output connectors, gain can be tuned by analog or TTL control. At minimum gain, typical output power at 1 dB compression is +28 dBm while at maximum gain the saturated output power is typically +31 dBm. Ideal for aerospace/defense, satellite and test applications, the amplifier runs on a single +10 to +15 VDC supply.

LTCC Highpass Filter

Mini-Circuits' model HFCN-3052+ is a low-temperature cofired-ceramic (LTCC) highpass filter with passband of 30.5 to 56.2 GHz. Passband insertion loss is typically 1.7 dB from 30.5 to 45.8 GHz and 2.5 dB to 56.2 GHz. Return loss is typically 14.1 dB from 30.5 to 45.8 dB and 12.8 dB from 45.8 to 56.2 GHz. Supplied in a 1206 ceramic form, the filter offers typical rejection of 21.4 dB from 0.1 to 11.2 GHz and 15 dB from 11.3 to 23.5 GHz.

www.minicircuits.com

Molex

Test and Measurement

Molex highlights our new high frequency products with performance up to 110 GHz. The newly released "Cardinal" line of high performance cable assemblies with Molex's ruggedized armored VNA test cables along with standard flex cables are ideal for bench top testing. Connector options include SMA, 3.5 mm, 2.92 mm, 2.4 mm, 1.85 mm and 1.0 mm series. In addition to the cable assemblies, Molex's new high frequency products include precision in-series and between-series adapters as well as their new line of End Launch PCB connectors.

www.molex.com

MPG

Broadband Diplexer

Whether you require dependable signal separation for defense ops, accurate measurement capabilities for electronic warfare or improved signal integrity for radar applications, MPG's SPCL-00734 broadband diplexer stands ready to meet your most demanding requirements. This device separates carriers below 5 GHz from their harmonics up to 40 GHz and prevents the carrier from reflecting to the device under test or entering the spectrum analyzer. MPG offers customizable options to meet your size and weight constraints without compromising performance.

www.mpgdover.com

Networks International Corp.

Ultra-Low-Profile LC Filters

NIC's engineering expertise in high-reliability RF products includes low-profile (< 0.1 in.) LC filters that span from 10 MHz to 11 GHz. These compact high performance filters are built on industry-standard PCBs such as Rogers 4350 or 4003 and have high selectivity with an out-of-band rejection of > 60 dB. These products can be customized to meet passband requirements from 1 to 100 percent and pass a wide range of environmental requirements as well. Please stop by Booth #433 for additional information.

www.nickc.com

NI

Vector Signal Transceiver

The PXIe-5842 vector signal transceiver combines a vector signal analyzer and generator with a user-programmable FPGA and high speed serial and parallel digital interfaces into a single instrument. With frequency coverage from 30 MHz up to 26.5 GHz, up to 2 GHz of instantaneous bandwidth and exceptional RF performance in just 4 PXI slots, the PXIe-5842 is a highly versatile and capable tool for wireless connectivity, cellular, aerospace and defense and general purpose RF applications.

www.ni.com

Norden Millimeter

Custom Transceivers

Norden designs custom transceivers for military and commercial applications including airborne, UAV and EW. They have "catalog" models which provide wideband RF and up to 1.5 GHz IF with low phase noise. Norden can provide custom designs which incorporate temperature compensation, variable gain and meet military environmental requirements. Norden also offers models in a low SWaP 3U VPX module which includes a built in LO. Norden engineers utilize proven designs to provide low risk, cost-effective solutions.

www.nordengroup.com

Nxbeam

Power Amplifier MMIC

VENDORVIEW

Nxbeam expands its Ka-Band power amplifier MMIC portfolio with the release of a 10 W GaN power amplifier. The NPA2040-DE operates from 27.5 to 31 GHz and provides an average saturated output power of 10 W, 31 percent power added efficiency, and 24.5 dB linear gain. This MMIC is ideal for satellite communication ground terminals and point-to-point communication links and lines up perfectly with Nxbeam's 20 W and 35 W GaN power amplifier MMICs.

www.nxbeam.com

Passive Plus

Broadband Multilayer Ceramic Capacitor

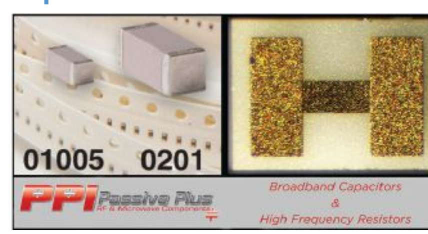

Passive Plus (PPI) has partnered its broadband capacitors with its high frequency resistors for similar case size and footprint to meet your high frequency needs. The 01005BB case size broadband multilayer ceramic capacitor is complemented by the R35-1209BB case size high frequency resistor, and the 0201BB case size broadband multilayer ceramic capacitor is complemented by the R35-2010BB case size high frequency resistor. Modelithics 3D Modeling Data available on the PPI website.

www.passiveplus.com

Piconics Inc.
NbTi Inductors

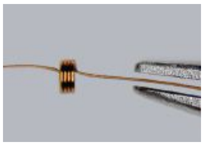

Piconics Inc. introduced a new line of Nobium Titanium (NbTi) wire air coil inductors for quantum computing applications. By utilizing NbTi wire the coils become superconductors at low temperature. The inductors range in inductance values of 10 to 250 nH and offer high frequency performance comparable to Piconics other fine wire air coil inductors. Typical applications include filters and hardware for quantum computing and other cryogenic applications. Custom NbTi wound solutions also available.
www.piconics.com

Quantic PMI
Phase Shifters & Bi-Phase Modulators
VENDORVIEW

Quantic PMI offers the highest quality phase shifters and bi-phase modulators for 5G, industrial and military applications in frequency ranges up to 70 GHz. Features include analog and digital control, fast speed and response time, low insertion loss, high phase accuracy, small size and standardized packaging. Available options are surface-mount or connectorized; custom packaging; form, fit and function designs; connector options; hermetic sealing, military or aerospace screening available. COTS availability.
www.quanticpmi.com

Quantic X-Microwave
3U and 6U OpenVPX Card Assemblies

Quantic X-Microwave offers 3U and 6U OpenVPX card assemblies leveraging their proven modular platform for quick turn prototypes and production IMAs. We offer the ability to integrate complex customer specified RF and microwave signal chains that interface with other VPX RF and control cards through a common backplane to realize complete systems, typically for aerospace and defense applications.
www.quanticxmw.com

Reactel Inc.
Filters, Multiplexers & Multifunction Assemblies
VENDORVIEW

Reactel will feature its full line of filters, multiplexers and multifunction assemblies covering up to 67 GHz at IMS2024 in Washington, DC. Supporting military, commercial, industrial and research needs, we can design the right unit for you. From small, lightweight units suitable for flight or portable systems to high power units capable of handling up to 25 kW, connectorized or surface-mount, large or small quantities, our talented engineers can design a unit specifically for your application. Visit Reactel in booth 814.
www.reactel.com

Remcom
Impedance Tuner Matching in XFdtd®
VENDORVIEW

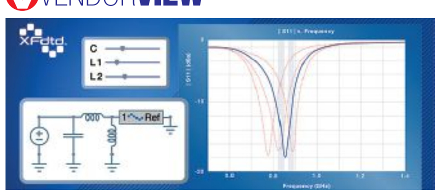

Remcom's XFdtd is a full-wave electromagnetic simulation tool that contains an integrated schematic editor and circuit solver for comprehensive matching network design. Intuitive sliders enable rapid manipulation of inductor and capacitor values to meet design goals and understand the behavior of a circuit. In addition, the schematic editor allows multi-state tuners to be incorporated into full-wave results and supports optimization on system efficiency. Visit Remcom's booth to learn more about Remcom's EM simulation solutions.
www.remcom.com

RF Lambda

600 W, 2 to 6 GHz, EMC Power Amplifier

This wideband EMC power amplifier spans an impressive frequency range of 2 to 6 GHz while delivering 600 W of CW output power. This advanced solution is built to provide engineers and researchers with a single broadband solution, offering high power-amplified signals over a wide frequency range without the need to source several amplifiers. Applications include test and measurement, EMC/EMI, wireless commercial communications, aerospace, military as well as research such as particle physics.

300 W, 2 to 20 GHz, EMC Power Amplifier

This 300 W CW EMC AC-powered amplifier is optimized to cover a broadband frequency of 2 to 20 GHz. This unit is packed with comprehensive protection features such as built in temperature compensation, automatic -calibration, as well as over current, temperature, VSWR, current imbalance and RF input protection. The unit also supports ethernet control and monitoring. Applications include test and measurement, EMC/EMI, wireless commercial communications, aerospace, military as well as research such as particle physics.

18 to 26 GHz, Hermetically Sealed Power Amplifier

Our ultra-wideband power amplifier spans 18 to 26.5 GHz with 51 dBm output power. The DC-powered series offers a compact package, easily integrated into RF systems or test setups. Any of RF Lambda's DC amplifiers can be provided in an AC-powered unit (RAMPXXX series). Hermetic seal, including 100 percent leak testing as per MIL-STD-883, is available for outdoor and harsh environments.

1 to 18 GHz, Hermetically Sealed SP2T Switch

RF Lambda's 1 to 18 GHz SP2T high-power 20 W switch combines robust power handling with rapid switching. Ideal for radar or TDD systems, it boasts low 1.8 dB insertion loss and a maximum 200 ns switching time. The comprehensive range of active RF switches, from SP2T to SP160T, supports power handling up to, ensuring longevity without cycle limitations. Perfect for sustained, reliable switching in demanding systems.

www.rflambda.com

RFMW

High Performance 50 Ω, 2.5+ GHz Transformer

VENDORVIEW

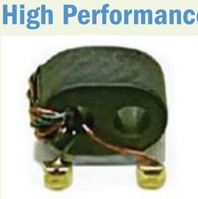

MiniRF's MRFXF0589 is a new high performance 50 Ω, 2.5+ GHz transformer in the new "Mini" 3 × 3.5 mm 4-pin surface mount package. It has excellent return loss, better than 20 dB typical across the band, and extremely low insertion loss of 0.5 dB typical. This transformer offers very good amplitude match which assists minimizing distortion for signal transfer from balanced to unbalanced circuits. MiniRF offers unsurpassed repeatability with 100 percent RF tested devices and low-cost manufacturing.

Smiths Planar X RF Filters for X-, Ku- and Ka-Bands

Smiths Interconnect's Planar X Series of standard RF filters provide system engineers with high performance, compact, light-weight solutions for critical RF filtering in X-Band, Ku-Band and Ka-Bands. Planar X Series compliments Smiths Interconnect's broad portfolio of RF/microwave components with an off-the-shelf product reducing the lead times of custom designs.

Spectrum Control Powerfilm Chip Attenuator Design Kit

Spectrum Control's Powerfilm chip attenuator design kit is ideal for rapid prototyping and development. It can significantly accelerate development and prototyping efforts and provide designers a great selection of popular Powerfilm chip attenuators for board-level RF module and system designs. The Powerfilm™ PCAAF_W-T9016 kit includes samples of 26 different part numbers in the PCAAW and PCAAF families, making it easy for designers to select the component appropriate for their design.

www.RFMW.com

Richardson RFPD
RadioCarbon and RadioThrorium Design Accelerators

VENDORVIEW

Start developing radio projects in minutes instead of months. Design Accelerators are standardized, off-the-shelf, hardware development platforms that help RF and radio product developers reduce risk and speed time to market. Each design accelerator includes full documentation, open source or licensable software and technical support. Design files of select design accelerators may also be available via license. RadioCarbon and RadioThrorium design accelerators were developed by Richardson RFPD to support high-power software defined radio, troposcatter, satcom and 5G mmWave communications applications.

www.richardsonrfpd.com

RLC Electronics
Panel Mount-SMT Filters

RLC Electronics is manufacturing 200 W cW panel mount-SMT filters. This tubular filter, which operates in UHF/L-Band, is designed to be panel mounted on one end and board mounted on the other end. The exposed pin is soldered directly to the customer's board, utilizing the mounting bracket to establish good ground. This saves at the customer end on cost and loss (no cables or mating connectors required). This filter is used in a handheld radio system. Similar designs available in higher/lower frequency and power combinations.

www.rlcelectronics.com

Rosenberger
Compact Calibration Kits – for MSO and MSOT Calibrations

Compact calibration kits from Rosenberger – available in various common coaxial interfaces, combine all necessary calibration standards in one compact unit, small, easy to handle and light weight. The 3-in-1 calibration kits can be applied for complete MSO calibrations (open – short – load) of single port VNAs, the 4-in-1 calibration kits can be used for complete MSOT calibrations (open – short – load - thru) of two or more port vector network analyzers. Rosenberger runs its own calibration laboratory accredited and controlled by the German accreditation body DAkkS (Deutsche Akkreditierungsstelle) – according to DIN EN 17025.

www.rosenberger.com

Saetta Labs
Sapphire Loaded Cavity Oscillators

Saetta Labs is introducing a line of 'whispering-gallery' Sapphire Loaded Cavity Oscillators (SLCO) at X-Band. These SLCOs are pure microwave oscillators exhibiting unparalleled low phase noise of -155 dBc/Hz at 10 kHz offset (8 GHz). Melding state of the art materials with meticulous engineering they are a complete subsystem operating free-running or locked to an external reference. 8 GHz, 10 GHz, 10.24 GHz, 12 GHz and customer specified. Visit us at IMS booth 344.

www.saettalabs.com

Samtec
Phase & Insertion Loss Stable Cable Assemblies

Samtec's Nitrowave™ high performance microwave cable offers improved phase and amplitude stability over flexure. Performance is optimized at frequencies that go beyond traditional industry targets to support emerging applications in the aerospace/defense, test and measurement and instrumentation markets. Initial product release includes LL043 Series with 2.92 mm, 2.40 mm and SMA connector end options. Additional Nitrowave™ cable assemblies coming soon.

www.samtec.com

SignalCore
40 GHz RF Down-converter

The SC5319A and SC5320A are Ka-Band single stage down-converters, with input RF range from 20 GHz to 40 GHz, external LO frequency range from 10 GHz to 20 GHz, output IF range from 100 MHz to 4 GHz and 3 dB bandwidth of 2 GHz. These modules feature an internal synthesized LO, selectable RF preamplifier and variable gain control. As being compact and versatile standalone down-converters, they are ideal for SISO and MIMO applications.

www.signalcore.com

Signal Hound
High Performance Spectrum Analyzer / Monitoring Receiver

Signal Hound's SM435C is a high performance spectrum analyzer/monitoring receiver tuning from 100 kHz to 43.5 GHz. This next-generation SM series analyzer includes a 10 Gb Ethernet SFP+ port, enabling communication with a PC over long distances using a fiber-optic cable. Designed for precision, remotely located, RF data analysis, the SM435C is perfect for 5G mmWave monitoring and analysis, 24 GHz ISM frequency monitoring, complete Ka-Band spectrum testing and analysis of emerging and new high frequency RF signals.

www.signalhound.com

Smiths Interconnect
HR TXS Series

Smiths Interconnect has extended its offering of high frequency surface-mount chip attenuators with the release of its HR TXS Series, a small, easy-to-implement, high-reliability product qualified for space and defense applications. The HR TSX Series is qualified to MIL-PRF-55342 and designed to offer excellent broadband performance up to 50 GHz, while

delivering increased power handling in a small 0604 surface-mount package. It allows wider coverage than traditional components while providing optimized return loss for multiple frequency ranges.
www.smithsinterconnect.com

Southwest Microwave
Flex Cable Connector

Newest SMI product offering is 54070-001B, a direct solder .047 SC flex cable connector with a built-in bullet. It combines the SSBB cable receptacle with the bullet interface creating a single-pc cable bullet. Frequency range is DC to 67+ GHz. As a standalone connector on a cable, it serves as a manual test probe. It also can be ganged together in a multipin configuration and thereby serve as the heart of the SSBB multipin cable harness.
www.mpd.southwestmicrowave.com

Spectrum Control Inc.
SCi Blocks

Spectrum Control Inc. (booth #208) will showcase two significant additions to its SCi blocks family of miniature, modular and intelligent RF+Digital system blocks. The new DirectRF mezzanine is the company's first RF-to-bits building block and an extension to its innovative SOSA-aligned wideband transceiver. Leveraging the Altera Agilex® 9 FPGA, it converts up to eight RF inputs and eight RF outputs at sample rates of up to 64 Gsps, with 32 GHz IBW. They will also unveil their new RF+Digital system-in-package platform, dramatically shrinking the RF frontend. The first SiP is a low noise, high gain wideband preselector in a standard BGA package.
spectrumcontrol.com

Stellant Systems
K-Band Quad Space nanoMPM®

Stellant Systems' K-Band Quad Space nanoMPM® is a state-of-the-art RF power amplifier for use in satellite downlink applications, specifically designed to enable the next generation of software-defined satellites utilizing phased-array antennas for increased flexibility while on-orbit. This product delivers the ultimate performance by leveraging the best of solid-state and TWT vacuum technology. Utilizing a high-gain pre-distortion solid-state linearizer, wideband high-power mini-TWT and proprietary compact nanoMPM® EPC designs, the B3400H series bridges the gap between solid-state amplifiers and traditional space LCTWTAs.
www.stellantsystems.com

SV Microwave
VITA RF 67

Amphenol SV Microwave's VITA 67.1, .2 and .3 product lines are the latest addition to the RF/coaxial section of the VPX platform. These modular solutions include contacts, cable assemblies, adapters and connector backplane and plug-in modules that support the entire RF signal path of your embedded system. SV's VITA products are designed for side-by-side implementation with other VITA connector standards. Visit SV Microwave at Booth #905 to learn more about their products and capabilities.
www.svmicrowave.com

Syscom Advanced Materials Inc.
Conductive Fiber Braiding Material

Liberator® conductive fiber braiding material provides cable manufacturers with the lightest weight alternative to traditional silver-plated copper braiding available today. Cables using Liberator® weigh 30 percent less on average. The fiber works with existing braiding equipment and is provided on spools or cores. Liberator® can be soldered or crimped and has proven shielding effectiveness equal to or better than traditional copper braiding. Superior flex-cycle durability over 1000x that of equivalent size copper provides an added benefit for repetitive bend applications.
www.metalcladfibers.com

Taitien
DTA-450 Atomic Clock

The DTA-450 atomic clock is distinguished by its exceptional features, notably its remarkably low power consumption, consuming a maximum of only 130 mW. It offers precise timing synchronization with 1 pps input and output capabilities. With remarkable accuracy, it disciplines to < 50 ns in phase and <10e-12 in frequency, ensuring unparalleled reliability. These features make the DTA-450 indispensable across diverse industries where precision and efficiency are paramount, setting a new standard in atomic timekeeping technology.
www.taitien.com

Tecdia
Wire-bondable Capacitors

Tecdia's new K4200 dielectric for single layer wire-bondable capacitors enables even more size, thickness and capacitance options for use as drop-in replacements in existing designs and entirely new designs alike. Visit us at IMS2024, booth 2131 to learn more about how we can solve your quality, lead-time and pricing issues with passive wire-bondable components. For more information please email us at sales@tecdia.com.
www.us.tecdia.com

Teledyne Storm
VITA Cable Assemblies

Teledyne Storm Microwave's VITA product line is expanding. We have created a new sample kit to display both NanoRF and SMPM contacts on StormFlex047 cable assemblies to demonstrate how easy they are to route. These are built to be reliable in harsh environmental conditions. For even more challenging needs we offer these contacts on StormFlex034 cable as well.
www.teledynedefenseelectronics.com

Pick Up Your T-Shirt
in the MWJ Booth 811

Times Microwave
High-Power Lineup

Experience unparalleled power and precision with Times Microwave Systems' High Power product lineup. Their StripFlex®, HPL, HP and HPQD™/MPQD™ connectors redefine connectivity, offering unmatched performance and durability for any application. StripFlex® provides exceptional flexibility without compromising performance, while HPL ensures reliability and efficiency in power distribution systems. HP connectors deliver robust connections for high-power applications, and HPQD/MPQD connectors offer quick-disconnect functionality and versatility. Trust in their commitment to excellence, revolutionize your power solutions today with Times Microwave Systems.
www.timesmicrowave.com

Transline Technology
High Performance PCB Laminates

With 30+ years' expertise, Transline Technology specializes in working closely with engineering innovators that push RF, microwave mmWave PCB boundaries. Our hands-on approach makes us an extension of your engineering team. We stock a wide variety of high performance PCB laminates enabling rapid prototype delivery.
www.translinetech.com

Vaunix
High-Resolution Digital Attenuator

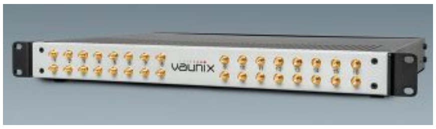

The LDA-802-32 digital attenuator is a rack-mounted 32-channel high dynamic range, bidirectional, 50 Ω step attenuator. It provides 120 dB of attenuation control range from 200 to 8000 MHz with a step size of 0.1 dB. The attenuators are easily programmable for fixed attenuation, swept attenuation ramps and user-defined fading profiles directly from the included graphical user interface (GUI). Alternatively, Vaunix supplies LabVIEW drivers, Windows API DLL files, macOS DYLIB files, Linux drivers, Python examples and more for users wishing to develop their own interface.
www.vaunix.com

WAFIOS
CNC Tube Bending Machine

The new BMZ 6 from WAFIOS is a unique and innovative CNC tube bending machine that has been specially developed for very small parts, such as those used in high frequency technology for semi-rigid coaxial cables. It is capable of bending small parts from tube or wire up to an outer diameter of 6 mm. The modular design enables the production of highly complex component geometries by combining different bending processes such as coiling and free forming. Visit us at booth 754.
www.wafios.com

WAKA Manufacturing

Cable Assembly

WAKA Manufacturing has introduced a new cable assembly featuring a 1.0 mmWave connector and rigid armor. This assembly ensures a balance between durability and flexibility by utilizing semi-rigid internal cables to maintain phase stability even when bent. It supports frequency up to 110 GHz and offers customizable lengths starting from a minimum of 150 mm, adjustable in 1.0 mm increments. Its high performance low reflection characteristics are achieved through WAKA's innovative soldering technology. A release of 1.85 mm armored cable is planned.

www.waka-manufacturing.com

Weinschel Associates

High-Power Attenuators and Loads

Weinschel Associates announces an improved line of high power attenuators and loads to accent their current high power offerings. The WA70/6 and WA1470/6 is a 1 KW attenuator and termination performing from DC to 6 GHz and is available with a variety of connector options to include N-Type, 4.3/10 and 7/16 DIN. Please visit us at IMS in booth #812 or contact Weinschel Associates at sales@weinschelassociates.com for more information.

www.weinschelassociates.com

West Bond

7KF Bonder

The 7KF bonder with West Bond new 7 in. capacitive touch sensing LCD displayed is designed with a gantry style chassis enabling unlimited part size capacity. The exclusive 8:1 ratio, purely orthogonal X-Y-Z Micromanipulator, allows the operator to place bonds very precisely, and is convertible between Ball Bonding and Wedge Bonding, presenting bond wire at both 45 and 90 degrees for deep access and ribbon bonding capabilities, is an excellent tool for RF, microwave, semiconductor, hybrid and medical device fields applications.

www.westbond.com

Z-Communications
DRO14000A for Radar, 5G, Satcom, Test and Measurement

The new DRO from Z-Communications, Inc. delivers 14 GHz while incorporating electrical and mechanical elements for fine and coarse tuning. This high performance DRO is optimized to feature superior low phase noise of -100 dBc/Hz at 10 kHz and -132 dBc/Hz at 1 MHz offsets and operates from a single 5 Vdc supply with low current draw of only 26 mA. Available in a surface-mount package for ease of manufacturing.
www.zcomm.com

Pick Up Your MWJ T-Shirt in Booth 811

REVOLUTIONARY HERMETIC SMP CONNECTORS

These SMPs meet the requirements of MIL-STD-348, but utilize unique housing interface features, which significantly improves reliability and production assembly yields. Proprietary techniques are used to independently control plating thickness on pin and housing.


For use with Aluminum, Kovar and other package materials

SPECIAL HERMETIC PRODUCTS, INC.
PO BOX 269 – WILTON – NH – 03086
(603) 654-2002 – Fax (603) 654-2533
E-mail: sales@shp-seals.com
Web: www.shp-seals.com

RF Amplifiers, Isolators and Circulators from 20MHz to 40GHz

- Super low noise RF amplifiers
- Broadband low noise amplifiers
- Input PIN diode protected low noise amplifiers
- General purpose gain block amplifiers
- High power RF amplifiers and broadband power amplifiers


- RF isolators and circulators
- High power coaxial and waveguide terminations
- High power coaxial attenuators
- PIN diode power limiters
- Active up and down converters

Wenteq Microwave Corporation
138 W Pomona Ave, Monrovia, CA 91016
Phone: (626) 305-6666, Fax: (626) 602-3101
Email: sales@wenteq.com, Website: www.wenteq.com

FEATURED e-Books

Check out this month's featured eBooks, online at
mwjournal.com/ebooks

KR ELECTRONICS
A Division of Networks International Corp.

Visit us at IMS Booth# 433

Custom & Standard Filters
40+ Years of Military & Commercial Applications

Bandpass	Lowpass
Anti-Aliasing	Notch
Highpass	Root Cosine
Video Filters	Equalizers
Diplexers	Linear Phase
Delayed Equalized	Absorptive
Surface Mount	Matched

sales@krfilters.com www.krfilters.com Ph: 913 685-3400

LOW NOISE AMPLIFIERS
WWW.SATELLINK.COM

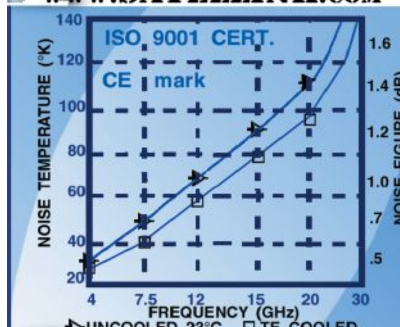

42nd
SATELLINK, INC.
3525 MILLER PARK DR.
GARLAND, TX 75042
CALL (972)487-1434
FAX (972)487-1204

ES MICROWAVE LLC.

Since 1985 we have offered our custom design filters and sub-assemblies in combline, interdigital and suspended-substrate technologies.

Broadband
Suspended-Substrate
Filters, Diplexers, Triplexers, Quadruplexers, Quintuplexers, Sextuplexers...

DC-40 GHz Filters
Multiplexers &
Switch Filter Banks

ES Microwave, LLC
8031 Cessna Avenue, Gaithersburg, MD 20879
P: 301-519-9407 F: 301-519-9418
www.esmicrowave.com

MAKING WAVES

5G Network Emulation Solutions

Discover more about Keysight's innovative 5G network emulation solutions in its latest catalog. Learn how Keysight's advanced solutions streamline 5G device workflow from development to deployment.

Keysight Technologies
ow.ly/8I5U50QH3Is

NI's New Open Innovation Laboratory

In cooperation with the ESA, NI's new Debrecen lab will focus on HiL and modular instrumentation that will drive new test strategies and advance emerging space applications.

NI
www.ni.com

The Future is Here: Integrating X-Band Radar for Next-Level Detection and Imaging

Radar technology has evolved dramatically over nearly a century. Today's radar is key to weather forecasting, air traffic management and vehicle safety. Dive into the future with Qorvo's latest blog on next-gen X-Band radar designs.

Qorvo
ow.ly/3T8g50QElul

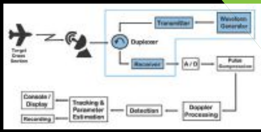

Remcom Updates Website

Remcom launched a new website with a major upgrade to their Resource Library. Sort by product, application and media format via the selectors. Choosing your desired combination will surface all the matching results from the library.

Remcom
www.remcom.com

Talking RF: Occupied Bandwidth - Keeping Communication Clean

In this episode of Talking RF, Signal Hound talks about occupied bandwidth (OBW), a regulatory requirement that is specified for equipment in some global regions.

Signal Hound
bit.ly/49gYAZ0

DDS Option for High Speed AWGs

Spectrum Instrumentation has released a new firmware option for its range of versatile 16-bit AWGs with sampling rates up to 1.25 GSPS and bandwidths up to 400 MHz. The new option allows users to define 23 DDS cores per AWG-card, that can be routed to the hardware output channels.

Spectrum Instrumentation
https://youtu.be/PoT0cReolRE

Review by: Dr. Ajay K. Poddar

Bookend

Developing Digital RF Memories and Transceiver Technologies for Electromagnetic Warfare

Phillip E. Pace

This book is an invaluable resource for a wide range of readers, including students and professionals working in AI and machine learning (ML)-inspired engineering. It focuses on the design trade-offs involved in developing multiple, structured, false target synthesis digital RF memory (DRFM) architecture and provides guidance on developing counter-DRFM techniques and distinguishing false targets from real ones. The book covers various transceiver technologies for electromagnetic (EM) warfare, including the latest advancements, emerging trends, case studies and best practices. It is an essential guide for anyone who wants to stay current with the latest developments in EM warfare.

This book is unique in that it provides a detailed table of contents and 11 chapters that delve into various relevant topics. There is a huge demand for sensors on unmanned vehicles, with the network-enabled DRFM serving as the eyes and ears for defense personnel. This book is divided into two parts. Part 1 deals with embedded transceiver design and architecture development for EM spectrum dominance and maneuver warfare. Part 2 introduces the concepts and techniques of modern spectral sensing using AI and ML for emitter modulation classification and electronic attack for counter-targeting to interrupt the kill web. A final chapter is included on recent counter-DRFM techniques, discussing the methods used to defeat the DRFM. One key feature of this book is the available online resources, including MATLAB software on the Artech House website. Readers can use these resources to reproduce the results published in this book, including problem exercises to enhance their understanding of the material.

Overall, this book is a must-read for anyone who wants to stay ahead in the field of DRFM transceivers, ML and deep learning in EM warfare.

ISBN 13: 9781630816971
Pages: 920
Digital download: $135
To order this book, contact:
Artech House (2022)
us.artechhouse.com

EXHIBITORS ARE HIGHLIGHTED IN BLUE

SPECIAL FOCUS ADVERTISERS ARE HIGHLIGHTED IN GREEN

Sales Representatives

Eastern and Central Time Zones
Carl Sheffres
Group Director
(New England, New York, Eastern Canada)
Tel: (781) 619-1949
Cell: (781) 363-0554
csheffres@horizonhouse.com

Michael Hallman
Associate Publisher
(NJ, Mid-Atlantic, Southeast, Midwest, TX)
Tel: (301) 371-8830
Cell: (781) 363-0338
mhallman@mwjournal.com

Pacific and Mountain Time Zones
Brian Landy
Western Reg. Sales Mgr.
(CA, AZ, OR, WA, ID, NV, UT, NM, CO, WY, MT, ND, SD, NE & Western Canada)
Tel: (831) 426-4143
Cell: (831) 713-9085
blandy@mwjournal.com

Submitting ad material?
Visit: www.adshuttle.com/mwj
(866) 774-5784
outside the U.S. call
+1-414-566-6940

Ed Kiessling
(781) 619-1963
ekiessling@mwjournal.com

International Sales
Richard Vaughan
International Sales Manager
Tel: +44 207 596 8742
rvaughan@horizonhouse.co.uk

Germany, Austria, and Switzerland (German-speaking)
Brigitte Beranek
Tel: +49 7125 407 31 18
bberanek@horizonhouse.com

France
Gaston Traboulsi
Tel: +44 207 596 8742
gtraboulsi@horizonhouse.com

Korea
Jaeho Chinn
JES MEDIA, INC.
Tel: +82 2 481-3411
corres1@jesmedia.com

China
Shanghai
Linda Li
ACT International
Tel: +86 136 7154 0807
lindal@actintl.com.hk

Wuhan
Phoebe Yin
ACT International
Tel: +86 134 7707 0600
phoebey@actintl.com.hk

Shenzhen
Annie Liu
ACT International
Tel: +135 9024 6961
anniel@actintl.com.hk

Beijing
Cecily Bian
ACT International
Tel: +86 135 5262 1310
cecilyb@actintl.com.hk

Hong Kong
Floyd Chun
ACT International
Tel: +852 28386298
floydc@actintl.com.hk

Taiwan, Singapore
Simon Lee
ACT International
Tel: +852 2838 6298
simonlee@actintl.com.hk

Japan
Katsuhiro Ishii
Ace Media Service Inc.
Tel: +81 3 5691 3335
amskatsu@dream.com

Corporate Headquarters: 685 Canton Street, Norwood, MA 02062 • Tel: (781) 769-9750

FABS and LABS

CML Micro: Customer-Centric, Continuous Innovation and Unwavering Quality



The story of what is now known as CML Micro began in 1968 when the company was founded as Consumer Microcircuits Limited in the U.K. Recognizing the growing demand for semiconductor solutions in the emerging field of wireless communications, the company shifted its focus toward the development of integrated circuits (ICs) for RF applications. To support this, they became the U.K.'s first company to adopt the rapidly emerging "fabless" semiconductor supply model.

The company grew steadily by expanding its product portfolio and customer base, leveraging advancements in semiconductor technology to develop new products for wireless communication systems. At its formation, CML considered its analog signal processing IP portfolio to be among the best in the world. This expertise evolved into digital signal processing (DSP) capabilities and in the early 1990s, the company introduced its first generation of DSP ICs for wireless communication applications. These DSP chips offered enhanced performance and flexibility compared to traditional analog solutions, paving the way for the widespread adoption of digital communication technologies.

As the demand for wireless communication devices grew, CML seized the opportunity to increase its market presence. In addition to expanding their product portfolio and range of market applications organically, the company began a string of acquisitions. In 2002, CML acquired Applied Technologies and formed the CML Radio Systems Group, specializing in DSP software and RF design solutions. The following year, CML acquired Hyperstone, a fabless semiconductor company that provided flash memory controller microchips and flash controller firmware complementary to these controllers. In 2016, the company acquired China-based SICOMM, a fabless semiconductor company specializing in integrated baseband processors and RF semiconductors. In 2020, PRFI, a U.K.-based design house specializing in the design and development of RFICs and MMICs, along with microwave and mmWave modules, was added to the portfolio. The most recent acquisition, MwT, specializes in GaAs and GaN-based MMICs, discrete devices and hybrid amplifier products for a variety of commercial, defense and industrial applications.

CML Micro has more than 400 products that come from nine global locations. The company sees good year-over-year financial growth with reported 2023 revenues of over $26 million.

The acquisitions and organic growth have greatly expanded the company's capabilities. The company continues to expand its "SμRF" line of high performance RF products and mixed-signal baseband/modem processors that address multiple wireless voice and data communication markets. In addition to these SμRF products, the company offers direct conversion receivers, transceivers and synthesizers for RF applications. With a broad range of products targeting analog front-end, baseband processing, voice coding, voice CODEC and Application/MMI applications, CML Micro can provide wireless communications solutions from the moment data is created until it is processed at the other end of a communications link. The main application focus areas for these products are critical communications, wireless networks and satellite, IoT, business and leisure wireless, aerospace and defense maritime communications and broadcast markets.

The CML Micro story is still being written. It is one of organic growth, coupled with strategic acquisitions to expand capabilities. The theme of the story is noble; helping the world to transform the way it communicates.

CML Micro
www.cmlmicro.com

Blueprints for Design: Building the New Age of Connectivity

What's Inside:

- True time delay technology overview
- New technologies for X-band radar applications
- Solutions for SATCOM user terminals
- Open RAN for 5G network resilience
- Advances in GaN technology
- Revolutionizing the mmWave 5G business case

True Time Delay: What It Is and How It Works

Steering in the Right Direction

Phased array antennas use phase shifters, true time delay, or a combination of both to point the summed beam more accurately toward the desired direction within an array's steered angle. This blog post reviews both of these methods and how wider bandwidth antenna arrays are driving the use of true time delay in their system design.

Phased array antennas change the shape and direction of the radiation pattern without physically moving the antenna. The antennas are uniquely placed into a larger array using individual elements – summing them up to provide more gain performance and directing the signal within the array's steering angle limits, as shown in the figure below.

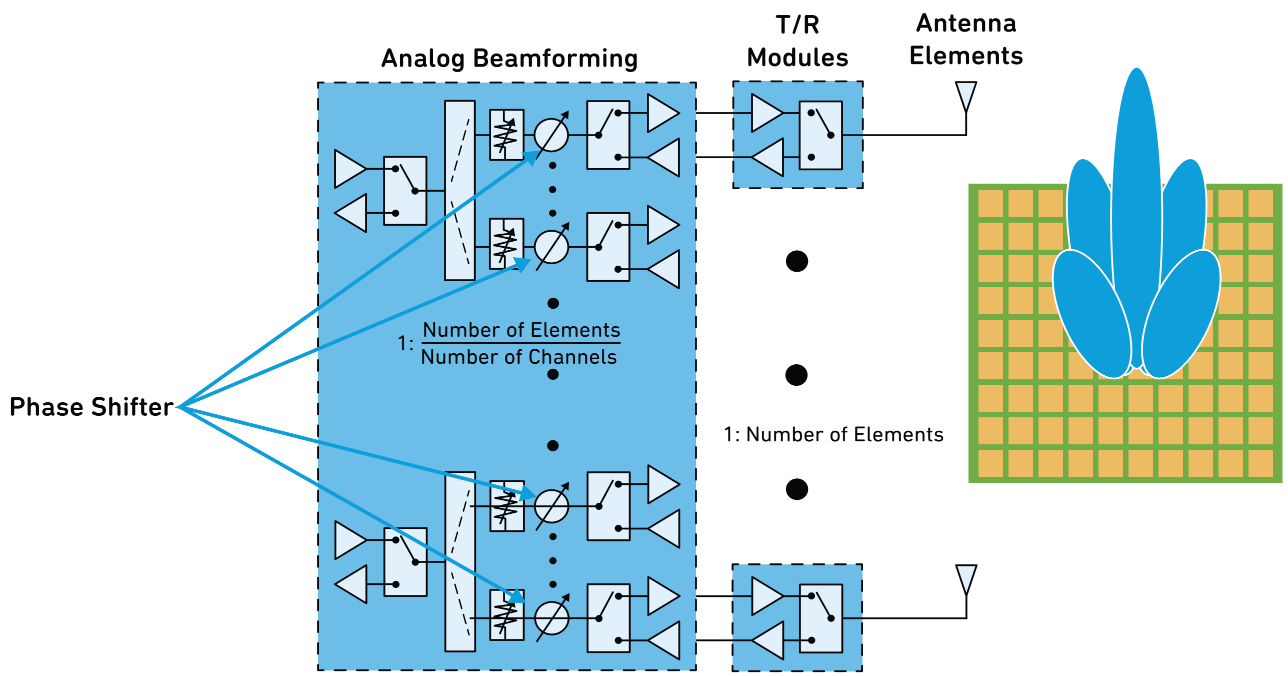

In today's phased array systems, the bandwidth is increasing to expand utility and flexibility. Wider bandwidth introduces system challenges that affect the phase shifting of the beam. Because of this trend, many AESA systems require true time delay to eliminate beam squint in larger bandwidth circumstances. We dig into this further in the following sections.

Background in Phased Arrays

The phased array antenna size is inversely proportional to the operational frequency. Therefore, the higher the frequency, the smaller the antenna element spacing. The opposite is true for lower-frequency applications.

So, how is the beam steering enabled? Traditionally for narrowband arrays, we convert the desired signal delay at a given frequency using phase shifters. In the phased array antenna, each antenna element can be fed with different phase shifters. Therefore, the beam direction of the array can be steered by changing the phase shift between each element to form a beam at the angle of interest.

For example, assume we have two antenna elements separated by distance "d," as shown in the graph below. The phase shifts between these two elements, altering the beam direction. Using a phase shifter at the alternative antenna element, the beam can be steered to alter its direction and improve antenna efficiency.

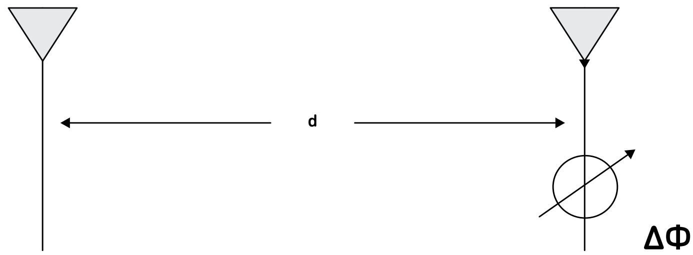

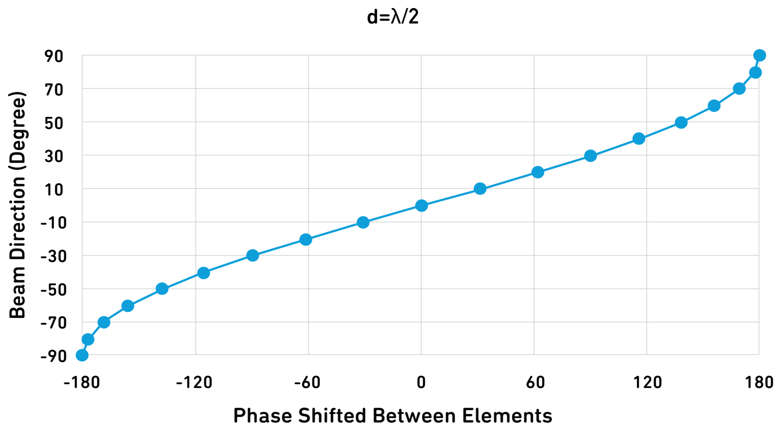

In the below image, we can see how the steering of a waveform in the antenna array creates a main lobe at a given angle and minimizes the side lobes. We also see measured data of phase angle and field pattern of these lobes.

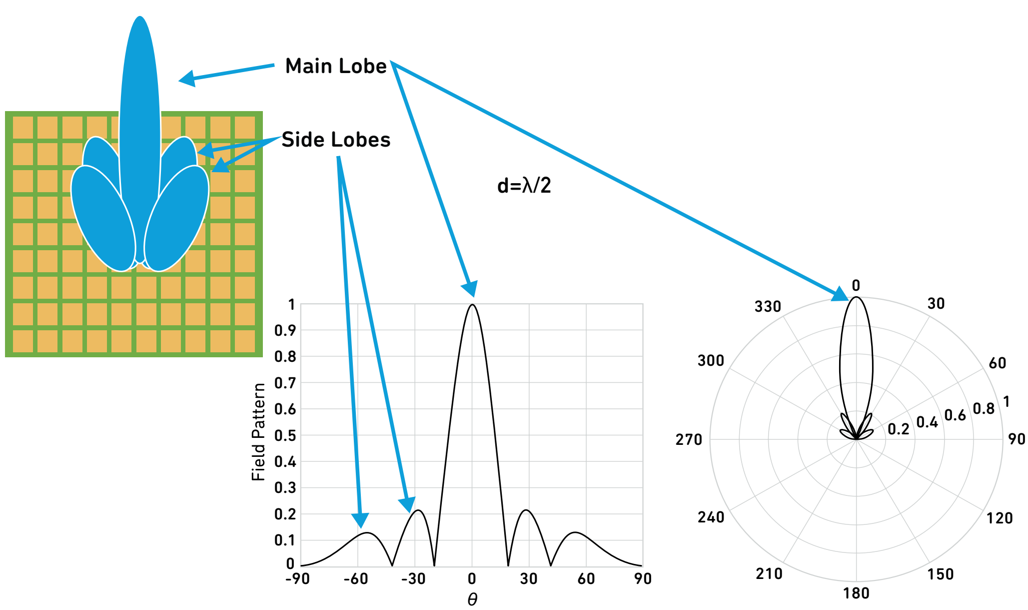

Below are two types of phased array antenna systems that are commonly used.

- Passive electronically steered array (PESA) uses a single transmit/receive module shared across all antenna elements.
- Active electronically steered array (AESA) uses phased array antennas with transmit/receive modules dedicated to each element.

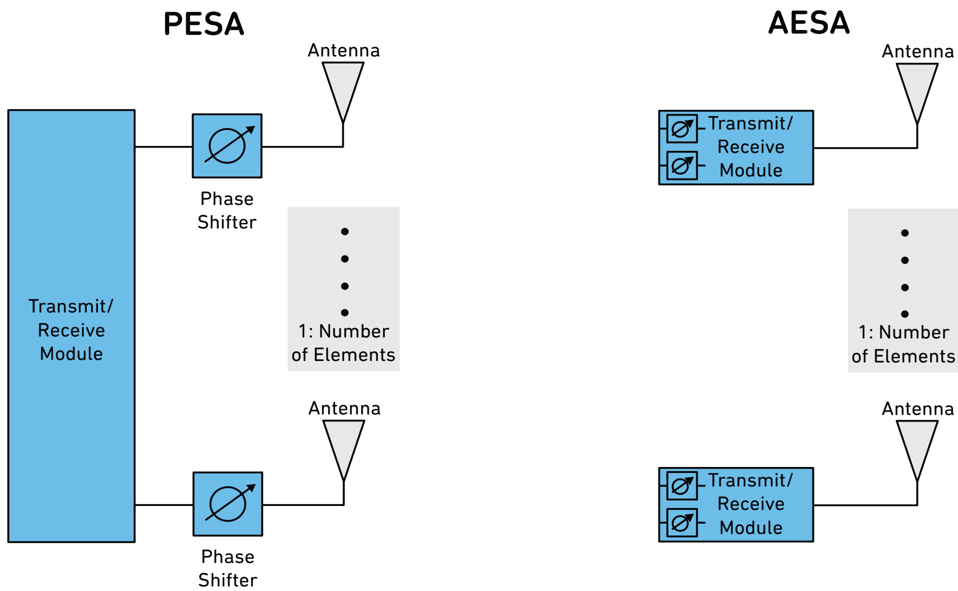

A Deeper Dive into AESAs
AESAs are the second generation of phased array antennas. In AESAs, there are separate transmitters controlled by microcontrollers for each antenna element. These AESAs are more advanced than PESAs and can transmit several radio waves at various frequencies simultaneously in different directions.

As higher performance and higher resolution systems are developed, the bandwidth requirements for the waveform increase. This presents a problem for AESAs that traditionally steer the beam using phase shifters because the beam will squint as a function of frequency. Beam squint can be calculated using the following equation.

$$\Delta\theta = \sin^{-1}\left(\frac{f_0}{f} \times \sin\theta_0\right) - \theta_0$$

$\Delta\theta$ = Peak Squint Angle

f_0 = Carrier Frequency

θ_0 = Maximum Beam Angle

f = Instantaneous Signal Frequency

For these wide instantaneous bandwidth waveforms and narrow beam widths, beam squint can be enough to steer the beam off target resulting in poor signal quality, reduced accuracy and resolution.

AESA: Phase Shifters Versus True Time Delay
AESAs use phase shifters or a time delay circuit, or a mix of both, to point the signal beam in the desired direction within the array's steering angle limits.

Phase shifters, as shown in the figure below, are used for directing the beams in phased array antennas and help improve efficiency in narrowband systems. Phase shifters have had a wide market dominance and provide a fixed insertion phase difference between the two states. They are typically used in applications with lower bandwidth because wideband phase shifting is more difficult and often comes with a penalty of increased insertion loss and phase accuracy across the operational frequency bandwidth. The two states are only slightly different in time delay, differing in path length by less than a wavelength. Phase shifters steer the beam at each antenna element but do not provide true time delay. Without this true time delay, the beam distorts, or "squints," over a larger frequency range as shown in the following graph. With newer, wider bandwidth array systems, beam squint has become more of an issue. True time delay units are used to mitigate this squinting effect.

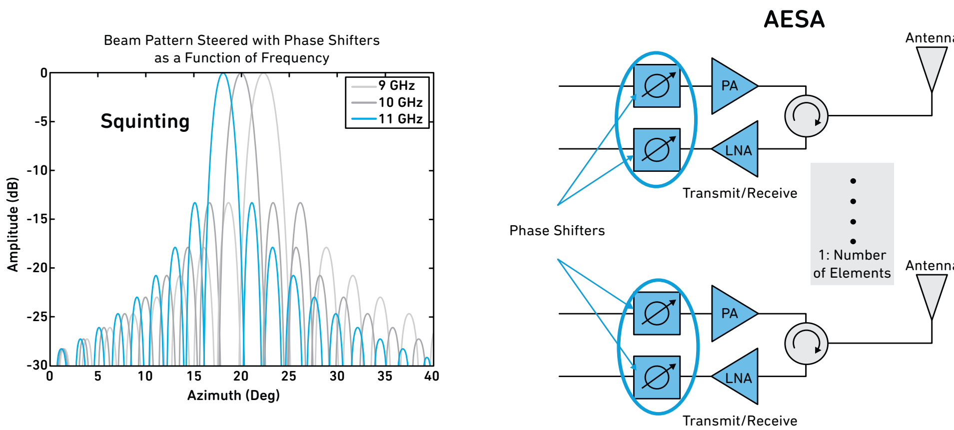

Time delay units provide many wavelengths of phase shifting, and the phase shift is exactly proportional to the frequency. This allows the group delay difference between the two states to create a flat phase over the entire frequency bandwidth.

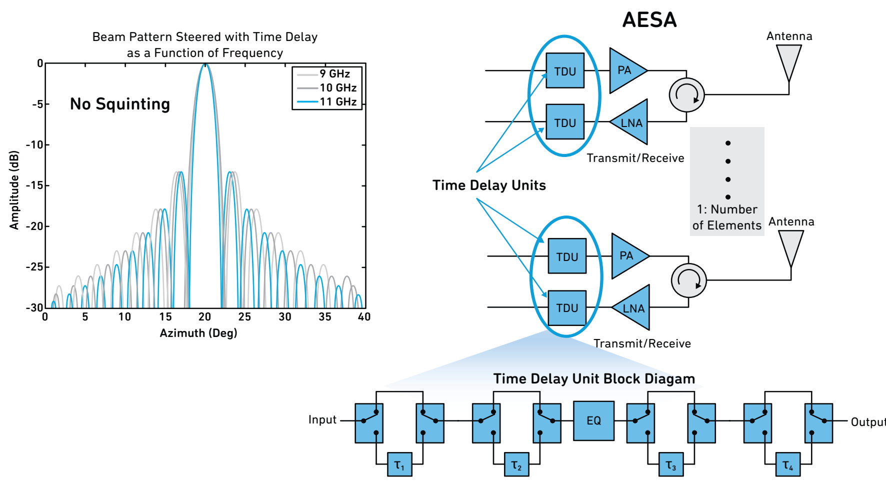

As you can see from the figure above, the time delay unit provides a noticeable benefit of squint reduction over the bandwidth frequency improving radar image resolution over the wider bandwidth.

True Time Delay MMICs

Time delay can be accomplished in many ways, e.g., coax, optical, microstrip, and strip-line. Electronic methods using MMICs are more popular due to their compact size and cost-benefit. Typical multi-bit time delay units include switches, time delay elements and equalizers to form both reference path and time delay pathways, as shown in the above figure. Overall delay range and delay steps can be generated by switching different path combinations. A reference line and delay element are typically created using different lengths of transmission lines. As the line length increases, so does the insertion loss and frequency. An equalizer is typically used to improve the overall time delay flatness over the frequency range.

Recent semiconductor developments and advances in modeling have helped to enable physically smaller delay circuits, which are useful in high-frequency array applications. Additionally, different semiconductor technologies like CMOS, GaAs and MEMs can be considered to help optimize performance requirements for some applications.

Key Takeaways

For today's broadband array antenna applications, true time delay is required to mitigate squint. As we have shown above, understanding the differences in using TDUs and phase shifters or using them together is an essential part of AESA system-level performance.

Take a deeper dive

Learn more about solutions to your challenges.

The Future is Here: Integrating X-band Radar for Next-Level Detection and Imaging

Basics of X-band Radar

As you can imagine, radar, originally developed by the military in the 1930s, has undergone significant changes. New technologies enable the delivery of transmitters and receivers with greater precision, more efficient power use, and significant size reduction. And in recent years, electronic control elements for beamforming have become increasingly popular, providing more flexibility and increased benefits in the latest generations of X-band solutions.

X-band radar occupies 8-12 GHz and has superior target resolution and improved support for operations that require higher accuracy. It operates with a smaller antenna size than lower frequency counterparts – enabling more compact antenna arrays – as well as offering greater sensitivity for detecting smaller objects because of the small wavelength used.

The advancements in X-band have given way to significant growth in the global radar industry. According to Allied Market Research, the industry was worth $32.56 billion in 2019 and is expected to grow at a CAGR of 4.7% from 2021 to 2028, reaching $44.35 billion, driven by increased demand in the automotive and defense industries, territorial battles, and advancements in technology.

Of course, with new advancements, there are also new design challenges. This blog post provides excerpts from a Qorvo Design Summit webinar on integration guidance for X-band applications.

Key Takeaways

In the Qorvo Design Summit webinar, X-band Radar Application with Integration Guidance, Fouad Boueri, Qorvo Senior Product Line Manager, covers the following key points:

- The fundamental building blocks for steering electronic phased arrays are the transmit/receive (T/R) modules (shown in Figure 1).
    - Circuits within these modules carry out basic tasks, including amplifying the transmit signals, filtering noise from the received signals, and using beamforming to shape and steer the elements in the radar system by varying the amplitude and phase of each element. As systems become increasingly configurable, solutions that offer expanded functionality – with several applications residing in one device – are becoming common.
    - Components included in the RF front end are the PAs and LNAs that provide signal amplification, phase shifters, attenuators, switches and filters that provide signal conditioning, and mixers and oscillators for signal translation (i.e., frequency up and down conversion).
    - An important trend in the industry is the increased integration of digital control over high-frequency functions. Other innovations include using a broadband front-end to support multi-function systems and controlling the elements precisely to improve digital beamforming.

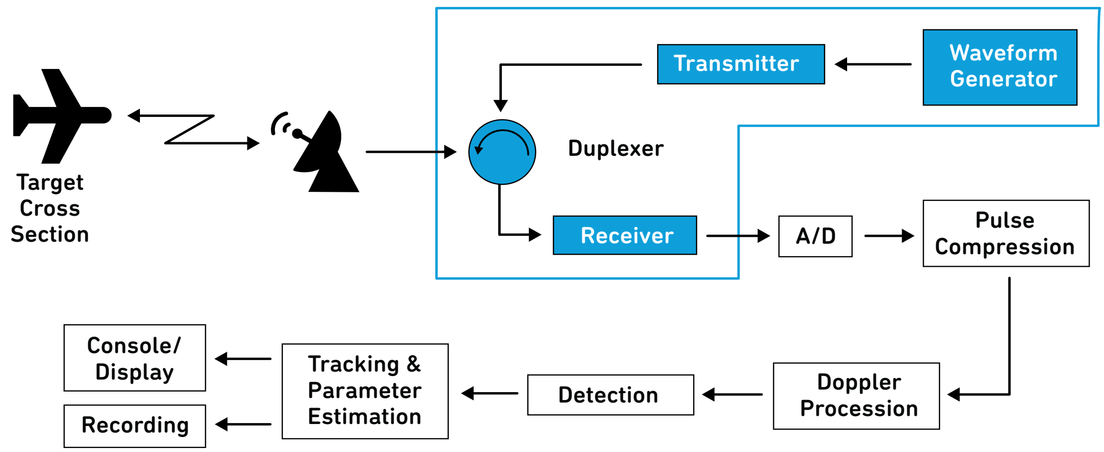

Figure 1. X-band radar T/R modules

The block diagram of a typical, modern X-band radar (**Figure 2**) shows the organization of key components. As with any system design, there are tradeoffs that are required to establish the most optimal performance. Below the block diagram is a list of transmit and receive attributes engineers must navigate through to attain optimal system performance.

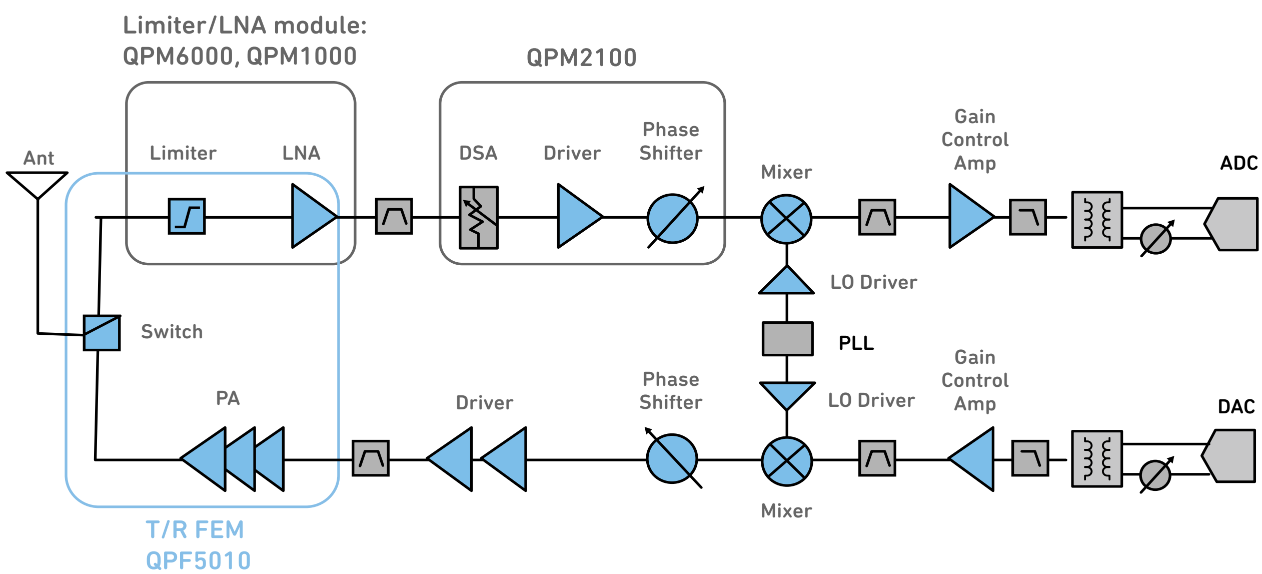

Figure 2. Next-gen X-band radar

The webinar provides details on each functional component area – defining the main function of the component in the system as well as what tradeoffs need to be considered during the design. Below is a short summary of this review. For more detail, refer to the webinar.

Component and function:

- Limiter: protects the LNA from damage by large incidents of power at the input.
- Switch: routes the RF signal between the transmit and receive paths with optimal signal-to-noise ratio (SNR), power level, and isolation between T/R and provides robustness on the input from the antenna.
- Phase shifter: controls the relative phase for each antenna element of the array system in order to electrically shape and steer the beam.
- Digital step attenuator: attenuates the RF signal by controlling power and gain for beam steering and tapering.
- Filter: provides signal conditioning such as isolation, coexistence and mitigation of interference.
- LNA: provides amplification of the received signal and provides system sensitivity.
- Power amplifier: amplifies the transmit signal with high efficiency.

Over the past couple of years, the above-listed individual discrete components have migrated toward integration – helping with system size reductions, performance and ease of design. Additionally, when integrating these individual functions, several designs also provide a fully matched module, making system design easier and less costly. As an example, let's compare the IMFET versus pre-matched transistor (**Figure 3**). The tradeoffs when comparing an internally matched field effect transistor (IMFET) with a pre-matched transistor package are shown in Figure 3. Note that for the IMFET, there is no matching network; all matchings happen within the transistor. The pre-matched transistor must be matched on the PCB before reaching the 50-ohm connector, as shown on the right side of the table.

Parameter	IMFET (Fully Internally Matched FET)	Pre-Matched Transistor
Price	Higher	Lower
Board Integration	Easy – no matching network design required	Hard – full PCB matching network required
Size	Very compact – no board space required for matching networks	Large – PCB must be able to fit the long matching networks
Design Cycle Time	Short – no design required	Long – must design, test and iterate until goals achieved
Design Flexibility	Only works in specific band with the specs as shown on he data sheet, very little tuning possible	Can match to other bands and optimize for power, efficiency, etc.
Stability	Already accounted for	Design must take this into consideration

Figure 3. IMFET vs. pre-matched transistor

Building Innovative Solutions for X-band Applications

With the recent acquisition of Anokiwave, Qorvo has strengthened its position in this market. As shown in **Figure 4**, by using Anokiwave's silicon beamformer ICs that integrate all core beam steering and control functions coupled with Qorvo's advanced GaN T/R FEMs, customers can fit all electronics within the radiating element lattice for planar X-band low-profile antennas that reduce wind drag and detectability.

The GaN T/R FEMs integrate high transmit output power, receiver low noise amplification, and front-end limiters while the silicon beamforming ICs feature single beam transmit and dual beam receive channels supporting monopulse or dual polarization operation. The SPI controlled beamformer ICs provide independent phase/amplitude settings at each element supporting independently steerable beams in Tx and dual pol Rx modes. These ICs are widely proven in military and commercial platforms and are available today with short lead time.

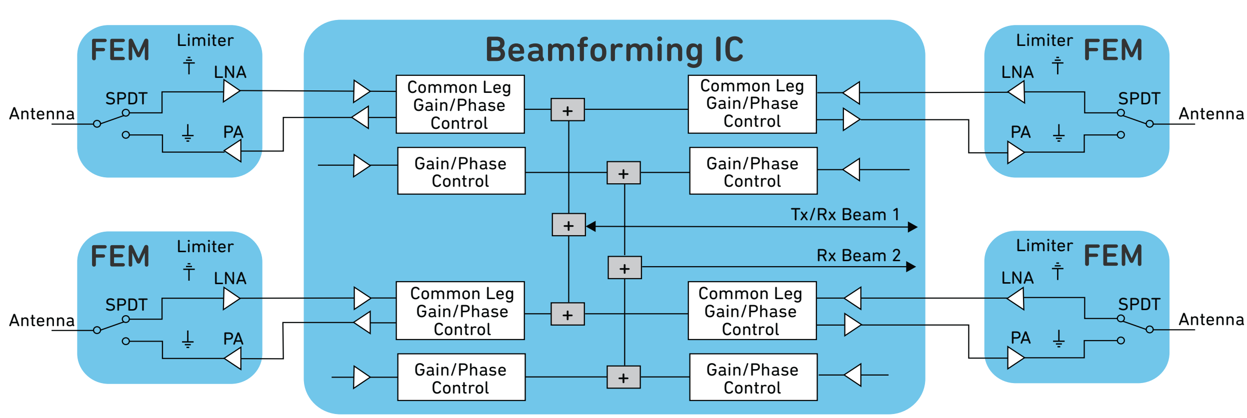

Figure 4. X-band radar block diagram with a silicon beamformer IC and complementary FEMs

Take a deeper dive

Explore this topic in greater detail as part of the Design Summit series with Qorvo experts. These webinar sessions cover advances that are enabling revolutionary next-generation technologies.

Cost-Effective Solutions Needed to Address the Exponential SATCOM Market Growth

The future has never looked brighter for satellite operators, given the record-setting number of satellite launches in recent years, the growing number of satellite-based applications and the huge capital investments being made in a host of planned space ventures.

The relentless quest for global connectivity has ushered in a new era in communication technologies, with satellite communications (SATCOM) at the forefront. The space economy, projected to exceed $1 trillion by 2040, underscores the vital role of satellites in extending the reach of terrestrial networks, thereby enabling ubiquitous connectivity across the globe. These investments are driving the demand for innovative technologies at lower price points, with new capabilities. As new SATCOM constellations become operational, unprecedented numbers of user terminals will be needed, and most of them will incorporate flat panel active phased array antennas to communicate when the satellite is in motion. The SATCOM flat panel user terminal market is about to explode.

By enabling the development of user terminals that are both cost-efficient and high-performing, Anokiwave (now Qorvo) is facilitating the widespread adoption of satellite services. These flat panel, electronically steered terminals are versatile enough to support multi-orbit SATCOM systems, from geostationary earth orbit (GEO) to medium earth orbit (MEO) and low earth orbit (LEO) satellites. This versatility ensures the SATCOM system can meet a broad spectrum of needs, from consumer broadband to critical emergency response communications.

SATCOM user terminals built with Anokiwave's (now Qorvo's) silicon-based SATCOM ICs result in systems with high performance, small form factor and low cost. Anokiwave's (now Qorvo's) ICs are designed to support FDD (frequency division duplex), however they can also support TDD (time division duplex), operation covering global SATCOM Ku, and Ka bands. Each IC in the family supports four (4) dual polarization radiating elements with full polarization flexibility. Each channel has its own individual control of phase and gain for maximum flexibility.

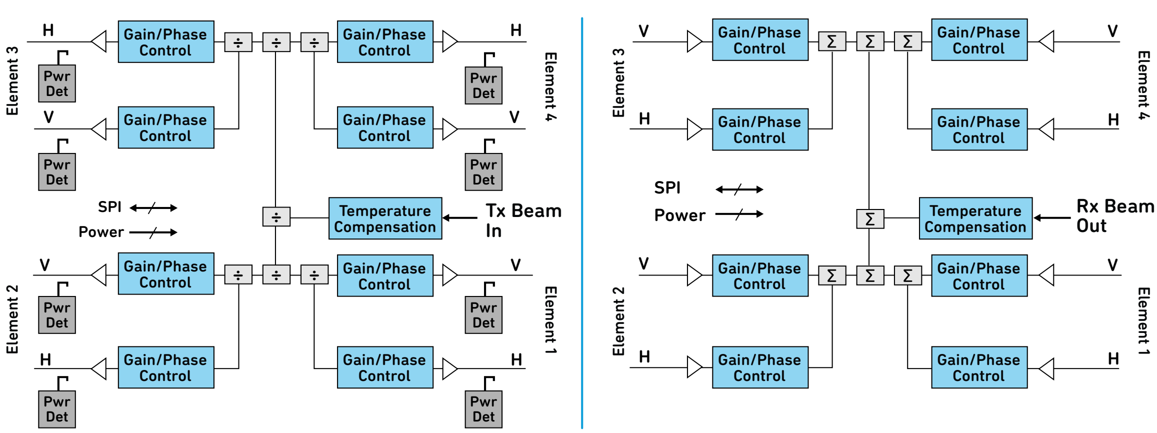

Anokiwave (now Qorvo) BFIC architecture supports four (4) dual polarization radiating elements with full polarization flexibility.

As demand for connectivity increases exponentially, satellites will serve areas outside highly networked cities for purposes such as connection on the move, critical emergency services, edge networking and connected devices (IoT).

By using Anokiwave's (now Qorvo's) SATCOM and 5G IC technology in the user terminals, OEMs gain unparalleled application expertise, allowing them to develop better array designs that are faster time-to-market as well as, and most importantly, the experience to support customers who are expanding their networks beyond traditional 5G or SATCOM use cases. This effort not only paves the way for enhanced communication services but also opens new avenues for applications and services in areas such as IoT, autonomous vehicles, and smart cities, thereby fueling economic growth and innovation.

The path towards global connectivity is illuminated by the relationship between terrestrial and non-terrestrial networks. A common intersection of these networks is the need to support both types of systems with mmWave phased array active antennas. Anokiwave (now Qorvo) has been in these markets for over 20 years. The company has multiple generations of both SATCOM and 5G products in volume production which have been widely adopted by the major equipment manufacturers. With the Qorvo acquisition of Anokiwave, the two companies' technologies bring innovation and scale to SATCOM and 5G applications. The system level support and broad portfolio of products are connecting the world through space.

Take a deeper dive

For a deeper discussion on this topic, download the full report.

Open RAN's Promising Future for 5G Design

Say the term "5G" and consumers often think about getting the most out of their smartphones or tablets, setting up a personal Wi-Fi hotspot, watching video on demand in an airport, or making video calls to their family on the other side of the country. Electronic engineers and designers may think that way too, but they must also consider the demands that 5G systems and infrastructure put on their work. Over the years, key players in the telecommunication industry have created an ecosystem that forces service providers like AT&T, T-Mobile and others to be locked with specific equipment vendors into various system configurations.

Open RAN (open radio access networks) is a standardized approach to RAN hardware and software disaggregation. Open RAN will foster network vendor competition and innovation. It is a methodology to open up these systems for manufacturers to be able to service these networks. Open RAN offers greater flexibility and choice in designing and implementing 5G products.

Traditionally, the radio access network components were tightly integrated and controlled by a single vendor, limiting the options for product designers. By using the Open RAN methodology, designers can leverage a more open and standardized architecture, allowing them to mix and match components from several vendors. This flexibility enables designers to select the hardware and software solutions that work best for them, leading to improved product performance, innovation and cost-effectiveness.

In the marketplace, Open RAN can promote increased competition benefiting both designers and consumers. By breaking down the traditional vendor lock-in and promoting interoperability, Open RAN encourages the participation of multiple vendors and start-ups. This more competitive landscape can lead to technological advancement reaching the market faster. As a result, designers can access a wider range of cutting-edge technologies, and consumers can take advantage of more diverse and innovative 5G products that cater to their specific needs.

Qorvo's Newest Open RAN 5G Support

Qorvo's most recent offering to promote Open RAN methodology is the QPB3810, QPB9362 and QPA9122 included in a full RF front-end reference design for 5G mMIMO applications. The reference design pictured below, provides a complete solution for a RF front end (RFFE) for an 8W average output power mMIMO 5G application in band n78 (3.4-3.8 GHz). It provides a transmit and receive solution from the digital front end to antenna filter in a compact layout, which can be directly implemented into an array.

The transmit chain features the QPA9122M as a wideband high linearity pre-driver and the QPB3810 as a highly efficient GaN final stage power amplifier module. The transmit chain also includes a directional coupler for DPD observation path as well as a circulator. For the receive chain, the reference design includes the low noise QPB9362 switch LNA.

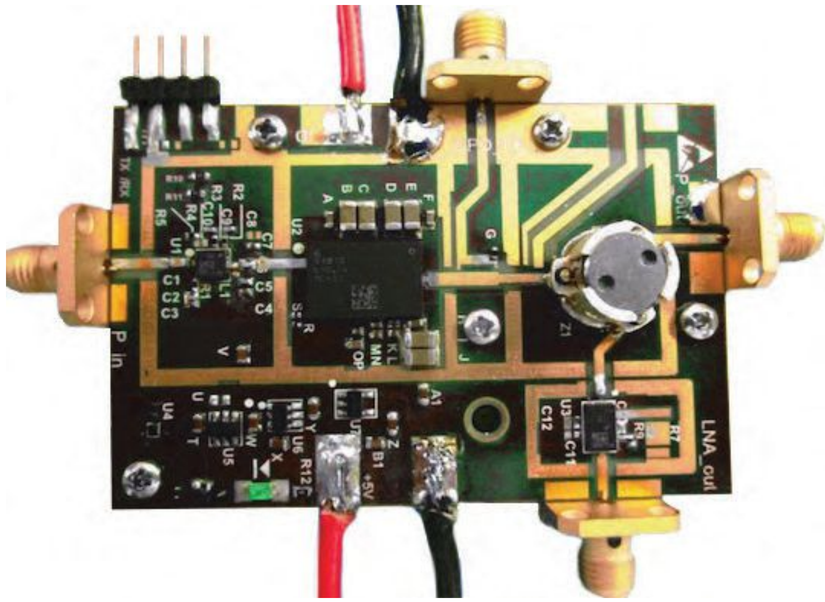

Reference design board: 8W mMIMO 3.4-3.8 GHz RF front end.

The QPB3810 is the first commercially released GaN-based module with an integrated bias controller factory programmed to set the optimal bias points of the Doherty® power amplifier module (PAM). The QPB3810 is a 48V, 8W average power PAM covering the 3.4-3.8 GHz band. The bias controller includes a temperature sensor allowing it to automatically adjust bias over temperature and includes an enable pin for fast TDD switching. The QPB3810 is available in a compact 12x8 mm SMT package, offering a much smaller footprint than traditional discrete component solutions; and similar to Qorvo's other PAM products which require minimal external circuitry.

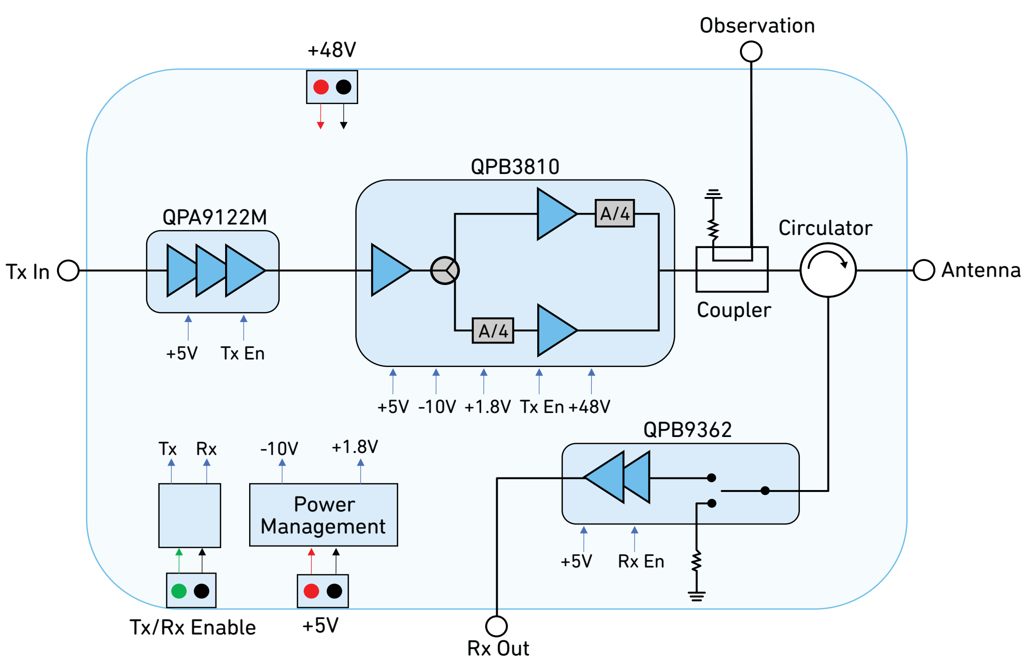

Also being released: Qorvo's QPB9362. This receive module is targeted for 5G wireless infrastructure applications configured for TDD-based mMIMO architectures. Its switch LNA module integrates an LNA with a high-power handling switch which can be used as a failsafe path to termination when a radio is in transmitting mode. The QPB9362 provides 34.5 dB of gain with 1.1 dB typical noise figure over the entire operating frequency band in the receiving mode and LNA power down mode is available via a transmit/receive control pin on the module. It is packaged in a RoHS-compliant, compact 5x3 mm LGA package.

Faster Development Plus Security

Open RAN clearly enables rapid deployment and scalability for 5G networks, benefiting both designers and consumers. The open and standardized interfaces allow for easier integration and interoperability of network components, simplifying the deployment process. This streamlined approach accelerates the time-to-market for electronic product designers, enabling them to introduce innovative 5G products more quickly. Consumers, on the other hand, benefit from faster network expansion and improved coverage, leading to enhanced connectivity and a better user experience.

Open RAN promotes greater security and resilience for 5G products and networks. With a closed network architecture, vulnerabilities or flaws in a single vendor's equipment can potentially compromise the entire network. In contrast, Open RAN's multi-vendor approach reduces the impact of security breaches, as components from different vendors can be independently assessed and updated. This enhanced security framework reassures electronic product designers and consumers, providing them with more confidence in the reliability and integrity of their 5G products and networks.

Take a Deeper Dive

Explore this topic in greater detail.

Gallium Nitride (GaN): Revolutionizing Industries with Advanced Semiconductor Technology

Introduction

In the realm of semiconductor technology, GaN has emerged as a transformative material, heralding new frontiers in various sectors, including military, aerospace and commercial applications. Thanks to continuous technological advancements, GaN's superior properties are increasingly preferred by engineers, setting a new standard in efficiency, reliability and performance. This article delves into GaN's significant impact across key markets, its current applications, potential future uses and the promising trajectory this technology is set to follow.

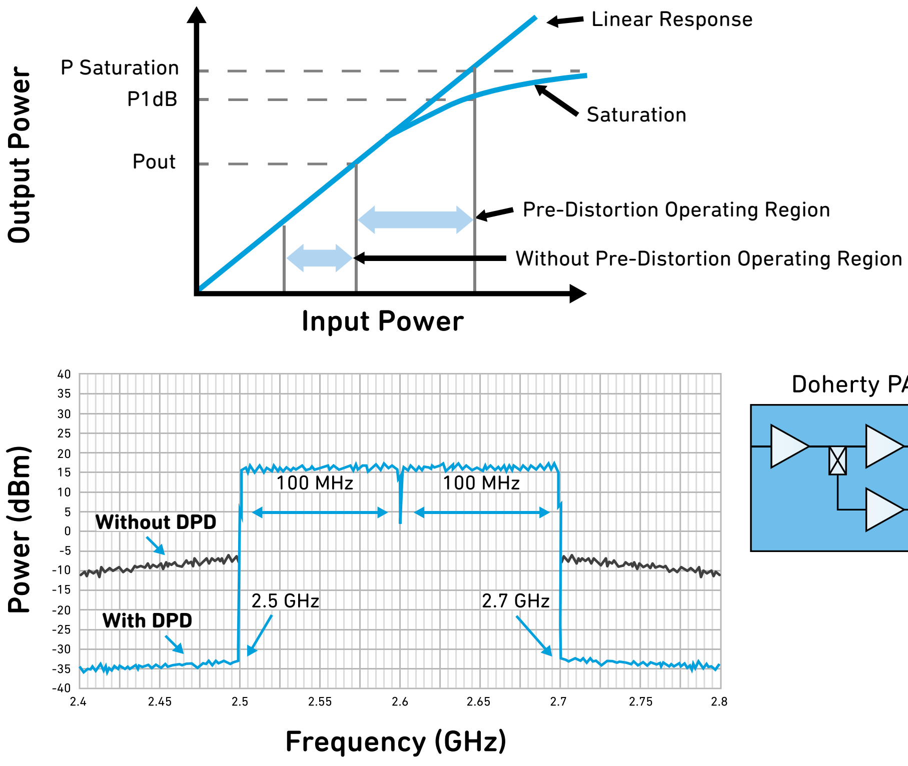

Figure 1: DPD and GaN Doherty PA configuration.

System Implementation

Exploring the design and implementation of GaN systems reveals a distinct advantage over mature technologies like GaAs, particularly in terms of power density and bandwidth capabilities. While GaAs high-electron-mobility transistors (HEMTs) remain useful for applications with lower power requirements and critical noise figures, GaN stands out for its superior power density and wide bandwidth. This not only enhances system survivability through higher input power tolerance but also simplifies RF matching due to GaN's high input impedance, reducing the number of components needed. In practical terms, GaN's attributes translate into longer RF ranges and higher signal resolution in applications such as radar, where the ability to detect smaller targets from greater distances is crucial. Moreover, GaN enables more efficient radar systems with potentially thousands of amplifiers, increasing range or reducing costs and complexity by requiring fewer devices per element. In advanced 5G antenna systems, GaN's efficiency at saturation is balanced with linearity through digital pre-distortion (DPD), optimizing performance for high-power applications.

DPD represents a critical advancement in combining hardware and software solutions to enhance PA performance, especially in cutting-edge RF systems like 5G base stations. By utilizing digital signal processing techniques, DPD allows for the optimization of PAs to achieve lower power dissipation, maximized output power, and high linearity simultaneously, all while reducing out-of-band distortion. A notable implementation is the integration of DPD with GaN PAs configured in a Doherty architecture, which is instrumental in increasing the PA's efficiency at back-off output power. This synergy between Doherty configurations and DPD not only achieves efficiencies exceeding 60%, significantly reducing the operational energy demands of power-intensive PA systems, but also ensures the attainment of higher efficiency and linearity, marking a substantial leap forward in PA system design and functionality.

GaN's Key Markets: Military and Aerospace

Military Satellites and Communications

The critical demand for robust, reliable components capable of delivering kilowatts of radio frequency (RF) output power in military and aerospace systems has historically been met by vacuum tube technology. However, the advent of high-power semiconductors initiated a paradigm shift towards solid-state power amplifiers (SSPAs), with GaN leading the way due to its enhanced reliability, robustness and bandwidth capabilities. In military satellite systems, which facilitate secure, high-speed data, video and voice communications, GaN's superior performance is increasingly pivotal. Systems previously dependent on traveling wave tube amplifier (TWTA) and GaAs technology are transitioning to GaN to meet the growing demands for power density, enabling significant advancements in satellite communication networks.

Figure 2: Qorvo Spatium® SSPA combining GaN in patented design.

Radar and Electronic Warfare

Radar and electronic warfare (EW) systems are critical for modern military operations, requiring high power, efficiency and reliability. GaN technology's attributes, such as linearity, power density and thermal efficiency, make it ideal for these applications. Its use in active electronically scanned array (AESA) radars contributes to more compact, efficient solutions, meeting stringent size, weight, power and cost (SWaP-C) requirements. Furthermore, in the evolving domain of EW, GaN enables the development of more compact, wide-bandwidth and powerful solutions, enhancing the capabilities of defense systems on land, air and sea.

Some of GaN's Commercial Applications

5G Infrastructure

The rollout of 5G technology has significantly benefited from GaN's capabilities, particularly for power amplifiers (PAs) in radio frequency front ends (RFFEs), where efficiency is critical. GaN's advantages, including higher power output, frequency operation and reduced power consumption, are vital for achieving the high efficiency required in 5G systems. This is especially true for millimeter-wave (mmWave) applications and massive MIMO antenna arrays, where GaN's efficiency enables higher capacity and coverage with lower energy costs.

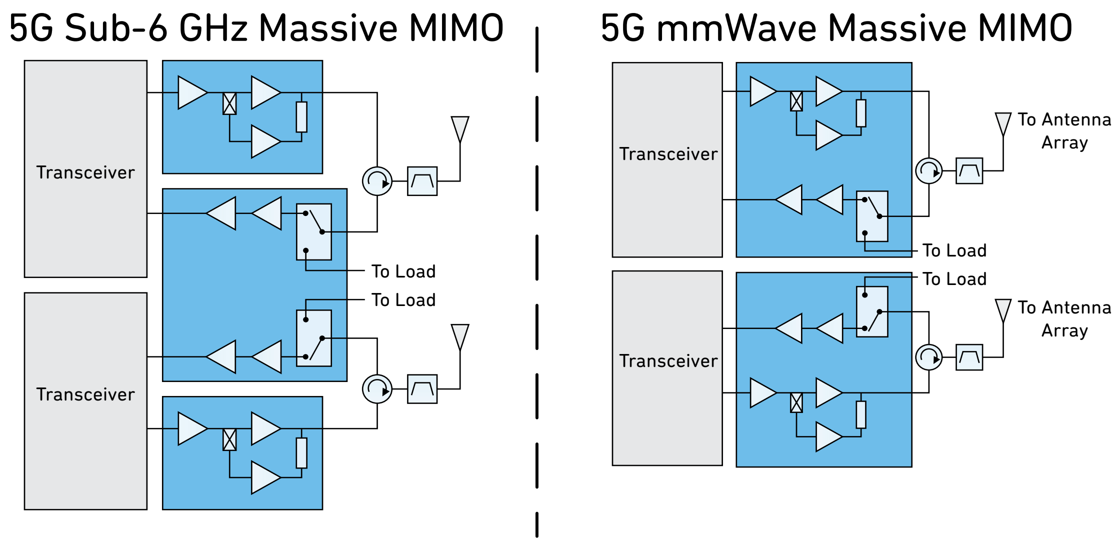

Figure 3: RF front-end block diagrams for 5G sub-6 GHz and mmWave.

CATV and Commercial Satellite
GaN's role in cable television (CATV) and commercial satellite communications underscores its importance in supporting high-throughput video, broadband services and global communication needs. GaN amplifiers offer the linearity and efficiency necessary for extending network reach and reliability, crucial for meeting the increasing consumer demand for data. Similarly, in commercial satellite applications, GaN facilitates more compact, lightweight components that support higher data throughput and frequency bands, essential for 5G backhaul, ultra-HD TV transmission and other advanced communications services.

GaN in Automotive
In the automotive sector, GaN is becoming a game-changer, particularly in the realm of electric vehicles (EVs). GaN's exceptional efficiency and power density are driving innovations in EV power systems, from inverters to onboard chargers and DC-DC converters. These advancements enable not only faster charging times but also more compact and lighter power electronics, contributing to an overall reduction in vehicle weight and an increase in range. Additionally, GaN's superior thermal management and fast switching capabilities are enhancing the performance of EVs, making it a key technology in the industry's shift towards more sustainable and efficient electric transportation solutions.

GaN's Future

Looking ahead, GaN technology's potential extends far into various sectors due to its high efficiency, power density and thermal performance. From data centers to EVs, wireless charging and medical equipment, GaN's contributions are set to revolutionize energy consumption, device miniaturization and system performance. In data centers, GaN's efficiency can significantly reduce energy consumption. For EVs, GaN enables more efficient, faster charging and power systems. In the medical field, GaN's high-resolution capabilities could lead to earlier, more accurate disease detection.

Conclusion

GaN is at the forefront of semiconductor technology, driving innovations across military, aerospace and a broad range of commercial applications. Its superior properties over traditional semiconductor materials, such as silicon and gallium arsenide, offer significant advantages in efficiency, power density and reliability. As GaN technology continues to evolve, its impact on industry standards and capabilities is expected to grow, heralding a future where GaN-based solutions redefine the technological landscape. The ongoing research and development in GaN technology promises to unlock even more applications, making it a cornerstone of modern electronic and electrical engineering.

Take a Deeper Dive

To learn more about GaN technology, download the GaN For Dummies® e-book.

Revolutionizing the mmWave 5G Business Case

The global deployment of 5G mmWave is now inevitable. Service providers will require mmWave bands to support the emerging trend of "mobility without boundaries" as well as to relieve stress on congested sub-6 GHz bands.

Abstract

The use of mmWave frequency is inevitable to achieve the full potential of 5G. 5G service providers will require mmWave bands to support the emerging trend of "mobility without boundaries." This exponential growth of demand for wireless data has quickly depleted spectrum resources in sub-1 GHz band (also called low band) in many countries. With the recent introduction of mid-band (frequencies between 1 GHz and 6 GHz) spectrum, the industry is experiencing a temporary relief of wireless congestion. If history is a guide, the relief will be short lived as the depletion of today's sub-6 GHz spectrum (low-band and mid-band) resource in major metro areas is projected to happen over next 3-5 years.

While mmWave 5G offers immense potential in terms of bandwidth, user capacity, and quality of service, developing a commercially realizable mmWave ecosystem has multiple challenges for providers. Using many of the first or second generation mmWave 5G solutions in the market today, the mmWave 5G business case often does NOT close, leading many to believe that mmWave is not the right solution to satisfy the immense (and growing) demand for data. Anokiwave's (now Qorvo's) IC technology is changing this perception.

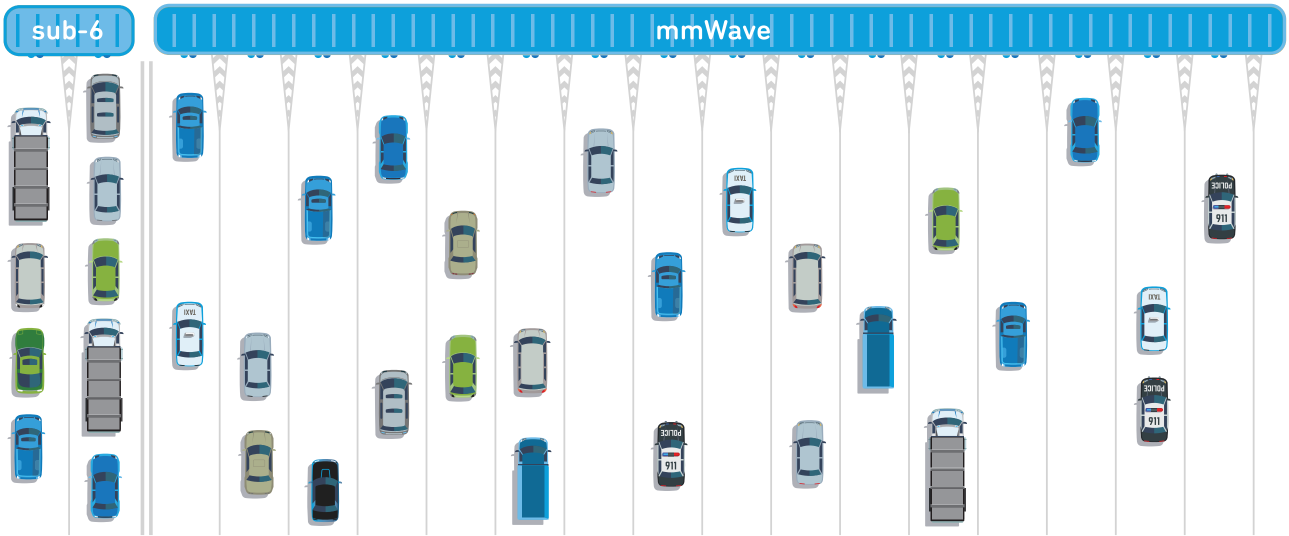

mmWave adds capacity to the busy 6 GHz spectrum allowing faster, less congested connections.

Many of the technical challenges of commercializing mmWave are solved with IC innovations. The latest ICs from Anokiwave (now Qorvo) provide orders of magnitude improvements of signal levels between the gNodeB and CPE in the system, allowing higher user capacity, larger coverage areas, and increased quality of service.

Although the thesis to support mmWave proliferation is strong, the industry must take the next step of commercializing mmWave 5G by leveraging the accomplishments already in place and by innovating further, improving performance, and reducing cost to that of a Wi-Fi connection to achieve true commercialization of mmWave networks.

Cost is an important piece of the mmWave 5G growth equation. If history can predict the price point that will proliferate a new mmWave CPE for 5G, look no further than the Wi-Fi router. Today, a mmWave 5G CPE cost is at several hundreds of dollars; although this sounds expensive in comparison with today's Wi-Fi router, one needs to understand that the innovations mentioned in this white paper will dramatically drive down the cost of the CPE.

The impact of Anokiwave's (now Qorvo's) technology extends beyond the technical realm, by shaping the economic landscape of 5G deployment. By reducing the cost and complexity of mmWave systems, Anokiwave (now Qorvo) has lowered the barrier to entry for service providers, facilitating the rapid expansion of 5G networks across different regions and markets. This democratization of mmWave technology is critical for achieving the global vision of 5G, enabling new applications and services, from ultra-high-definition video streaming to autonomous vehicles, and IoT (Internet of Things) ecosystems.

The excitement around the mmWave market emergence is something we see in our careers maybe once or twice if we are lucky. For many, the viability of mmWave is a question of cost, knowhow and technical expertise, spanning everything from waveforms and frequency bands to antenna power, sensitivity and the production and manufacturability of phased array antennas. Anokiwave (now Qorvo) has always understood these technical issues, and recognized that radio level cost would drive the commercial viability of mmWave 5G networks.

Looking at the connectivity market as it stands today with multiple commercial mmWave networks in operation, the focus of the industry is shifting to ways that proliferate mmWave 5G into regions and countries where it can create impactful economic, societal and environmental benefits. Anokiwave (now Qorvo) is enabling that industry focus.

Take a Deeper Dive

For a deeper discussion on this topic, please download the full whitepaper.

Anokiwave Is Now

qorvo

Anokiwave is now Qorvo. Anokiwave's innovative portfolio of active antenna ICs, combined with Qorvo's complementary products, global scale, and significant market reach, provide new options for high integration and high-performance that will democratize phased array active antennas. The two companies' technologies enable a unique combination of innovation + commercial scale + reputation to deliver with proven commercial success across mmWave 5G, SATCOM and D&A.

Qorvo SATCOM Solutions: Connecting Through Space

Space Applications

Space Payload

Ku-Band

Rx: 13.75 to 14.5 GHz; Tx: 10.7 to 12.75 GHz

17.5 or 35 W GaN Tx Power Amplifiers
QPA1006D, QPA1009D

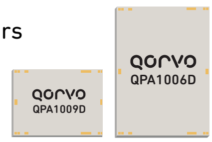

GaAs Rx Low Noise Amplifier
QPA2735
Market leading NF=1.3 dB, 25.5 dB gain with no external DC blocks or RF matching required.

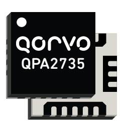

Ka-Band

Rx: 27.5 to 31.0 GHz; Tx: 17.7 to 21.2 GHz

20 or 30 W GaN Tx Power Amplifiers
QPA1721D, QPA1724

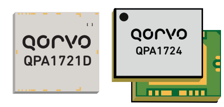

GaAs Rx Low Noise Amplifier
QPA2628
Market leading NF=1.6 dB, 23 dB gain with no external DC blocks or RF matching required.

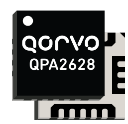

Ground Applications

Flat Panel Arrays

Ku-Band

Rx: 10.7 to 12.75 GHz; Tx: 13.75 to 14.5 GHz

Ku-Band Quad Beamformer ICs
AWMF-0146, AWMF-0147
Quad 4x2 Tx and Rx highly integrated ICs simplifying active antenna design.
Recommended Rx Gain Stage: CMD264P3
Recommended Tx Driver: CMD264P3

Ka-Band

Rx: 17.7 to 21.2 GHz; Tx: 27.5 to 31.0 GHz

Ka-Band Quad Beamformer ICs
AWMF-0197; AWMF-0198
Quad 4x2 Tx and Rx highly integrated ICs simplifying active antenna design.
Recommended Rx Gain Stage: QPA2626
Recommended Tx Driver: QPA2628

Visit qorvo.com/go/satcom to see our complete portfolio for SATCOM

SATCOM Terminals

Ku-Band

Rx: 10.7 to 12.75 GHz; Tx: 13.75 to 14.5 GHz

8, 15, or 25 W GaN Tx Power Amplifiers
QPA0015, QPA0016, QPA0017
SMT package

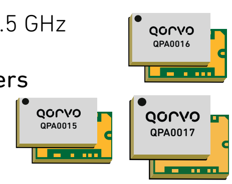

Ultra-Low Noise Rx Amplifier
CMD320C3
Market leading NF=1.07 dB, 18 dB gain with no external DC blocks or RF matching required. Low power dissipation.

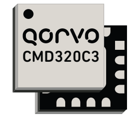

Ka-Band

Rx: 17.7 to 21.2 GHz; Tx: 27.5 to 31.0 GHz

25 W GaN Tx Power Amplifier
QPA2212D

GaAs Rx Low Noise Amplifier
CMD298C4
Market leading NF=1.07 dB, 18 dB gain with no external DC blocks or RF matching required. Low power dissipation.

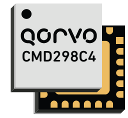

all around you